UNIVERSIDADE FEDERAL DO RIO GRANDE – FURG
INSTITUTO DE OCEANOGRAFIA
PROGRAMA DE PÓS-GRADUAÇÃO EM OCEANOGRAFIA BIOLÓGICA

DINÂMICA ESPAÇO-TEMPORAL DA DISTRIBUIÇÃO VERTICAL DO MESO E MACROZOOPLÂNCTON AO NORTE DA PENÍNSULA ANTÁRTICA

LETÍCIA CAZARIN BALDONI

Tese apresentada ao Programa de Pós-graduação em Oceanografia Biológica daUniversidade Federal do Rio Grande - FURG, como requisito parcial à obtenção do título de DOUTORA

Orientador: Prof. Dr. Erik Muxagata
Coorientadora: Dra. Vanessa Ochi Agostini

RIO GRANDE
Março de 2025

Ficha Catalográfica

B178d Baldoni, Letícia Cazarin.
Dinâmica espaço-temporal da distribuição vertical do meso e *macrozooplâncton* ao norte da Península Antártica / Letícia Cazarin Baldoni. – 2025.
181 f.

Tese (doutorado) – Universidade Federal do Rio Grande – FURG, Programa de Pós-Graduação em Oceanografia Biológica, Rio Grande/RS, 2025.
Orientador: Dr. Erik Muxagata.
Coorientadora: Dra. Vanessa Ochi Agostini.

1. *Mesozooplâncton* 2. Distribuição vertical 3. Migração nictemeral 4. Oceano Austral I. Muxagata, Erik II. Agostini, Vanessa Ochi III. Título.

CDU 551.46

Catalogação na Fonte: Bibliotecário José Paulo dos Santos CRB 10/2344

UNIVERSIDADE FEDERAL DO RIO GRANDE - FURG
IO – INSTITUTO DE OCEANOGRAFIA
PROGRAMA DE PÓS-GRADUAÇÃO EM OCEANOGRAFIA BIOLÓGICA
E-mail: ccpgob@furg.br – home-page: www.ppgocbio.furg.br

ATA DE DEFESA DE TESE DE DOUTORADO – 01/2025

Às treze horas e trinta minutos do dia dez de março do ano de dois mil e vinte e cinco, na sala virtual: https://us05web.zoom.us/j/85719585012, reuniu-se a Comissão Examinadora de Tese de Doutorado da Oc. **Letícia Cazarin Baldoni**, composta pelos seguintes membros: Prof. Dr. Erik Muxagata – Orientador - (PPGOB-IO/FURG); Profa. Dra. Vanessa Ochi Agostini – Coorientadora- (REGENERA BIOTECNOLOGIA); Prof. Dr. Maurício Shimabukuro (PPGOB-IO/FURG); Prof. Dr. Lohengrin Dias de Almeida Fernandes - (IEAPM); Prof. Dr. Charrid Resgalla Junior – (UNIVALI); Dr. Octavio Esquivel Garrote - (PPGOB-IO/FURG). Título da Tese: "DINÂMICA ESPAÇO-TEMPORAL DA DISTRIBUIÇÃO VERTICAL DO MESO E MACROZOOPLÂNCTON AO NORTE DA PENÍNSULA ANTÁRTICA". Dando início à reunião, a Coordenadora do PPGOB, agradeceu a presença de todos e fez a apresentação da Comissão Examinadora. Logo após, explicou que a candidata teria um tempo de 45 a 60 min. para explanação do tema, e cada membro da Comissão, um máximo de 30 min. para perguntas. Dando prosseguimento, passou à palavra a candidata que apresentou o tema e respondeu às perguntas formuladas. Após explanação, a Comissão aprovou o que segue: As sugestões de todos os membros da Comissão Examinadora foram aceitas pelo orientador/candidata e foram incorporadas na versão final. Foi atribuída a seguinte classificação a candidata: Prof. Dr. Maurício Shimabukuro – Classificação: Aprovada; Prof. Dr. Lohengrin Dias de Almeida Fernandes – Classificação: Aprovada; Prof. Dr. Charrid Resgalla Junior – Classificação: Aprovada e Dr. Octavio Esquivel Garrote – Classificação: Aprovada. A candidata foi considerada APROVADA por UNANIMIDADE. Nada mais havendo a tratar, eu, Clabisnei Moura de Melo – Secretário do PPGOB, lavro a presente ata, que após lida e aprovada, será assinada pela Comissão Examinadora, pela aluna e pelo Coordenador Adjunto do PPGOB.

Documento assinado digitalmente
gov.br ERIK MUXAGATA
Data: 10/03/2025 18:08:23-0300
Verifique em https://validar.iti.gov.br

Prof. Dr. Erik Muxagata

Documento assinado digitalmente
gov.br VANESSA OCHI AGOSTINI
Data: 14/03/2025 08:51:37-0300
Verifique em https://validar.iti.gov.br

Profa. Dra. Vanessa Ochi Agostini

Documento assinado digitalmente
gov.br MAURICIO SHIMABUKURO
Data: 14/03/2025 15:10:16-0300
Verifique em https://validar.iti.gov.br

Prof. Dr. Maurício Shimabukuro

Prof. Dr. Lohengrin Dias de Almeida Fernandes

Documento assinado digitalmente
gov.br LOHENGRIN DIAS DE ALMEIDA FERNANDES
Data: 13/03/2025 19:52:26-0300
Verifique em https://validar.iti.gov.br

Documento assinado digitalmente
gov.br CHARRID RESGALLA JUNIOR
Data: 10/03/2025 20:05:23-0300
Verifique em https://validar.iti.gov.br

Prof. Dr. Charrid Resgalla Junior

Dr. Octavio Esquivel Garrote

Documento assinado digitalmente
gov.br OCTAVIO ESQUIVEL GARROTE
Data: 14/03/2025 13:49:20-0300
Verifique em https://validar.iti.gov.br

Profa. Dra. Silvina Botta
Coordenador PPGOB

Oc. Letícia Cazarin Baldoni

Documento assinado digitalmente
gov.br SILVINA BOTTA
Data: 14/03/2025 17:49:06-0300
Verifique em https://validar.iti.gov.br

Documento assinado digitalmente
gov.br LETICIA CAZARIN BALDONI
Data: 14/03/2025 15:32:31-0300
Verifique em https://validar.iti.gov.br

Dedico este trabalho às minhas amadas avós,
que, mesmo distantes, sempre foram luz e força em minha vida.
Seus exemplos, orações e amor incondicional me sustentaram nos momentos mais difíceis,
me inspirando a nunca desistir e a seguir em frente com coragem e determinação.
Este é também um tributo à presença eterna que elas têm em meu coração,
guiando cada passo rumo aos meus sonhos.

"O mar, uma vez que lança seu feitiço, mantém-nos

em sua rede de maravilha para sempre."

Jacques-Yves Cousteau

Agradecimentos

Ao meu orientador, Erik, por esses dez anos de caminhada juntos no laboratório, agradeço por todo conhecimento passado, pelas conversas e pelos puxões de orelha, também necessários. Obrigada por me permitir mergulhar no fascinante mundo do zooplâncton.

À minha coorientadora, Vanessa, pela sabedoria, paciência e prontidão em ajudar. Suas palavras e parceria foram fundamentais em todos os momentos desta jornada.

À CAPES, pela bolsa concedida ao longo do doutorado, e ao CNPq, pela bolsa dentro do Projeto MARES durante o último ano, que tornaram possível a concretização deste trabalho.

Aos projetos INTERBIOTA e NAUTILUS, a toda a equipe do PROANTAR e ao GOAL (Grupo de Oceanografia de Altas Latitudes), pelo suporte, disponibilidade e viabilidade dos dados que foram a base desta pesquisa.

Ao Instituto de Oceanografia e ao Programa de Pós-Graduação em Oceanografia Biológica, pela oportunidade de aprendizado e desenvolvimento deste trabalho, sempre com excelência e suporte.

Ao Professor Rodrigo, ao Thiago e à Andrea, por acreditarem no meu potencial e me acolherem no Projeto MARES.

Aos meus familiares, por serem o alicerce da minha vida. Obrigada por todo apoio, incentivo e amor incondicional, mesmo nos momentos em que eu duvidei de mim mesma. Sem vocês, nada disso seria possível.

Ao Rubens, meu companheiro de vida, por estar ao meu lado em todas as fases desta jornada. Sua paciência, apoio e amor foram um porto seguro em meio aos desafios e conquistas.

Aos meus amigos queridos – André, Giovana, Douglas, Natália, e tantos outros que a vida me deu a sorte de encontrar. Vocês foram minha rede de apoio, alegria e amizade, tornando este caminho menos difícil.

Aos meus amigos de laboratório, pela troca de ideias, companheirismo e pela amizade que tornou cada dia mais especial.

Aos meus afilhados, que trazem brilho e alegria à minha vida. O amor e a conexão que construímos são inigualáveis, mostrando-me que os vínculos mais preciosos da vida são aqueles que vêm do coração.

Aos "alunos" que tive no último ano, sempre entusiasmados pelo ambiente marinho, suas curiosidades me renovaram a cada encontro, me inspirando e marcando minha vida.

E, por fim, aos meus pets, que foram meus "cãopanheiros" fiéis, trazendo leveza e carinho em meio aos dias intensos de escrita e trabalho.

ÍNDICE

LISTA DE TABELAS....6
LISTA DE FIGURAS....7
LISTA DE ABREVIAÇÕES....11
Estrutura da Tese....13
Resumo....14
Abstract....15
1. Introdução....16
2. Hipóteses....23
3. Objetivos....24
3.1. Objetivo Geral....24
3.2. Objetivos Específicos....24
4. Material e Métodos....25
4.1. Caracterização da área de estudo....25
4.2. Amostragens Oceanográficas....27
4.3. Experimento....30
4.4. Análise estatísticas dos dados....31
5. Principais Resultados e Discussões....34
5.1. Variabilidade Hidrográfica....34
5.2. Composição do fitoplâncton....38
5.3. Composição, abundância e variabilidade interanual da comunidade de meso e macrozooplâncton....39
5.3.1. Novos Registros para o NPA....45
5.4. Distribuição vertical do meso e macrozooplâncton....47
5.5. Acoplamento trófico e distribuição do zooplâncton na coluna de água durante o ciclo de 20 horas....56
6. Conclusões e Perspectivas futuras....60
Referências Bibliográficas....64
APÊNDICE 1....81
APÊNDICE 2....134
APÊNDICE 3....165
ANEXOS (Dados)....175

LISTA DE TABELAS

Tabela 1: Lista de todos os taxa identificados nas 141 amostras analisadas.

Tabela 2: Porcentagem de contribuição das espécies que apresentaram diferenças significativas (p < 0,001) entre os anos amostrados (2017–2019) na análise SIMPER.

Table 1 - 1: Summary of zooplankton sampling stations across the three years and locations. A dash (-) indicates that the station was not sampled that year.

Tabela Ap. 1 - 2: Taxonomic groups identified in the samples collected from 2017 to 2019. FO = Frequency of Occurrence, RA = Relative Abundance, Max. Ab. = Maximum Abundance, and N = Number of specimens found. N.I. = Not Identified.

Tabela Ap. 1 - 3: Percentage of contributions from species that demonstrated significant dissimilarities (p-value< 0.001) between sampled years (2017 – 2019) from SIMPER analysis.

Tabela Ap. 1 - 4: Species indicators for each Depth Strata combination with significant values (p-value <0.05)

Tabela Ap. 2 – 1: Diversity indexes calculated for each strata and each sampling time. Species richness (S), Exponential of Shannon-Waver index (Exp H'), the inverse of Simpson index (1/D) and Pielou's evenness index (J)

Tabela Ap. 2 - OR 1: Macronutrient concentrations during the sampling intervals from T1 to T5. DIN = Dissolved Inorganic Nitrogen

Tabela Ap. 2 - OR 2: Taxonomic groups found in the 25 zooplankton samples collected at station B42. FO = Frequency of occurrence, RA = Relative Abundance, Max. Ab. = Maximum Abundance and N = Number of specimens found, N.I. = Not identified

LISTA DE FIGURAS

Figura 1: Mapa da área de estudo (NPA), incluindo o Estreito de Bransfield (EB), Estreito de Gerlache (EG), Mar de Bellingshausen (MBL), com uma representação esquemática da influência das águas adjacentes, seguindo Zhou et al. (2002), Huneke et al. 2016 e Sangrà et al. (2017). As setas representam o fluxo das águas do Mar de Bellingshausen, Estreito de Gerlache e Mar de Weddell no Estreito de Bransfield. A linha tracejada mostra a Frente da Península (FP).

Figura 2: Mapa da área de estudo mostrando as estações oceanográficas onde foram realizadas coletas de zooplâncton ao longo de três anos (2017, 2018, 2019), incluindo o ponto de amostragem em 20 horas.

Figura 3: Mapas mostrando a distribuição superficial da temperatura e salinidade do NPA durante os três anos amostrados.

Figura 4: Distribuição da concentração de clorofila-*a* ($mg.m^{-3}$) na superfície em toda a estação de amostragem. As estações marcadas com "D" foram amostradas durante o dia, enquanto aquelas marcadas com "C" foram amostradas durante o crepúsculo. EG = Estreito de Gerlache, MBL= Mar de Bellingshausen, EB = Estreito de Bransfield.

Figura 5: Variação temporal e contribuição (%) dos principais grupos taxonômicos por ano e região. GS = Estreito de Gerlache, BL = Mar de Bellingshausen, BS = Estreito de Bransfield. Em 2018, os dados não foram amostrados em BL

Figura 6: Espécime de éfira de *Desmonema glaciale* amostrado no Estreito de Bransfield. A) visão oral, a seta branca indica um broto de tentáculo. B) Vista aboral. C) Vista lateral. D) Detalhe dos lóbulos (*lappet*)

Figura 7: Índices de diversidade: (A) Shannon-Weaver (Exp H′) e (B) Simpson (1/D) para cada estação amostrada ao longo dos anos (#01–#05: Estreito de Gerlache; #06–#07: Mar de Bellingshausen; #08–#17: Estreito de Bransfield). Estações marcadas com 'D' indicam amostragem diurna, enquanto 'C' indica amostragem crepuscular.

Figura 8: Distribuição vertical dos principais taxa das comunidades de meso e macrozooplâncton em todas as estações amostradas em Gerlache (#01, #02, #03, #04 e #05) e no Mar de Bellingshausen (#06 e #07) ao longo de três anos (2017 – 2019).

Figura 9: Distribuição vertical dos principais taxa das comunidades de meso e macrozooplâncton em todas as estações amostradas em Bransfield ao longo de três anos (2017 – 2019).

Figura 10: Análise de Correspondência Canônica (ACC) da comunidade de meso e macrozooplâncton de superfície em relação aos principais grupos fitoplanctônicos dentro dos 100 metros superiores nos 3 anos de amostragem (2017, 2018 e 2019)

Figura 11: Análise de Correspondência Canônica (ACC) da comunidade meso e macrozooplâncton em relação às variáveis ambientais mais significativas durante os 3 anos amostrados

Figura 12: Distribuição vertical dos principais taxa meso e macrozooplanctônicos em cada horário de amostragem da estação B42 em 2017 onde: T1 - 17:07; T2 - 22:28; T3 - 1:08; T4 - 5:49 e T5 - 9:05. Período diurno e crepuscular também são indicados.

Figura 13: Concentração de pigmentos biomarcadores nas pelotas fecais de krill e salpa em comparação com a amostragem de linha de base. As barras pretas, cinzas e azuis representam as médias de fucoxantina (Fuco), clorofila-c1 (Chl-c1) e aloxantina (Allo), respectivamente. Os pontos pretos indicam valores individuais. As concentrações de pigmentos nos experimentos foram subtraídas dos valores da amostragem de linha de base, representando a diferença entre eles. A média de cada pigmento foi calculada a partir desses valores subtraídos. A figura inserida exibe uma escala ampliada para a média e os valores individuais de Chl-c1 nos experimentos com krill e salpa.

Figura 14: (a – e) Perfis verticais de temperatura da coluna de água (°C), salinidade, densidade (kg m^{-3}) e estabilidade (x^{10-6} m^{-1}) no painel superior. (f - j) Distribuição de profundidade da biomassa dos grupos fitoplanctônicos (mg m^{-3} Chl-*a*), índice de pastejo (%) e índice de senescência (%) no painel inferior. Diatomáceas (azul), dinoflagelados (vermelho escuro), *P. antarctica* (verde), criptófitas (roxo) e flagelados verdes (azul claro) são mostrados. A linha cinza tracejada representa a profundidade da camada de mistura (PCM; m).

Figura Ap. 1 – 1: Map of the study area with 17 zooplankton sampling stations over 3 years (2017, 2018, and 2019).

Figura Ap. 1 – 2: Maps showing the distribution of surface temperature and salinity of the NAP during the three years sampled.

Figura Ap. 1 – 3: TS diagram showing temperature and salinity profiles from 2017, 2018, and 2019.

Figura Ap. 1 – 4: Distribution of chlorophyll-*a* concentration ($mg.m^{-3}$) at the surface across sampling station. Stations labeled with "D" were sampled during the daytime, while those labeled with "T" were sampled during twilight. The spatial distribution is as follows: #01 - #05 = Gerlache Strait (GS); #06 - #07 = Bellingshausen Sea (BL); #08 - #17 = Bransfield Strait (BS). The bars indicate the proportion of different phytoplankton groups: Diatoms, Dinoflagellates, *P. antarctica*, Cryptophytes, and Green flagellates.

Figura Ap. 1 – 5: Temporal variation and contribution (percentage %) of the main taxonomic groups per year and location. GS = Gerlache Strait, BL = Bellingshausen Sea, BS = Bransfield Strait. In 2018, data was not sampled in BL

Figura Ap. 1 – 6: A: Shannon-Weaver (Exp H′) and B: the inverse of the Simpson (1/D) for each station sampled (#01 - #05 = Gerlache Strait; #06 - #07 = Bellingshausen Sea;

#08 - #17 = Bransfield Strait) across years. Stations with 'D' indicate daytime sampling, and 'T' indicate twilight sampling.

Figura Ap. 1 – 7: Vertical distribution of the meso- and macrozooplankton groups across all stations sampled in Gerlache (#01, #02, #03, #04, and #05) and Bellingshausen (#06 and #07) over three years (2017 – 2019).

Figura Ap. 1 – 8: Vertical distribution of the meso- and macrozooplankton groups across all stations sampled in Bransfield over three years (2017 – 2019).

Figura Ap. 1 – 9: Vertical distribution of the main taxa from the meso- and macrozooplankton communities across all stations sampled in Gerlache (#01, #02, #03, #04 and #05) and Bellingshausen (#06 and #07) over three years (2017 – 2019)

Figura Ap. 1 – 10: Vertical distribution of the main taxa from the meso- and macrozooplankton communities across all stations sampled in Bransfield over three years (2017 – 2019)

Figura Ap. 1 – 11: nMDS plot with the meso and macrozooplankton community distribution across three years, categorized by depth layers: Surface layer (0-100 m), subsurface layer (100-200 m), mid layers (200-400 m) and deep layer (400-500 m).

Figura Ap. 1 - 12: Canonical correspondence analysis (CCA) of surface meso- and macrozooplankton community relative to major phytoplankton groups within the upper 100 meters in the 3 years of sampling (2017, 2018, and 2019)

Figura Ap. 1 – 13: Canonical Correspondence Analysis (CCA) of the meso and macrozooplankton community in relation to the most significant environmental variables during the 3 years sampled

Figura Ap. 2 – 1: Map of the Northern Antarctic Peninsula showing the location of the B42 oceanographic station in the Bransfield Strait (B42), with a schematic representation of the influence of adjacent waters, following Zhou et al. (2002), Huneke et al. 2016 and Sangrà et al. (2017). Arrows represent the inflow of Bellingshausen Sea, Gerlache Strait and Weddell Sea waters in Bransfield Strait. SSI = South Shetland Islands, EI = Elephant Island. Dashed line show the surface Peninsula Front (PF)

Figura Ap. 2 – 2: (a – e) Vertical profiles of water column temperature (°C), salinity, density (kg m^{-3}) and stability (x10^{-6} m^{-1}) in the top panel. (f - j) Depth distribution of phytoplankton groups' biomass (mg m^{-3} Chl-*a*), grazing index (%) and senescence index (%) in the lower panel. Diatoms (blue), dinoflagellates (dark red), *P. antarctica* (green), cryptophytes (purple) and green flagellates (light blue) are shown. Dashed gray line represents mixed layer depth (MLD; m)

Figura Ap. 2 – 3: T–S diagram for B42 oceanographic station from the Bransfield Strait with the waters masses observed: Transitional Zonal Water with Bellingshausen Sea influence (TBW), Transitional Zonal Water with Weddell Sea influence (TWW)

Figura Ap. 2 – 4: Vertical distribution of the main zooplanktonic groups in each sampling time of B42 station in 2017 where: T1 -5:07 pm; T2 -10:28 pm; T3 - 1:08 am; T4 -5:49 am and T5 - 9:05 am. Day and night period is also indicated

Figura Ap. 2 – 5: Vertical distribution of the main meso- and macrozooplanktonic taxa in each sampling time of B42 station in 2017 where: T1 -5:07 pm; T2 -10:28 pm; T3 - 1:08 am; T4 -5:49 am and T5 - 9:05 am. Day and night period is also indicated

Figura Ap. 2 – 6: Non-metric multidimensional scaling (nMDS) of the main zooplanktonic species collected in B42 station in 2017. Vectors show the significant species (a) and environmental variables (b) with nMDS ordination of samples

Figura Ap. 3 – 1: Specimen of *Desmonema glaciale* sampled at Bransfield Strait. A) oral view, the white arrow indicates tentacle bud. B) Aboral view. C) Lateral view. D) Lappet detail

LISTA DE ABREVIAÇÕES

ACC - Análise Canônica de Correspondência

ACP –Água Circumpolar Profunda

ACPM - Água Circumpolar Profunda Modificada

ADP – Água Densa de Plataforma

ANOVA - Análise de Variância, do inglês Analysis of Variance

ASAA – Água Superficial Antártica

ATB – Água de Transição de Bellingshausen

ATW – Água de Transição de Weddell

CCA –Corrente Circumpolar Antártica

Chl-c1 - Clorofila-c1

CPR – do inglês Continuous Plankton Recorder, ou Amostrador Contínuo de Plâncton

CTD – do inglês Conductivity, Temperature and Depth

EB – Estreito de Bransfield

EG – Estreito de Gerlache

ENSO – El-Niño Oscilação Sul, do inglês El-Niño Southern Oscillation

FB –Frente da Península

FURG – Universidade Federal do Rio Grande

GOAL – Grupo de Oceanografia de Altas Latitudes

HPLC - Cromatografia Líquida de Alta Eficiência, do inglês High Performance Liquid Chromatography

INTERBIOTA – INTERações BIOlógicas em ecossisTemas marinhos próximo à Península Antártica sob diferentes impactos de câmbios climáticos

ISS – Ilhas Shetland do Sul

LEOC – Laboratório de Estudos dos Oceanos e Clima

MAS – Módulo Anular Sul, do inglês, SAM - South Annular Mode

MBL – Mar de Bellingshausen

MN – Migração Nictemeral

NMDS – Escalonamento Multidimensional Não Métrico, do inglês Non Metric Multidimensional Scalling

NOAA - National Oceanic and Atmospheric Administration

NPA – Norte da Península Antártica

OA - Operação Antártica

OPERANTAR – Operação Antártica

PCM - Profundidade da Camada de Mistura

PERMANOVA – Análise Multivariada de Variância por Permutação, do inglês Permutational Multivariate Analysis of Variance

PROANTAR – Programa Antártico Brasileiro

RAMS – Registro de Espécies Marinhas da Antártica, do inglês Register of Antarctic Marine Species

SIMPER – do inglês Similarity Percentage, ou Percentual de Similaridade

UE – Unidade Experimental

Estrutura da Tese

Esta Tese explora as mudanças na composição e na estrutura vertical das comunidades de meso e macrozooplâncton no Norte da Península Antártica, em escalas interanuais e diária. A pesquisa foi conduzida no âmbito dos projetos INTERBIOTA e NAUTILUS, como parte do Grupo de Oceanografia de Altas Latitudes (GOAL). A Tese é composta por duas partes complementares. A primeira, apresentada em português, que reúne os seguintes elementos: Resumo e Abstract com as palavras-chave, Introdução, Hipóteses, Objetivos, Material e Métodos, uma Síntese dos Resultados e as Conclusões, oferecendo uma visão geral do estudo. A segunda parte, em inglês, contém três apêndices que destacam os artigos científicos gerados a partir desta pesquisa, ampliando o alcance e a relevância dos resultados obtidos. Sendo eles:

1. "*Spatiotemporal Patterns and Environmental Drivers of Meso- and Macrozooplankton Communities in the Northern Antarctic Peninsula (2017–2019)*". O artigo aborda as mudanças interanuais na composição taxonômica e distribuição vertical do meso e macrozooplâncton ao longo de três anos consecutivos. Foi submetido ao periódico *Progress in Oceanography* e encontra-se em processo de revisão.

2. "*Meso and macrozooplankton distribution across water column during a 20-hours experiment in the Bransfield Strait, northern Antarctic Peninsula*". O artigo investiga o comportamento da migração vertical diária, utilizando dados de amostras estratificadas coletadas nas zonas epipelágica e mesopelágica, em um ponto estratégico do Estreito de Bransfield. Foi submetido ao periódico *Polar Biology* e encontra-se em processo de revisão.

3. "*First Record of Desmonema glaciale Larson, 1986 ephyrae in the Northern Antarctic Peninsula*". O artigo apresenta o primeiro registro de éfira de *Desmonema glaciale* na região central do Estreito de Bransfield. Está em estágio final de revisão a ser submetido ao periódico *Ocean and Coastal Research*.

Resumo

Os organismos zooplanctônicos conectam os produtores primários aos níveis tróficos superiores e, transferem matéria e carbono verticalmente das águas superficiais para as zonas profundas. A eficiência desses processos depende da composição taxonômica e ecologia trófica dessas comunidades, uma questão particularmente importante no ambiente antártico, sensível às mudanças climáticas globais e com impactos evidentes em todo ecossistema. Aos arredores do Norte da Península Antártica (NPA), o rápido aquecimento regional tem alterado a composição do fitoplâncton e, consequentemente, pode estar modificando a estrutura e a dinâmica do zooplâncton, influenciando sua distribuição e interações tróficas. Este estudo analisou as dinâmicas de meso e macrozooplâncton em escalas temporais curtas, essenciais para entender a estrutura da comunidade planctônica em um ambiente sensível às mudanças climáticas. Amostragens verticais (0-500 m) foram realizadas no verão de 2017, 2018 e 2019 para analisar as mudanças interanuais na composição zooplanctônica nos estreitos de Gerlache, Bransfield e no Mar de Bellingshausen. Ainda em 2017, uma estação no Estreito de Bransfield também foi amostrada para investigar a migração vertical do zooplâncton e a alimentação de krill e salpas por meio de um experimento com pelotas fecais. Dados físicos e de fitoplâncton permitiram testar as relações das comunidades com variáveis ambientais. Temperaturas superficiais excepcionalmente altas em 2017 (3,2 °C), resultaram em uma alta estabilidade da coluna d'água, que associada a predominância de criptófitas e dinoflagelados, favoreceram altas abundâncias de *Salpa thompsoni* e copépodes maiores (>2000 μm), como *Metridia gerlachei*. Em contraste, 2018 e 2019 condições térmicas mais amenas, menor estabilidade e a ausência de *S. thompsoni*, favoreceram maiores abundâncias de copépodes menores (<2000 μm) como *Ctenocalanus citer* e *Oithona* spp. Além disso, este estudo registrou pela primeira vez a presença de uma éfira de *Desmonema glaciale* na região e expandiu a distribuição do tunicado *Dolioletta* spp. para águas polares, reforçando a contribuição do meroplâncton e a importância do monitoramento da biodiversidade antártica, essencial para compreender os efeitos das mudanças climáticas nos ecossistemas marinhos polares. Durante o ciclo de 20 horas de amostragens, as salpas permaneceram abundantes na superfície, e, ao reduzirem suas abundâncias ainda no período noturno, tornou-se evidente a migração nictemeral de *Euphausia superba* e a migração ontogenética de *M. gerlachei*. Já os organismos carnívoros e detritívoros permaneceram mais abundantes na zona mesopelágica. Essas dinâmicas destacam a complexidade dos padrões de distribuição vertical. O experimento mostrou que as salpas ingerem criptófitas, o que pode ter impulsionado sua proliferação devido à disponibilidade dessa fonte alimentar. Este estudo revelou mudanças significativas na composição e abundância do zooplâncton antártico no NPA em escalas diárias a interanuais, que podem impactar os ciclos biogeoquímicos e as dinâmicas das redes alimentares a longo prazo, caso as condições observadas persistam. Para avançar na compreensão das mudanças observadas, estudos futuros devem integrar amostragens diurnas e noturnas em estratos menores, conduzidas de forma contínua ao longo dos anos, permitindo uma análise mais detalhada da influência das variações ambientais na estrutura e dinâmica do zooplâncton antártico.

Palavras-chave: Mesozooplâncton, Distribuição Vertical, Migração nictemeral, Oceano Austral

Abstract

Zooplankton organisms connect primary producers to higher trophic levels and transfer matter and carbon vertically from surface waters to deeper zones. The efficiency of these processes depends on the taxonomic composition and trophic ecology of these communities, a particularly important issue in the Antarctic environment, which is highly sensitive to global climate change and has profound impacts on the entire ecosystem. Around the Northern Antarctic Peninsula (NAP), rapid regional has altered the composition of phytoplankton and, consequently, may be modifying the structure and dynamics of zooplankton, influencing their distribution and trophic interactions. This study analyzed the dynamics of meso- and macrozooplankton on short timescales, essential to understand the the structure of the plankton community in an environment sensitive to climate change. Vertical sampling (0-500 m) was conducted in the summer of 2017, 2018 and 2019 to analyze interannual changes in zooplankton composition in the Gerlache and Bransfield Straits and the Bellingshausen Sea. Also in 2017, an additional station in the Bransfield Strait was sampled to investigate the vertical migration of zooplankton and the feeding behavior of krill and salps through a fecal pellet experiment. Physical and phytoplankton data allowed testing the relationships of communities with environmental variables. Exceptionally high surface temperatures in 2017 (3.2 °C) resulted in strong stratification and high water column stability. This stability was the most significant variable influencing zooplankton distribution, being associated with the predominance of cryptophytes and dinoflagellates, which favored high abundances of *Salpa thompsoni* and larger copepods (>2000 μm), such as *Metridia gerlachei*. In contrast, the milder thermal conditions of 2018 and 2019, coupled with lower stability and the absence of *S. thompsoni*, favored higher abundances of smaller copepods (<2000 μm), such as *Ctenocalanus citer* and *Oithona* spp.. Additionally, this study recorded, for the first time, the presence of a *Desmonema glaciale* ephyra in the region and expanded the known distribution of the tunicate Dolioletta spp. into polar waters. These findings reinforce the contribution of meroplankton and the importance of monitoring Antarctic biodiversity, which is crucial for understanding the effects of climate change on polar marine ecosystems. During the 20-hour sampling cycle, salps remained abundant at the surface. However, as their abundance decreased at night, the diel vertical migration of Euphausia superba and the ontogenetic migration of *M. gerlachei* became evident. In contrast, carnivorous, detritivorous, and seasonally migratory organisms remained more abundant in the mesopelagic zone, playing an essential role in the trophic structure. These dynamics highlight the complexity of vertical distribution patterns. The experiment showed that salps ingest cryptophytes, which may have driven their proliferation due to the availability of this food source. This study revealed significant changes in the composition and abundance of Antarctic zooplankton in the NPA on a daily to interannual scale, which may affect biogeochemical cycles and food web dynamics in the long term if the observed conditions persist. To advance the understanding of the observed changes, future studies should integrate daytime and nighttime sampling in shallow strata, conducted continuously over the years, allowing a more detailed analysis of the influence of environmental variations on the structure and dynamics of Antarctic zooplankton.

Key Words: Mesozooplankton, Vertical Distribution, Diel Vertical Migration, Southern Ocean

1. Introdução

O Oceano Austral cobre aproximadamente 20% da área dos oceanos do planeta e desempenha um papel fundamental no equilíbrio climático global (Knox 2006). Sua dinâmica é influenciada por fatores ambientais como temperatura, salinidade, cobertura de gelo (Meredith et al. 2013, Deppeler & Davidson 2017) e fenômenos climáticos, como o Modo Anular Sul (MAS) e o El Niño-Oscilação Sul (ENSO) (Ruiz-Barlett et al. 2018). Esses fenômenos alteram padrões de ventos, pressão atmosférica e distribuição de calor, afetando a circulação oceânica, como as intrusões da Corrente Circumpolar Antártica (CCA) (Ruiz-Barlett et al. 2018) e a extensão do gelo marinho (Turner 2004, Marshall et al. 2011).

Nas últimas décadas, o aumento da temperatura da água no Oceano Austral vem sendo reportado, principalmente na região do Norte da Península Antártica (NPA) (Skvarca et al. 1999, Meredith & King 2005, Henley et al. 2019). A região do NPA se destaca por ser uma área de transição entre as regiões subpolares e polares, caracterizada por condições hidrográficas complexas e dinâmicas sazonais de gelo marinho. Ela inclui os estreitos de Bransfield e Gerlache, uma porção do noroeste do Mar de Weddell e parte do Mar de Bellingshausen, bem como a porção sul da Passagem de Drake (Kerr et al. 2018a). Esse ecossistema único oferece abrigo para diversas comunidades biológicas e é crucial para compreender os processos do Oceano Antártico e os impactos da variabilidade climática (Mendes et al. 2013, 2018b, Dotto et al. 2016, Orselli et al. 2022). O rápido aumento da temperatura nessa região intensifica as mudanças sazonais e interanuais da cobertura de gelo marinho e altera as condições hidrográficas da região (Henley et al. 2019). Essas variações têm impacto direto nos perfis de temperatura e salinidade, que por sua vez influenciam a estrutura e função das comunidades de fitoplâncton e zooplâncton, refletindo-se na biodiversidade e na distribuição das espécies dessa região (Cisewski et al. 2010, Mendes et al. 2013, Flores et al. 2014).

O fitoplâncton, base da cadeia trófica marinha, desempenha um papel fundamental na regulação dos ciclos sazonais e da variabilidade interanual na abundância e distribuição do meso e macrozooplâncton, servindo como a principal fonte de alimento para diversas espécies dessas comunidades (Gleiber et al. 2016, Schofield et al. 2024). O mesozooplâncton abrange organismos com tamanhos que variam de 0,2 a 20 mm e o

macrozooplâncton de 20 a 200 mm, os quais caracterizam-se por uma grande diversidade, incluindo representantes de quase todos os filos animais (Richardson & Kunz 2006). Esses organismos exibem uma ampla gama de estratégias de vida e formas corporais distintas, como os holoplanctônicos que passam todo ciclo de vida no plâncton e os meroplanctônicos, que passam apenas parte do ciclo de vida no plâncton (Calbet 2024). Ainda, desempenham um papel crucial na cadeia trófica marinha, sendo o elo entre os produtores primários e os níveis tróficos superiores, como peixes, aves e mamíferos (Banse 1995). Por terem ciclos de vidas curtos e por serem sensíveis às mudanças no ambiente (Sabatini 2008) são utilizados como indicadores biológicos de massas de água, correntes oceânicas (Grant 1991), mudanças climáticas (Bednaršek et al. 2016) e poluição (Ferdous & Muktadir 2009). Sendo assim, alterações na abundância e/ou ocorrência de determinadas espécies podem indicar mudanças importantes no ambiente (Richardson 2006).

Os organismos zooplanctônicos também desempenham um papel fundamental na ciclagem de elementos e nos fluxos verticais de energia e matéria, atuando no processo de acoplamento pelágico-bentônico (Marcus & Boero 1998), e no processo da bomba biológica, que nada mais é do que o transporte de carbono das camadas superficiais para maiores profundidades (Griffiths et al. 2017, Aumont et al. 2018). Estes dois processos tornam-se ainda mais fundamentais no oceano Austral, um dos ecossistemas mais dinâmicos do planeta, caracterizado por uma biodiversidade única. Nesse ambiente, a eficiência da bomba biológica e do acoplamento pelágico-bentônico está intimamente relacionada à composição taxonômica e à ecologia trófica das comunidades zooplanctônicas (Mayzaud & Pakhomov 2014). A biodiversidade local é fortemente influenciada pelas condições oceanográficas e se mostra particularmente sensível às mudanças na circulação das correntes oceânicas e aos impactos das mudanças climáticas (David & Saucède 2015). Diante disso, monitorar as variações na composição e abundância das espécies é fundamental para entender como essas transformações globais afetam os processos da bomba biológica e do acoplamento pelágico-bentônico (Mackas et al. 2001). Os organismos zooplanctônicos participam desses processos por meio da liberação de suas pelotas fecais e exúvias e, através de diferentes padrões de migração, que ocorrem em diferentes escalas temporais e são influenciadas tanto por fatores ambientais quanto pelo ciclo de vida dos organismos (Bandara et al. 2021).

As migrações nictemerais (MN), comuns em copépodes, krill e salpas, ocorrem diariamente, com organismos subindo à superfície durante a noite para se alimentar e descendo durante o dia para evitar predadores (Hays 2001, Gili et al. 2006). As ontogenéticas envolvem mudanças na distribuição vertical ao longo do ciclo de vida, com juvenis ocupando camadas mais superficiais e adultos águas mais profundas, como ocorre com algumas espécies de copépodes (Schnack-Schiel 2002, Yang et al. 2017). Já as migrações sazonais são influenciadas por variações ambientais ao longo do ano, especialmente em ambientes polares, onde nos meses de inverno a luz solar é praticamente inexistente e ocorre o congelamento da superfície do mar. Nessas condições, algumas espécies se deslocam para camadas mais profundas, reduzindo o metabolismo para evitar essas condições adversas, sendo este um comportamento comum em algumas espécies de copépodes (King & LaCasella 2003, Flores et al. 2014, Conroy et al. 2023).

Estes comportamentos de migração, junto aos processos oceanográficos físicos, moldam a distribuição vertical do meso e macrozooplâncton (Barange 1990, Atkinson & Sinclair 2000, Ibáñez-Tejero et al. 2018). Entretanto, nos ambientes polares, existe uma variabilidade da magnitude dessas migrações diante dos períodos de luz contínua (durante o verão) ou escuridão (durante o inverno), onde algumas espécies realizam migrações mais rasas (Flores et al. 2014, Ludvigsen et al. 2018, Conroy et al. 2020). As MN podem ocorrer para maximizar a obtenção de alimento (Guglielmo et al. 2011), minimizar a predação (Nishikawa & Tsuda 2001) e/ou reduzir a competição entre as espécies (Romero-Romero et al. 2019).

Nos ecossistemas polares, sobretudo, essas dinâmicas migratórias refletem as variações sazonais na estrutura e dinâmica da produtividade primária. No NPA, por exemplo, altas concentrações de clorofila-*a* ocorrem perto da superfície no verão, especialmente em áreas próximas à borda do gelo marinho, como o Estreito de Gerlache (Smith et al. 1999, Arrigo et al. 2008, Mendes et al. 2012, 2013, 2018), normalmente com altas concentrações de diatomáceas (Ducklow et al. 2007). No entanto, o aumento da temperatura nas camadas superiores do oceano, ocasionam maior derretimento do gelo, reduzindo a salinidade e aumentando a estratificação da coluna d'água. Esses efeitos são evidenciados por alterações na composição do fitoplâncton, com a substituição de diatomáceas por células menores, como criptófitas (Montes-Hugo et al. 2009, Mendes et

al. 2018, Costa et al. 2021), gerando consequências diretas para as comunidades de meso e macrozooplâncton e para toda cadeia trófica (Atkinson et al. 2004, 2019, Clarke et al. 2007, Deppeler & Davidson 2017, Seyboth et al. 2018).

Uma das consequências é a redução nas abundâncias do krill antártico (*Euphausia superba* Dana, 1850), relatada nos últimos anos (Atkinson et al. 2004, 2019, Steinberg et al. 2015, Bitiutskii et al. 2022). O krill, uma espécie-chave da região do NPA, dependente do gelo marinho e alimenta-se predominantemente de partículas maiores, como diatomáceas (Nishikawa et al. 1995, Atkinson et al., 2001). Por outro lado, um aumento substancial na abundância de salpas tem sido reportado (Criales-Hernández et al. 2022, Kasyan et al. 2022, Gorbatenko & Yakovenko 2023). As salpas prosperam em águas mais quentes e livres de gelo (Pakhomov et al. 2002, Henschke & Pakhomov 2019, Henschke et al. 2021).

A relação entre krill e salpas é fortemente influenciada pelas condições ambientais e pela disponibilidade de alimento, afetando o fluxo de matéria e energia de formas distintas (Nishikawa et al. 1995; Moline et al. 2000; Smith et al. 2014). O krill se alimenta predominantemente de diatomáceas, forma densos cardumes e atua como um elo essencial na transferência de carbono para níveis tróficos superiores, servindo de alimento para diversos predadores (Atkinson et al. 2004). Em contraste, as salpas, que consomem células fitoplanctônicas menores e partículas em suspensão na coluna d'água, possuem uma alta taxa de filtração e geram pelotas fecais maiores e mais densas, que afundam rapidamente, promovendo uma exportação eficiente de carbono para o oceano profundo (Perissinotto & Pakhomov 1998, Moline et al. 2004, Henschke et al. 2021). Assim, enquanto o krill sustenta redes tróficas mais complexas, as salpas aceleram o transporte de matéria orgânica para profundidades maiores (Perissinotto & Pakhomov 1998, Smith et al. 2014, Belcher et al. 2019). Além disso, as salpas já foram registradas em altas abundâncias em maiores profundidades (Gili et al. 2006), indicando que esses organismos estão entre os que possuem distribuições verticais mais amplas relacionadas ao comportamento migratório nictemeral no ambiente antártico (Nishikawa & Tsuda 2001).

Além do krill e das salpas, outros grupos zooplanctônicos, como quetognatos, cnidários e copépodes, desempenham papéis fundamentais na estrutura trófica e distribuição vertical das comunidades zooplanctônicas no Oceano Austral. A composição

dessas comunidades varia com os diferentes estratos de profundidade, refletindo diferenças nos hábitos alimentares e no gradiente ambiental das massas de água (Yang et al. 2017, Conroy et al. 2020). Estudos ao redor da Península Antártica e no Ártico indicam que a distribuição vertical desses organismos está relacionada ao máximo de clorofila-*a* subsuperficial e à profundidade da camada de mistura, onde alguns copépodes tendem a se concentrar logo abaixo dessa camada (Berge et al. 2014, Conroy et al. 2020). Já os quetognatos e cnidários, predominantemente carnívoros, ocupam camadas mais profundas, onde encontram maior disponibilidade e diversidade de presas, incluindo indivíduos da própria espécie (Conroy et al. 2020, Venkataramana et al. 2022). Os copépodes, por sua vez, podem ser onívoros, carnívoros ou herbívoros e apresentam uma distribuição mais ampla, abrangendo toda a coluna d'água conforme a disponibilidade de fitoplâncton e presas menores (Giraldo et al. 2019, Conroy et al. 2020).

Outras pesquisas na Antártica destacam estruturas verticais distintas, com algumas agregações formadas para dividir verticalmente o habitat, reduzindo potencialmente a competição intra e interespecífica (Mackas et al. 1993). Estudos realizados no Mar de Weddell e no setor Pacífico do Oceano Austral, destacam a separação entre comunidades epipelágicas (0–200 m) e de estratos mais profundos, com maior abundância e dominância de copépodes nas camadas superiores, enquanto as camadas mais profundas apresentam menor abundância total e dominância de outros grupos (Hopkins & Torres 1989, Marrari et al. 2011, Liu et al. 2024). Em águas ao redor do NPA, as distribuições verticais são atribuídas a comportamentos específicos da espécie, para evitar a competição (Marrari et al. 2011). Além disso, a composição das comunidades pode variar ao longo do dia, com alguns taxa carnívoros mais abundantes na zona mesopelágica e copépodes e ostracodes ajustando suas distribuições na zona epipelágica conforme o fotoperíodo (Conroy et al. 2020).

Na região do NPA, no Estreito de Bransfield, as variações nas abundâncias entre as diferentes profundidades amostradas podem estar relacionadas aos estágios de desenvolvimento e padrões do ciclo de vida de alguns copépodes, com copepoditos mais próximos à superfície, onde há maior disponibilidade de alimento, e adultos em camadas mais profundas. Em termos espaciais, pode ocorrer uma alternância na dominância das espécies, com copépodes mais abundantes em algumas estações, enquanto salpas e

eufausiáceos predominam em outras. Essa alternância na dominância pode estar relacionada à fase reprodutiva ou ao estágio de desenvolvimento dos copépodes (Lee et al. 2004). Além disso, variações interanuais nos padrões de distribuição superficial do mesozooplâncton entre os Estreitos de Gerlache e Bransfield já foram identificadas, com dados obtidos por meio do *Continuous Plankton Recorder* (CPR) (Leonor & Muxagata 2025). Em 2016, por exemplo, copépodes dominaram as comunidades, enquanto em 2017 houve predominância de salpas, associada a condições ambientais anômalas, como temperaturas de superfície mais altas. Também foram observadas maiores abundâncias de mesozooplâncton na superfície durante o período crepuscular, evidenciando padrões de migração nictemeral no Estreito de Bransfield (Leonor & Muxagata 2025).

Além disso, a variabilidade interanual e sazonal nas condições ambientais e na disponibilidade de alimentos, combinada com os processos de vida do zooplâncton, como reprodução e crescimento, contribui ainda mais para variações significativas de ano para ano nos padrões de distribuição vertical (Mackas et al. 2012, Conroy et al. 2020). Esses fatores reforçam a complexidade das interações entre comportamento, ambiente e disponibilidade de recursos, que mudam diariamente e anualmente e são essenciais para a compreensão da dinâmica dos ecossistemas polares.

Embora estudos anteriores aqui citados tenham identificado padrões distintos na distribuição vertical do meso- e macrozooplâncton em outros ambientes antárticos (Constable et al. 2014, Conroy et al. 2020, Liu et al. 2024), a compreensão das variações interanuais entre as comunidades epipelágicas e mesopelágicas no NPA permanece limitada. Poucos estudos detalham a composição específica e variabilidade temporal do zooplâncton nessas camadas, especialmente em regiões dinâmicas como os estreitos de Gerlache e Bransfield, onde fortes gradientes ambientais e a interação de diferentes massas de água, tornam-se pontos-chave para investigar como as comunidades respondem às mudanças ambientais (Kerr et al. 2018, Mendes et al. 2023). Investigar a biodiversidade e as interações biológicas dessas comunidades é essencial para compreender o funcionamento dos ecossistemas polares, pois alterações na biodiversidade e biomassa do zooplâncton podem indicar a saúde e resiliência desses ecossistemas, altamente sensíveis às mudanças climáticas (Henley et al. 2019, Steiner et al. 2021, Schofield et al. 2024).

Ao integrar a variabilidade interanual e diária da composição zooplanctônica com fatores ambientais, este estudo contribui para uma melhor compreensão dos processos que regulam a estrutura e dinâmica das comunidades de meso e macrozooplâncton no NPA. Isso é essencial para avaliar possíveis impactos das mudanças climáticas e das variações oceanográficas sobre essas comunidades, fornecendo subsídios para futuras pesquisas em um dos ambientes mais sensíveis às mudanças globais.

2. Hipóteses

A distribuição do meso e macrozooplâncton no ambiente antártico apresenta alta variabilidade, refletindo a complexidade dos processos oceanográficos que influenciam essas comunidades. Nesse contexto, esta tese testou as seguintes hipóteses:

1. A variabilidade interanual e espacial do meso e macrozooplâncton no NPA é influenciada pelas diferenças na temperatura e pela composição dos grupos fitoplanctônicos. No Estreito de Gerlache, onde ocorre maior produtividade primária, as camadas superficiais apresentam maiores abundâncias da comunidade, enquanto o Estreito de Bransfield, caracterizado por águas com temperaturas heterogêneas, apresenta maior variabilidade vertical na estrutura da comunidade.

2. O zooplâncton mantém um padrão de migração nictemeral durante o verão austral, mesmo sob condições de estratificação da coluna d'água e variação mínima no fotoperíodo, com diferenças significativas nas abundâncias entre as zonas epipelágica (0-200 m) e mesopelágica (201-500 m).

3. Krill e salpas possuem estratégias tróficas distintas, com o krill exibindo maior proporção de pigmentos de diatomáceas em suas pelotas fecais, enquanto as salpas apresentam uma composição mais variada, incluindo outros pigmentos em suas pelotas além dos pigmentos característicos de diatomáceas.

3. Objetivos

3.1. Objetivo Geral

Investigar a composição, distribuição e dinâmica da comunidade do meso e macrozooplâncton no Norte da Península Antártica, analisando sua variabilidade espacial, temporal e sua relação com fatores ambientais ao longo da coluna d'água (0-500 m).

3.1.1. Objetivos específicos

1. Realizar um levantamento da biodiversidade meso e macrozooplanctônica no Norte da Península Antártica, da superfície até 500 m de profundidade;

2. Investigar as mudanças interanuais (2017 – 2019) na composição da comunidade assim como na distribuição de espécies dominantes dentro e entre as camadas epipelágica (0-200 m) e mesopelágica superior (201 - 500 m);

3. Determinar a variabilidade vertical das espécies da comunidade zooplanctônica durante as migrações nictemerais (ciclo de 24 horas);

4. Analisar a relação entre a estrutura da comunidade e os fatores ambientais, incluindo a composição do fitoplâncton.

5. Avaliar como as diferenças nas estratégias alimentares de krill e salpas se refletem na composição fitoplanctônica de suas pelotas fecais, explorando a seletividade alimentar e suas possíveis implicações na estrutura trófica no NPA

4. Material e Métodos

4.1. Caracterização da área de estudo

A área de estudo abrangiu o norte da Península Antártica (NPA), incluindo uma porção do mar de Bellingshausen (MBL), o Estreito de Gerlache (EG) e o Estreito de Bransfield (EB) (Kerr et al., 2018a) (Fig. 1). O NPA é uma região estratégica para investigações sobre as mudanças climáticas contemporâneas, evidenciando alterações constantes na interação entre atmosfera, oceano e criosfera (Kerr et al. 2018a, Henley et al. 2019, Ferreira et al. 2020).

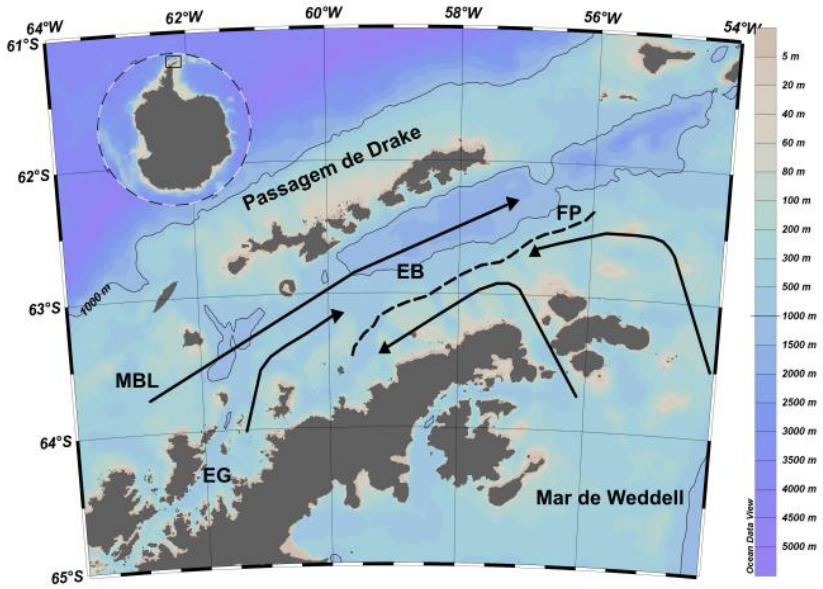


Figura 1: Mapa da área de estudo (NPA), incluindo o Estreito de Bransfield (EB), Estreito de Gerlache (EG), Mar de Bellingshausen (MBL), com uma representação esquemática da influência das águas adjacentes, seguindo Zhou et al. (2002), Huneke et al. 2016 e Sangrà et al. (2011). As setas representam o fluxo das águas do Mar de Bellingshausen, Estreito de Gerlache e Mar de Weddell no Estreito de Bransfield. A linha tracejada mostra a Frente da Península (FP).

Essa região ainda se destaca por sua hidrografia complexa, influenciada principalmente pelo fluxo contínuo da Corrente Circumpolar Antártica (CCA), no sentido leste. Esta corrente oceânica possui um fluxo ininterrupto por massa continental e conecta todos os oceanos, transferindo propriedades físicas cruciais para o controle do clima no planeta (Orsi et al. 1995, Ward et al. 2002). A CCA transporta a Água Circumpolar Profunda (ACP), uma massa de água quente (> 1°C) e rica em nutrientes, que adentra nos

estreitos do NPA em camadas intermediárias (Prézelin et al. 2000, Garcia et al. 2002, Ruiz-Barlett et al. 2018). As propriedades dessa massa de água se modificam conforme as misturas com águas mais frias e menos salinas, formando a Água Circumpolar Profunda Modificada (ACPM) (Couto et al 2017).

Localizado ao sul do NPA, o EG apresenta profundidades predominantemente rasas, em torno de 800 m, com áreas mais rasas de até 200 ou 300 m (García et al. 2002). Ele se conecta ao norte com o EB e ao MBL através de dois canais principais: Schollaert, ao centro, e Bismarck, ao sul (Kerr et al. 2018). Essa região é marcada por uma alta concentração de gelo marinho e é fortemente influenciada pelo derretimento de gelo proveniente das geleiras continentais (Parra et al. 2020, Meredith et al. 2022).

O EB, por sua vez, é uma região paralela à costa da Península Antártica e apresenta profundidades que ultrapassam os 2000 m (Gordon & Nowlin 1978). Por ser uma região mais profunda, o EB possui uma circulação dinâmica, recebendo águas superficiais provenientes do MBL e do EG que carregam a ACPM, ricas em nutrientes. Em maiores profundidades o volume deste estreito é ocupado por uma mistura de águas oriundas do mar de Weddell, como a Água Densa de Plataforma (ADP), com baixas temperaturas e altas salinidades. Esta massa de água se mistura com a ACPM em níveis intermediários e superiores, alterando suas propriedades físicas (Dotto et al. 2016, Damini et al. 2022). Parte do fluxo procedente do mar de Weddell também pode adentrar ao estreito de Gerlache (Zhou et al. 2002, Ruiz Barlett et al. 2018). Já a circulação superficial no EG, possui uma vazão em direção ao norte do estreito, a qual se une ao fluxo norte da Corrente de Bransfield (Zhou et al. 2002). Em níveis de sub-superfície e mais profundos, este estreito também é influenciado pelas massas de água que fluem do MBL, com entradas irregulares da ACP (García et al. 2002).

Tokarczyk (1987) classificou essas águas que advectam aos estreitos em duas massas distintas: a porção influenciada pelas características do MBL foi denominada Água de Transição com influência de Bellingshausen (ATB), enquanto a porção influenciada pelas características do Mar de Weddell foi chamada de Água de Transição com influência do Mar de Weddell (ATW). Essas massas de água são separadas na superfície pela Frente da Península (FP), que pode ser identificada pela isoterma de 1 °C (Sangrà et al. 2011) (Fig. 1).

As águas do NPA são essenciais para a produtividade biológica do Oceano Austral, sustentando uma densa rede trófica com florações fitoplanctônicas (Costa et al. 2020), altas densidades de zooplâncton (Kasyan et al. 2022) e a presença de grandes predadores, como baleias (Secchi et al. 2020).

4.2. Amostragens Oceanográficas

Todas as amostras utilizadas neste trabalho foram coletadas a bordo do Navio Polar Almirante Maximiano, com o apoio do Programa Antártico Brasileiro (PROANTAR), durante três cruzeiros diferentes no NPA. Esses cruzeiros fizeram parte do projeto INTERBIOTA ("Interações Biológicas em Ecossistemas Marinhos ao redor da Península Antártica sob diferentes impactos das mudanças climáticas"), como parte dos projetos do GOAL (Grupo de Oceanografia de Altas Latitudes). Esses cruzeiros ocorreram no final do verão de 2017 (fevereiro - março), 2018 (fevereiro) e início do verão de 2019 (janeiro - fevereiro), coletando dados físicos, químicos e biológicos. Para este trabalho, foram utilizadas 141 amostras coletadas durante esses cruzeiros, onde as amostragens de zooplâncton foram realizadas em 29 estações oceanográficas. No entanto, devido a desafios logísticos, condições adversas do mar e outras atividades de cruzeiro, nem todas as estações foram amostradas nos mesmos pontos ao longo dos três anos (Tabela 1).

Tabela 1: Resumo das estações de amostragem de zooplâncton nos três anos e locais. O traço (-) indica que a estação não foi amostrada em determinado ano.

Ano/Locais	Estreito de Gerlache					Mar de Bellingshausen		Estreito de Bransfield								
2017	-	-	#03	#04	-	#06	-	#08	-	#10	#11	#12	-	-	-	-
2018	#01	#02	#03	-	#05	-	-	#08	#09	#10	#11	#12	#13	-	#15	#16
2019	-	-	#03	-	#05	#06	#07	#08	-	-	#11	#12	-	#14	-	-

Das estações oceanográficas, a estação denominada B42 (62°17'09''S; 57°02'53''W) em 2017, foi amostrada a cada quatro horas para avaliação da variabilidade meso e macrozooplanctônica durante as migrações nictemerais. Esta estação foi escolhida por ser uma região dinâmica, próxima da FP (Fig. 2; Ferreira et al. 2020).

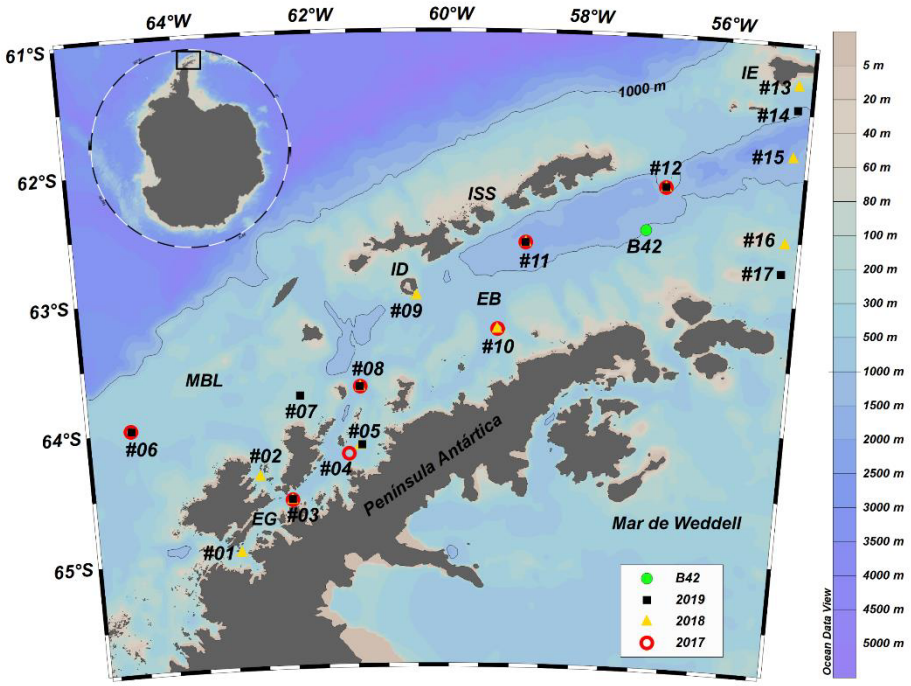


Figura 2: Mapa da área de estudo mostrando as estações oceanográficas onde foram realizadas coletas de zooplâncton ao longo de três anos (2017, 2018, 2019), incluindo o ponto de amostragem em 20 horas.

Dados hidrográficos (temperatura e salinidade) e amostras de água para avaliar a composição do fitoplâncton e a dinâmica da coluna de água foram coletados com um CTD Sea-Bird (do inglês condutividade-temperatura-profundidade) + Carrousel 911+system® equipado com 24 garrafas Niskin de cinco litros em todas as estações realizadas pelo GOAL (Fig. 2; mesmas estações utilizadas por Avelina et al. 2024).

Mapas com os dados superficiais (~5m) de temperatura e salinidade foram elaborados utilizando o programa Ocean Data View– ODV (Schlitzer, R., Ocean Data View, http://odv.awi.de, 2024), com a interpolação DIVA (Data-Interpolating Variational Analysis), a qual permite a interpolação espacial dos dados de forma otimizada, levando em consideração incertezas nas observações (Barth et al. 2014).

Para examinar a estrutura física da coluna de água, a profundidade da camada de mistura (MLD; m) foi calculada como a profundidade na qual a densidade potencial da água do mar desvia de seu valor de profundidade de 10 m, por um limite de 0,03 $kg.m^{-3}$ (de Boyer Montégut et al. 2004). Além disso, também se utilizou a densidade potencial

da água do mar para calcular a estabilidade da coluna de água ($x10^{-6}.m^{-1}$), como uma função da frequência de flutuabilidade pela gravidade local, conforme descrito por Costa et al. (2020).

A concentração de clorofila-*a* e pigmentos acessórios específicos de classe foram medidos por Cromatografia Líquida de Alta Eficiência (do inglês – *High-Performance Liquid Chromatography* - HPLC), conforme descrito em Costa et al. (2020). A contribuição absoluta ($mg.m^{-3}$) e relativa (%) dos grupos quimiotaxonômicos do fitoplâncton foi estimada pelo software CHEMTAX v1.95 (Mackey et al. 1996). Sete grupos de algas foram escolhidos para análise CHEMTAX, com base nas proporções iniciais de pigmento derivadas para o NPA (Mendes et al. 2018, Costa et al. 2022). Os grupos incluem diatomáceas Tipo A, diatomáceas Tipo B, dinoflagelados Tipo A, dinoflagelados Tipo B, criptófitas, haptófitas Tipo 8 (*Phaeocystis antarctica* Karsten, 1905) e flagelados verdes. As diatomáceas (soma das diatomáceas Tipo A e diatomáceas Tipo B) e os dinoflagelados (soma dos dinoflagelados Tipo A e dinoflagelados Tipo B) foram agrupados como o mesmo grupo quimiotaxonômico. Os resultados do CHEMTAX foram otimizados seguindo Wright et al. (2009). O procedimento de controle de qualidade foi realizado por análise microscópica. Todos os dados utilizados constam no banco de dados do GOAL, sendo os físicos fornecidos pelo Laboratório de Estudos dos Oceanos e Clima (LEOC) e os dados de fitoplâncton pelo Laboratório de Fitoplâncton e Microorganismos Marinhos, ambos localizados na Universidade Federal do Rio Grande (FURG).

As comunidades de meso e macrozooplâncton foram amostradas em 7, 12 e 9 estações em 2017, 2018 e 2019, respectivamente. Essas amostras foram coletadas por uma MultiNet® (Tipo Midi - Hydrobios), equipada com redes de 300 μm, fluxômetros, CT-Set, fluorímetro e turbidímetro. Conforme a batimetria local, arrastos verticais foram conduzidos em cinco estratos (500-400 m; 400-300 m; 300-200 m; 200-100 m e 100-0 m). Esses mesmos estratos foram utilizados para a avaliação da variabilidade meso e macrozooplanctônica durante as migrações verticais (ciclo de 20 horas). O volume filtrado foi obtido usando fluxômetros acoplados à Multinet. As amostras foram fixadas com uma solução de formalina a 4% neutralizada com bórax (Steedman 1976) logo após as coletas. Em laboratório as amostras foram analisadas em sua totalidade, sendo feita a

identificação de todos os organismos presentes nas amostras ao menor nível taxonômico possível. Os resultados foram expressos em ind.1000 m^{-3}.

4.3. Experimento

Durante a OA 35 (2017) foi realizado um experimento de produção de pelotas fecais de salpas (*Salpa thompsoni*) e eufausiáceos (*Euphausia superba*). A coleta dos organismos utilizados no experimento foi realizada em 24 de fevereiro de 2017, também na estação B42 com uma rede tipo Bongo de 300 μm. Após a coleta, o material coletado foi transferido para o laboratório de bordo, onde os organismos foram imediatamente confinados em unidades experimentais (UE). A UE consistiu em seis frascos de vidro, sendo três contendo krill e três contendo salpas (um indivíduo por frasco de vidro), com 300 ml de água do mar não filtrada. Os organismos foram mantidos por 24h em temperatura ambiente, sem alimentação e/ou oxigenação (ou seja, apenas as células alimentares/fitoplâncton que já estavam disponíveis na água do mar e sem aeração).

Após esse período, os organismos foram retirados dos frascos e fixados em uma solução de formalina a 4% (Steedman 1976). As pelotas fecais presentes no fundo dos frascos de vidro, juntamente com a água do mar, foram cuidadosamente removidas e filtrada com filtros GF/F Whatman®. Em seguida, os filtros foram congelados em nitrogênio líquido para posterior análise por HPLC, conforme o método de Mendes et al. (2007). Essa análise permitiu a separação, quantificação e identificação dos pigmentos fitoplanctônicos presentes nas pelotas fecais de krill e salpa, visando determinar a composição da comunidade fitoplanctônica predada pelos mesmos.

A análise de pigmentos foi concentrada em diatomáceas e criptófitas, pois ambos os grupos possuem pigmentos biomarcadores específicos (Chl-c1 e aloxantina, respectivamente) e representam os principais grupos fitoplanctônicos ao longo do NPA (Mendes et al. 2018, Mendes et al. 2023). Para calcular o acúmulo de pigmentos biomarcadores nas pelotas fecais de krill e salpas provenientes da ingestão de células fitoplanctônicas, a água do mar coletada antes do experimento também foi filtrada (amostragem de linha de base) e processada em HPLC. Os valores obtidos nessa amostragem indicaram as concentrações esperadas na água do mar de fucoxantina, clorofila-c1 (Chl-c1) e aloxantina. Assim, a diferença entre a concentração de pigmentos

biomarcadores antes (amostragem de linha de base) e depois do experimento reflete se o krill ou as salpas consumiram determinado grupo de fitoplâncton (diatomáceas ou criptófitas). Essa diferença foi calculada subtraindo a concentração inicial (amostragem de linha de base) da concentração final (com as pelotas fecais). Valores positivos indicaram acúmulo de pigmentos biomarcadores, sugerindo consumo de diatomáceas ou criptófitas. Por outro lado, valores negativos indicaram que não houve acúmulo de pigmentos biomarcadores, uma vez que as concentrações de pigmentos na água do mar antes do experimento eram maiores do que após o experimento, evidenciando que diatomáceas ou criptófitas não foram consumidas.

Além disso, alguns produtos de degradação de clorofila-*a*, como feopigmentos, têm sido observados há muito tempo em pelotas fecais de organismos zooplanctônicos (Coelho et al. 2011). Sendo assim, clorofilida-*a* (Chlide-*a*), feofitina-*a* (Phytin-*a*) e feoforbídeo-*a* (Phide-*a*) foram analisados também por HPLC e a soma de Phytin-*a* e Phide-*a* foi usada como um indicador da pressão de pastejo, e Chlide-*a* como a senescência das células fitoplanctônicas. Esses dois índices foram divididos pelo total de produtos de degradação, mais a clorofila-*a* (soma de Chl-*a*, Phytin-*a*, Phide-*a* e Chlide-*a*) e aqui foram representados como uma porcentagem (Costa et al. 2021).

4.4. Análises estatísticas dos dados

Valores médios e índices de variação de temperatura, salinidade e clorofila-*a* foram calculados para cada estrato de 100 metros de profundidade amostrado. Os índices de variação foram calculados tomando a diferença entre os valores de temperatura, salinidade e clorofila-*a* encontrados na superfície (5 m) e os valores encontrados na profundidade máxima que a Multinet atingiu. Esses índices foram calculados para determinar o quanto esses parâmetros variaram dentro de cada estrato de 100 metros e posteriormente utilizados nas análises estatísticas. Além disso, foram calculados valores médios dos dados de turbidez e densidade da água, coletados pela Multinet, para cada estrato de profundidade e incluídos nas análises estatísticas para avaliar a influência dos parâmetros ambientais na migração nictemeral dos organismos.

Análises de escalonamento multidimensional não métrico (nMDS) com similaridade de Bray-Curtis foram geradas para resumir os padrões da estrutura das

comunidades de meso e macrozooplâncton ao longo dos três anos e dos estratos amostrados. A função "*envfit*", do pacote "vegan" (Oksanen et al. 2022), foi aplicada à ordenação nMDS para explorar a relação entre a comunidade zooplanctônica e as variáveis ambientais utilizadas na análise de migração nictemeral. Um teste de permutação foi realizado para obter valores de significância associados à influência de cada variável ambiental na distribuição das espécies, e os vetores resultantes foram sobrepostos aos gráficos nMDS.

Para todas as análises estatísticas da comunidade de meso e macrozooplâncton, utilizou-se a transformação de Hellinger na abundância (ind.1000m^{-3}). A transformação de Hellinger, balaceia a heterogeneidade dos dados de abundância, equilibrando a influência de espécies raras e dominantes (Legendre e Legendre 2012). As espécies que apareceram em menos de duas amostras ou cuja abundância relativa foi menor que 0,6% foram excluídas da análise para evitar que taxa raros não dominassem a análise.

Testes PERMANOVA foram realizados com base em 999 permutações para determinar se haviam diferenças significativas na composição da comunidade e abundância de meso e macrozooplâncton encontradas entre anos, locais e em diferentes estratos amostrados. As amostras foram classificadas de acordo com a localidade que foram amostradas: Mar de Bellingshausen (MBL), Estreito de Bransfield (EB) e Estreito de Gerlache (EG). Além disso, o teste PERMANOVA foi realizado para avaliar diferenças na composição e abundância das comunidades planctônicas entre os períodos (dia e crepúsculo). Para cada amostragem, os períodos de "dia" e "crepúsculo" foram definidos com base nos horários de amostragem recuperados do site da NOAA (National Oceanic and Atmospheric Administration - https://gml.noaa.gov/grad/solcalc/sunrise.html). Análises de similaridade (SIMPER) (Clarke & Warwick 2001) foram realizadas para determinar a contribuição dos taxa nas diferenças entre os anos analisados. Os índices de riqueza e diversidade de espécies dos diferentes estratos para cada estação foram calculados por meio de números de Hill, com o exponencial do índice de Shannon-Weaver (Exp H′) e o inverso do índice de Simpson (1/D) (Hill 1973).

Para explorar as relações entre as variações interanuais da comunidade de meso e macrozooplâncton com variáveis ambientais, foi elaborada uma Análise de

Correspondência Canônica (ACC; Ter Braak & Prentice 1988) também utilizando o pacote "*vegan"* (Oksanen et al. 2022). Para a variabilidade interanual, as variáveis ambientais compreenderam a temperatura, salinidade e clorofila-*a* média para cada intervalo de profundidade de 100 m; os índices de variação para temperatura, salinidade e clorofila-*a*; estabilidade da coluna de água (10^{-6} m^{-1}); a profundidade da camada de mistura (PCM); e também, os valores máximos e mínimos de temperatura, salinidade e clorofila-*a*. Um teste ANOVA para a ACC foi conduzido para identificar as variáveis que foram mais significativas na análise (valor de $p < 0,05$). Posteriormente, a ACC foi recalculada usando apenas as variáveis significativas. Além disso, outra análise ACC foi feita apenas com os dados do primeiro estrato da coluna d'água (0–100 m), para avaliar a relação das comunidades meso e macrozooplâncton com os diferentes grupos fitoplanctônicos.

Por fim, uma Análise de Espécies Indicadoras com o pacote "indicspecies" (De Cáceres et al. 2010) também foi conduzida para identificar espécies fortemente associadas a estratos específicos. O nível de confiança de 95% (valor de $p \leq 0,05$) foi usado para identificar as espécies indicadoras (Dufrêne e Legendre 1997). Todos os índices de diversidade e análises estatísticas foram feitos no R v.4.2.0 (R Core R Development Core Team 2022). As análises estatísticas foram realizadas utilizando o pacote R "vegan" (Oksanen et al. 2022) e, todos os gráficos foram gerados utilizando o pacote "ggplot2" (Wickham 2016).

5. Principais Resultados e Discussões

5.1. Variabilidade Hidrográfica

A variabilidade hidrográfica no NPA entre 2017 e 2019 demonstrou padrões distintos de temperatura e salinidade, especialmente na superfície (Fig. 3), refletindo a influência de massas de água adjacentes (Huneke et al. 2016) e destacando mudanças interanuais na profundidade da camada de mistura (PCM) e na estabilidade da coluna d'água (Fig. 4). O ano de 2017, foi caracterizado por águas superficiais mais quentes e menos salinas (Fig. 3), com um máximo de temperatura de 3,2 °C na superfície do primeiro estrato (0-100 m) no Mar de Bellingshausen (#06) e 2,5 °C na estação #12 do EB. Em contraste, as menores temperaturas foram registradas em maiores profundidades, especificamente no estrato de 200 – 300 m (-1,2 °C; Fig. 4). No geral, as condições de temperaturas mais elevadas na superfície favoreceram uma PCM mais rasa (13-36 m), maior estratificação e estabilidade da coluna d'água no ano de 2017 (Fig. 4).

De fato, temperaturas mais altas na superfície do mar e na atmosfera foram detectadas ao redor da Antártica no início de 2017 (Hartfield et al. 2018), tendência confirmada por medições da Estação Palmer, que indicaram valores acima da média climatológica. Além disso, as elevadas temperaturas na região em 2017 estiveram associadas a uma fase negativa do Modo Anular Sul (MAS) no ano anterior (2016), que modificou a direção dos ventos superficiais e intensificou a advecção de águas mais quentes para o NPA no ano de 2017 (Fig. 3 e 4) (Parra et al. 2020, Leonor & Muxagata 2025).

Nos anos de 2018 e 2019, as temperaturas superficiais médias foram menores em comparação a 2017 (Fig. 3), com média de 1,3°C em 2018, e de 1,2° C em 2019. Nesse período, as camadas de mistura foram ~2x mais profundas, chegando a 76 m em 2018 e 70 m em 2019, sendo observado também uma menor estabilidade da coluna d'água, principalmente no leste do EB, onde evidenciou-se uma coluna d'água praticamente homogênea. Ainda, de modo geral, as menores salinidades nos três anos (~33.4) foram registradas na superfície do EG (Fig. 3 e 4), provavelmente associadas ao derretimento das geleiras continentais e do gelo marinho (Cook et al. 2016), enquanto valores mais elevados (~34.6) ocorreram em maiores profundidades (Fig. 4).

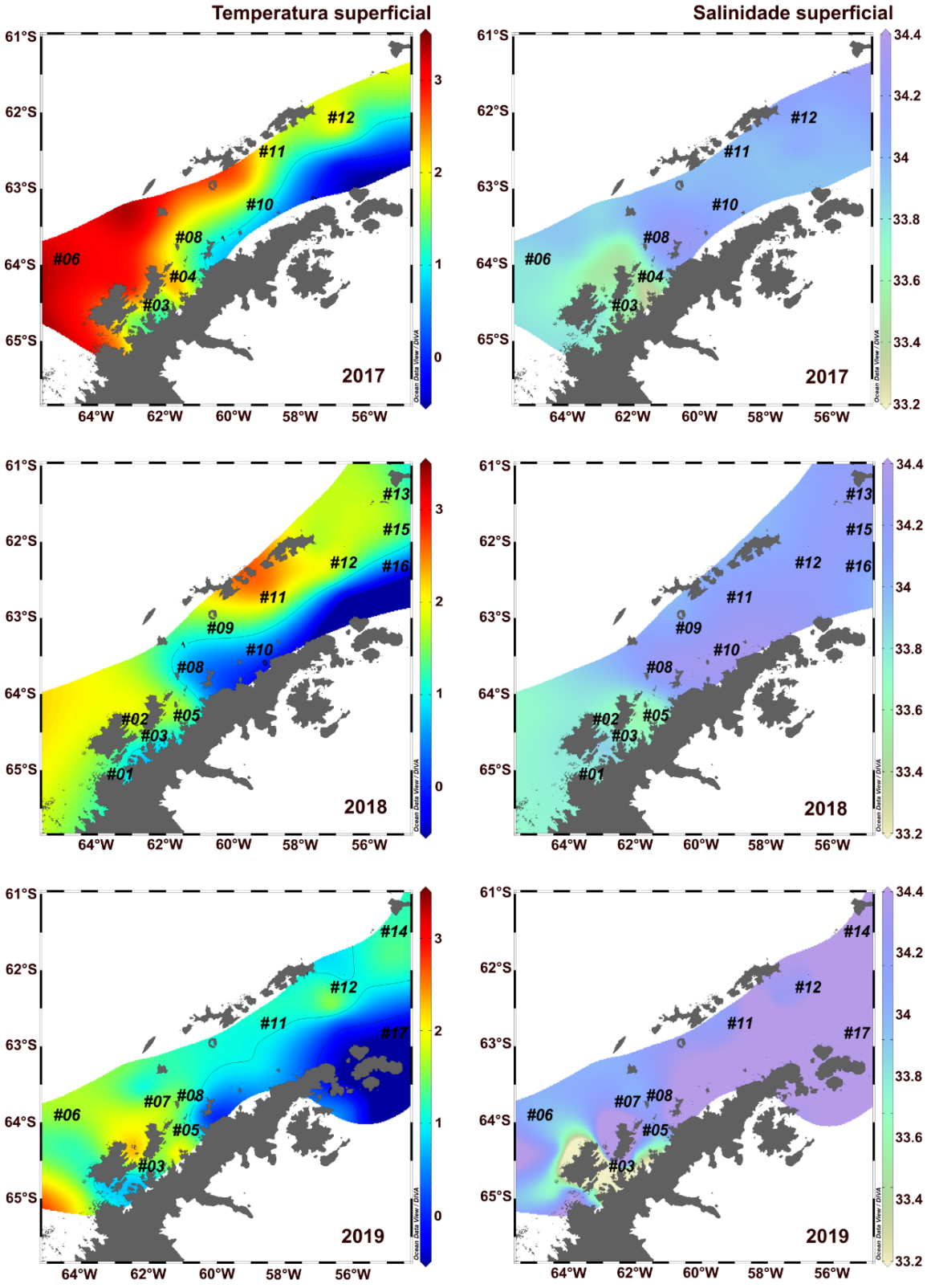


Figura 3: Mapas mostrando a distribuição superficial da temperatura e salinidade do NPA durante os três anos amostrados.

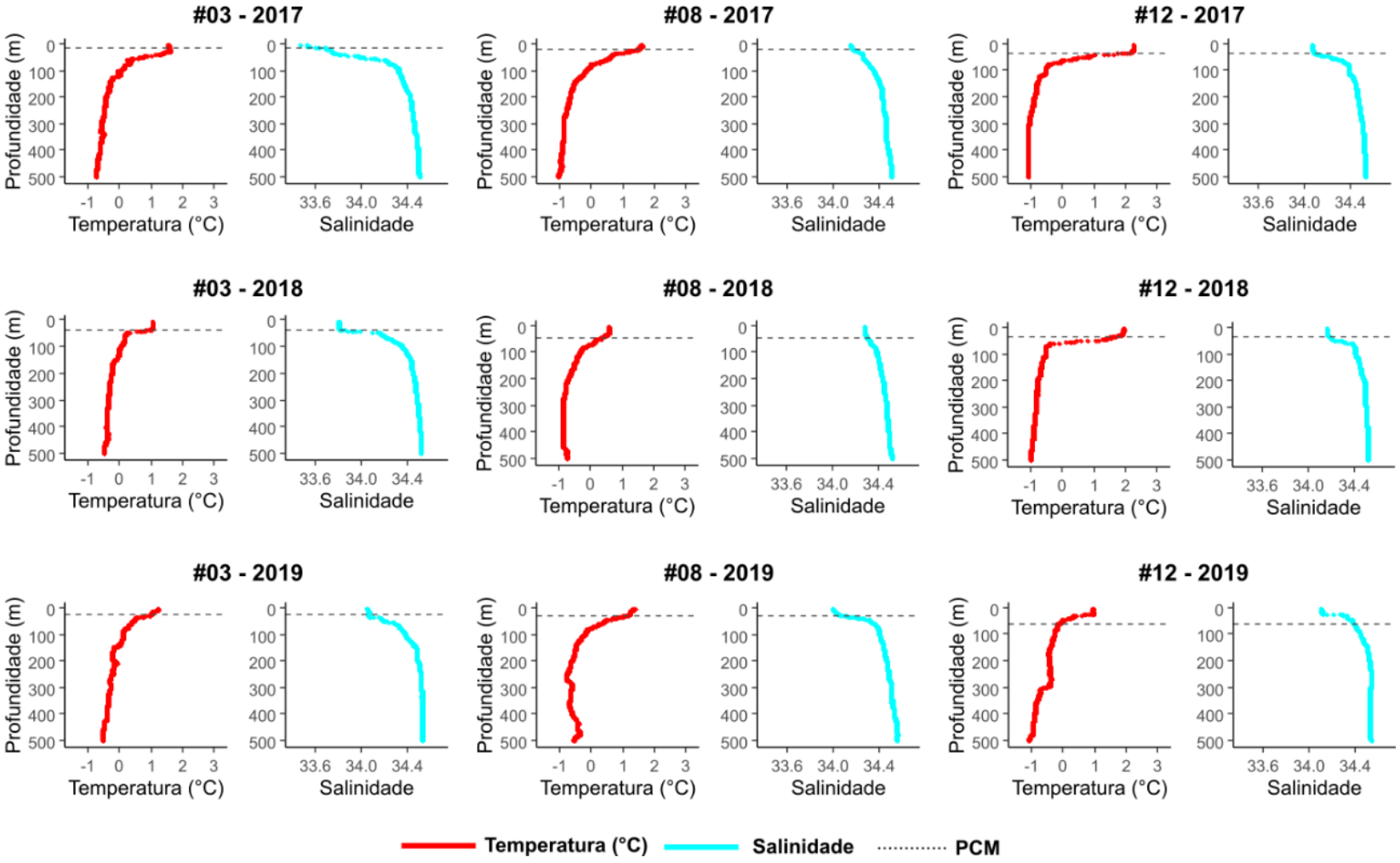


Figura 4: Perfis de temperatura (em vermelho) e salinidade (em azul claro) de três estações oceanográficas representativas da área de estudo, amostradas no mesmo ponto nos três anos. A linha tracejada indica a profundidade da camada de mistura (PCM).

Apesar dessas diferenças pronunciadas, a intrusão de massas de água adjacentes criou um gradiente hidrográfico nos três anos avaliados, já observado por outros autores (Sangrà et al. 2011, Huneke et al. 2016, Leonor & Muxagata 2025). Águas mais quentes e menos salinas foram registradas na superfície do EG, MBL e no oeste do EB, enquanto águas mais frias e salinas predominaram no leste e sudeste do EB, influenciadas pela Água Densa de Plataforma (ADP) (Fig. 5), oriunda do Mar de Weddell (Sangrà et al. 2011, Huneke et al. 2016, Ruiz-Barlett et al. 2018, Frey et al. 2022). Além disso, a Água Superficial Antártica (ASAA) dominou os primeiros 150 m ao longo dos três anos (Fig.5), enquanto a Água Circumpolar Profunda Modificada (ACPM) esteve em profundidades intermediárias mais rasas em 2017 (140-270 m) e progressivamente mais profundas em 2018 e 2019 (170-360 m e 225-470 m, respectivamente). A interação entre essas massas de água, associada à influência da Corrente Circumpolar Antártica (CCA), provavelmente intensificou a estratificação e reforçou o gradiente horizontal nas propriedades superficiais, como já observado por outros autores (Sangrà et al. 2011, Huneke et al. 2016, Ruiz-Barlett et al. 2018).

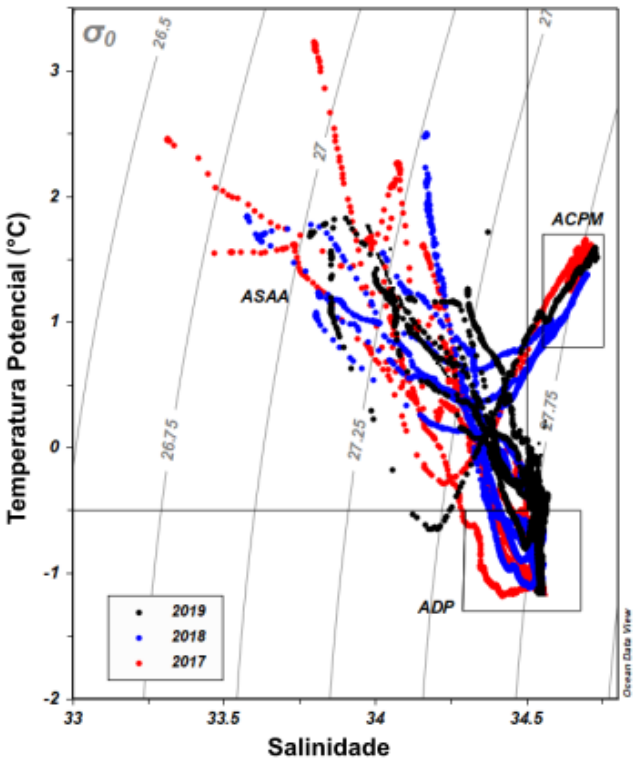


Figura 5: Diagrama TS das estações amostradas até 500 m, com dados de temperatura e salinidade coletados ao longo dos três anos de estudo (2017, 2018 e 2019).

A convecção de águas mais quentes do Mar de Bellingshausen contribui para águas ricas em nutrientes nas camadas superficiais, provenientes de áreas costeiras produtivas, particularmente o Estreito de Gerlache (Zhou et al. 2002, Ferreira et al. 2020, Costa et al. 2021).

5.2. Composição do fitoplâncton

A composição da comunidade fitoplanctônica exibiu uma variabilidade interanual, refletindo as mudanças nas condições oceanográficas. A distribuição da comunidade de plâncton é moldada por essas massas de água, que desempenham um papel fundamental em diferentes camadas oceânicas e regiões do NPA (Mendes et al. 2018a, Costa et al. 2020, Criales-Hernández et al. 2022). Em 2017, as temperaturas elevadas e as baixas salinidades superficiais favoreceram células menores de fitoplâncton como dinoflagelados e criptófitas, que predominaram no NPA, especialmente no EB, onde as diatomáceas eram escassas (Fig. 6). Em 2018, as diatomáceas passaram a predominar em toda a região, provavelmente devido às condições mais amenas na temperatura e ao leve aprofundamento da camada de mistura (Mendes et al. 2023). Já em 2019, padrões distintos entre os locais foram observados, com as criptófitas dominando a comunidade fitoplanctônica no EG e no MBL e as diatomáceas dominando no EB. As menores salinidades observadas no EG, influenciadas pelo derretimento de geleiras, criou uma estratificação favorável às criptófitas (Mendes et al. 2018, 2023, Costa et al. 2021), enquanto o aprofundamento da PCM no EB favoreceu as diatomáceas (Mendes et al. 2023). Essas variações podem estar relacionadas à competição ou segregação entre os grupos, um fenômeno ainda não totalmente compreendido.

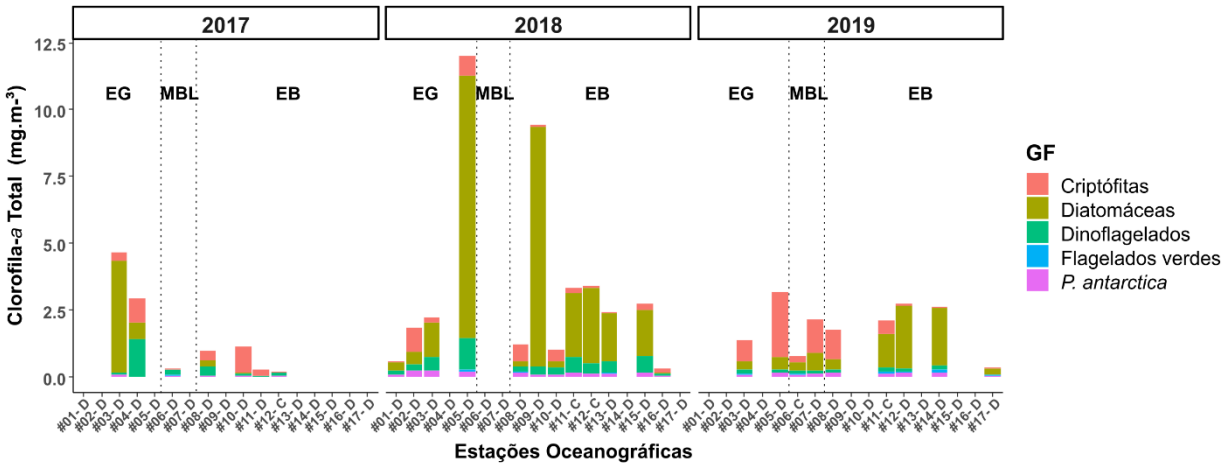


Figura 6: Distribuição da concentração de clorofila-*a* (mg.m^{-3}) e da (%) dos grupos fitoplanctônicos na superfície em todas estações oceanográficas amostradas. As estações marcadas com "D" foram amostradas durante o dia, enquanto aquelas marcadas com "C" foram amostradas durante o crepúsculo. EG = Estreito de Gerlache, MBL= Mar de Bellingshausen, EB = Estreito de Bransfield.

Apesar das variações interanuais nos grupos fitoplanctônicos, as altas concentrações de clorofila-*a* observadas estiveram fortemente associadas à presença de diatomáceas (Fig. 6). No NPA, um gradiente de concentração de clorofila-*a* é comumente identificado, com maiores valores no oeste e menores no leste (Aracena et al. 2018). Este mesmo padrão de gradiente foi confirmado neste estudo, com as maiores concentrações de clorofila-*a* registradas em 2018 no EG (est. #05, 12,02 mg.m^{-3}) e perto da Ilha Deception (est. #09, 9,44 mg.m^{-3}), no oeste do EB, associadas à predominância de diatomáceas (Fig. 6). Em contraste, os menores valores (em 2017) ocorreram no leste do EB (est. #12, 0,19 mg.m^{-3}), onde a comunidade fitoplanctônica era composta principalmente por células menores.

5.3. Composição, abundância e variabilidade interanual da comunidade de meso e macrozooplâncton

Neste estudo, 41.490 indivíduos foram contados e identificados em 162 taxa distintos. Destes, 100 foram identificados ao nível de espécie, 43 ao nível de gênero e 19 em níveis taxonômicos mais altos (Tabela 1). Os grupos mais representativos foram Copepoda (Calanoida e Cyclopoida), Salpidae, Ostracoda, Chaetognatha, Cnidaria, Polychaeta, Euphausiidae e Amphipoda, com diferentes composições entre os anos (Fig.

7). Os copépodes da ordem Calanoida tiveram o maior número de espécies identificadas, com um total de 47 espécies, seguidos por Amphipoda com 11 espécies, Polychaeta com 10, Cyclopoida com 9 e Cnidaria com 7 espécies (Tabela 1).

Tabela 1: Lista de todos os taxa identificados nas 141 amostras analisadas (1 de 2). N.I. = Não identificado e Cop = copepoditos.

Taxa	
Siphonophorae	**Copepoda Calanoida**
Dimophyes arctica (Chun, 1897)	*Calanoides acutus* (Giesbrecht, 1902)
Diphyes antarctica Moser, 1925	*Calanoides brevicornis* (Lubbock, 1856)
Diphyes dispar Chamisso & Eysenhardt, 1821	*Calanoides carinatus* (Krøyer, 1849)
Lensia spp.	*Calanus simillimus* Giesbrecht, 1902
N.I.	*Calanus propinquus* Brady, 1883
Hydrozoa	*Calanus* spp.
Leuckartiara brownei Larson & Harbison, 1990	*Nannocalanus minor* (Claus, 1863)
Solmundella bitentaculata (Quoy & Gaimard, 1833)	*Neocalanus tonsus* (Brady, 1883)
Corymorpha sp.	*Neocalanus gracilis* (Dana, 1849-1852)
Cosmetirella davisi (Browne, 1902)	Cop *Neoclanus* spp.
Arctapodema spp.	Cop *Calanoides* spp.
Rhopalonematidae	Cop *Calanus* spp.
Leptothecata	Calanidae N.I.
Scyphozoa	*Calocalanus styliremis* Giesbrecht, 1888
Ephyra *Desmonema glaciale* Larson, 1986	Calocalanus sp.
Polychaeta	*Paracalanus parvus parvus* (Claus, 1863)
Larva N.I.	*Paracalanus* sp.
Vanadis antarctica (McIntosh, 1885)	Paracalanidae N.I.
Vanadis longissima (Levinsen, 1885)	*Rhincalanus gigas* Brady, 1883
Vanadis spp.	*Rhincalanus nasutus* Giesbrecht, 1888
Maupasia coeca Viguier, 1886	Cop *Subeucalanus* spp.
Pelagobia longicirrata Greeff, 1879	Cop *Eucalanus* spp.
Tomopteris planktonis Apstein, 1900	*Clausocalanus ingens* Frost & Fleminger, 1968
Tomopteris carpenteri Quatrefages, 1866	*Clausocalanus* spp.
Tomopteris lingulata Rosa, 1908	*Ctenocalanus citer* Heron & Bowman, 1971
Tomopteris spp.	*Ctenocalanus* sp.
Typhloscolex mulleri Busch, 1851	*Drepanopus* spp.
Travisiopsis coniceps (Chamberlin, 1919)	*Microcalanus pygmaeus* (Sars G.O., 1900)
Traviopsis levinseni Southern, 1910	Clausocalanidae N.I.
Travisiopsis spp.	*Aetideus arcuatus* (Vervoort, 1949)
Pteropoda	*Aetideus pseudarmatus* Bradford, 1971
Limacina antarctica S. P. Woodward, 1854	*Aetideopsis antarctica* (Wolfenden, 1908)
Limacina retroversa australis (Eydoux & Souleyet, 1840)	*Chiridius gracilis* Farran, 1908
Clione limacina (Phipps, 1774)	*Chiridius polaris* Wolfenden, 1911
Spongiobranchaea australis d'Orbigny, 1836	*Chiridius* sp.
Ostracoda N.I.	*Euchirella rostromagna* Wolfenden, 1905

Tabela 1: Lista de todos os taxa identificados nas 141 amostras analisadas (2 de 2).

Taxa	
Gaetanus tenuispinus (Sars G.O., 1900)	**Amphipoda**
Cop *Gaetanus* sp.	Estágio Manca
Cop *Aetideopsis* spp.	*Eusirus* sp.
Paraeuchaeta antarctica (Giesbrecht, 1902)	*Eusirus microps* Walker, 1906
Paraeuchaeta austrina (Giesbrecht, 1902)	*Eusirus properdentatus* Andres, 1979
Paraeuchaeta biloba Farran, 1929	*Eusirus perdentatus* Chevreux, 1912
Paraeuchaeta exigua (Wolfenden, 1911)	*Orchamenella* spp.
Paraeuchaeta pseudotonsa (Fontaine, 1967)	*Scina* spp.
Cop *Paraeuchaeta* spp.	*Cyllopus lucasi* Spence Bate, 1862
Undinella simplex (Wolfenden, 1906)	*Vibilia armata* Bovallius, 1887
Amallothrix sp.	*Vibilia antarctica* Stebbing, 1888
Pseudoamallothrix hadrosoma (Park, 1980)	*Vibilia* spp.
Pseudoamallothrix cetonelis (Park, 1980)	*Hyperiella* spp.
Pseudoamallothrix spp.	*Hyperiella antarctica* Bovallius, 1887
Scaphocalanus curtus (Farran, 1926)	*Hyperoche medusarum* (Kröyer, 1838)
Scaphocalanus elongatus Scott A., 1909	*Hyperoche* sp.
Scaphocalanus spp.	*Themisto gaudichaudi* Guérin, 1825
Scolecithricella minor minor (Brady, 1883)	*Primno macropa* Guérin-Méneville, 1836
Scolecithricella vittata (Giesbrecht, 1893)	*Phronimella elongata* (Claus, 1862)
Scolecithricella spp.	**Euphausiidae**
Scolecithrix danae (Lubbock, 1856)	Náuplio
Scottocalanus securifrons (Scott T., 1894)	Calyptopis
Cop Scolecitrichidae N.I.	Furcília
Haloptilus ocellatus Wolfenden, 1905	*Euphausia superba* Dana, 1850
Haloptilus oxycephalus (Giesbrecht, 1889)	*Euphausia crystallorophias* Holt & Tattersall, 1906
Haloptilus longicornis (Claus, 1863)	*Thysanoessa macrura* G.O. Sars, 1883
Cop *Eugaliptilus* spp.	**Cirripedia**
Heterorhabdus austrinus Giesbrecht, 1902	Náuplio
Heterorhabdus lobatus Bradford, 1971	Cipris
Heterorhabdus spinifrons (Claus, 1863)	**Echinodermata**
Heterorhabdus spp.	Brachiolaria
Lucicutia ovalis (Giesbrecht, 1889)	**Chaetognatha**
Metridia gerlachei Giesbrecht, 1902	N.I.
Metridia longa (Lubbock, 1854)	*Eukrohnia hamata* (Möbius, 1875)
Metridia lucens Boeck, 1865	*Eukrohnia* spp.
Cop *Metridia* spp.	*Pseudosagitta maxima* (Conant, 1896)
Cop. *Centropages* sp.	*Pseudosagitta gazellae* (Ritter-Záhony, 1909)
Candacia maxima Vervoort, 1957	*Pseudosagitta* spp.
Paralabidocera antarctica (Thompson I.C., 1898)	*Solidosagitta marri* (David, 1956)
Labidocera sp.	**Appendicularia**
Copepoda Cyclopoida	*Oikopleura* spp.
Oithona frigida Giesbrecht, 1902	*Fritilaria* spp.
Oithona similis Claus, 1866	N.I.
Oithona spp.	**Doliolida**
Triconia antarctica (Heron, 1977)	*Dolioletta* spp.
Oncaea mediterranea (Claus, 1863)	**Salpidae**
Oncaea venusta Philippi, 1843	*Salpa maxima* Forskål, 1775
Oncaea spp.	*Salpa thompsoni* Foxton, 1961
Agetus flaccus (Giesbrecht, 1891)	*Ihlea racovitzai* (Van Beneden & De Selys Longchamp, 1913)
Corycaeus speciosus Dana, 1849	*Ihlea magallanica* (Apstein, 1894)
Onychocorycaeus pacificus (Dahl F., 1894)	**Larva de Peixe N.I.**
Farranula gracilis (Dana, 1849-1852)	
Copepoda N.I.	

Os copépodes, especialmente os da ordem Calanoida, foram os taxa mais frequentes, abundantes e diversos no NPA ao longo dos três anos, representando 58% da abundância relativa em 2017, 68% em 2018 e 62% em 2019 (Fig. 7). Esse grupo é comumente reconhecido como um dos principais componentes da região (Plum et al. 2021, Criales-Hernández et al. 2022, Kasyan 2023). De 2017 a 2019, houve um aumento significativo nas abundâncias relativas dos copépodes, com os da ordem Cyclopoida dobrando suas contribuições no meso e macrozooplâncton no NAP. Em contraste, as salpas, que em 2017 representaram 34% da abundância no EB (dominando em algumas estações, como #11 e #12), foram pouco expressivas no EG (2%) e ausentes no MBL, não sendo sequer identificadas nos anos seguintes (2018 e 2019).

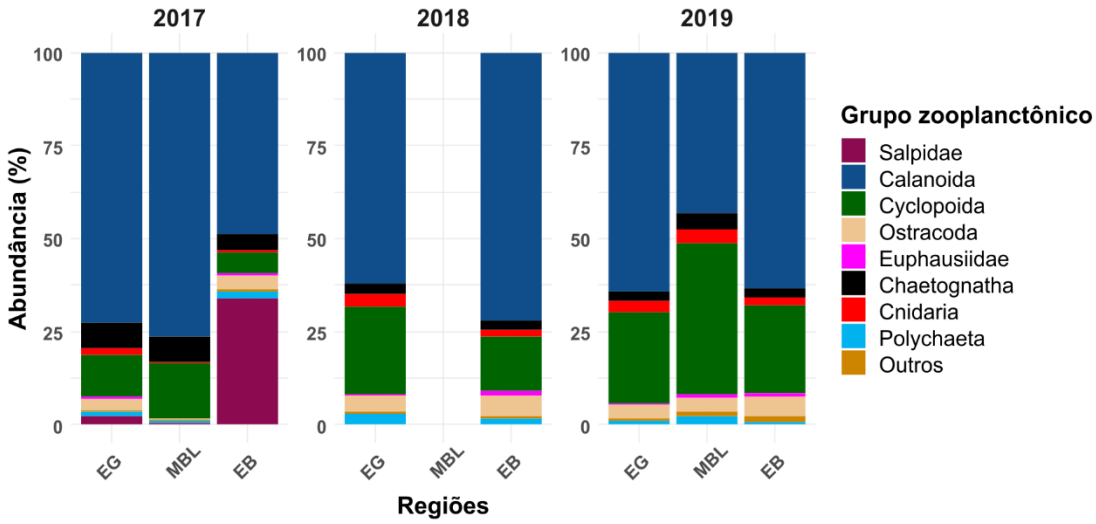


Figura 7: Variação temporal e contribuição (%) dos principais grupos taxonômicos por ano e região. EG = Estreito de Gerlache, MBL = Mar de Bellingshausen, EB = Estreito de Bransfield. Em 2018, os dados não foram amostrados em MBL.

O teste PERMANOVA (p-valor < 0,001) confirmou diferenças significativas na composição e abundância das comunidades entre as regiões (EG, MBL e EB) e entre os anos. Após 2017, a dominância foi mantida pelos calanoides, seguidos por copépodes Cyclopoida e ostrácodes em todas as localidades. Chaetognatha foi um grupo que se destacou em 2017, sendo o quarto mais abundante, representando 7% da abundância em EG e MBL, e 4% no EB, mas com um declínio nos anos posteriores. *Eukrohnia hamata* foi a espécie mais abundante desse grupo, assim como observado em outras regiões do

oceano Austral (Øresland 1990, Mackas et al. 2012, Venkataramana et al. 2022). No NPA, essa espécie também é amplamente registrada, com sua distribuição acompanhando a de copépodes, sua principal presa (Øresland 1990, Giesecke & González 2012). Os poliquetas, embora presentes, tiveram abundâncias relativamente baixas em comparação com outros grupos do zooplâncton, sendo representados principalmente por larvas. Sua ocorrência foi mais expressiva no EB em 2017, no EG em 2018 e no MBL em 2019. Altas abundâncias de larvas de poliquetas foram relatadas em regiões como a Baía Marguerita, na Península Antártica Ocidental (Ameneiro et al. 2012), e na Baía Prydz (Venkataramana et al. 2022). No NPA, a distribuição dessas larvas ainda é pouco conhecida, mas acredita-se que esteja associada a regiões mais rasas, como o EG, que são propícias para o desenvolvimento das mesmas e as distribuem de acordo com a circulação da água. Esse processo desempenha um papel fundamental no recrutamento bentônico em áreas polares (Venkataramana et al. 2022). Já os cnidários, em 2017 e 2018 apresentaram as maiores abundâncias no EG. No EB, suas abundâncias aumentaram gradativamente ao longo dos anos e no MBL atingiram um máximo de 4% da abundância total em 2019.

A proporção entre os grupos restantes manteve-se estável ao longo dos três anos. Os Euphausiidae apresentaram abundâncias muito baixas, com a maioria dos espécimes coletados sendo juvenis. Esse fato provavelmente está relacionado ao uso de redes MultiNet em arrastos verticais, uma vez que o krill adulto, conhecido por sua agilidade, tende a escapar desse tipo de equipamento devido à lentidão dos arrastos verticais (Yang et al. 2017). Pteropoda, Amphipoda, Cirripedia, Echinodermata, Doliolida e larvas de peixes foram os grupos menos abundantes e, portanto, foram categorizados como "Outros" (Fig. 7). Essas variações destacam os padrões distintos na distribuição e dominância dos grupos ao longo do tempo e entre as localidades. Isso se deve ao fato da complexidade hidrodinâmica do NPA, com intensas trocas nas propriedades físicas das massas de água adjacentes, que formam um gradiente horizontal de temperatura, salinidade e clorofila-*a* e moldam a estrutura da coluna de água (Huneke et al. 2016).

Conforme já relatado por Leonor & Muxagata (2024), em 2017 houve a predominância de copépodes maiores (>2000μm), aqui identificados principalmente como a espécie *Metridia gerlachei* (máx. 22609 ind.1000 m^{-3}, no EG). Esta espécie não

só foi a mais abundante e frequente em 2017 como ao longo dos três anos analisados, amplamente reportada com alta biomassa em águas antárticas (King & LaCasella 2003, Yebra et al. 2009, Conroy et al. 2020, 2023).

Os copepoditos de *Metridia* spp. também apresentaram alta abundância, exibindo um padrão de distribuição semelhante ao dos adultos de *M. gerlachei*. Esse padrão provavelmente está relacionado ao período reprodutivo da espécie, que ocorre predominantemente em março (King & LaCasella 2003), quando atingiram sua maior abundância (máx. 46.467 ind.1000 m^{-3}) observada neste estudo, registrada no EB em 2018. Embora as abundâncias desses copépodes calanóides tenham permanecido altas nos outros dois anos (2018 e 2019), houve um aumento nas abundâncias de copépodes menores (<2000 μm), como *C. citer*, *M. pygmaeus* e *Oithona* spp., em 2018 e 2019. Estudos anteriores sugerem que a comunidade de copépodes passa por mudanças relacionadas ao tamanho ao longo do verão austral, com uma transição de espécies menores para maiores (Atkinson & Shreeve 1995, Hernández-León et al. 2013, Garcia et al. 2016, 2020). Essa variação pode ser influenciada por fatores como temperatura e disponibilidade de alimentos (Hernández-León et al. 2013). Além disso, foi relatado que a presença de criptófitas também favorece espécies menores, como *Oithona similis*, enquanto copépodes maiores tendem a migrar para camadas mais profundas, onde consomem partículas maiores (Atkinson & Shreeve 1995). De fato, em 2019, a amostragem ocorreu mais cedo (janeiro/fevereiro) em comparação com os anos anteriores, e as maiores abundâncias de *C. citer* e *Oithona* spp. foram observadas em estações dominadas por criptófitas, principalmente no EG.

Além dos copépodes, os agregados da espécie *S. thompsoni* foram um dos principais contribuintes para as diferenças observadas entre os anos, conforme análise SIMPER (Tabela 2), estando presentes apenas em 2017 (máx. 12600 ind.1000 m^{-3}), principalmente no EB, quando altas temperaturas na superfície foram observadas e ausentes nos anos subsequentes. Estudos anteriores identificaram que fortes correlações entre temperaturas mais altas e o influxo de águas quentes, como a entrada de CCA, impulsionam a dinâmica populacional de *S. thompsoni*, elevando suas abundâncias (Pakhomov et al. 2002, 2011, Criales-Hernández et al. 2022, Kasyan et al. 2022, Leonor & Muxagata 2024). Por outro lado, temperaturas mais baixas podem reduzir sua

capacidade reprodutiva (Henschke et al. 2019), resultando em menores abundâncias ou ausência da espécie na região. No NPA, Plum et al. (2021) relataram que a presença desses organismos favoreceu espécies de mesozooplâncton maiores (> 2000 µm), enquanto afetou negativamente copépodes menores (< 2000 µm). Assim, assume-se que a ausência de salpas nas amostras de 2018 e 2019, além de estar relacionada a temperaturas mais amenas observadas nestes anos, pode ter contribuído para o aumento da abundância dos copépodes menores aqui relatados. Esses resultados reforçam o impacto significativo das salpas na estruturação das comunidades de meso e macrozooplâncton no NPA, como também observado por Plum et al. (2021), Kasyan et al. (2022) e Criáles-Hernandez et al. (2022).

Tabela 2: Porcentagem de contribuição das espécies que apresentaram diferenças significativas ($p < 0,001$) entre os anos amostrados (2017–2019) na análise SIMPER.

Espécies/Ano	2017 - 2018	2017 - 2019	2018 - 2019
Calanoides acutus	-	0,75	-
Microcalanus pygmaeus	-	-	0,044
Ctenocalanus citer	-	-	0,053
Oithona spp.	-	-	0,108
Triconia antarctica	-	-	0,026
Eukrohnia hamata	2,4	2,7	-
Salpa thompsoni	14,6	17,7	-

5.3.1. Novos Registros para o NPA

No geral, a comunidade zooplanctônica observada durante este estudo foi semelhante em composição de espécies àquelas relatadas anteriormente para a região (Plum et al. 2021, Criales-Hernández et al. 2022, Kasyan 2023, Esquivel-Garrote & Muxagata 2023, Esquivel-Garrote et al. 2023, Leonor & Muxagata 2024, 2025) e no Oceano Antártico (Yang et al. 2017, Conroy et al. 2020, 2023, Venkataramana et al. 2022, Liu et al. 2024). No entanto, pela primeira vez, registramos a presença do tunicado do gênero *Dolioletta* spp. em duas estações diferentes (#10 e #15) do EB em 2018, a qual não havia sido relatada anteriormente na região antártica e no NPA, de acordo com o Registro de Espécies Marinhas da Antártica (RAMS - https://www.marinespecies.org/rams./index.php). Esses organismos podem ocorrer

abundantemente em áreas neríticas de regiões subtropicais (Paffenhöfer & Gibson 1999). Além disso, espécies deste gênero já foram observadas na PCM superior em regiões de quebra de plataforma (Pinchuk et al. 2021). Entretanto, neste estudo, os dois espécimes de *Dolioletta* spp. foram registrados em maiores profundidades (200 - 400 m), sob influência de águas mais frias e salinas. Neste contexto, a presença deste gênero no NPA indica que estes organismos também aproveitam condições ambientais diferentes das conhecidas, potencialmente expandindo sua distribuição para águas polares.

Além disso, uma éfira medindo 12,2 mm de diâmetro foi identificada na amostra do primeiro estrato (0-100 m) na estação #10, localizada no EB, em 2018 (Fig. 8). As éfiras, liberadas de pólipos bentônicos de cnidários da classe Scyphozoa, são definidas por sua morfologia distinta e curta duração, representando um período crítico de transição para o estágio adulto (Schiariti et al. 2008).

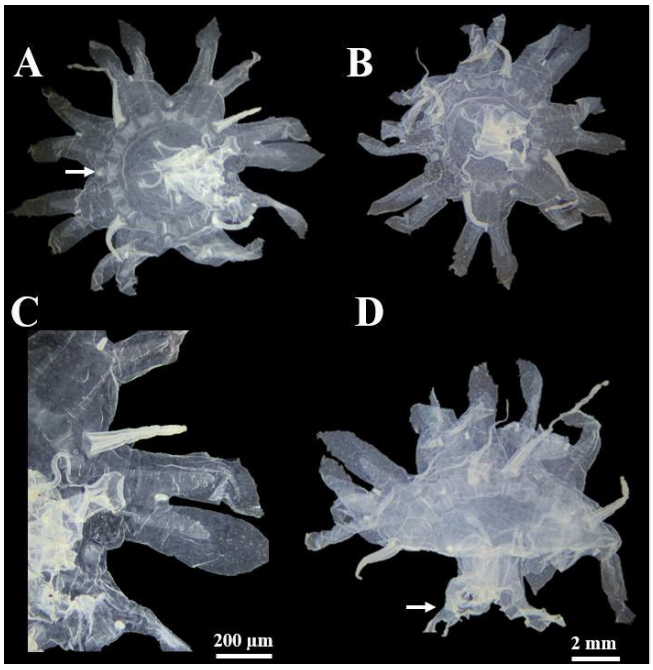


Figura 8: Espécime de éfira de *Desmonema glaciale* amostrado no Estreito de Bransfield. A) visão oral, a seta branca indica um broto de tentáculo. B) Vista aboral. C) Vista lateral. D) Detalhe dos lóbulos (*lappet*)

A éfira era transparente, com ausência de lobos velares, braços orais pouco desenvolvidos e apenas quatro tentáculos e quatro brotos tentaculares (em contraste com os oito tentáculos presentes em estágios mais avançados, observados em registros de espécimes mais antigos, e.g. Browne 1909), o que indica que se tratava de um indivíduo

em estágio inicial de desenvolvimento. Apesar disso, o espécime apresentou características morfológicas que permitiram classificá-lo como uma éfira de Semaeostomeae (Fig. 8). A presença de lobos lisos na umbrella reforça essa identificação (Jordano et al. 2022).

Entre os gêneros de Semaeostomeae reportados nas águas da Antártica, destaca-se *Desmonema* spp., especialmente a espécie *Desmonema glaciale*. Browne (1908) encontrou espécimes de éfiras juvenis dessa espécie ao redor das Ilhas Malvinas, com diâmetros entre 14 mm e 25 mm, enquanto o espécime coletado no NPA mede apenas 12,2 mm. Considerando que o diâmetro da umbrela é um parâmetro determinante para o surgimento de novas estruturas em águas-vivas (Jordano et al. 2022), o menor tamanho do nosso espécime indica que ele se encontra em um estágio de desenvolvimento anterior ao descrito na literatura, possivelmente o mais jovem já registrado para a espécie.

A identificação deste espécime como *Desmonema glaciale* foi apoiada por sua localização geográfica e similaridades morfológicas com espécimes descritos (Browne, 1909, Larson 1986). A detecção de éfiras no ambiente natural pode fornecer informações detalhados sobre o sucesso reprodutivo e a dinâmica populacional das águas-vivas (Straehler-Pohl & Jarms 2010), ainda mais em um ambiente complexo, como as águas do NPA. Embora espécimes de *Desmonema* já tenha sido observado em águas frias próximas à Antártica e à costa da Argentina (Larson 1986), ainda há lacunas sobre sua biologia e ecologia, especialmente em seus primeiros estágios de vida. A presença de um espécime em estágio tão inicial de desenvolvimento na Antártica não apenas contribui para a biodiversidade local, mas também sugere que essas águas-vivas podem estar desempenhando um papel ecológico cada vez mais relevante em um ecossistema polar em transformação, atuando como predadoras bentopelágicas (White & Bone 1972), e como presas para aves marinhas e peixes, especialmente quando as abundâncias de krill estão baixas (Brierley & Watkins 1996).

5.4. Distribuição vertical do meso e macrozooplâncton

O teste PERMANOVA (p-valor<0,001) indicou diferenças nas abundâncias e composição de espécies entre os estratos. Apesar dessas diferenças, o domínio dos

copépodes em todas as profundidades e anos (Fig. 9 e 10) reforça o papel central desses organismos nas comunidades de zooplâncton do Oceano Austral (Marrari et al. 2011b).

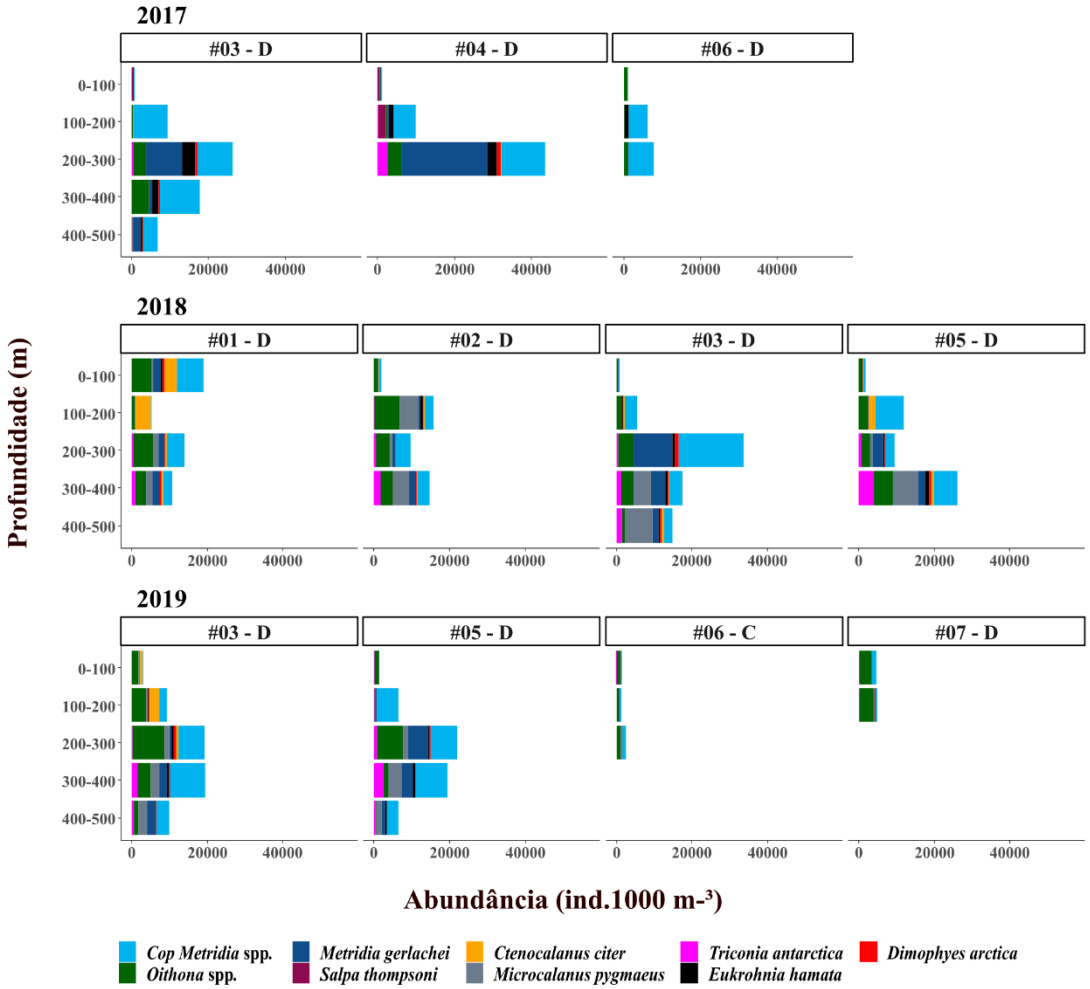


Figura 9: Distribuição vertical dos principais taxa das comunidades de meso e macrozooplâncton em todas as estações amostradas em Gerlache (#01, #02, #03, #04 e #05) e no Mar de Bellingshausen (#06 e #07) ao longo de três anos (2017 – 2019).

Metridia gerlachei tem uma das distribuições verticais mais amplas e emergiu como uma espécie-chave contribuindo para as diferenças entre estratos, reforçando sua importância ecológica Lopez & Huntley (1995). Os copepoditos de *Metridia* spp. parecem seguir a distribuição vertical adulta. Essas distribuições podem estar relacionadas às estratégias do ciclo de vida desta espécie e para evitar predadores, como sugerido por Atkinson et al. (1992) e King e LaCasella (2003). Espécies menores, como

C. citer e *Oithona spp.*, foram associadas às camadas superiores, enquanto *T. antarctica* foi encontrada em águas mais profundas (Fig. 9 e 10).

Apesar de ser amplamente distribuído por toda a coluna d'água, *S. thompsoni* foi registrado em maior abundância nas camadas superiores (0 – 100 e 100 – 200 m). Em regiões de alta produtividade, como áreas com altas concentrações de clorofila-*a*, as salpas tendem a se concentrar nas camadas superficiais (Conroy et al. 2020, Henschke et al. 2021, Liu et al. 2024). No entanto, as altas abundâncias no primeiro estrato, observadas durante o estudo, coincidiram com concentrações muito baixas de clorofila-*a*, o que sugere uma possível relação entre a presença desses organismos e a redução na produtividade primária. As salpas são filtradoras eficientes, podendo exercer um controle de cima pra baixo ("*top-down*") da comunidade fitoplanctônicas (Stukel et al. 2021). Isso significa que a pressão de predação pelas salpas pode ter limitado a abundância do fitoplâncton, resultando em uma queda nas concentrações de clorofila-*a*, nessas estações oceanográficas (#11 e #12 de 2017).

Embora menos frequentes, as salpas também podem ser encontradas em maiores profundidades (Nishikawa & Tsuda 2001, Pakhomov et al. 2011, Conroy et al. 2020, Henschke et al. 2021), como observado aqui (Fig. 10). Isso depende das condições locais, como estabilidade da coluna de água (maior em 2017) e disponibilidade de alimentos (Conroy et al. 2020, Henschke et al. 2021). Essa movimentação vertical contribui para o transporte ativo de carbono e nutrientes entre camadas da coluna de água (Nishikawa & Tsuda 2001, Pakhomov et al. 2011, Henschke et al. 2021). Além disso, observamos um padrão de migração durante o período crepuscular na estação #12 de 2017, no EB, onde suas abundâncias aumentam no primeiro estrato (Fig. 10).

Os eufausiáceos, quando presentes, foram mais frequentes nas camadas intermediárias. No entanto, as abundâncias de superfície podem estar subestimadas devido à possível evasão da rede, especialmente durante o dia (quando a maioria das amostragens ocorreu), possibilitando maior visibilidade do equipamento, o que facilitaria a fuga (Flores et al. 2014).

Os ostracodes foram predominantes em águas profundas, mas em algumas estações amostradas ao crepúsculo, também migraram para camadas superiores, reforçando a influência da migração nictemeral.

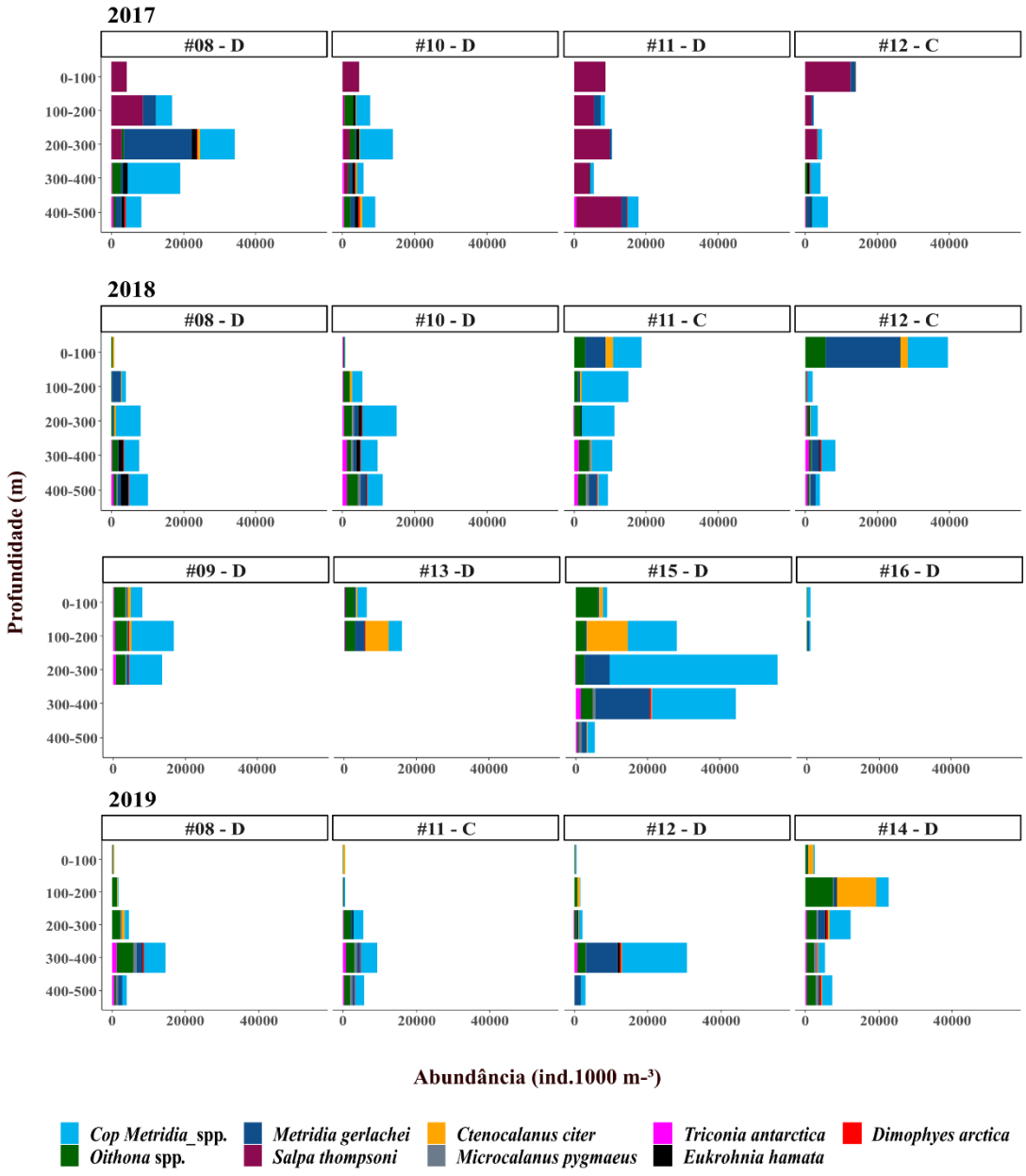


Figura 10: Distribuição vertical dos principais taxa das comunidades de meso e macrozooplâncton em todas as estações amostradas em Bransfield ao longo de três anos (2017 – 2019).

Grupos carnívoros, como quetognatos, representados por *E. hamata*, poliquetas e cnidários, representados por *Dimophyes artica*, apresentaram maiores densidades em camadas mais profundas (Fig. 9 e 10), seguindo o padrão amplamente documentado na Antártica, onde os carnívoros tendem a ser mais prevalentes em maiores profundidades (Marrari et al. 2011b, Venkataramana et al. 2022, Liu et al. 2024). Essa distribuição está possivelmente relacionada aos benefícios de maior sedimentação de partículas e à disponibilidade de uma base alimentar mais diversa nesses estratos (Øresland 1990, Flores et al. 2014). Durante as amostragens crepusculares foi observado uma migração de hidromedusas para o primeiro estrato (Fig. 10), possivelmente acompanhando os copépodes, suas principais presas (Hopkins 1985).

Embora as abundâncias de anfípodes tenham sido baixas nas amostras analisadas, alguns autores destacam seu papel ecológico crucial em ecossistemas pelágicos temperados e polares, onde podem atingir altos níveis de biomassa e atuar como presas essenciais para estoques de peixes e lulas comercialmente importantes. Em área próximas ao NPA, a abundância desses organismos pode ser tão expressiva que chegam a desempenhar um papel ecológico semelhante ao do krill antártico (Havermans et al. 2019). No presente estudo, especificamente em 2017, esses organismos foram mais frequentes nos primeiros estratos da coluna d'água, um padrão que pode estar associado a interações alimentares com as salpas, conforme já descrito em outros estudos. (Donnelly et al. 2006).

A análise PERMANOVA revelou diferenças significativas (p-valor=0,041) entre a composição e abundâncias observadas nas amostras coletadas durante o crepúsculo e o dia, confirmando padrões previamente observados. Diversos estudos já registraram a migração vertical nictemeral do zooplâncton, com aumento da biomassa próximo à superfície durante a noite devido à maior atividade alimentar (Yebra et al. 2009, Marrari et al. 2011, Flores et al. 2014, Conroy et al. 2020, Leonor & Muxagata 2025). Entretanto, ao contrário do que se esperava, a diversidade não aumentou na superfície durante o período crepuscular, sendo maior nos estratos mais profundos (Fig. 11). Isso está de acordo com Park & Wormuth (1993), o que implica que nem todas as espécies realizam essa migração vertical.

Além disso, acredita-se que a intrusão de águas em EB e EG tenha criado nichos favoráveis à diversidade em determinadas profundidades (Loeb et al. 2010). Este efeito foi observado nas camadas intermediárias (200 - 400 m), onde houve um aumento da diversidade, possivelmente devido às condições que oferecerem refúgio contra predadores e apresentam variações menores de temperatura e salinidade, em comparação com a superfície (Ward et al. 2014, Conroy et al. 2020, Henschke et al. 2021). Além disso, é importante considerar que a maioria das estações oceanográficas foi amostrada durante o período diurno, quando a maior parte dos organismos tende a ocorrer em maiores profundidades (Hays et al. 2001).

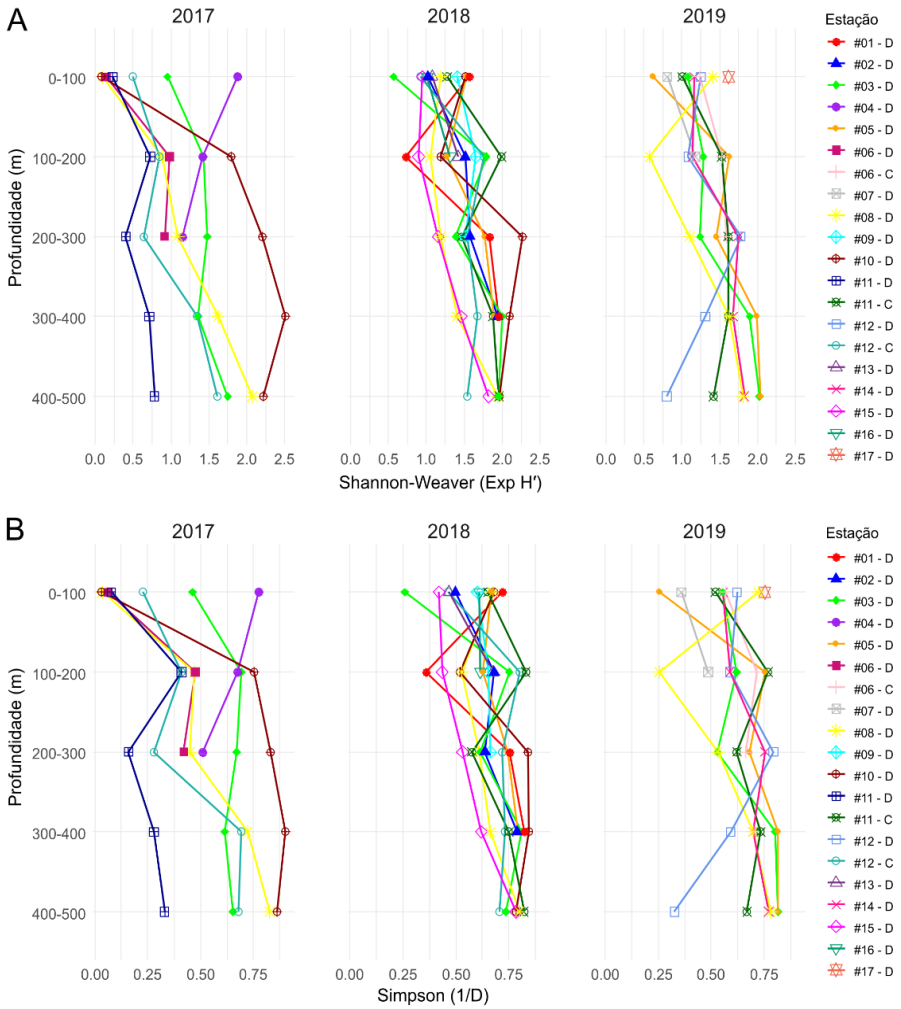


Figura 11: Índices de diversidade: (A) Shannon-Weaver (Exp H′) e (B) Simpson (1/D) para cada estação amostrada ao longo dos anos (#01–#05: Estreito de Gerlache; #06–#07: Mar de Bellingshausen; #08–#17: Estreito de Bransfield). Estações marcadas com 'D' indicam amostragem diurna, enquanto 'C' indica amostragem crepuscular.

A influência da composição fitoplanctônica na diâmica interanual do meso e macrozooplâncton ficou evidente na análise de ACC, revelando que os grupos fitoplanctônicos explicaram 52,3% da variação total da comunidade no primeiro estrato (0-100 m), com os dois primeiros eixos explicando 49,3% da variância (Fig. 12). A relação entre os anos amostrados e os grupos taxonômicos foi distinta: as amostras de 2017 estavam associadas a dinoflagelados e criptófitas; as de 2018 com diatomáceas; e as de 2019 foram mais dispersas. *S. thompsoni* apresentou uma associação positiva com dinoflagelados e criptófitas, enquanto mostrou uma relação inversa com diatomáceas. *M. gerlachei* e *C. propinquus* foram espécies associadas às diatomáceas, principalmente em 2018. Esses padrões são consistentes com Atkinson & Shreeve (1995), que observou que *C. propinquus* e *M. gerlachei* se alimentam de células maiores. Esse comportamento alimentar sugere que o pastoreio por esses copépodes pode ter contribuído para a menor abundância de diatomáceas em 2017, destacando a influência da composição fitoplanctônica na dinâmica interanual dos copépodes (Garcia et al. 2020).

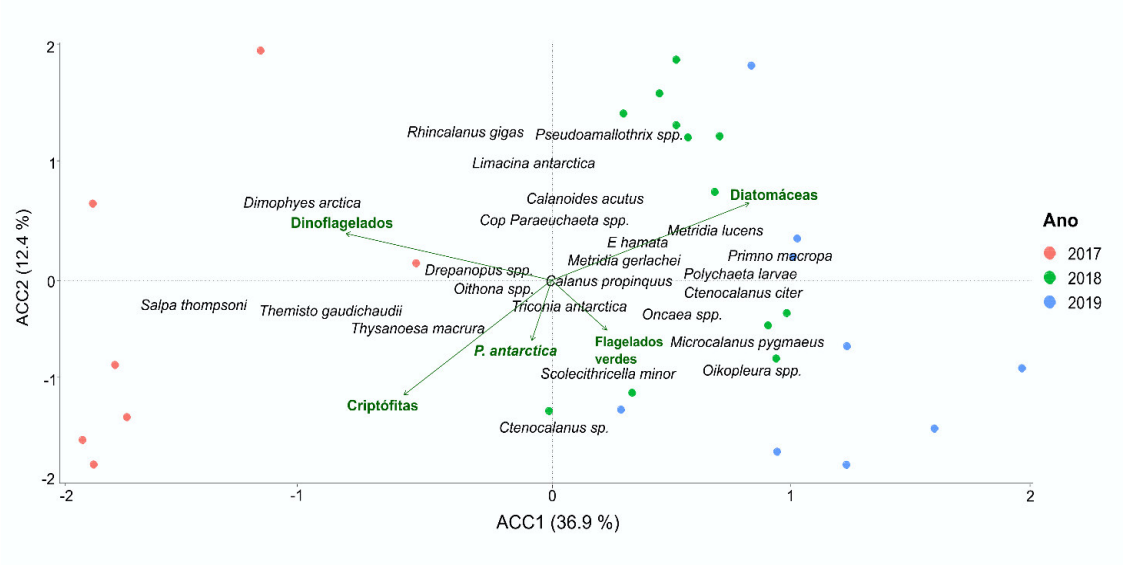


Figura 12: Análise de Correspondência Canônica (ACC) da comunidade de meso e macrozooplâncton de superfície em relação aos principais grupos fitoplanctônicos dentro dos 100 metros superiores nos 3 anos de amostragem (2017, 2018 e 2019)

Além da relação com dinoflagelados e criptófitas (Fig. 12), as análises também indicaram que as abundâncias de salpas estiveram associadas a condições ambientais específicas, como temperaturas mais elevadas na superfície e maior estabilidade da

coluna d'água, refletidas por altos índices de variação térmica (Fig. 13). Essas relações corroboram estudos anteriores (Hunt & Hosie 2006, Loeb & Santora 2012, Henschke et al. 2021, Plum et al. 2021, Criales-Hernández et al. 2022) e destacam a forte interação entre a estrutura fitoplacntônica e os fatores oceanográficos na distribuição do zooplâncton antártico.

Os gradientes verticais na abundância e diversidade do meso e macrozooplâncton foram diretamente ligados à estratificação da coluna d'água, com a estabilidade sendo o principal fator de variação da comunidade ao longo dos anos e locais, segundo a ACC (Fig. 13), que explicou 23% da variância total na abundância das espécies, revelando padrões significativos na distribuição espacial das espécies. Em 2017, a maior estabilidade, impulsionada por temperaturas superficiais elevadas, principalmente no EB, favoreceu a abundância de salpas, as quais se reproduzem rapidamente e prosperam em águas mais quentes (Plum et al. 2021). Na estação #11, a distribuição quase homogênea das salpas ao longo da coluna d'água demonstra um comportamento ativo desses organismos, que possuem grande mobilidade e podem se distribuir amplamente na coluna d'água em busca de alimento, independentemente da estratificação física. Isso reforça a plasticidade ecológica das salpas e sua capacidade de explorar diferentes camadas da coluna d'água de acordo com a disponibilidade de recursos (Henschke et al. 2021).

Já em 2018 e 2019, a estabilidade decorreu de uma redução da salinidade, associada ao aporte de água de degelo, criando condições favoráveis para pequenos copépodes, que tendem a se beneficiar da maior disponibilidade de alimento em ambientes estratificados (Giraldo et al. 2020). A estratificação também afetou a composição fitoplanctônica, com criptófitas apresentando forte correlação com algumas espécies do meso e macrozooplâncton (Fig. 12). Por outro lado, em áreas de menor estratificação, como na estação #15 em 2018, a homogeneidade da coluna d'água até 500 m esteve associada a um aumento significativo da abundância zooplanctônica, destacando a complexidade vertical dessa comunidade.

Além disso, deve-se levar em conta o fato de que a maioria das amostras foi coletada durante o período diurno, o qual os organismos zooplanctônicos tendem a ocupar maiores profundidades (Hays 2001).

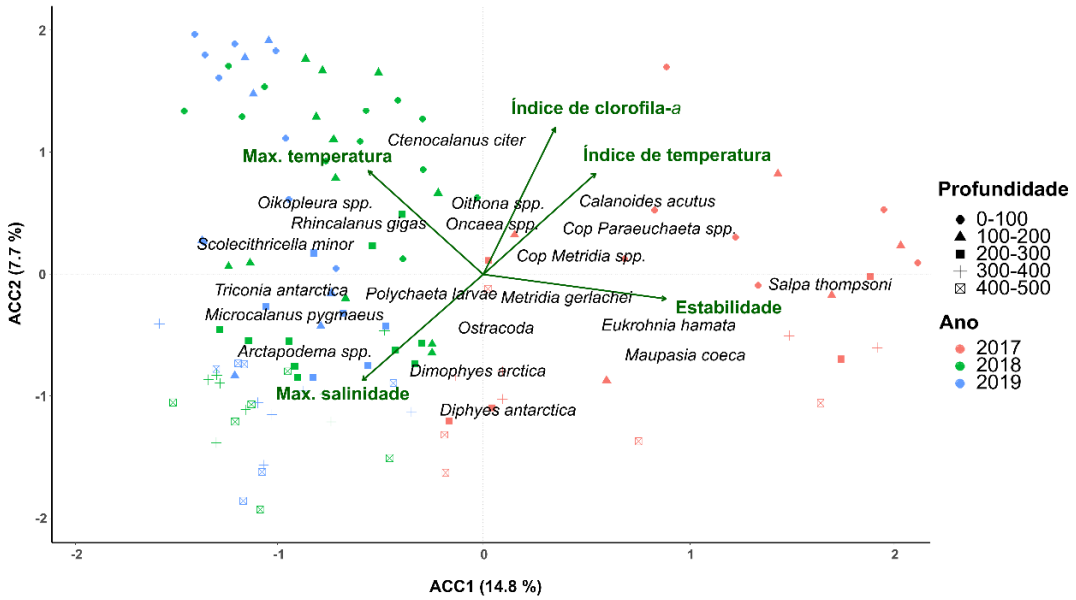


Figura 13: Análise de Correspondência Canônica (ACC) da comunidade de meso e macrozooplâncton em relação às variáveis ambientais mais significativas durante os três anos amostrados (Máximo de temperatura, máximo de salinidade, índice da variação de clorofila-*a*, índice da variação de temperatura e estabilidade).

Além das diferenças particulares de cada taxa quanto a distribuição na coluna de água, padrões de migração vertical foram evidentes, conforme indicado pelo teste PERMANOVA (p-valor=0,041), com organismos concentrando-se no primeiro estrato (0-100 m) durante amostragens crepusculares e em maiores profundidades, nas amostragens diurnas. No entanto, a expectativa de encontrar maior abundância de espécies nas camadas superficiais (0-100 m), especialmente no EB, devido às temperaturas mais elevadas, não foi confirmada. Ao contrário, as maiores abundâncias, e também diversidade, foram observadas em profundidades maiores no EB, possivelmente devido à menor variabilidade das propriedades físico-químicas da água em comparação à superfície e ao comportamento migratório dos organismos, que tendem a ocupar águas mais profundas durante o dia. Por outro lado, as maiores variações na estrutura da coluna d'água foram registradas no EG (#03; Fig. 4), onde oscilações de salinidade e temperatura impulsionaram uma alta estabilidade, influenciando as diferenças verticais na composição e abundância das espécies entre os três anos analisados.

As análises relevaram mudanças interanuais na composição de espécies, especialmente relacionadas a temperatura mais elevadas na superfície, como em 2017.

Além disso, os resultados indicam que a distribuição vertical do zooplâncton no NPA é de fato complexa e moldada por um conjunto de fatores, como: condições ambientais, disponibilidade de alimento e estratégias ecológicas específicas. A inclusão de coletas futuras no período crepuscular é essencial para capturar a amplitude total da migração vertical e evitar subestimação da diversidade e abundância na superfície. Tendo isto em vista, o próximo tópico a ser apresentado nesta tese focou nos principais achados das amostragens realizadas ao longo de um ciclo diário no EB, sob influência de uma coluna de água estratificada e altas abundâncias de *S. thompsoni*.

5.5. Acoplamento trófico e distribuição do zooplâncton na coluna de água durante o ciclo de 20 horas

Durante as amostragens contínuas ao longo de um ciclo circadiano, foram observadas variações significativas nas abundâncias (p-valor > 0,001) e na distribuição vertical de grupos específicos em diferentes períodos do dia (Fig. 14), mesmo com a pouca variação de luz durante o verão austral. Nossos resultados revelaram principalmente duas comunidades distintas de meso e macrozooplâncton: uma na camada superficial dominada pelos agregados de *S. thompsoni* e outra nas camadas mais profundas (200-500 m), dominadas por copépodes calanóides, onde *M. gerlachei* foi a espécie mais abundante (Fig. 14).

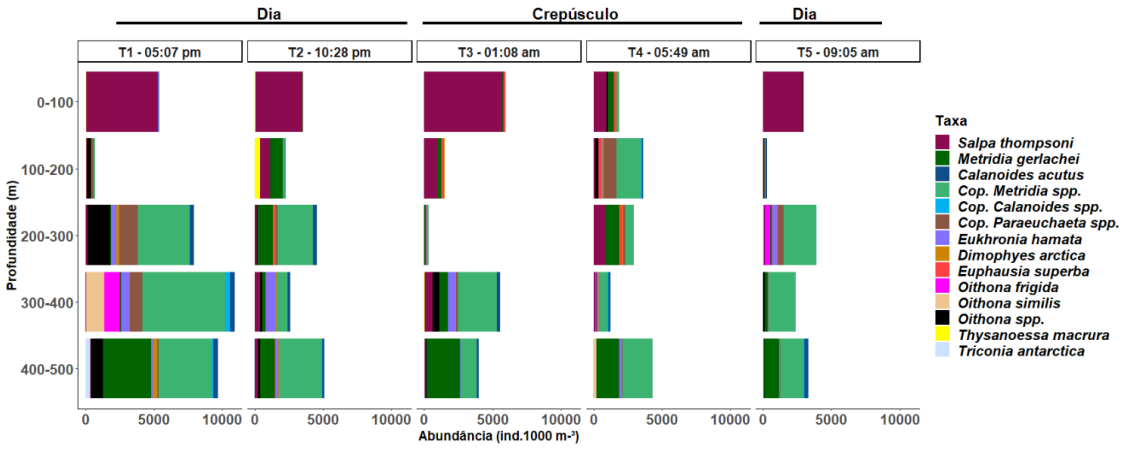


Figura 14: Distribuição vertical dos principais taxa de meso e macrozooplâncton em cada horário de amostragem da estação B42 em 2017, onde: T1 - 17:07; T2 - 22:28; T3 - 1:08; T4 - 5:49 e T5 - 9:05. Os períodos diurno e crepuscular também estão indicados.

Em T4, quando as abundâncias de salpas diminuíram no primeiro estrato durante o crepúsculo, observou-se um aumento nas abundâncias de copépodes, krill e outras espécies, principalmente *M. gerlachei* e *E. superba* (Fig. 14), indicando potencial competição por espaço e alimento. Isso porque, apesar da espécie *M. gerlachei* ser considerada uma espécie de águas intermediárias (Hopkings &Torres 1989), ela adapta suas estratégias de alimentação com base na disponibilidade de alimentos em diferentes profundidades, permitindo que explore múltiplos nichos ecológicos e minimize a competição (Yang et al. 2017). Já foi relatado que *M. gerlachei* inicia sua migração para profundidades mais rasas, para se alimentar principalmente durante a noite (Lopez & Huntley 1995), apesar de sua natureza onívora (Hopkins 1985), consumindo fitoplâncton, especialmente durante os meses de verão e primavera (Hopkins & Torres 1989).

Vários copepoditos da ordem Calanoida foram identificados nos diferentes horários amostrados. Observamos uma pequena migração ontogenética para *Calanoides* spp., *Metridia* spp. e *Paraeuchaeta* spp., durante o período noturno (T3 e T4; Fig. 14), quando houve aumento nas abundâncias dos adultos (531 ind.1000 m^{-3}) entre 200-300 m e copepoditos (2759 ind.1000 m^{-3}) nos dois primeiros estratos (0-200 m), em comparação com as abundâncias encontradas durante o dia (T1) nos mesmos estratos (32 ind.1000 m^{-3} para adultos e 276 ind. 1000 m^{-3} para copepoditos). De fato, durante a amostragem T5 observamos uma escassa abundância desses calanoides na superfície e um aumento (6756 ind.1000 m^{-3}) nos estratos mais profundos (200 – 500 m) (Fig. 14). Esse comportamento de migração ontogenética também já foi observado para esses gêneros da ordem Calanoida em outros locais da Antártica (Schnack-Schiel 2002b, Michels et al. 2012, Yang et al. 2017).

Embora tenham mantido suas distribuições em camadas profundas, os cnidários (representados por *D. arctica*) e ostrácodes foram encontrados em menores abundâncias (103 ind. 1000 m^{-3}, 172 ind.1000 m^{-3}, respectivamente) na camada de 100-200 m durante o período noturno (Fig. 14), indicando uma migração nictemeral desse grupo para menores profundidades. Além desses grupos, a espécie *Eukrohnia hamata* também realizou migração, principalmente dentro da zona mesopelágica superior (200-400 m, Fig. 14), seguindo a distribuição de copépodes, o que indica um acoplamento de predador-presa (Conroy et al. 2020).

Por fim, realizou-se um experimento controlado com krill e salpas para avaliar o conteúdo de pigmentos em suas pelotas fecais, visando identificar seus padrões alimentares. Nesse contexto, esperava-se que a concentração de produtos de degradação e pigmentos biomarcadores (derivados de células fitoplanctônicas ingeridas) fosse maior na água do mar filtrada do experimento em comparação com a amostragem de base (B42, coletada em 24 de fevereiro). Por outro lado, pigmentos associados a grupos fitoplanctônicos não consumidos deveriam apresentar concentrações menores na água filtrada. Os resultados confirmaram o consumo de diatomáceas tanto por krill quanto por salpas, evidenciado pela presença de fucoxantina nas pelotas fecais de ambos os ogranismos. Além disso, o acúmulo de Chl-c1 nas pelotas fecais de krill reforça a ingestão desse grupo fitoplanctônico. No entanto, as salpas apresentaram uma maior concentração de aloxantina em suas pelotas fecais, indicando uma predação preferencial sobre criptófitas, apesar de também consumirem diatomáceas (Fig. 15).

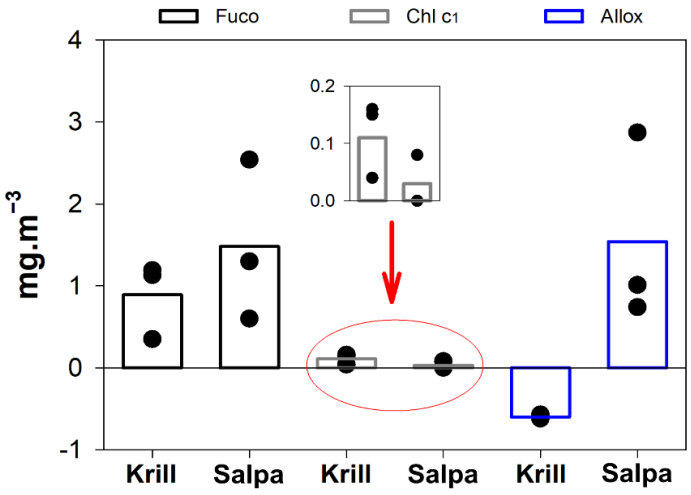


Figura 15: Concentração de pigmentos biomarcadores nas pelotas fecais de krill e salpa em comparação com a amostragem de linha de base. As colunas pretas, cinzas e azuis representam as médias de fucoxantina (Fuco), clorofila-c1 (Chl-c1) e aloxantina (Allo), respectivamente. Os pontos pretos indicam valores individuais. As concentrações de pigmentos nos experimentos foram subtraídas dos valores da amostragem de linha de base, representando a diferença entre eles. A proporção média de cada pigmento foi calculada a partir desses valores subtraídos. A figura inserida exibe uma escala ampliada para a média e os valores individuais de Chl-c1 nos experimentos com krill e salpa.

Além disso, durante o período de amostragem, observou-se um aumento rápido nos valores do índice de pastejo abaixo da camada de mistura (PCM), sugerindo um processo de afundamento das pelotas fecais e deterioração da comunidade fitoplanctônica, com valores crescentes do índice de senescência (Fig. 16). Esse padrão está correlacionado com a pressão de pastejo exercida pelas comunidades de meso e macrozooplâncton, que influenciaram diretamente a composição da comunidade fitoplanctônica ao longo do tempo.

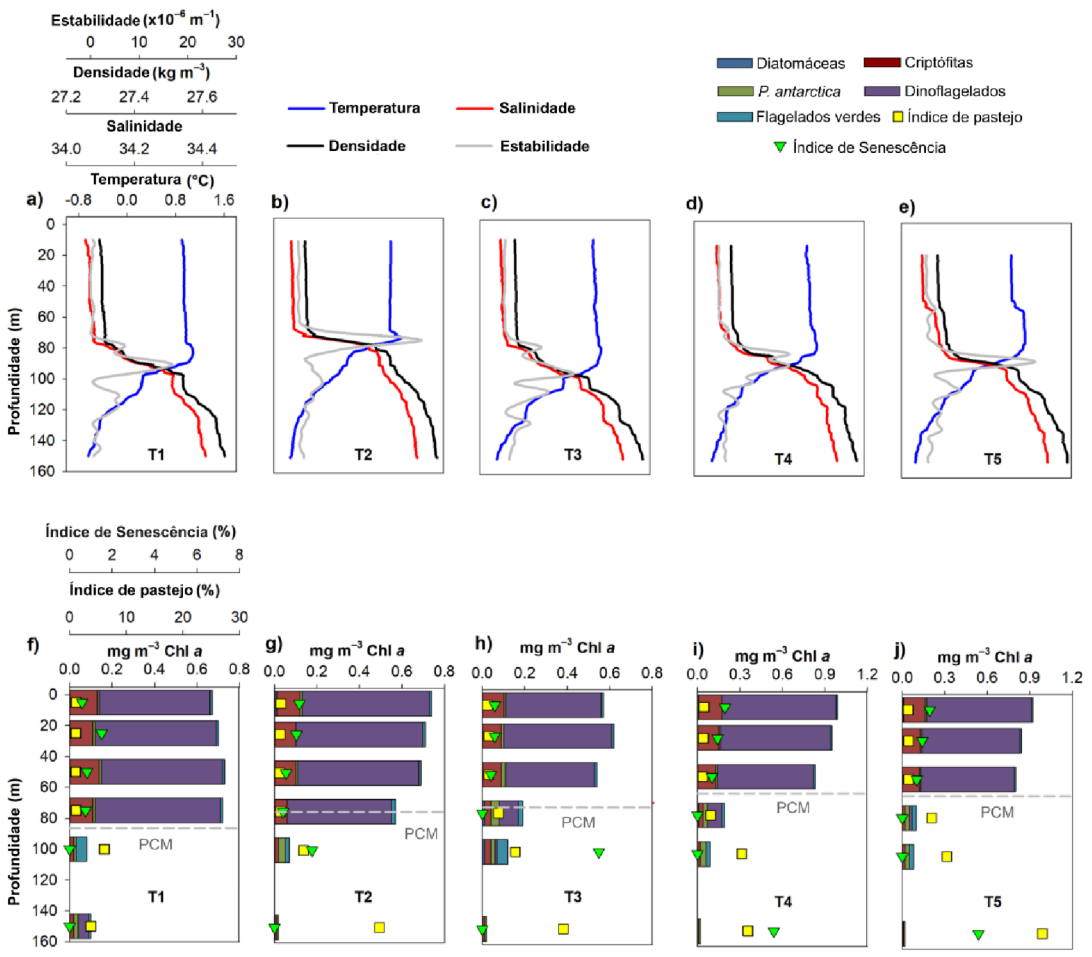


Figura 16: (a – e) Perfis verticais de temperatura da coluna de água (°C), salinidade, densidade (kg m^{-3}) e estabilidade (x$^{10-6}$ m^{-1}) no painel superior. (f - j) Distribuição de profundidade da biomassa dos grupos fitoplanctônicos (mg m^{-3} Chl-*a*), índice de pastejo (%) e índice de senescência (%) no painel inferior. Diatomáceas (azul), dinoflagelados (vermelho escuro), *P. antarctica* (verde), criptófitas (roxo) e flagelados verdes (azul

claro) são mostrados. A linha cinza tracejada representa a profundidade da camada de mistura (PCM; m).

Os achados reforçam a importância da atividade de pastejo na estruturação das comunidades planctônicas e na dinâmica dos ecossistemas marinhos antárticos. As diferenças nas dietas de krill e salpas influenciam diretamente a ciclagem de nutrientes e o transporte de carbono. Enquanto o krill se alimenta preferencialmente de células maiores, como as diatomáceas — microalgas eficientes no sequestro de carbono devido ao seu maior tamanho e à formação de cadeias celulares (Smetacek 1999) —, as salpas são mais eficientes na filtragem de células de menor tamanho e consomem preferencialmente criptófitas, que, por serem menores e menos propensas à formação de agregados, apresentam menor eficiência no sequestro de CO_2 (Brown et al. 2021, Ferreira et al. 2020). O aumento das criptófitas no NPA, impulsionado pelo rápido aquecimento dos últimos anos (Ferreira et al. 2020, Mendes et al. 2023), pode, portanto, alterar a base da cadeia trófica, favorecendo organismos filtradores como as salpas, e na ausência delas, copépodes menores, em detrimento de espécies dependentes de diatomáceas, como o krill com potenciais impactos no fluxo de energia e no equilíbrio do ecossistema marinho antártico (Moline et al 2004, Seyboth et al. 2018, Ferreira et al. 2020).

Nossos resultados corroboram com a segunda hipótese e indicam que, mesmo sob um fotoperíodo relativamente estável no verão austral, a distribuição vertical do zooplâncton foi influenciada por fatores ambientais e disponibilidade de alimento. A variação na abundância entre os períodos diurno e crepuscular, especialmente nas camadas epipelágicas e mesopelágicas superiores, sugere que a migração vertical não é apenas um reflexo de respostas circadianas, mas também um mecanismo dinâmico regulado pela estrutura da coluna d'água e pela oferta de alimento. *Salpa thompsoni*, em particular, demonstrou um papel central nessas variações verticais, reforçando sua relevância ecológica nesse ambiente.

6. Conclusões e Perspectivas futuras

Esta tese aprofunda a compreensão da distribuição, abundância e composição do meso e macrozooplâncton em amplas regiões do Norte da Península Antártica.

As abundâncias e a composição taxonômica do meso e macrozooplâncton antártico variam significativamente entre anos, dentro do próprio verão, e entre diferentes regiões do NPA (estreitos de Gerlache e Bransfield e Mar de Bellingshausen). Essas variações nas comunidades estão intimanete associadas às flutuações de temperatura e salinidade, que afetam a estabilidade da coluna d'água. Em Gerlache essas diferenças são influenciadas pelas baixas salinidades superficiais, enquanto em Bransfield e Bellingshausen, pela maior temperatura da superfície. Esses resultados indicam que a composição de espécies se altera frente a mudanças interanuais na estabilidade da coluna d'água, impulsionadas pela intrusão de águas mais quentes das áreas adjacentes, fato este que também reflete nas estratégias de vida de algumas espécies, como *Salpa thompsoni* e os copepoditos de *Metridia* spp.. Além disso, a tese expandiu a distribuição conhecida do tunicado *Dolioletta* spp. para águas polares, contribuindo para o entendimento da biodiversidade na região. Estes resultados fazem parte do artigo "*Spatiotemporal Patterns and Environmental Drivers of Meso- and Macrozooplankton Communities in the Northern Antarctic Peninsula (2017–2019)*", apresentado no apêndice 1 deste documento.

Apesar da luz solar quase contínua no verão, foi observada a migração vertical diária de alguns taxa. No entanto, o domínio de *S. thompsoni* foi observado em camadas superiores (0-100 m) com números significativos, independentemente do horário de coleta. A maior concentração de fitoplâncton na superfície pode ter favorecido a permanência de alguns organismos nas camadas superficiais para alimentação, interrompendo sua migração vertical entre os ambientes epipelágico e mesopelágico superior. Apesar disso, os padrões de distribuição vertical observados variaram entre os grupos, provavelmente refletindo a disponibilidade de alimento e a diferentes estratégias do ciclo de vida, como as migrações ontogenéticas de copépodes calanóides observadas. Esses resultados indicam a necessidade de amostragens mais estratificadas no primeiro estrato da coluna d'água (0-100 m), já que muitas espécies realizam migrações de menor amplitude durante o verão austral. Estes resultados fazem parte do artigo "*Meso and macrozooplankton distribution across water column during a 20-hours experiment in the Bransfield Strait, Northern Antarctic Peninsula*", apresentado no apêndice 2 deste documento.

A forte relação entre as altas abundâncias de *Salpa thompsoni* e a presença de criptófitas foi evidenciada através do experimento de suas pelotas fecais. A estabilidade elevada da coluna d'água, causada pelo aumento da temperatura superficial, aliada à preferência alimentar por nanoplâncton, favoreceu o sucesso dessa espécie em 2017.

Um novo registro da éfira de *Desmonema glaciale* na região central do Estreito de Bransfield reforçou a presença dessa espécie em águas aos arredores da Península Antártica e contribuiu para a documentação de seus estágios iniciais de desenvolvimento. Esse achado é relevante para o entendimento da biodiversidade de cnidários na Antártica e do papel ecológico das medusas nos ecossistemas polares, onde atuam como predadoras e presas, podendo influenciar a dinâmica de outros organismos marinhos. Além disso, a presença desse estágio larval em águas frias e relativamente salinas do NPA levanta questões sobre os fatores que regulam sua distribuição e o impacto da proliferação desses organismos no Oceano Austral. Este registro faz parte de um terceiro artigo - "*First Record of Desmonema glaciale Larson, 1986 ephyrae in the Northern Antarctic Peninsula*", o qual está apresentado no apêndice 3 deste documento.

Embora a estabilidade da coluna de água e composição fitoplanctônica parecem ser os principais fatores reguladores da distribuição espacial do meso e macrozooplâncton na NPA, as particularidades do ciclo de vida das diferentes espécies também devem ser consideradas, pois influenciam sua distribuição vertical e dinâmica na região.

Esses achados fornecem direções para futuras pesquisas. Caso essas oscilações na composição de espécies persistam nos próximos anos, com um aumento na frequência de florações de salpas, impactos ecológicos significativos poderão ocorrer na teia alimentar e no ciclo do carbono. Isso afetaria comunidades tanto de águas superficiais quanto profundas, pois as salpas não são o alimento preferido dos predadores antárticos de topo. Esses resultados reforçam a necessidade de investigar mais profundamente o papel crescente das salpas e suas interações ecológicas, bem como quantificar o impacto da migração nictemeral (MN) na bomba biológica de carbono.

Por fim, compreender as mudanças futuras exige a continuidade de programas de pesquisa de longo prazo. O GOAL tem sido essencial no monitoramento das propriedades físicas, biogeoquímicas e biológicas no NPA, contribuindo significativamente para os

estudos desta tese. No entanto, um monitoramento contínuo, sistemático e padronizado da região é crucial para avaliar as mudanças na biodiversidade e abundância do zooplâncton, especialmente em resposta às alterações físico-químicas da coluna d'água.

Para aprimorar a qualidade dos dados, o uso de técnicas complementares e novas abordagens analíticas seria fundamental. Amostragens com redes de maior abertura, como IKMT (Isaacs-Kidd Midwater Trawl), permitiria arrastos mais eficientes para a captura de organismos como o krill antártico, reduzindo a subestimativa das populações em comparação com a Multinet utilizada neste estudo. O emprego da Multinet em diferentes estratégias, como arrastos horizontais ou oblíquos, possibilitaria uma amostragem mais eficiente ao longo dos estratos da coluna d'água, provavelmente capturando essas variações na distribuição do krill.

Para otimizar a identificação taxonômica, o uso de sistemas de imagens, como o ZooScan ou o Flowcam poderia automatizar as identificações dos organismos, dando agilidade às análises. Além disso, técnicas de eDNA permitiriam uma caracterização mais precisa da biodiversidade, incluindo organismos frágeis ou de difícil identificação por métodos tradicionais. No que se refere às interações tróficas das comunidades de meso e macrozooplâncton, experimentos de incubação com outras espécies chaves, como os copépodes *M. gerlachei*, *Oithona* spp., e o anfípoda *Themisto gaudichaudii*, por exemplo, e estudos isotópicos mais detalhados ajudariam a esclarecer as complexas relações alimentares no ambiente antártico. Por fim, o uso de armadilhas de sedimentação possibilitaria o monitoramento do fluxo de matéria orgânica e a caracterização do material exportado para o fundo, contribuindo para a quantificação do carbono exportado pelos organismos zooplanctônicos. Esse processo é fundamental para o acoplamento pelágico-bentônico, que sustenta a vida no fundo marinho, tornando-se ainda mais crítico em uma região tão inóspita como a Antártica.

Referências Bibliográficas:

Ameneiro J, Mouriño-Carballido B, Parapar J, Vázquez E (2012) Abundance and distribution of invertebrate larvae in the Bellingshausen Sea (West Antarctica). Polar Biol 35:1359–1373.

Arrigo KR, Van Dijken GL, Bushinsky S (2008) Primary production in the Southern Ocean, 1997–2006. J Geophys Res 113:2007JC004551.

Atkinson A, Hill SL, Pakhomov EA, Siegel V, Reiss CS, Loeb VJ, Steinberg DK, Schmidt K, Tarling GA, Gerrish L, Sailley SF (2019) Krill (Euphausia superba) distribution contracts southward during rapid regional warming. Nature Clim Change 9:142–147.

Atkinson A, Shreeve RS (1995) Response of the copepod community to a spring bloom in the Bellingshausen Sea. Deep Sea Research Part II: Topical Studies in Oceanography 42:1291–1311.

Atkinson A, Siegel V, Pakhomov E, Rothery P (2004) Long-term decline in krill stock and increase in salps within the Southern Ocean. Nature 432:100–103.

Atkinson A, Sinclair JD (2000) Zonal distribution and seasonal vertical migration of copepod assemblages in the Scotia Sea. Polar Biology 23:46–58.

Atkinson A, Ward P, Williams R, Poulet SA (1992) Diel vertical migration and feeding of copepods at an oceanic site near South Georgia. Marine Biology 113:583–593.

Atkinson A, Whitehouse M, Priddle J, Cripps G, Ward P, Brandon M (2001) South Georgia, Antarctica: a productive, cold water, pelagic ecosystem. Mar Ecol Prog Ser 216:279–308.

Aumont O, Maury O, Lefort S, Bopp L (2018) Evaluating the Potential Impacts of the Diurnal Vertical Migration by Marine Organisms on Marine Biogeochemistry. Global Biogeochemical Cycles 32:1622–1643.

Avelina R, Cunha LCD, Kerr R, Farias CO, Hamacher C, Mata MM (2024) Drivers and fluxes of dissolved organic carbon along the northern Antarctic Peninsula during late summer. An Acad Bras Ciênc 96:e20240573.

Bandara K, Varpe Ø, Wijewardene L, Tverberg V, Eiane K (2021) Two hundred years of zooplankton vertical migration research. Biological Reviews 96:1547–1589.

Banse K (1995) Zooplankton: Pivotal role in the control of ocean production. ICES Journal of Marine Science 52:265–277.

Barange M (1990) Vertical migration and habitat partitioning of six euphausiid species in the northern Benguela upwelling system. J Plankton Res 12:1223–1237.

Barth A, Beckers JM, Troupin C, Alvera-Azcárate A, and Vandenbulcke L (2014) DIVAnd-1.0: n-dimensional variational data analysis for ocean observations, Geosci. Model Dev., 7, 225-241.

Bathmann U, Fischer G, Müller PJ, Gerdes D (1991) Short-term variations in particulate matter sedimentation off Kapp Norvegia, Weddell Sea, Antarctica: relation to water mass advection, ice cover, plankton biomass and feeding activity. Polar Biol 11.

Bednaršek N, Harvey CJ, Kaplan IC, Feely RA, Možina J (2016) Pteropods on the edge: Cumulative effects of ocean acidification, warming, and deoxygenation. Progress in Oceanography 145:1–24.

Berge J, Cottier F, Varpe Ø, Renaud PE, Falk-Petersen S, Kwasniewski S, Griffiths C, Søreide JE, Johnsen G, Aubert A, Bjærke O, Hovinen J, Jung-Madsen S, Tveit M, Majaneva S (2014) Arctic complexity: a case study on diel vertical migration of zooplankton. Journal of Plankton Research 36:1279–1297.

Bitiutskii DG, Samyshev EZ, Minkina NI, Melnikov VV, Chudinovskih ES, Usachev SI, Salyuk PA, Serebrennikov AN, Zuev OA, Orlov AM (2022) Distribution and Demography of Antarctic Krill and Salps in the Atlantic Sector of the Southern Ocean during Austral Summer 2021–2022. Water 14:3812.

Brierley A, Watkins J (1996) Acoustic targets at South Georgia and the South Orkney Islands during a season of krill scarcity. Mar Ecol Prog Ser 138:51–61.

Brown MS, Bowman JS, Lin Y, Feehan CJ, Moreno CM, Cassar N, Marchetti A, Schofield OM (2021) Low diversity of a key phytoplankton group along the West Antarctic Peninsula. Limnology & Oceanography 66:2470–2480.

Browne ET (1909) X.—The Medusæ of the Scottish National Antarctic Expedition. Trans R Soc Edinb 46:233–251.

Calbet A (2024) Holoplankton and Meroplankton: Two Peculiar Terms for Common Creatures. In: The Wonders of Marine Plankton. Springer, Cham.

Calbet A, Alcaraz M, Atienza D, Broglio E, Vaqué D (2005) Zooplankton biomass distribution patterns along the western Antarctic Peninsula (December 2002). Journal of Plankton Research 27:1195–1203.

Cisewski B, Strass VH, Rhein M, Krägefsky S (2010) Seasonal variation of diel vertical migration of zooplankton from ADCP backscatter time series data in the Lazarev Sea, Antarctica. Deep Sea Research Part I: Oceanographic Research Papers 57:78–94.

Clarke A, Murphy EJ, Meredith MP, King JC, Peck LS, Barnes DKA, Smith RC (2007) Climate change and the marine ecosystem of the western Antarctic Peninsula. Phil Trans R Soc B 362:149–166.

Clarke K, Warwick R (2001) A further biodiversity index applicable to species lists: variation in taxonomic distinctness. Mar Ecol Prog Ser 216:265–278.

Conroy J, Steinberg D, Thomas M, West L (2023) Seasonal and interannual changes in a coastal Antarctic zooplankton community. Mar Ecol Prog Ser 706:17–32.

Conroy JA, Steinberg DK, Thibodeau PS, Schofield O (2020) Zooplankton diel vertical migration during Antarctic summer. Deep Sea Research Part I: Oceanographic Research Papers 162:103324.

Constable AJ, Melbourne-Thomas J, Corney SP, Arrigo KR, Barbraud C, Barnes DKA, Bindoff NL, Boyd PW, Brandt A, Costa DP, Davidson AT, Ducklow HW, Emmerson L, Fukuchi M, Gutt J, Hindell MA, Hofmann EE, Hosie GW, Iida T, Jacob S, Johnston NM, Kawaguchi S, Kokubun N, Koubbi P, Lea M, Makhado A, Massom RA, Meiners K, Meredith MP, Murphy EJ, Nicol S, Reid K, Richerson K, Riddle MJ, Rintoul SR, Smith WO, Southwell C, Stark JS, Sumner M, Swadling KM, Takahashi KT, Trathan PN, Welsford DC, Weimerskirch H, Westwood KJ, Wienecke BC, Wolf-Gladrow D, Wright SW, Xavier JC, Ziegler P (2014) Climate change and Southern Ocean ecosystems I: how changes in physical habitats directly affect marine biota. Global Change Biology 20:3004–3025.

Cook AJ, Holland PR, Meredith MP, Murray T, Luckman A, Vaughan DG (2016) Ocean forcing of glacier retreat in the western Antarctic Peninsula. Science 353:283–286.

Costa RR, Mendes CRB, Ferreira A, Tavano VM, Dotto TS, Secchi ER (2021) Large diatom bloom off the Antarctic Peninsula during cool conditions associated with the 2015/2016 El Niño. Commun Earth Environ 2:252.

Costa RR, Mendes CRB, Tavano VM, Dotto TS, Kerr R, Monteiro T, Odebrecht C, Secchi ER (2020) Dynamics of an intense diatom bloom in the Northern Antarctic Peninsula, February 2016. Limnology & Oceanography 65:2056–2075.

Couto N, Martinson DG, Kohut J, Schofield O (2017) Distribution of U pper C ircumpolar D eep W ater on the warming continental shelf of the W est A ntarctic P eninsula. JGR Oceans 122:5306–5315.

Criales-Hernández MI, Jerez-Guerrero M, Latandret-Solana SA, Gómez-Sánchez MD (2022) Spatial distribution of meso- and macro-zooplankton in the Bransfield Strait and around Elephant Island, Antarctic Peninsula, during the 2019–2020 austral summer. Polar Science 32:100821.

Damini BY, Kerr R, Dotto TS, Mata MM (2022) Long-term changes on the Bransfield Strait deep water masses: Variability, drivers and connections with the northwestern Weddell Sea. Deep Sea Research Part I: Oceanographic Research Papers 179:103667.

David B, Saucède T (2015) History of Biodiversity in the Southern Ocean. In: *The Southern Ocean*. Elsevier, p 59–70

De Cáceres M, Legendre P, Moretti M (2010) Improving indicator species analysis by combining groups of sites. Oikos 119:1674–1684.

Deppeler SL, Davidson AT (2017) Southern Ocean Phytoplankton in a Changing Climate. Front Mar Sci 4.

Donnelly J, Sutton TT, Torres JJ (2006) Distribution and abundance of micronekton and macrozooplankton in the NW Weddell Sea: relation to a spring ice-edge bloom. Polar Biol 29:280–293.

Dotto TS, Kerr R, Mata MM, Garcia CAE (2016) Multidecadal freshening and lightening in the deep waters of the Bransfield Strait, Antarctica. JGR Oceans 121:3741–3756.

Dufrene M, Legendre P (1997) Species Assemblages and Indicator Species: The Need for a Flexible Asymmetrical Approach. Ecological Monographs 67:345.

Esquivel-Garrote O, Muxagata E (2023) Composition patterns of surface mesozooplankton in the zonal fronts of Drake Passage. Journal of Plankton Research 45:853–869.

Esquivel-Garrote O, Muxagata E, Hosie GW (2023) Spatial and temporal variation and distribution of mesozooplankton in the Drake Passage sampled with the continuous Plankton Recorder. Deep Sea Research Part I: Oceanographic Research Papers 192:103936.

Ferdous Z, Muktadir AKM (2009) A Review: Potentiality of Zooplankton as Bioindicator. American J of Applied Sciences 6:1815–1819.

Ferreira A, Costa RR, Dotto TS, Kerr R, Tavano VM, Brito AC, Brotas V, Secchi ER, Mendes CRB (2020) Changes in Phytoplankton Communities Along the Northern Antarctic Peninsula: Causes, Impacts and Research Priorities. Front Mar Sci 7:576254.

Flores H, Hunt BPV, Kruse S, Pakhomov EA, Siegel V, Van Franeker JA, Strass V, Van De Putte AP, Meesters EHWG, Bathmann U (2014) Seasonal changes in the vertical distribution and community structure of Antarctic macrozooplankton and micronekton. Deep Sea Research Part I: Oceanographic Research Papers 84:127–141.

Frey DI, Krechik VA, Morozov EG, Drozd ID, Gordey AS, Latushkin AA, Mekhova OS, Mukhametianov RZ, Murzina SA, Ostroumova SA, Ponomarev VI, Salyuk PA, Smirnova DA, Shutov SA, Zuev OA (2022) Water Exchange between Deep Basins of the Bransfield Strait. Water 14:3193.

Garcia MD, Dutto MS, Chazarreta CJ, Berasategui AA, Schloss IR, Hoffmeyer MS (2020) Micro- and mesozooplankton successions in an Antarctic coastal environment during a warm year. PLoS ONE 15:e0232614.

Garcia MD, Hoffmeyer MS, Abbate MCL, Barría De Cao MS, Pettigrosso RE, Almandoz GO, Hernando MP, Schloss IR (2016) Micro- and mesozooplankton responses during two contrasting summers in a coastal Antarctic environment. Polar Biol 39:123–137.

García MA, Castro CG, Ríos AF, Doval MD, Rosón G, Gomis D, López O (2002) Water masses and distribution of physico-chemical properties in the Western Bransfield Strait and Gerlache Strait during Austral summer 1995/96. Deep Sea Research Part II: Topical Studies in Oceanography 49:585–602.

Giesecke R, González HE (2012) Distribution and feeding of chaetognaths in the epipelagic zone of the Lazarev Sea (Antarctica) during austral summer. Polar Biol 35:689–703.

Gili J, Rossi S, Pagès F, Orejas C, Teixidó N, López-González P, Arntz W (2006) A new trophic link between the pelagic and benthic systems on the Antarctic shelf. Mar Ecol Prog Ser 322:43–49.

Gleiber MR, Steinberg DK, Schofield OME (2016) Copepod summer grazing and fecal pellet production along the Western Antarctic Peninsula. J Plankton Res 38:732–750.

Gorbatenko KM, Yakovenko VA (2023) Spatial Variability of Macro- and Mesozooplankton in the Bransfield Strait in January 2020. Oceanology 63:559–567.

Gordon AL, Nowlin WD (1978) The Basin Waters of the Bransfield Strait. J Phys Oceanogr 8:258–264.

Grant GC (1991) Chaetognatha From The Central And Southern Middle Atlantic Bight - Species Composition, Temperature-Salinity Relationships, And Interspecific Associations. VIMS Articles 89:33–40.

Griffiths JR, Kadin M, Nascimento FJA, Tamelander T, Törnroos A, Bonaglia S, Bonsdorff E, Brüchert V, Gårdmark A, Järnström M, Kotta J, Lindegren M, Nordström MC, Norkko A, Olsson J, Weigel B, Žydelis R, Blenckner T, Niiranen S, Winder M (2017) The importance of benthic–pelagic coupling for marine ecosystem functioning in a changing world. Global Change Biology 23:2179–2196.

Guglielmo L, Minutoli R, Bergamasco A, Granata A, Zagami G, Antezana T (2011) Short-term changes in zooplankton community in Paso Ancho basin (Strait of Magellan): functional trophic structure and diel vertical migration. Polar Biol 34:1301–1317.

Hartfield G, Blunden J, Arndt DS (2018) State of the Climate in 2017. Bulletin of the American Meteorological Society 99:Si-S310.

Havermans C, Auel H, Hagen W, Held C, Ensor NS, A. Tarling G (2019) Predatory zooplankton on the move: Themisto amphipods in high-latitude marine pelagic food webs. In: *Advances in Marine Biology*. Elsevier, p 51–92

Hays GC, Kennedy H, Frost BW (2001) Individual variability in diel vertical migration of a marine copepod: Why some individuals remain at depth when others migrate. Limnology & Oceanography 46:2050–2054.

Henley SF, Schofield OM, Hendry KR, Schloss IR, Steinberg DK, Moffat C, Peck LS, Costa DP, Bakker DCE, Hughes C, Rozema PD, Ducklow HW, Abele D, Stefels J, Van Leeuwe MA, Brussaard CPD, Buma AGJ, Kohut J, Sahade R, Friedlaender AS, Stammerjohn SE, Venables HJ, Meredith MP (2019) Variability and change in the west Antarctic Peninsula marine system: Research priorities and opportunities. Progress in Oceanography 173:208–237.

Henschke N, Blain S, Cherel Y, Cotte C, Espinasse B, Hunt BPV, Pakhomov EA (2021) Population demographics and growth rate of Salpa thompsoni on the Kerguelen Plateau. Journal of Marine Systems 214:103489.

Henschke N, Pakhomov EA (2019) Latitudinal variations in *Salpa thompsoni* reproductive fitness. Limnology & Oceanography 64:575–584.

Hernández-León S, Sangrà P, Lehette P, Lubián L, Almeida C, Putzeys S, Bécognée P, Andrade MP (2013) Zooplankton biomass and metabolism in the frontal zones of the Bransfield Strait, Antarctica. Journal of Marine Systems 111–112:196–207.

Hill MO (1973) Diversity and Evenness: A Unifying Notation and Its Consequences. Ecology 54:427–432.

Hopkins TL (1985) Food web of an Antarctic midwater ecosystem. Mar Biol 89:197–212.

Hopkins TL, Torres JJ (1989) Midwater food web in the vicinity of a marginal ice zone in the western Weddell Sea. Deep Sea Research Part A Oceanographic Research Papers 36:543–560.

Huneke WGC, Huhn O, Schröeder M (2016) Water masses in the Bransfield Strait and adjacent seas, austral summer 2013. Polar Biol 39:789–798.

Hunt BPV, Hosie GW (2006) The seasonal succession of zooplankton in the Southern Ocean south of Australia, part I: The seasonal ice zone. Deep Sea Research Part I: Oceanographic Research Papers 53:1182–1202.

Ibáñez-Tejero L, Ladah LB, Sánchez-Velasco L, Barton ED, Filonov A (2018) Vertical distribution of zooplankton biomass during internal tidal forcing under mesoscale conditions of upwelling and relaxation. Continental Shelf Research 171:1–11.

Jordano MDA, Miyake H, Nagata RM, Morandini AC (2022) Patterns of morphological development in Scyphozoa ephyrae (Cnidaria, Medusozoa). Mar Biodivers 52:31.

Kasyan VV (2023) Structure and Spatial Distribution of Mesozooplankton Communities in the Atlantic Sector of the Southern Ocean. Oceanology 63:550–558.

Kasyan VV, Bitiutskii DG, Mishin AV, Zuev OA, Murzina SA, Sapozhnikov PV, Kalinina OYu, Syomin VL, Kolbasova GD, Voronin VP, Chudinovskikh ES, Orlov AM (2022) Composition and Distribution of Plankton Communities in the Atlantic Sector of the Southern Ocean. Diversity 14:923.

Kerr R, Mata MM, Mendes CRB, Secchi ER (2018) Northern Antarctic Peninsula: a marine climate hotspot of rapid changes on ecosystems and ocean dynamics. Deep Sea Research Part II: Topical Studies in Oceanography 149:4–9.

King A, LaCasella EL (2003) Seasonal variations in abundance, diel vertical migration, and population structure of Metridia gerlachei at Port Foster, Deception Island, Antarctica. Deep Sea Research Part II: Topical Studies in Oceanography 50:1753–1763.

Knox GA (2006) Biology of the Southern Ocean.

Larson RJ (1986) Pelagic Scyphomedusae (Scyphozoa: Coronate and Semaeostomeae of the Southern Ocean. Antarctic Research Series 41:59–165.

Lee W, Kim S, Kang S-H, Bang HW, Lee KH, Kwak I-S (2004) Distribution and Abundance of Zooplankton in the Bransfield Strait and the Western Weddell Sea during Austral Summer. Ocean Polar Res 26:607–618.

Legendre P, Legendre L (2012) Ecological resemblance. In: *Developments in Environmental Modelling*. Elsevier, p 265–335

Leonor CM, Muxagata E (2025) Interannual variability in surface mesozooplankton in the Western Antarctic Peninsula during two anomalous years. Deep Sea Research Part I: Oceanographic Research Papers 217:104444.

Leonor CM, Muxagata E (2024) Vertical distribution of the zooplankton in the Antarctic Peninsula during the austral summer of 2017. An Acad Bras Ciênc 96:e20240144.

Liu Y, Wang Y, Sun Y, Yang G, Swadling KM (2024) Zooplankton vertical stratification in the East-pacific and Indian sectors of the Southern Ocean. Front Mar Sci 11:1274582.

Loeb V, Hofmann EE, Klinck JM, Holm-Hansen O (2010) Hydrographic control of the marine ecosystem in the South Shetland-Elephant Island and Bransfield Strait region. Deep Sea Research Part II: Topical Studies in Oceanography 57:519–542.

Loeb VJ, Santora JA (2012) Population dynamics of Salpa thompsoni near the Antarctic Peninsula: Growth rates and interannual variations in reproductive activity (1993–2009). Progress in Oceanography 96:93–107.

Lopez MDG, Huntley ME (1995) Feeding and diel vertical migration cycles of Metridia gerlachei (Giesbrecht) in coastal waters of the Antarctic Peninsula. Polar Biol 15.

Ludvigsen M, Berge J, Geoffroy M, Cohen JH, De La Torre PR, Nornes SM, Singh H, Sørensen AJ, Daase M, Johnsen G (2018) Use of an Autonomous Surface Vehicle reveals small-scale diel vertical migrations of zooplankton and susceptibility to light pollution under low solar irradiance. Sci Adv 4:eaap9887.

Mackas DL, Greve W, Edwards M, Chiba S, Tadokoro K, Eloire D, Mazzocchi MG, Batten S, Richardson AJ, Johnson C, Head E, Conversi A, Peluso T (2012) Changing zooplankton seasonality in a changing ocean: Comparing time series of zooplankton phenology. Progress in Oceanography 97–100:31–62.

Mackas DL, Sefton H, Miller CB, Raich A (1993) Vertical habitat partitioning by large calanoid copepods in the oceanic subarctic Pacific during Spring. Progress in Oceanography 32:259–294.

Mackas DL, Thomson RE, Galbraith M (2001) Changes in the zooplankton community of the British Columbia continental margin, 1985-1999, and their covariation with oceanographic conditions. Can J Fish Aquat Sci 58:685–702.

Manno C, Stowasser G, Enderlein P, Fielding S, Tarling GA (2015) The contribution of zooplankton faecal pellets to deep-carbon transport in the Scotia Sea (Southern Ocean). Biogeosciences 12:1955–1965.

Marrari M, Daly KL, Timonin A, Semenova T (2011) The zooplankton of Marguerite Bay, western Antarctic Peninsula—Part II: Vertical distributions and habitat partitioning. Deep Sea Research Part II: Topical Studies in Oceanography 58:1614–1629.

Marshall GJ, Di Battista S, Naik SS, Thamban M (2011) Analysis of a regional change in the sign of the SAM–temperature relationship in Antarctica. Clim Dyn 36:277–287.

Mayzaud P, Pakhomov EA (2014) The role of zooplankton communities in carbon recycling in the Ocean: the case of the Southern Ocean. Journal of Plankton Research 36:1543–1556.

Mendes CR, Cartaxana P, Brotas V (2007) HPLC determination of phytoplankton and microphytobenthos pigments: comparing resolution and sensitivity of a C_{18} and a C_{8} method. Limnology & Ocean Methods 5:363–370.

Mendes CRB, Costa RR, Ferreira A, Jesus B, Tavano VM, Dotto TS, Leal MC, Kerr R, Islabão CA, Franco ADODR, Mata MM, Garcia CAE, Secchi ER (2023) Cryptophytes: An emerging algal group in the rapidly changing Antarctic Peninsula marine environments. Global Change Biology 29:1791–1808.

Mendes CRB, De Souza MS, Garcia VMT, Leal MC, Brotas V, Garcia CAE (2012) Dynamics of phytoplankton communities during late summer around the tip of the Antarctic Peninsula. Deep Sea Research Part I: Oceanographic Research Papers 65:1–14.

Mendes CRB, Tavano VM, Dotto TS, Kerr R, De Souza MS, Garcia CAE, Secchi ER (2018) New insights on the dominance of cryptophytes in Antarctic coastal waters: A case study in Gerlache Strait. Deep Sea Research Part II: Topical Studies in Oceanography 149:161–170.

Mendes CRB, Tavano VM, Leal MC, De Souza MS, Brotas V, Garcia CAE (2013) Shifts in the dominance between diatoms and cryptophytes during three late summers in the Bransfield Strait (Antarctic Peninsula). Polar Biol 36:537–547.

Meredith MP, Inall ME, Brearley JA, Ehmen T, Sheen K, Munday D, Cook A, Retallick K, Van Landeghem K, Gerrish L, Annett A, Carvalho F, Jones R, Naveira Garabato AC,

Bull CYS, Wallis BJ, Hogg AE, Scourse J (2022) Internal tsunamigenesis and ocean mixing driven by glacier calving in Antarctica. Sci Adv 8:eadd0720.

Meredith MP, King JC (2005) Rapid climate change in the ocean west of the Antarctic Peninsula during the second half of the 20th century. Geophysical Research Letters 32:2005GL024042.

Meredith MP, Schofield O, Newman L, Urban E, Sparrow M (2013) The vision for a Southern Ocean Observing System. Current Opinion in Environmental Sustainability 5:306–313.

Michels J, Schnack-Schiel SB, Pasternak A, Mizdalski E, Isla E, Gerdes D (2012) Abundance, population structure and vertical distribution of dominant calanoid copepods on the eastern Weddell Sea shelf during a spring phytoplankton bloom. Polar Biol 35:369–386.

Moline MA, Claustre H, Frazer TK, Schofield O, Vernet M (2004) Alteration of the food web along the Antarctic Peninsula in response to a regional warming trend. Global Change Biology 10:1973–1980.

Montes-Hugo M, Doney SC, Ducklow HW, Fraser W, Martinson D, Stammerjohn SE, Schofield O (2009) Recent Changes in Phytoplankton Communities Associated with Rapid Regional Climate Change Along the Western Antarctic Peninsula. Science 323:1470–1473.

Nishikawa J, Naganobu M, Ichii T, Ishii H, Terazaki M, Kawaguchi K (1995) Distribution of salps near the South Shetland Islands during austral summer, 1990?1991 with special reference to krill distribution. Polar Biol 15.

Nishikawa J, Tsuda A (2001) Diel vertical migration of the tunicate Salpa thompsoni in the Southern Ocean during summer. Polar Biol 24:299–302.

Oksanen J (2022) Vegan: Community Ecology Package.

Øresland V (1990) Feeding and predation impact of the chaetognath Eukrohnia hamata in Gerlache Strait, Antarctic Peninsula. Mar Ecol Prog Ser 63:201–209.

Orselli IBM, Carvalho ACO, Monteiro T, Damini BY, Carvalho-Borges MD, Albuquerque C, Kerr R (2022) The marine carbonate system along the northern Antarctic Peninsula: current knowledge and future perspectives. An Acad Bras Ciênc 94:e20210825.

Orsi AH, Whitworth T, Nowlin WD (1995) On the meridional extent and fronts of the Antarctic Circumpolar Current. Deep Sea Research Part I: Oceanographic Research Papers 42:641–673.

Paffenhöfer G-A, Gibson DM (1999) Determination of generation time and asexual fecundity of doliolids (Tunicata, Thaliacea). J Plankton Res 21:1193–1189.

Pakhomov EA, Froneman PW, Perissinotto R (2002) Salp/krill interactions in the Southern Ocean: spatial segregation and implications for the carbon flux. Deep Sea Research Part II: Topical Studies in Oceanography 49:1881–1907.

Pakhomov EA, Hall J, Williams MJM, Hunt BPV, Stevens CJ (2011) Biology of Salpa thompsoni in waters adjacent to the Ross Sea, Southern Ocean, during austral summer 2008. Polar Biol 34:257–271.

Park C, Wormuth JH (1993) Distribution of antarctic zooplankton around Elephant Island during the austral summers of 1988, 1989, and 1990. Polar Biol 13.

Pinchuk AI, Batten SD, Strasburger WW (2021) Doliolid (Tunicata, Thaliacea) Blooms in the Southeastern Gulf of Alaska as a Result of the Recent Marine Heat Wave of 2014–2016. Front Mar Sci 8:625486.

Plum C, Cornils A, Driscoll R, Wenta P, Badewien TH, Niggemann J, Moorthi S (2021) Mesozooplankton trait distribution in relation to environmental conditions and the presence of krill and salps along the northern Antarctic Peninsula. Journal of Plankton Research 43:927–944.

Prézelin BB, Hofmann EE, Mengelt C, Klinck JM (2000) The linkage between Upper Circumpolar Deep Water (UCDW) and phytoplankton assemblages on the west Antarctic Peninsula continental shelf. Journal of Marine Research 58:165–202.

Richardson AJ (2008) In hot water: zooplankton and climate change. ICES Journal of Marine Science 65:279–295.

Richardson AJ, Kunz TJ (2006) Impacts of Climate Change on Zooplankton. In: *Impacts of Climate Change on Australian Marine Life, Part C: Literature Review*. Hobday, A.J., Okey, T.A., Poloczanska, E.S., Kunz, T.J. & Richardson, A.J., Canberra, Australia, p 19–25

Romero-Romero S, Choy CA, Hannides CCS, Popp BN, Drazen JC (2019) Differences in the trophic ecology of micronekton driven by diel vertical migration. Limnology & Oceanography 64:1473–1483.

Ruiz Barlett EM, Tosonotto GV, Piola AR, Sierra ME, Mata MM (2018) On the temporal variability of intermediate and deep waters in the Western Basin of the Bransfield Strait. Deep Sea Research Part II: Topical Studies in Oceanography 149:31–46.

Sabatini ME (2008) El Ecosistema de la Plataforma Patagónica Austral, Marzo-Abril 2000. Composición, Abundancia y Distribuición del Zooplancton. Rev Invest Desarr Pesq 19:5–21.

Sangrà P, Gordo C, Hernández-Arencibia M, Marrero-Díaz A, Rodríguez-Santana A, Stegner A, Martínez-Marrero A, Pelegrí JL, Pichon T (2011) The Bransfield current system. Deep Sea Research Part I: Oceanographic Research Papers 58:390–402.

Schiariti A, Kawahara M, Uye S, Mianzan HW (2008) Life cycle of the jellyfish Lychnorhiza lucerna (Scyphozoa: Rhizostomeae). Mar Biol 156:1–12.

Schnack-Schiel SB (2002a) Aspects of the study of the life cycles of Antarctic copepods. In: *Copepoda: Developments in Ecology, Biology and Systematics*. Developments in Hydrobiology, Lopes RM, Reid JW, Rocha CEF (eds) Kluwer Academic Publishers, Dordrecht, p 9–24

Schnack-Schiel SB (2002b) Aspects of the study of the life cycles of Antarctic copepods. In: *Copepoda: Developments in Ecology, Biology and Systematics*. Developments in Hydrobiology, Lopes RM, Reid JW, Rocha CEF (eds) Kluwer Academic Publishers, Dordrecht, p 9–24

Schofield O, Cimino M, Doney S, Friedlaender A, Meredith M, Moffat C, Stammerjohn S, Van Mooy B, Steinberg D (2024) Antarctic pelagic ecosystems on a warming planet. Trends in Ecology & Evolution:S0169534724002003.

Secchi ER, Dalla Rosa L, Kinas PG, Nicolette RF, Rufino ANM, Azevedo AF (2020) Encounter rates and abundance of humpback whales (Megaptera novaeangliae) in Gerlache and Bransfield Straits, Antarctic Peninsula. JCRM:107–111.

Seyboth E, Botta S, Mendes CRB, Negrete J, Dalla Rosa L, Secchi ER (2018) Isotopic evidence of the effect of warming on the northern Antarctic Peninsula ecosystem. Deep Sea Research Part II: Topical Studies in Oceanography 149:218–228.

Skvarca P, Rack W, Rott H, Donángelo TI (1999) Climatic trend and the retreat and disintegration of ice shelves on the Antarctic Peninsula: an overview. Polar Research 18:151–157.

Smetacek V (1999) Diatoms and the Ocean Carbon Cycle. Protist 150:25–32.

Smith DA, Hofmann EE, Klinck JM, Lascara CM (1999) Hydrography and circulation of the West Antarctic Peninsula Continental Shelf. Deep Sea Research Part I: Oceanographic Research Papers 46:925–949.

Smith WO, Ainley DG, Arrigo KR, Dinniman MS (2014) The Oceanography and Ecology of the Ross Sea. Annu Rev Mar Sci 6:469–487.

Steedman H (1976) Monographs on oceanographic methodology No 4 - Zooplankton fixation and preservation, 4th ed.

Steinberg DK, Ruck KE, Gleiber MR, Garzio LM, Cope JS, Bernard KS, Stammerjohn SE, Schofield OME, Quetin LB, Ross RM (2015) Long-term (1993–2013) changes in macrozooplankton off the Western Antarctic Peninsula. Deep Sea Research Part I: Oceanographic Research Papers 101:54–70.

Steiner NS, Bowman J, Campbell K, Chierici M, Eronen-Rasimus E, Falardeau M, Flores H, Fransson A, Herr H, Insley SJ, Kauko HM, Lannuzel D, Loseto L, Lynnes A, Majewski A, Meiners KM, Miller LA, Michel LN, Moreau S, Nacke M, Nomura D,

Tedesco L, Van Franeker JA, Van Leeuwe MA, Wongpan P (2021) Climate change impacts on sea-ice ecosystems and associated ecosystem services. Elementa: Science of the Anthropocene 9:00007.

Straehler-Pohl I, Jarms G (2010) Identification key for young ephyrae: a first step for early detection of jellyfish blooms. Hydrobiologia 645:3–21.

Stukel MR, Décima M, Selph KE, Gutiérrez-Rodríguez A (2021) Size-specific grazing and competitive interactions between large salps and protistan grazers. Limnol Oceanogr, 66: 2521-2534.

Ter Braak CJF, Prentice IC (1988) A Theory of Gradient Analysis. In: *Advances in Ecological Research*. Elsevier, p 271–317

Tokarczyk R (1987) Classification of water masses in the Bransfield Strait and southern part of the Drake Passage using a method of statistical multidimensional analysis. Polish Polar Research 8:333–366.

Torres Parra RR, Caicedo Laurido AL, Iriarte Sánchez JD (2020) Hydrographic conditions during two austral summer situations (2015 and 2017) in the Gerlache and Bismarck straits, northern Antarctic Peninsula. Deep Sea Research Part I: Oceanographic Research Papers 161:103278.

Turner J (2004) The El Niño–southern oscillation and Antarctica. Intl Journal of Climatology 24:1–31.

Venkataramana V, Kerkar AU, Mishra RK, Sabu P, Anilkumar N (2022) Hydrodynamics and zooplankton assemblages in Prydz Bay, East Antarctica, during the austral summer of 2017. Regional Studies in Marine Science 52:102341.

Ward P, Tarling GA, Thorpe SE (2014) Mesozooplankton in the Southern Ocean: Spatial and temporal patterns from Discovery Investigations. Progress in Oceanography 120:305–319.

Ward P, Whitehouse M, Meredith M, Murphy E, Shreeve R, Korb R, Watkins J, Thorpe S, Woodd-Walker R, Brierley A, Cunningham N, Grant S, Bone D (2002) The Southern

Antarctic Circumpolar Current Front: physical and biological coupling at South Georgia. Deep Sea Research Part I: Oceanographic Research Papers 49:2183–2202.

Wickham H (2016) Ggplot2: Elegant Graphics for Data Analysis.

Yang G, Li C, Wang Y, Zhang Y (2017) Vertical profiles of zooplankton community structure in Prydz Bay, Antarctica, during the austral summer of 2012/2013. Polar Biol 40:1101–1114.

Yebra L, Hernández-León S, Almeida C, Bécognée P (2009) Metabolism and biomass vertical distribution of zooplankton in the Bransfield Strait during the austral summer of 2000. Polar Research 28:415–425.

Zhou M, Niiler PP, Hu J-H (2002) Surface currents in the Bransfield and Gerlache Straits, Antarctica. Deep Sea Research Part I: Oceanographic Research Papers 49:267–280.

APÊNDICE 1

Artigo submetido ao periódico *Progress in Oceanography*, o qual encontra-se em revisão.

Spatiotemporal Patterns and Environmental Drivers of Meso- and Macrozooplankton Communities in the Northern Antarctic Peninsula (2017–2019)

Spatiotemporal Patterns and Environmental Drivers of Meso- and Macrozooplankton Communities in the Northern Antarctic Peninsula (2017–2019)

Letícia Cazarin Baldoni*[a,b], Vanessa Ochi Agostini[c] and Erik Muxagata[a,b]

[a]Laboratório de Zooplâncton, Universidade Federal do Rio Grande, Instituto de Oceanografia, Av. Itália, km 8, 96203-900 Rio Grande, RS, Brazil

[b]Programa de Pós-Graduação em Oceanografia Biológica, Universidade Federal do Rio Grande, Instituto de Oceanografia, Av. Itália, km 8, 96203-900 Rio Grande, RS, Brazil

[c]Regenera Moléculas do Mar, Prédio 43421, Av. Bento Gonçalves, 9500 - 117 - Agronomia, 91501-970 Porto Alegre, RS, Brazil

***Corresponding author (e-mail):** l.baldoni.lb@gmail.com

Abstract

Identifying variations in species composition in marine environments is crucial to monitor climate change effects, particularly in the Northern Antarctic Peninsula (NAP), one of the fastest warming regions on the planet. This study examined the spatial and vertical distribution of meso- and macrozooplankton in the Gerlache and Bransfield Straits and part of the Bellingshausen Sea over three austral summers (2017-2019). The water column structure influenced zooplankton composition, with higher abundances recorded at depths of 200-300 m in 2018, linked to lower water column stability. A notable predominance of *Salpa thompsoni* was observed associated with higher surface temperatures, greater water column stability, and a dominance of small phytoplankton such as cryptophytes and dinoflagellates. In 2018, cooler conditions and a slight deepening of the mixed layer favored diatoms and copepods, including *Metridia* spp. copepodites. In 2019, greater stability related to lower surface salinity favored cryptophytes and small copepod species like *Ctenocalanus citer* and *Oithona* spp. in the Gerlache Strait, while diatoms and calanoid copepods remained dominant in Bransfield. Diel vertical migration influenced distribution patterns, with higher surface abundances during twilight and at greater depths during the day, benefiting *Metridia* spp. This study emphasizes that the presence of *Salpa thompsoni* significantly alters meso- and macrozooplankton community structure, primarily affecting small copepods and early developmental stages, which increased in abundance in its absence, becoming important components of the community. These changes affect the Southern Ocean plankton food

web, with implications for energy and carbon transport and potential cascading effects on the Antarctic ecosystem.

Keywords: Zooplankton, Northern Antarctic Peninsula, *Salpa thompsoni*, Water column stability

1. Introduction

In recent decades, notable impacts of the increased ocean and air temperatures, shifts in ocean fronts, and regional variations in sea ice extent during winter have been reported in the Southern Ocean (SO) [1,2]. These changes are particularly evident in the Northern Antarctic Peninsula (NAP), a transition area between subpolar and polar regions, with complex hydrographic conditions and seasonal sea ice dynamics that impact abiotic and biotic components of the ecosystem [3–6].

The NAP includes the Bransfield and Gerlache Straits, northwestern Weddell Sea and portions of the northeastern Bellingshausen Sea as well as the southern portion of the Drake Passage. This region provides a unique habitat for diverse biological communities and is critical for studying Southern Ocean processes and the impacts of climate variability [7]. Seasonal and interannual changes in sea ice cover and hydrographic conditions, including intrusions of Antarctic Circumpolar Current (ACC), affect temperature and salinity profiles, which are closely linked to the structure and function of both phytoplankton and zooplankton communities [4,8].

Phytoplankton are crucial in driving zooplankton seasonal cycles and interannual variability in abundance and distribution, as they serve as the primary food source for many meso- and macrozooplanktonic species [9,10]. In the NAP high concentrations of chlorophyll-*a* occur near the surface, particularly in areas close to the sea ice edge, such as the Gerlache Strait [3,11]. However, rapid warming of the ocean upper layers, linked to ice melt that reduces salinity and increases water column stratification, drives shifts in phytoplankton composition from large diatoms to smaller cells like cryptophytes [11,12]. These changes can significantly affect the composition, distribution, and abundance of meso- and macrozooplankton communities, since cryptophytes are efficiently grazed by salps, while Antarctic krill have selective feeding habits, preferring to graze on diatoms [10,12,13].

In addition to krill and salps, other zooplankton groups such as chaetognaths, cnidarians, and copepods play pivotal roles in shaping community structure. These animals can reach high abundances, exhibiting carnivorous, omnivorous, or herbivorous feeding habits, with some even preying on other members of the zooplankton community, which influences how they are structured throughout the water column [14]. Additionally, studies have shown that the mixed layer depth (MLD), along with the subsurface chlorophyll-*a* maximum, significantly impacts vertical distribution patterns in polar environments, where meso- and macrozooplankton organisms tend to concentrate just below the MLD [15,16]. Thus, in the SO, distinct depth strata can harbor unique zooplankton communities, driven by food availability [16] and the environmental gradients shaped by regional factors such as sea ice extent, salinity and temperature [17]. Therefore, understanding the biodiversity and biological interactions within these communities is essential to unravel the functioning of polar ecosystems.

Previous studies in the Antarctic environment highlight distinct vertical structures among various groups, with some aggregations forming to vertically partition the habitat, potentially reducing both intra- and interspecific competition [18]. Hopkins and Torres [19] observed greater diversity below the epipelagic strata (0–200 m) in the Weddell Sea. Similarly, Liu et al. [20] identified a clear distinction between epipelagic (0–200 m) and deeper strata communities in the SO Pacific sector, however, with higher abundance and dominance of copepods in the upper layers, while deeper layers were characterized by reduced abundance and dominance by other zooplankton groups.

In waters surrounding the NAP, Marrari et al. [21] also found distinct vertical distributions, attributed to species-specific behaviors, with some distributing themselves in a stratified manner to avoid competition, while others remained in the surface layers. Conroy et al. [16] observed different patterns of vertical distribution between the mesopelagic and epipelagic zones, with carnivorous taxa more abundant in the mesopelagic zone, while in the epipelagic zone, copepods and ostracods varied their abundances according to the photoperiod. In the NAP region, in the Bransfield Strait, Lee et al. [22] reported that the differences between the sampled depths were related to the life cycle patterns of copepods, with copepodites close to the surface and adults in deeper layers. Spatially, copepods dominated in some seasons, while salps and euphausiids dominated in others. Yebra et al. [23] observed that zooplankton abundances between the

epipelagic and mesopelagic layers were similar. Furthermore, Leonor and Muxagata [24] identified distinct patterns in the surface distribution of mesozooplankton between the Gerlache and Bransfield Straits, with data obtained through the Continuous Plankton Recorder (CPR). In 2016, the Copepoda group dominated the communities, while in 2017 there was a predominance of Salpidae, associated with anomalous environmental conditions, such as higher surface temperatures. The authors also observed higher surface abundances during the twilight period, evidencing diel vertical migration (DVM) patterns in the Bransfield Strait.

Despite minimal light variation during the polar summer, vertical differences in zooplankton distribution are often associated with diel, seasonal and ontogenetic migrations. These migrations play an important role in community structuring and can be driven by factors such as food search [16], predator avoidance or reduced competition [21]. They can occur in small amplitudes, concentrated in the upper 30 m of the water column [8], or asynchronously, in response to environmental changes, reproductive cycles or food availability [25].

In addition to vertical migrations, interannual variability in environmental conditions and food supply exerts a significant influence on distribution patterns. Biological processes such as reproduction, growth, and vertical shifts of zooplankton amplify differences between years, resulting in significant changes in the vertical organization of communities [16,26]. These factors reinforce the complexity of interactions between behavior, environment, and resource availability, which change annually and are essential to understanding the dynamics of polar ecosystems.

Although previous studies have identified distinct patterns in the vertical distribution of meso- and macrozooplankton in Antarctic environments [16,17,20], understanding of interannual variations between epipelagic and mesopelagic communities in the Northern Antarctic Peninsula (NAP) remains limited, especially between dynamic regions such as the Gerlache and Bransfield Straits. These straits, characterized by strong environmental gradients and the interaction of different water masses, represent key points for investigating how communities respond to environmental changes [7,27]. Leonor and Muxagata [28] assessed the vertical distribution of zooplankton in 2017, partially using subsets of the data analyzed in this work; however, applied to a broader group approach.

Understanding the composition and vertical distribution of zooplankton in these straits is essential to elucidate their role in biogeochemical fluxes, particularly in carbon export, complementing the knowledge already obtained in studies of specific taxa [28–30].

Given this, our study aimed to explore the spatial and temporal variation in the vertical composition of meso- and macrozooplankton communities in the NAP, correlating these patterns with environmental parameters and phytoplankton composition over three distinct years. The objective was to understand whether there is any pattern in the structure of these zooplankton communities in response to interannual environmental variations.

2. Materials and methods

2.1. Oceanographic sampling

Sampling was conducted on board the NPo Almirante Maximiano of the Brazilian Navy, during three different oceanographic cruises in the northern of the Antarctic Peninsula (NAP) (Figure 1), as part of the INTERBIOTA project ("Biological Interactions in marine ecosystems around the Antarctic Peninsula under different impacts of climate change") from GOAL (Grupo de Oceanografia de Altas Latitudes). These cruises took place in the late summer of 2017 (February - March), 2018 (February), and early summer of 2019 (January - February), collecting physical, chemical, and biological data. During these cruises, zooplankton sampling was conducted at 17 different oceanographic stations, resulting in 116 samples (Figure 1). However, due to logistical challenges, adverse sea conditions, and other cruise activities, not all stations were sampled consistently across the three years (Table 1).

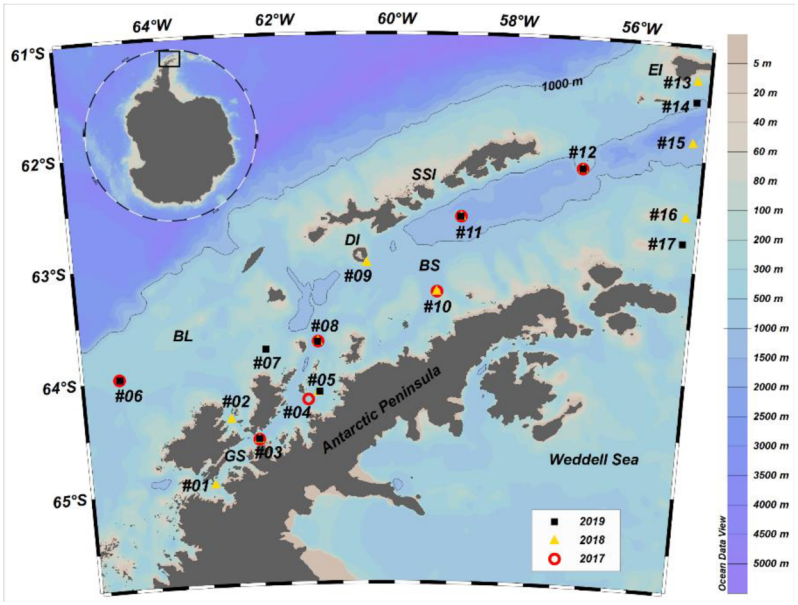


Figure 1: Map of the study area with 17 zooplankton sampling stations over 3 years (2017, 2018, and 2019).

Hydrographic data (temperature and salinity) and water samples to evaluate phytoplankton composition and the dynamics of the water column were collected with a Sea-Bird CTD (conductivity–temperature–depth instrument)/Carrousel 911+system® equipped with 24 five-liter Niskin bottles in all GOAL stations (Figure 1; see Avelina et al. [31]). The seawater was filtered under low vacuum through Glass fiber filters (Whatman ® GF/F) and the filters were frozen in liquid nitrogen for later High-Performance Liquid Chromatography (HPLC)/Chemical Taxonomy (CHEMTAX) analysis [32] to ascertain pigments and phytoplankton community composition.

Table 1: Summary of zooplankton sampling stations across the three years and locations. A dash (-) indicates that the station was not sampled that year.

Year/Locations	Gerlache Strait					Bellingshausen Sea		Bransfield Strait									
2017	-	-	#03	#04	-	#06	-	#08	-	#10	#11	#12	-	-	-	-	-
2018	#01	#02	#03	-	#05	-	-	#08	#09	#10	#11	#12	#13	-	#15	#16	-
2019	-	-	#03	-	#05	#06	#07	#08	-	-	#11	#12	-	#14	-	-	#17

The meso- and macrozooplankton communities were sampled with a MultiNet® (Type Midi - Hydrobios), equipped with 300 µm nets on 7, 12, and 9 stations in 2017, 2018, and 2019, respectively. Vertical trawls were conducted in five strata (500-400 m; 400-300 m; 300-200 m; 200-100 m and 100-0 m) if the depth of the location allowed. The filtered

volume was obtained using flowmeters coupled to the Multinet. The samples were fixed with a 4% formalin solution neutralized with borax [33].

2.2. Physical properties of seawater analysis

Seawater thermodynamic calculations were performed with the Thermodynamic Equation of Seawater - 2010 (TEOS-10). Based on seawater conservative temperature, absolute salinity, and pressure data, the seawater potential density (kg m–3) referenced to 0 dbar was determined for each CTD cast. To examine the water column physical structure, the mixed layer depth (MLD; m) was calculated as the depth at which seawater potential density deviates from its 10 m depth value by a threshold of 0.03 kg m–3 (de Boyer Montégut et al. 2004). We also used the seawater potential density to calculate water column stability (x10–6 m–1) as a function of buoyancy frequency by the local gravity, as described by Costa et al. [34].

2.3. Laboratory analysis

The concentration of Chl-*a* and class-specific accessory pigments was measured by high-performance liquid chromatography (HPLC), as described in Costa et al. [34]. The absolute (mg m Chl-*a*) and relative (%) contribution of phytoplankton chemotaxonomic groups were estimated via Chemical taxonomy (CHEMTAX) software v1.95 [32]. Seven algal groups were chosen for CHEMTAX analysis based on initial pigment ratios derived for the NAP [4,35]. The groups include diatoms Type-A, diatoms Type-B, dinoflagellates Type-A, dinoflagellates Type-B, cryptophytes, haptophytes Type 8 (*Phaeocystis antarctica* Karsten, 1905), and green flagellates. The two types of diatoms and dinoflagellates were grouped as the same chemotaxonomic group: the diatoms (sum of diatoms Type-A and diatoms Type-B) and the dinoflagellates (sum of dinoflagellates Type-A and dinoflagellates Type-B), respectively. CHEMTAX results were optimized following Wright et al. [36]. The procedure of quality control was performed by microscopic analysis. We focus our pigment analysis on diatoms and cryptophytes, as both groups show specific biomarker pigments (Chl-c1 and alloxanthin, respectively) and compose the main phytoplankton groups along the NAP [4,27].

The organisms present in the zooplankton samples were quantified and identified in a stereo microscope. The analysis was performed on the entire sample, ensuring all

organisms were accounted for. Immature stages (e.g. copepodites) were identified and quantified to a higher taxonomic level (because of difficulties in identification) while adults were identified to the lowest possible taxonomic level. The abundances were expressed as ind.1000 m-3.

2.4. Statistical analysis

Values of temperature, salinity, and chlorophyll-*a* were averaged for each 100-meter depth stratum sampled. The variation indices for these variables were calculated as the difference between the values at the subsurface (5 m) and those at the maximum depth reached by the Multinet. These indices represent how much salinity, temperature, and chlorophyll-*a* varied within each 100-meter stratum. Higher indices indicate greater differences between surface and deeper layers, with higher values of temperature, salinity, and chlorophyll-*a* concentrated in the surface layer of each stratum in the water column.

Multiple linear regression were calculated to evaluate the contribution of each phytoplankton group in relation to the total chlorophyll-*a* concentration considering the pigments of five phytoplankton groups: Diatoms, Dinoflagellates, *Phaeocystis antarctica*, Cryptophytes and Green flagellates.

Non-Metric Multidimensional Scaling (nMDS) with Bray-Curtis similarity was obtained to summarize the patterns of the structure of the meso- and macrozooplankton communities across the three years. For all statistical analyses of the meso- and macrozooplankton community, we used the "Hellinger" transformation in the abundance (ind.1000m^{-3}) of each taxa that occurred in more than 20% of the samples. We used this transformation because it better handles the heterogeneity of abundance data, balancing the influence of rare and dominant species [37]. Those species that appeared in less than two samples or whose relative abundance was less than 0.6% were excluded from the analysis to avoid rare, poorly resolved taxa dominating the analysis.

A PERMANOVA test was performed, based on 999 permutations to determine if there were significant differences in the community composition and abundance of phytoplankton and zooplankton found between years, sites, and in different sampled strata. We divided the samples according to the locations that were sampled: Bellingshausen Sea (BL), Bransfield Strait (BS,) and Gerlache Strait (GS). In addition,

the PERMANOVA test was performed to evaluate differences in the composition and abundance of the planktonic communities between periods (day and twilight). For each sampling, "day" and "twilight" periods were defined based on sampling times retrieved from the NOAA website [38]. All these analyses were calculated using the R “vegan” package [39], and all plots were generated using the “ggplot2” package [40]. Similarity analyses (SIMPER) [41] were performed to determine the contribution of taxa to discriminate between the years. Indicator Species Analysis (ISA) with the “indicspecies” package [42] was also conducted to identify species strongly associated with specific strata. The 95% confidence level (p-value ≤ 0.05) was used to identify indicator species [43].

Species richness and diversity indexes of the different strata for each station were calculated through Hill numbers, with the exponential of the Shannon-Weaver index (Exp H′) and the inverse of the Simpson index (1/D) [44].

We also applied a canonical correspondence analysis to explore the relationships between meso- and macrozooplankton community variations with environmental variables (CCA; [45] using the Vegan package [39]. The environmental variables comprised the mean water column temperature, salinity, and chlorophyll-*a* for each 100 m depth interval; the variation indexes for temperature, salinity, and chlorophyll-*a*; water column stability; the mixed layer depth (MLD); and the maximum and minimum values of temperature, salinity, and chlorophyll-*a* of each 100 m depth interval. An ANOVA test for the CCA was conducted to identify the variables that were most significant in the analysis (p-value < 0.05). Subsequently, the CCA was recalculated using only the significant variables. Furthermore, we applied another CCA analysis only to the surface stratum data (0–100 m) to evaluate the relationship of these meso and macrozooplankton communities with the different phytoplankton groups. All diversity indexes and statistical analyses were made in R v.4.2.0 (R Core R Development Core Team 2022).

3. Results

3.1. Oceanographic data

Maximum temperatures were recorded in 2017 in the northwestern sector of the BS, and BL, with the highest temperature (3.2°C) recorded at the surface of 0-100 m layer at

station #06 in the Bellingshausen Sea. In contrast, the minimum temperatures were observed in the eastern and southeastern of the BS in 2018, with the lowest temperature (-1.3°C) occurring in the 100–200 layer, at station #16. During the three years, lower salinities on the surface of the 0-100 layer were consistent in the GS, while high salinities were recorded in the southeastern portion of the BS (Figure 2).

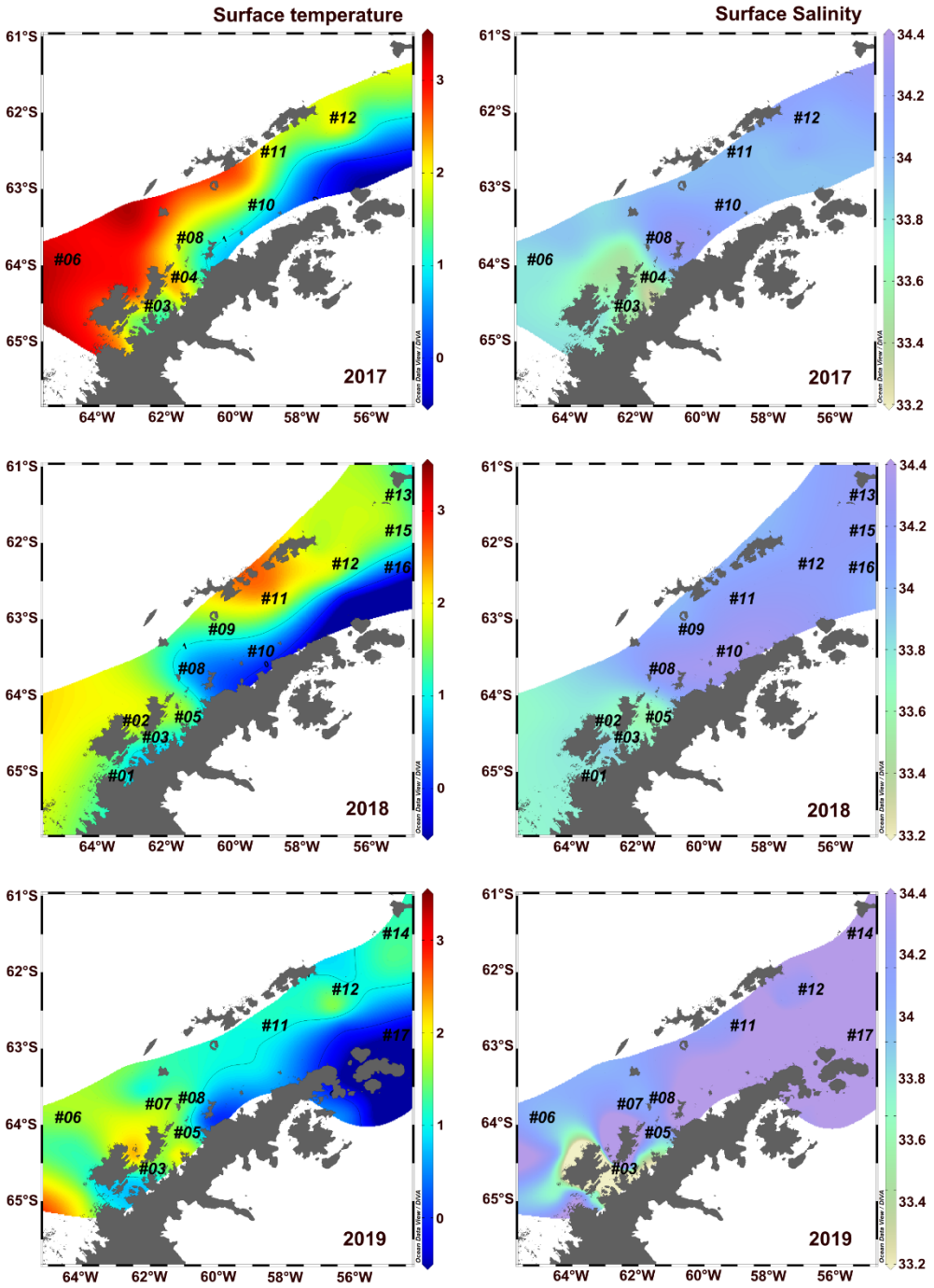


Figure 2: Maps showing the distribution of surface temperature and salinity of the NAP during the three years sampled.

The NAP was under the influence of water masses from surrounding areas over the three years analyzed. Warmer, lower-salinity waters were found in 2017 on top layers contrasted with cooler, higher-salinity conditions in 2018 and 2019, as evidenced by the T-S diagram. (Figure 3). The Antarctic Surface Water (AASW) was observed in the upper 150 m of the water column, characterized by temperatures ranging from -0.6°C to 3.2°C and salinities between 33.3 and 34.4. Modified Circumpolar Deep Water (mCDW) was identified at intermediate layers, with interannual variability in its distribution and properties, only in select stations of NAP (Figure 3). In 2017, mCDW was present at station #07 between 140–270 m, with maximum temperatures of 1.7 °C. In subsequent years, mCDW depths deepened to 170–360 m (#01, #02 and #09) in 2018 and 225–470 m in 2019 (#06 and #07). Dense Shelf Water (DSW) occupied the deeper layers, with higher salinity levels consistently observed in 2019 compared to 2017 and 2018 (Figure 3).

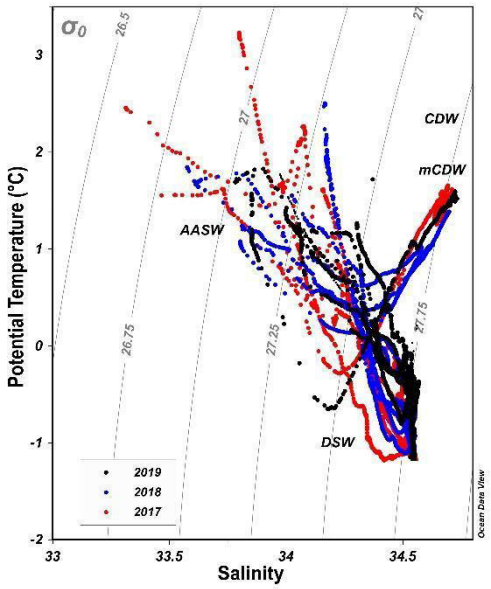


Figure 3: TS diagram showing temperature and salinity profiles from 2017, 2018, and 2019.

The water column up to 500 m had a temperature range of 3.2 °C and -1.3 °C and salinity between 33.3 and 34.75. Overall, stations in BL, GS and western part of BS were more stratified, across years. The thermocline varied according to the location of each station. In 2017 the thermocline was shallower than recorded in other years varying between 35 - 60 m. In the eastern part of BS (e.g., stations #13, #15, and #16 in 2018; #14 and #17 in 2019), we observed a practically homogeneous water column.

The mixed layer depths (MLD) varied annually, ranging from 13–36 m in 2017, 15–76 m in 2018, and 20–70 m in 2019. The shallowest MLD was observed at station #07 in the GS (2017), while the deepest occurred at station #13 in the BS (2018). A moderate negative correlation (R = -0.46) between MLD and water column stability highlights that deeper MLDs corresponded to reduced stratification.

3.2. Phytoplankton community

The highest concentration of chlorophyll-*a* in the 0-100 layer was recorded in 2018, at station #05 (12.02 $mg.m^{-3}$) localized in GS and at #09 (9.44 $mg.m^{-3}$), situated near Deception Island (DI). These elevated chlorophyll levels were associated with the shallowest mixed layer depth and the presence of diatoms (Figure 4). Conversely, the lowest chlorophyll-*a* concentration (0.19 $mg.m^{-3}$) was observed in 2017 at station #12 in the BS, associated with a deep mixed layer and smaller phytoplankton cells. Figure 4 illustrates the contribution of major phytoplankton groups to the total chlorophyll-*a* concentration at the surface.

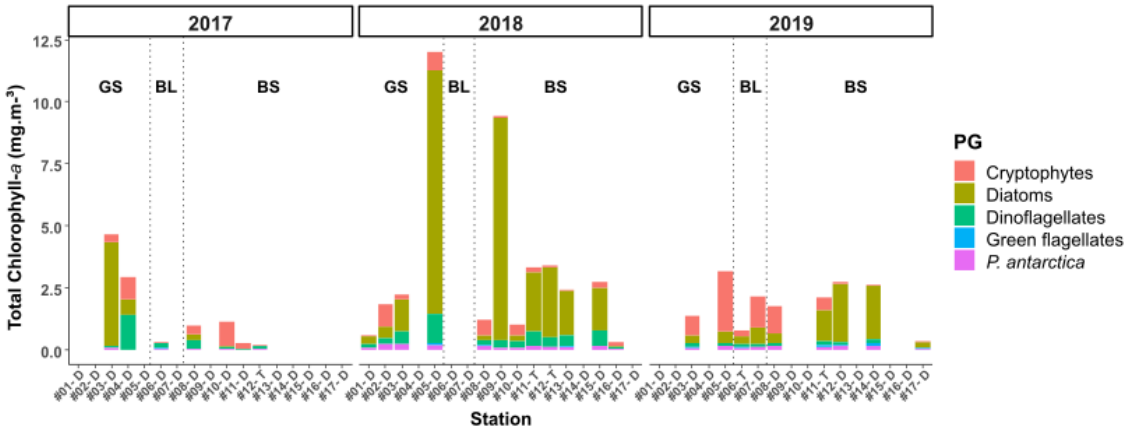


Figure 4: Distribution of chlorophyll-*a* concentration ($mg.m^{-3}$) at the surface across sampling station. Stations labeled with "D" were sampled during the daytime, while those labeled with "T" were sampled during twilight. The spatial distribution is as follows: #01 - #05 = Gerlache Strait (GS); #06 - #07 = Bellingshausen Sea (BL); #08 - #17 = Bransfield Strait (BS). The bars indicate the proportion of different phytoplankton groups: Diatoms, Dinoflagellates, *P. antarctica*, Cryptophytes, and Green flagellates.

Overall, high chlorophyll-*a* concentrations were primarily related to diatoms, which explained approximately 93.7% of the total chlorophyll-*a* variability across the three years, with a significant linear relationship ($F(1.26) = 405.6$, adjusted $R^2 = 0.937$, $p <$

0.001). In 2017, the phytoplankton community was dominated by smaller cells, such as dinoflagellates and cryptophytes, particularly in the BS, where diatoms were scarce. However, diatoms dominated at station #03 in the GS. In 2018, diatoms became the predominant group. By 2019, the distribution shifted significantly, with diatoms dominating in BS, while cryptophytes prevailed in GS and BL (Figure 4).

3.3. Meso and macrozooplankton community composition

Over the three years of sampling, 37451 individuals were counted and identified in 147 distinct taxonomic groups. Of these, 90 taxa were identified to species level, 37 to genus, and 20 at a higher taxonomic level (Table 2). In 2017, we identified 105 taxa, including 65 species, from a total of 9,943 organisms. In 2018, 113 taxonomic groups were recorded from 18,385 organisms, with 60 identified to species. In 2019, 9,123 organisms were found across 82 taxa, of which 45 were identified to species.

The most representative groups within the community were Calanoida, Cyclopoida, Salpidae, Ostracoda, Chaetognatha, Cnidaria, Polychaeta, Euphausiidae and Amphipoda, each displaying varying degrees of abundance and composition throughout the years. Calanoida copepods had the highest number of identified species, with a total of 44, followed by Amphipoda with 10 species, planktonic Polychaete with 9 species, and Cyclopoida with 7 species (Table 2).

Calanoid copepods were the most abundant and dominant group over the years, with 58% of total abundance in 2017, 68% in 2018, and 62% in 2019 (Figure 5). Over the years, we observed a slight increase in the relative abundances of copepods with cyclopoid doubling their contribution and salps disappearing from the samples (Figure 5). The proportion of the remaining groups was stable over the years. Euphausiids had very low abundances and the majority of specimens collected were juveniles. Pteropoda, Amphipoda, Cirripedia, Echinodermata, Doliolida and Fish larvae were the least abundant groups and were therefore categorized as "Others" (Figure 5).

Table 2: Taxonomic groups identified in the samples collected from 2017 to 2019. FO = Frequency of Occurrence, RA = Relative Abundance, Max. Ab. = Maximum Abundance, and N = Number of specimens found. N.I. = Not Identified.

Taxa	2017			2018			2019		
	FO (%)	AR (%)	Max. Ab. (ind.1000 m^{-3})	FO (%)	AR (%)	Max. Ab. (ind.1000 m^{-3})	FO (%)	AR (%)	Max. Ab. (ind.1000 m^{-3})
Dimophyes arctica	51.6	0.9	957	59.2	0.9	917	61.1	1.4	708
Diphyes antarctica	22.6	0.1	174	28.6	0.2	200	27.8	0.3	269
Diphyes dispar	3.2	0.0	43	0.0	0.0	0	0.0	0.0	0
Lensia spp.	0.0	0.0	0	0.0	0.0	0	2.8	0.0	43
Siphonophorae N.I.	0.0	0.0	0	34.7	0.4	679	47.2	0.4	259
Leuckartiara brownei	0.0	0.0	0	4.1	0.0	37	0.0	0.0	0
Solmundella bitentaculata	0.0	0.0	0	22.4	0.1	143	22.2	0.1	77
Corymorpha sp.	0.0	0.0	0	2.0	0.0	38	0.0	0.0	0
Cosmetirella davisi	6.5	0.0	40	6.1	0.1	429	2.8	0.0	38
Arctapodema spp.	3.2	0.0	38	32.7	0.4	474	36.1	0.5	385
Ephyra *Desmonema* sp.	0.0	0.0	0	2.0	0.0	37	0.0	0.0	0
Lepthotecatha	3.2	0.0	87	4.1	0.2	1238	0.0	0.0	0
Polychaeta larvae	41.9	0.5	565	79.6	1.5	1143	63.9	0.8	542
Vanadis antarctica	6.5	0.0	40	2.0	0.0	37	0.0	0.0	0
Vanadis spp.	3.2	0.0	40	4.1	0.0	80	0.0	0.0	0
Maupasia coeca	32.3	0.4	522	26.5	0.1	185	2.8	0.0	43
Pelagobia longicirrata	16.1	0.5	962	8.2	0.1	250	2.8	0.0	48
Tomopteris planktonis	0.0	0.0	0	10.2	0.0	74	2.8	0.0	143
Tomopteris carpenteri	0.0	0.0	0	14.3	0.1	111	0.0	0.0	0
Tomopteris lingulata	3.2	0.0	43	4.1	0.0	77	0.0	0.0	0
Tomopteris spp.	19.4	0.1	77	18.4	0.1	333	8.3	0.0	38
Typhloscolex mulleri	0.0	0.0	0	0.0	0.0	0	5.6	0.0	95
Travisiopsis coniceps	0.0	0.0	0	2.0	0.0	34	0.0	0.0	0
Traviopsis levinseni	3.2	0.0	43	0.0	0.0	0	0.0	0.0	0
Travisiopsis spp.	0.0	0.0	0	10.2	0.0	71	5.6	0.0	53
Limacina antarctica	6.5	0.0	120	2.0	0.0	71	5.6	0.0	77
Limacina retroversa australis	0.0	0.0	0	2.0	0.0	37	0.0	0.0	0
Clione limacina	6.5	0.0	43	2.0	0.0	77	0.0	0.0	0
Spongiobranchaea australis	6.5	0.0	40	2.0	0.0	42	2.8	0.0	36
Ostracoda N.I.	71.0	3.3	2000	83.7	5.1	3455	88.9	4.6	1643
Calanoides acutus	74.2	1.2	654	65.3	0.5	769	80.6	0.7	208
Calanoides brevicornis	6.5	0.1	333	0.0	0.0	0	0.0	0.0	0
Calanoides carinatus	3.2	0.0	77	2.0	0.0	74	0.0	0.0	0
Calanus simillimus	0.0	0.0	0	12.2	0.0	100	5.6	0.0	38
Calanus propinquus	12.9	0.1	87	14.3	0.1	200	2.8	0.0	36
Calanus spp.	0.0	0.0	0	4.1	0.0	77	0.0	0.0	0
Nannocalanus minor	3.2	0.0	120	0.0	0.0	0	0.0	0.0	0
Neocalanus tonsus	12.9	0.1	167	2.0	0.0	43	0.0	0.0	0
Neocalanus gracilis	0.0	0.0	0	4.1	0.0	71	0.0	0.0	0
Cop *Neoclanus* spp.	3.2	0.1	227	2.0	0.0	71	0.0	0.0	0
Cop *Calanoides* spp.	22.6	0.1	214	0.0	0.0	0	0.0	0.0	0
Cop *Calanus* spp.	3.2	0.0	40	0.0	0.0	0	0.0	0.0	0
Calanidae N.I.	25.8	0.1	160	30.6	1.1	3429	25.0	0.4	481
Calocalanus styliremis	3.2	0.0	40	0.0	0.0	0	0.0	0.0	0
Calocalanus sp.	0.0	0.0	0	0.0	0.0	0	2.8	0.0	115
Paracalanus parvus parvus	3.2	0.0	74	0.0	0.0	0	0.0	0.0	0
Paracalanus sp.	9.7	0.1	261	2.0	0.0	40	5.6	0.0	36
Paracalanidae N.I.	0.0	0.0	0	0.0	0.0	0	0.0	0.0	0

Rhincalanus gigas	38.7	0.2	167	40.8	0.2	214	38.9	0.4	200
Rhincalanus nasutus	3.2	0.0	43	0.0	0.0	0	0.0	0.0	0
Cop *Subeucalanus* spp.	0.0	0.0	0	6.1	0.0	69	0.0	0.0	0
Cop *Eucalanus* spp.	0.0	0.0	0	2.0	0.0	37	0.0	0.0	0
Clausocalanus ingens	0.0	0.0	0	2.0	0.0	36	0.0	0.0	0
Clausocalanus spp.	3.2	0.0	77	4.1	0.0	133	22.2	0.5	607
Ctenocalanus citer	32.3	0.5	565	87.8	5.2	11385	61.1	5.8	10704
Ctenocalanus sp.	0.0	0.0	0	4.1	0.2	1679	38.9	2.2	1846
Drepanopus spp.	3.2	0.0	154	38.8	0.9	1464	0.0	0.0	0
Microcalanus pygmaeus	0.0	0.0	0	57.1	5.1	7308	75.0	5.4	3333
Clausocalanidae N.I.	6.5	0.3	1217	12.2	0.7	4048	2.8	0.1	480
Aetideus pseudarmatus	3.2	0.0	69	0.0	0.0	0	0.0	0.0	0
Chiridius polaris	0.0	0.0	0	4.1	0.0	77	0.0	0.0	0
Chiridius sp.	3.2	0.0	34	0.0	0.0	0	2.8	0.0	43
Euchirella rostromagna	0.0	0.0	0	2.0	0.0	40	0.0	0.0	0
Gaetanus tenuspinus	12.9	0.1	200	24.5	0.3	462	19.4	0.2	286
Cop *Gaetanus* sp.	6.5	0.0	80	2.0	0.0	231	11.1	0.1	120
Cop *Aetideopsis* spp.	3.2	0.0	87	4.1	0.0	42	2.8	0.0	48
Paraeuchaeta antarctica	3.2	0.0	38	12.2	0.0	77	13.9	0.1	50
Paraeuchaeta austrina	3.2	0.0	80	0.0	0.0	0	0.0	0.0	0
Paraeuchaeta exigua	6.5	0.1	125	0.0	0.0	0	0.0	0.0	0
Paraeuchaeta pseudotonsa	3.2	0.0	83	0.0	0.0	0	0.0	0.0	0
Cop *Paraeuchaeta* spp.	64.5	5.3	4692	85.7	1.9	1357	72.2	2.6	1833
Undinella simplex	0.0	0.0	0	4.1	0.0	37	0.0	0.0	0
Amallothrix sp.	0.0	0.0	0	4.1	0.0	125	5.6	0.0	33
Pseudoamallothrix hadrosoma	6.5	0.0	130	0.0	0.0	0	0.0	0.0	0
Pseudoamallothrix cetonelis	3.2	0.0	38	0.0	0.0	0	0.0	0.0	0
Pseudoamallothrix spp.	0.0	0.0	0	32.7	0.2	375	16.7	0.1	111
Scaphocalanus enlogatus	3.2	0.0	38	2.0	0.0	38	0.0	0.0	0
Scaphocalanus spp.	9.7	0.1	174	6.1	0.0	190	2.8	0.0	48
Scolecithricella minor	29.0	0.3	391	42.9	0.5	593	44.4	0.6	474
Scolecithricella vittata	3.2	0.0	40	0.0	0.0	0	0.0	0.0	0
Scolecithricella spp.	3.2	0.0	77	0.0	0.0	0	2.8	0.0	63
Scolecithrix danae	0.0	0.0	0	2.0	0.0	50	0.0	0.0	0
Cop Scolecitrichidae N.I.	16.1	0.1	192	73.5	2.1	2174	72.2	1.2	760
Haloptilus ocellatus	0.0	0.0	0	6.1	0.0	36	8.3	0.0	53
Haloptilus oxycephalus	0.0	0.0	0	2.0	0.0	36	0.0	0.0	0
Haloptilus longicornis	0.0	0.0	0	2.0	0.0	111	0.0	0.0	0
Cop *Eugaliptilus* spp.	3.2	0.0	182	0.0	0.0	0	0.0	0.0	0
Heterorhabdus austrinus	3.2	0.0	77	6.1	0.0	95	0.0	0.0	0
Heterorhabdus lobatus	3.2	0.0	40	0.0	0.0	0	2.8	0.0	38
Heterorhabdus spinifrons	0.0	0.0	0	2.0	0.0	37	0.0	0.0	0
Heterorhabdus spp.	0.0	0.0	0	26.5	0.2	333	16.7	0.1	95
Lucicutia ovalis	0.0	0.0	0	2.0	0.0	37	0.0	0.0	0
Metridia gerlachei	83.9	17.2	22609	85.7	12.7	20643	83.3	10.0	8429
Metridia longa	16.1	0.3	448	18.4	0.3	880	13.9	1.2	2143
Metridia lucens	0.0	0.0	0	6.1	0.4	3077	22.2	0.5	893
Cop *Metridia* spp.	90.3	31.7	14565	98.0	36.4	46467	100.0	30.7	17821
Candacia maxima	0.0	0.0	0	0.0	0.0	0	2.8	0.0	38
Paralabidocera antarctica	0.0	0.0	0	0.0	0.0	0	2.8	0.0	43
Oithona spp.	67.7	6.3	4609	100.0	14.0	6667	100.0	21.6	8500
Triconia antarctica	48.4	1.4	2565	73.5	3.1	4048	75.0	3.5	2571
Oncaea mediterranea	6.5	0.0	77	0.0	0.0	0	0.0	0.0	0
Oncaea venusta	0.0	0.0	0	12.2	0.1	286	2.8	0.0	34
Oncaea spp.	12.9	0.1	125	42.9	0.8	1143	52.8	0.3	111
Agetus flaccus	6.5	0.0	40	0.0	0.0	0	0.0	0.0	0
Corycaeus speciosus	3.2	0.0	37	0.0	0.0	0	0.0	0.0	0
Onychorycaeus pacificus	3.2	0.0	80	0.0	0.0	0	0.0	0.0	0
Farranula gracilis	3.2	0.0	120	8.2	0.0	48	0.0	0.0	0

Manca stage	9.7	0.0	40	10.2	0.1	429	2.8	0.0	80
Eusirus sp.	0.0	0.0	0	8.2	0.0	71	0.0	0.0	0
Eusirus properdentatus	0.0	0.0	0	0.0	0.0	0	2.8	0.0	31
Eusirus perdentatus	3.2	0.0	38	0.0	0.0	0	0.0	0.0	0
Orchamenella spp.	3.2	0.0	43	4.1	0.0	40	0.0	0.0	0
Scina spp.	0.0	0.0	0	2.0	0.0	36	2.8	0.0	34
Cyllopus lucasi	9.7	0.0	45	0.0	0.0	0	5.6	0.0	77
Vibilia armata	12.9	0.1	148	0.0	0.0	0	0.0	0.0	0
Vibilia antarctica	9.7	0.1	120	0.0	0.0	0	0.0	0.0	0
Vibilia spp.	3.2	0.0	120	0.0	0.0	0	0.0	0.0	0
Hyperiella spp.	0.0	0.0	0	4.1	0.0	167	0.0	0.0	0
Hyperiella antarctica	0.0	0.0	0	0.0	0.0	0	2.8	0.0	105
Hyperoche medusarum	0.0	0.0	0	4.1	0.0	115	0.0	0.0	0
Hyperoche sp.	0.0	0.0	0	4.1	0.0	40	5.6	0.0	43
Themisto gaudichaudi	0.0	0.0	0	6.1	0.0	143	0.0	0.0	0
Primno macropa	3.2	0.0	38	10.2	0.0	67	5.6	0.0	67
Phronomella enlogata	3.2	0.0	37	0.0	0.0	0	0.0	0.0	0
Nauplio Euphausiidae	6.5	0.0	43	10.2	0.0	111	2.8	0.0	43
Calyptopis	19.4	0.2	348	24.5	0.3	846	58.3	0.5	370
Furcilia	0.0	0.0	0	20.4	0.1	321	5.6	0.0	42
Euphausia superba	9.7	0.0	40	2.0	0.0	36	2.8	0.0	71
Euphausia crystallorophias	0.0	0.0	0	2.0	0.0	37	5.6	0.0	38
Thysanoesa macrura	22.6	0.3	360	24.5	0.5	1680	5.6	0.0	63
Nauplio Cirripedia	3.2	0.0	77	0.0	0.0	0	2.8	0.0	31
Cipris Cirripedia	6.5	0.1	280	10.2	0.1	208	0.0	0.0	0
Brachiolaria Echinodermata	12.9	0.0	43	34.7	0.3	792	16.7	0.3	308
Eukrohnia hamata	67.7	4.6	3348	49.0	1.4	1880	41.7	1.4	750
Eukrohnia spp.	25.8	0.2	348	6.1	0.1	286	0.0	0.0	0
Pseudosagitta maxima	9.7	0.1	87	6.1	0.0	95	0.0	0.0	0
Pseudosagitta gazellae	3.2	0.0	38	4.1	0.0	77	5.6	0.0	36
Pseudosagitta spp.	9.7	0.0	43	6.1	0.0	115	2.8	0.0	43
Solidosagitta marri	0.0	0.0	0	2.0	0.0	45	0.0	0.0	0
Oikopleura spp.	3.2	0.0	115	26.5	0.2	231	33.3	0.2	120
Fritilaria spp.	0.0	0.0	0	16.3	0.1	148	19.4	0.3	741
Appendicularia N.I.	3.2	0.0	34	0.0	0.0	0	8.3	0.0	74
Dolioletta spp.	0.0	0.0	0	4.1	0.0	77	0.0	0.0	0
Salpa thompsoni	71.0	21.3	12600	0.0	0.0	0	0.0	0.0	0
Ihlea racovtzai	6.5	0.0	37	0.0	0.0	0	0.0	0.0	0
Ihlea magallanica	3.2	0.2	720	0.0	0.0	0	0.0	0.0	0
Fish larvae	3.2	0.0	37	2.0	0.0	43	5.6	0.0	42

The PERMANOVA test (p-value < 0.001) confirmed significant differences in community composition and abundances between the locations (GS, BL, and BS) over the years. In 2017 calanoids copepods were the dominant taxa accounting for 73% of the total abundance in GS, 76% in BL, and 49% in BS, followed by cyclopoids copepods with 11% in GS and in 15% in BL (Figure 5). However, in BS salps were the second major group that dominated the total of abundance, accounting 34%. Salps were scarce in GS (2%) and absent in BL. Chaetognatha was another important group in 2017 with 7% of total abundance in GS and BL, decreasing to 4% in BS, following the calanoids abundance.

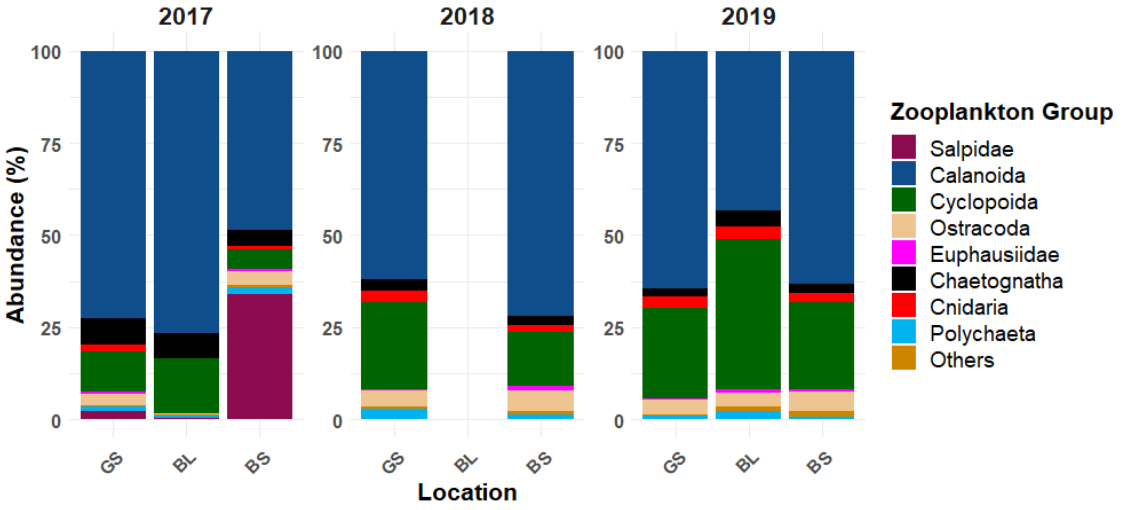


Figure 5: Temporal variation and contribution (percentage %) of the main taxonomic groups per year and location. GS = Gerlache Strait, BL = Bellingshausen Sea, BS = Bransfield Strait. In 2018, data was not sampled in BL.

Salps were absent in 2018 and 2019 (Figure 5). Among the samples of 2018 and 2019, calanoids, followed by cyclopoids and ostracods, dominated the total abundance in all locations. Cnidaria was also an important group in both years, with a slight decrease in its abundance from 2018 to 2019 in GS and an increase in BS, accounting for 4% of the total abundance in BL during 2019.

Among the 105 taxa found in 2017, adults of *M. gerlachei* were the most abundant taxa (max 22609 ind.1000 m^{-3}; see Table 2), recorded in GS, followed by unidentified *Metridia* copepodites (max 14565 ind.1000 m^{-3}), and salps aggregates of *Salpa thompsoni* (max 12600 ind.1000 m^{-3}), both recorded in BS. In 2018, copepodites of *Metridia* spp. reached a maximum abundance of 46467 ind.1000 m^{-3} in BS, being the most abundant taxa, followed by *M. gerlachei* (max 20643 ind.1000 m^{-3}). Other smaller copepods, like the calanoids *Ctenocalanus citer* (max 11385 ind.1000 m^{-3}), *Microcalanus pygmaeus* (max 7308 ind.1000 m^{-3}), and the cyclopoid *Oithona* spp. (6667 ind.1000 m^{-3}), were also recorded in great numbers in this year.

Small copepods dominated the taxa from 2019, with unidentified *Metridia* copepodites (max 17821 ind.1000 m^{-3}) and *C. citer* (max 10704 ind.1000 m^{-3}) being the most abundant in BS, followed by the cyclopoid *Oithona* spp. (max 8500 ind.1000 m^{-3}; see Table 2).

3.4. Spatial and temporal variation in the vertical distributions of meso- and macrozooplankton communities

Overall, in almost all stations, a vertical gradient was observed, mainly between the first two strata (0-200 m) and those from 200 to 500 m, reinforcing some vertical segregations. We observed that species richness increased with depth, with the lowest values in the first layer (0–100 m) and the highest values in the intermediate layers (from 200 to 400 m). The diversity indices followed a similar trend, with higher values associated with deeper or mid layers and lower diversity in upper layers. In 2017, the higher richness (22) was between 200-300 m, at station #10 in the BS, which also had the highest diversity indices across years (Shannon-Weaver Exp H': 2.5; Simpson 1/D: 0.9). In 2018 and 2019, higher species richness were reported at stations #02 and #05 (22 and 17, respectively) in the GS. However, in 2018 station #10 showed the highest diversity indices in intermediate layers (200- 400 m). Among 2019 stations, at #03 and #05, we recorded the higher diversity indices in deeper layers (400-500 m) (Figure 6).

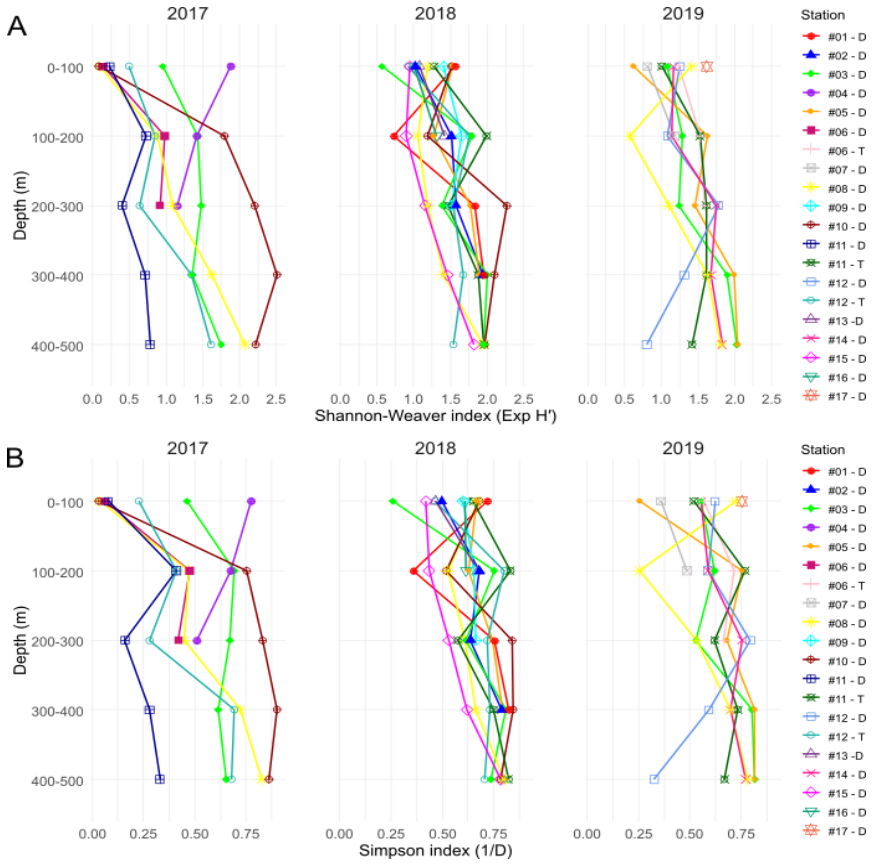


Figure 6: A: Shannon-Weaver (Exp H′) and B: the inverse of the Simpson (1/D) for each station sampled (#01 - #05 = Gerlache Strait; #06 - #07 = Bellingshausen Sea; #08 - #17 = Bransfield Strait) across years. Stations with 'D' indicate daytime sampling, and 'T' indicate twilight sampling.

Despite interannual and spatial variations, the dominance of copepods, particularly calanoids, was a common feature across all years, depths, and locations. In the stations sampled in GS (Figure 7), during 2017, they were dominant especially between depths of 200-300 m and 300-400 m, standing out at stations #04 and #06. Cyclopoida were less abundant than calanoids, but consistently present in the 100-400 m layers. The highest concentration of organisms was observed in the intermediate layers (200-400 m), while shallower layers (0-100 m) showed lower diversity and abundance (Figure 7). Station #04 exhibited the highest abundance of meso and macrozooplankton community from 2017, with 50,695 ind.1000 m^{-3} between 200-300 m.

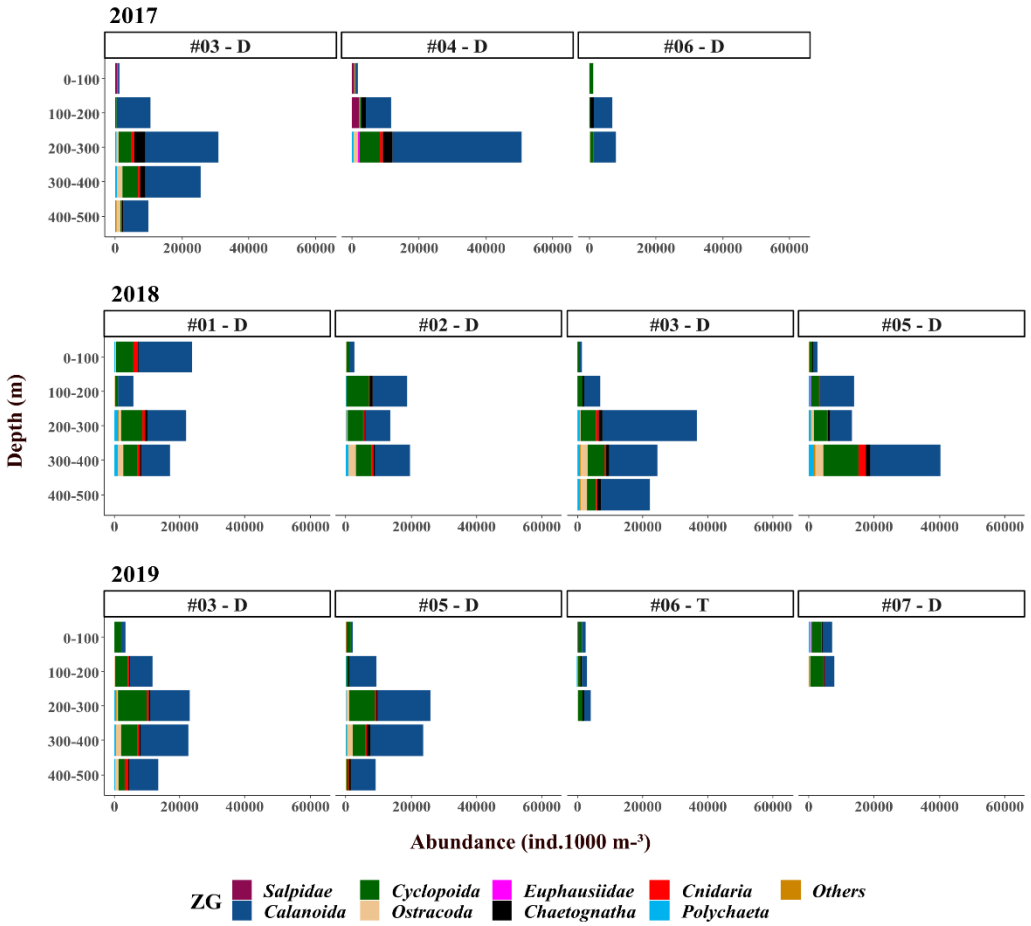


Figure 7: Vertical distribution of the meso- and macrozooplankton groups across all stations sampled in Gerlache (#01, #02, #03, #04, and #05) and Bellingshausen (#06 and #07) over three years (2017 – 2019).

Salps had a very limited presence in the GS and only in 2017, being observed in small abundances at the first layer (0-100 m) at stations #03 and #04. Their abundance was low compared to other groups. Ostracods appeared in small quantities, but mainly in the deepest layers of each station (200-400 m; #03 and #04). Euphausiids, chaetognaths, and polychaetes showed a modest presence, mainly at intermediate depths (200-400 m), but without reaching considerable abundances, while cnidarians, although poorly represented at all depths, were more notable in the upper layers (Figure 7). During 2018 and 2019 in GS stations, the community maintained their patterns through the water column, with increased presence of cyclopoids and polychaetes in intermediate and deep layers. Samples collected in BL also showed a dominance of calanoids through the water column. On the only twilight station (#06 from 2019), we observed a decrease in the abundance, mainly in the 0-100 m layer. The considerable presence of chaetognaths between 100-200 m was noted (Figure 7).

Regarding the samples gathered from the BS, we observed significant differences (p-value = 0.041) in the abundances between sampling periods (daytime and twilight). Although abundances in the first stratum (0 - 100 m) were low in almost all stations, we observed an increase in abundances during the twilight period, mainly in salps evident in stations #12 in 2017 and cyclopoids and calanoids at #11 and #12 in 2018, for example (Figure 8). However, in the twilight station #11 of 2019, there was no increase in abundances in the first strata.

Despite this, copepods still dominated the water column in BS (Figure 8). However, in 2017, when salps were present, both cyclopoids and calanoids were particularly abundant in the deeper layers (300-500 m), except at station #11, where salps were highly abundant throughout the water column. Cyclopoids were also common across all depths. During the samplings conducted in 2018, their abundances increased in the upper strata (0-100 m) during twilight samples, alongside a rise in euphausiid abundance. Furthermore, it was observed that euphausiids were more abundant in the first three strata of station #08 and the upper layers (0-200 m) of station #15, both during the day.

Overall, chaetognaths and ostracods showed more scattered distributions, with a notable presence in the upper and intermediate layers (200-500 m), over the years, while

polychaetes were mostly observed in 2018 samples, in intermediate and deeper layers (200 – 500 m).

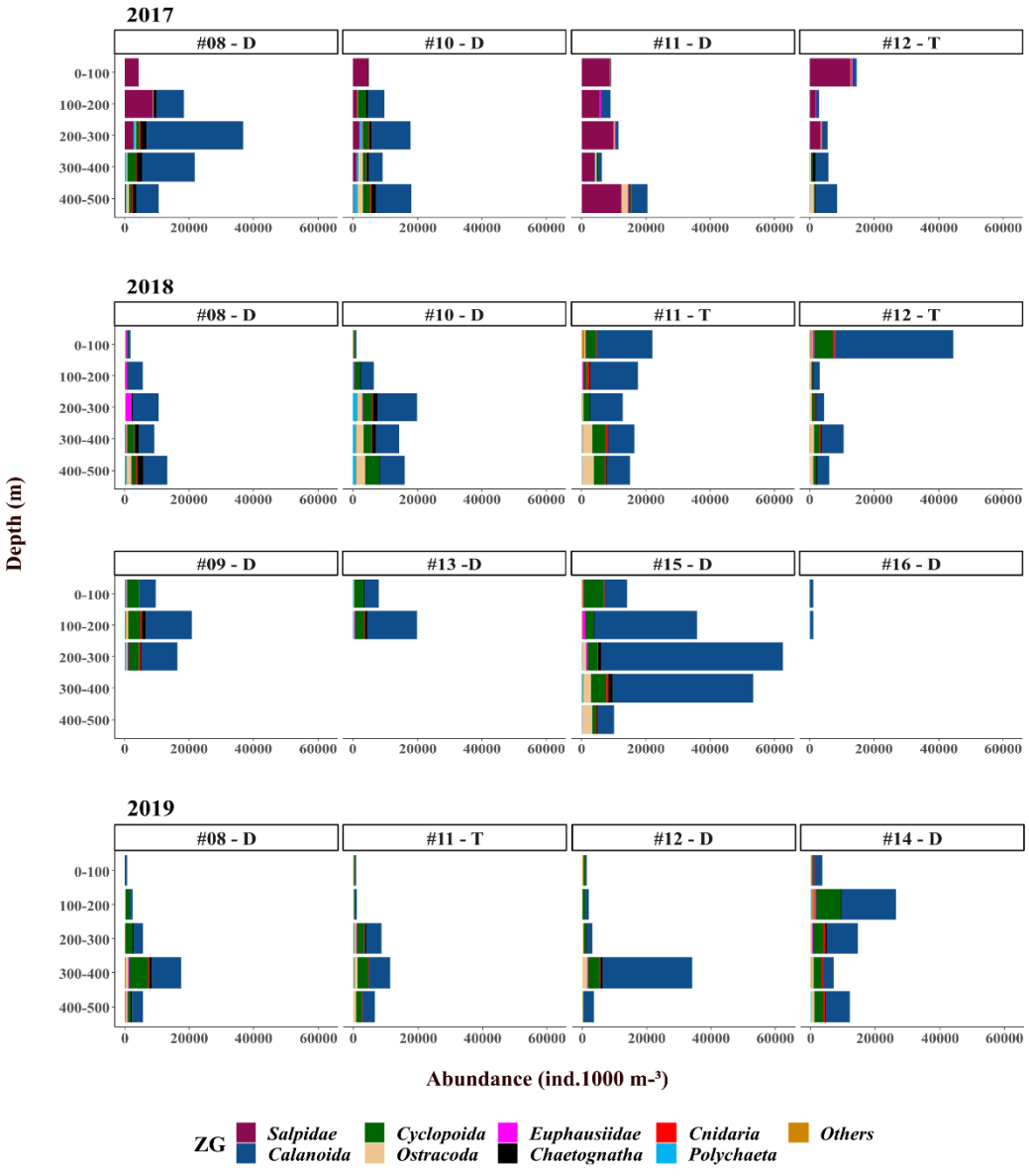


Figure 8: Vertical distribution of the meso- and macrozooplankton groups across all stations sampled in Bransfield over three years (2017 – 2019).

In 2018, we recorded the highest total abundance of the meso- and macrozooplankton community (62,600 ind.1000 m^{-3}), observed between 200-300 m at station #15, located in the eastern part of BS (Figure 8). For 2019, the highest abundance was recorded between 300-400 m at station #12, with 34035 ind.1000 m^{-3} (Figure 8). Additionally, in

2019, the lowest total abundance of the meso and macrozooplankton community between years was observed in the first stratum (0-100 m) at station #08 (682 ind.1000 m^{-3}), located in the western part of BS.

Of the remaining groups “Others" found in GS, BL, and BS, amphipods, were generally present in low abundances across all stations and years sampled, with higher abundances in intermediate layers (200–300 m), when present. Appendicularia and pteropods were identified in all years with lower abundances, with appendicularian concentrations more evident in the first two strata (0–200 m), while pteropods in intermediate and deeper strata, with contributions up to 300 m depth. Fish larvae were observed twice at station #11 in 2017, during the day in the first stratum, and in 2018, during the twilight, between (200-300 m). Doliolida (*Dolioletta* spp.) also were recorded twice only in 2018, at station #10 (200- 300 m) and #15 (300 – 400 m) for the first time in the region.

In general, larval stages in 2017 were concentrated in the 200-300 m strata, with a particular emphasis on Calyptopis larvae. These larvae were found at the surface during twilight at station #12, while in daytime samples, they were present at intermediate depths. In 2018, the highest abundance of larvae occurred in the 300-400 m strata during the day, whereas twilight samples showed higher concentrations in the upper strata (0-100 m). Polychaete larvae were restricted to greater depths, regardless of the sampling period. The highest surface abundances were observed during twilight, driven by the presence of echinoderm and furcilia larvae. While furcilia larvae were also found at the surface during the day, their numbers were smaller. Calyptopis followed a similar pattern, appearing in the first strata at twilight but with greater abundance in daytime samples. In 2019, larvae were most abundant between 200-300 m, but the first strata of twilight samples (stations #6 and #11) showed very low larval abundances or none at all. Despite these observed patterns, no significant differences in the vertical distribution of larvae were observed between daytime and twilight samples.

Among calanoids, *Metridia gerlachei* exhibited a broad vertical and spatial distribution but was more abundant in the mid layers (200–400 m; Figure 9 and 10), in all locations. The vertical pattern of *Metridia* spp. copepodites mirrored that of adults that were broadly distributed across all depth layers but were particularly abundant in intermediate and deeper layers (200–400 m; Figure 9 and 10). Other main species, such as *C. citer*,

concentrated their abundances between 100–200 m in GS and BS (Figs. 9 and 10), while *Microcalanus pygmaeus* was more abundant in the stations sampled in Gerlache and generally found in middle layers (200–300 m; Figure 9), also being collected on deeper strata (300–500 m), mainly in BS (Figure 10).

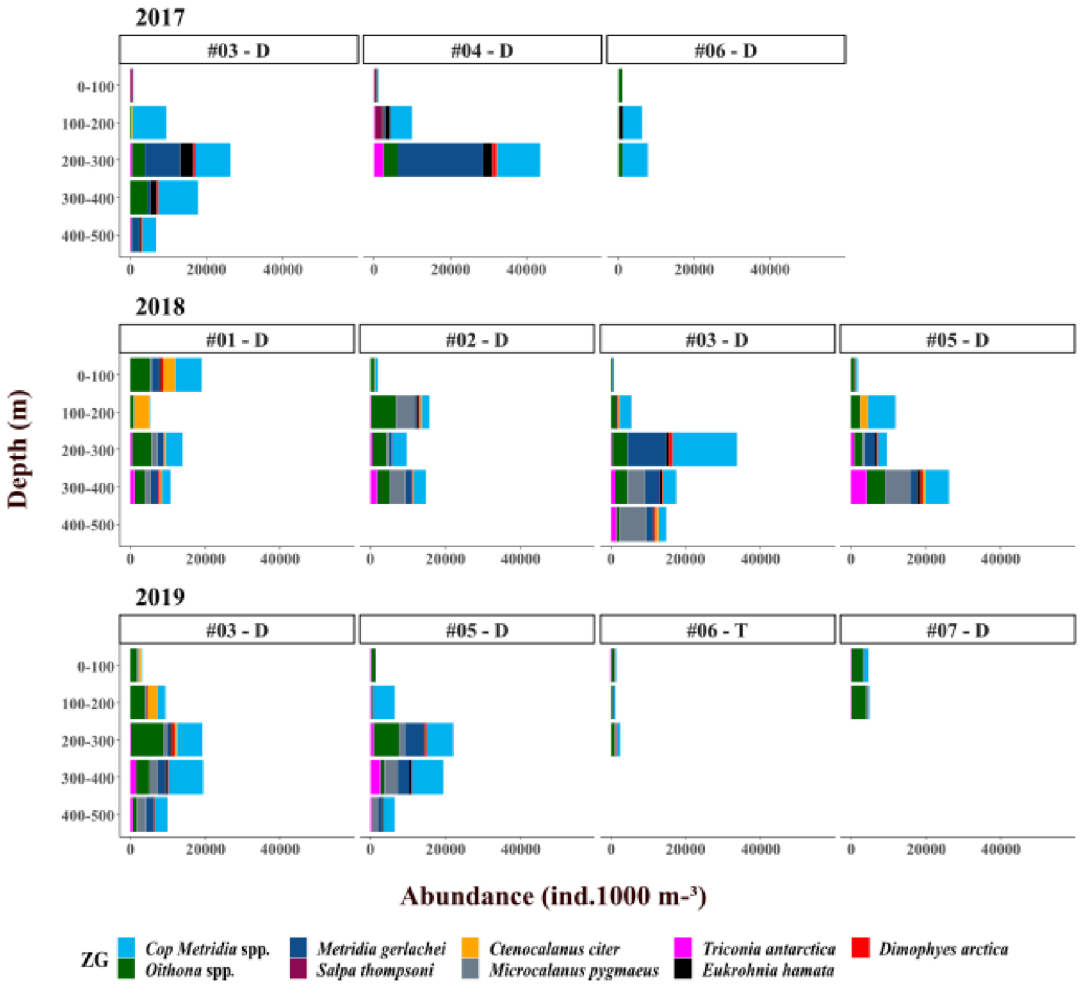


Figure 9: Vertical distribution of the main taxa from the meso- and macrozooplankton communities across all stations sampled in Gerlache (#01, #02, #03, #04 and #05) and Bellingshausen (#06 and #07) over three years (2017 – 2019)

Triconia antarctica exhibited a notable presence between 200–500 m, with consistent contributions across all years, but more evident in GS (Figure 9). Similarly, *Oithona* spp. was widely distributed across all depths but showed peaks in abundance in the mid layers (200 - 300 m) in GS (Figure 9) and upper layers (0–200 m) in BS (Figure 10).

Among other groups, *S. thompsoni* was more common in the first two strata (0 – 200 m), mainly in BS (Figure 10). *E. hamata*, the most representative species of Chaetognatha, showed notable variation across depth layers, with higher abundances concentrated in the

mid layers (200–300 m), although occasional presence was recorded in deeper strata in BS (Figure 10). The siphonophore *Dimophyes arctica*, was more abundant in the 200 – 300 m layers in GS (Figure 9), with sporadic occurrences in deeper layers, while in BS, its presence was more restricted to the bottom (Figure 10).

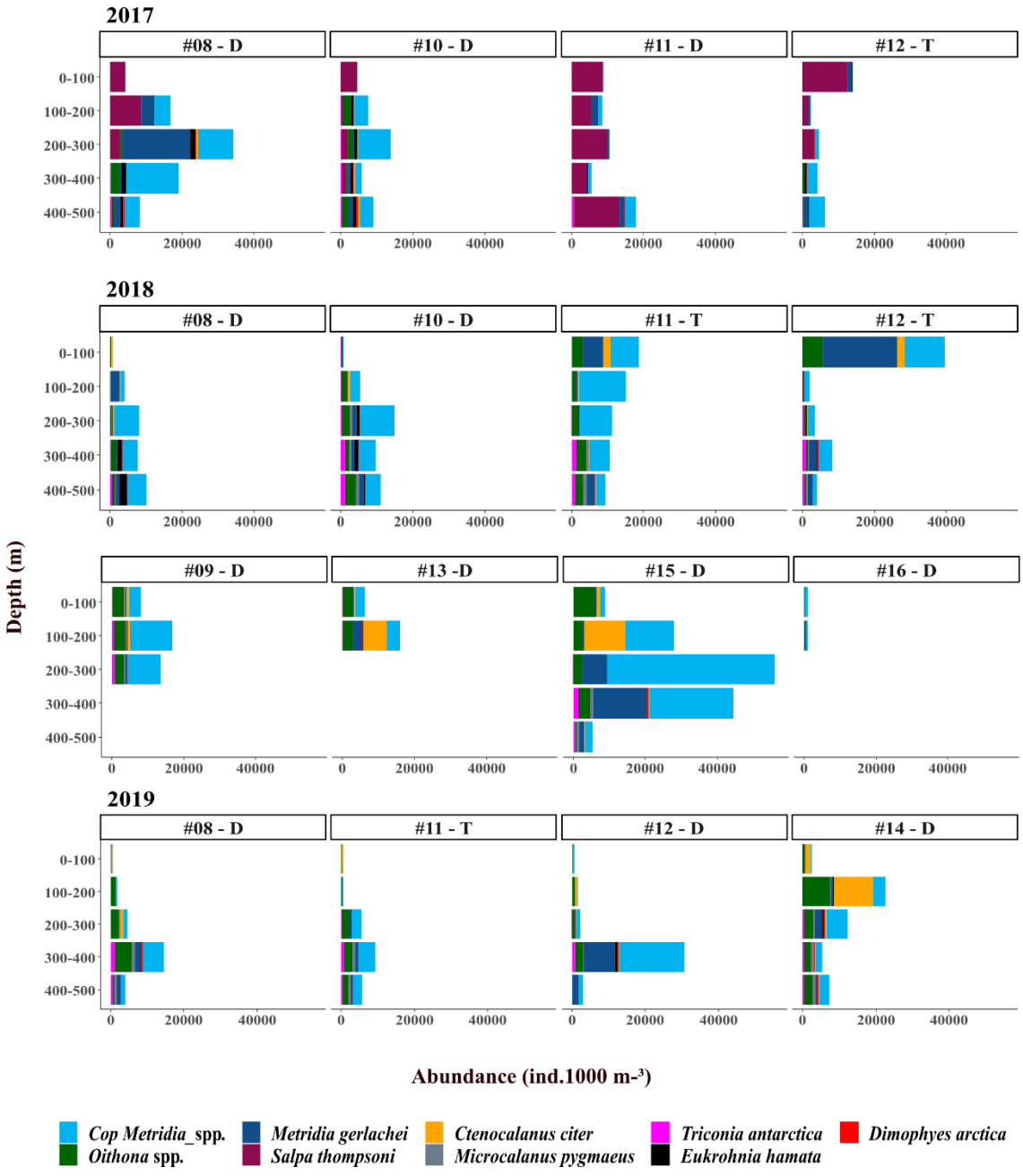


Figure 10: Vertical distribution of the main taxa from the meso- and macrozooplankton communities across all stations sampled in Bransfield over three years (2017 – 2019)

Variations in the proportions of these dominant taxa likely contributed to observed interannual and vertical patterns. The nMDS analysis (Figure 11) highlights the clear

difference in the composition and abundance of the meso- and macrozooplankton communities across years and depth strata. The 2017 samples are notably distinct, clustering separately from those collected in 2018 and 2019. Even with some overlaps, it was possible to highlight differences mainly between the upper layers and the deepest ones, confirming significant interannual and vertical differences (p-value < 0.001) observed in the PERMANOVA test results.

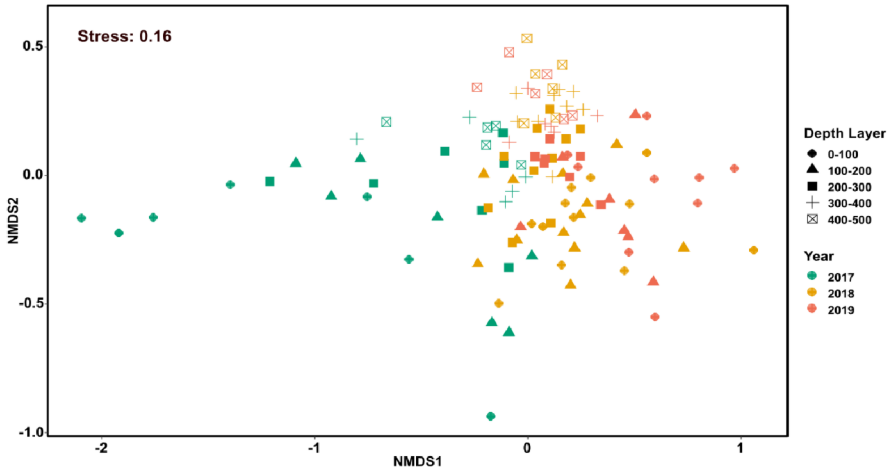


Figure 11: nMDS plot with the meso and macrozooplankton community distribution across three years, categorized by depth layers: Surface layer (0-100 m), subsurface layer (100-200 m), mid layers (200-400 m) and deep layer (400-500 m).

The SIMPER analysis indicated that *S. thompsoni* was the species that most contributed to the dissimilarities between years. *M. pygmaeus*, *C. citer*, *Oithona* spp. and *T. antarctica* contributed to the differences observed between 2018 and 2019. Contribution of *C. acutus* and *E. hamata* was recorded for 2017 and 2019 dissimilarities (Table 3).

Table 3: Percentage of contributions from species that demonstrated significant dissimilarities (p-value< 0.001) between sampled years (2017 – 2019) from SIMPER analysis.

Species/Year	2017 - 2018	2017 - 2019	2018 - 2019
Calanoides acutus	-	0.75	-
Microcalanus pygmaeus	-	-	0.044
Ctenocalanus citer	-	-	0.053
Oithona spp.	-	-	0.108
Triconia antarctica	-	-	0.026
Eukrohnia hamata	2.4	2.7	-
Salpa thompsoni	14.6	17.7	-

The species indicator analysis showed the most significant taxa, which were preferentially associated with determinate depth ranges (Table 4). *Oithona* spp. exclusively was the taxa that showed a significant association with the first stratum (0-100 m). *C. citer* showed an extremely significant association with the first two strata (0-200 m) and *S. minor* with the 100-300 m strata. For the 200-300 and 400-500 m depths, *M. gerlachei* was the most significantly associated taxa. Three taxa were associated with the two deepest strata (300-400 and 400-500 m): *T. antarctica*, *Arctapodema* spp., and *M. pygmaeus*. In the intermediate (200-400 m) and deep (400-500 m) strata, species such as *D. arctica*, D. antarctica and *E. hamata* were strongly associated. The copepodites of *Metridia* spp. showed an extremely significant association in all strata except the first (0-100 m) (Table 4).

Table 4: Species indicators for each Depth Strata combination with significant values (p-value <0.05)

Depth Strata	Taxa	p-value	
0-100	*Oithona* spp.	0.016	*
0-100 + 100-200	*Ctenocalanus citer*	0.0001	***
100-200 + 200-300	*Scolecithricella minor*	0.0037	**
200-300 + 400-500	*Metridia gerlachei*	0.0035	**
300-400 + 400-500	*Triconia antarctica*	0.0001	***
	Arctapodema spp.	0.0001	***
	Microcalanus pygmaeus	0.0002	***
200-300 + 300-400 + 400-500	*Dimophyes arctica*	0.0001	***
	Diphyes antarctica	0.0004	***
	Eukrohnia hamata	0.0019	**
100-200 + 200-300 + 300-400 + 400-500	Cop *Metridia* spp.	0.0001	***

3.5. Relationship between surface meso- and macrozooplankton community with phytoplankton groups

Through CCA analysis of the first stratum, we found that phytoplankton groups accounted for 52.3% of the total variation in the meso- and macrozooplankton community, with the first two axes explaining 49.3% of the variance. A distinct relationship emerged between the sampled years and the taxonomic groups: 2017 samples were closely associated with the presence of *S. thompsoni*, related to dinoflagellates, and cryptophytes; 2018 samples showed a stronger connection to diatoms; and 2019 samples were more broadly dispersed across the plot (Figure 12).

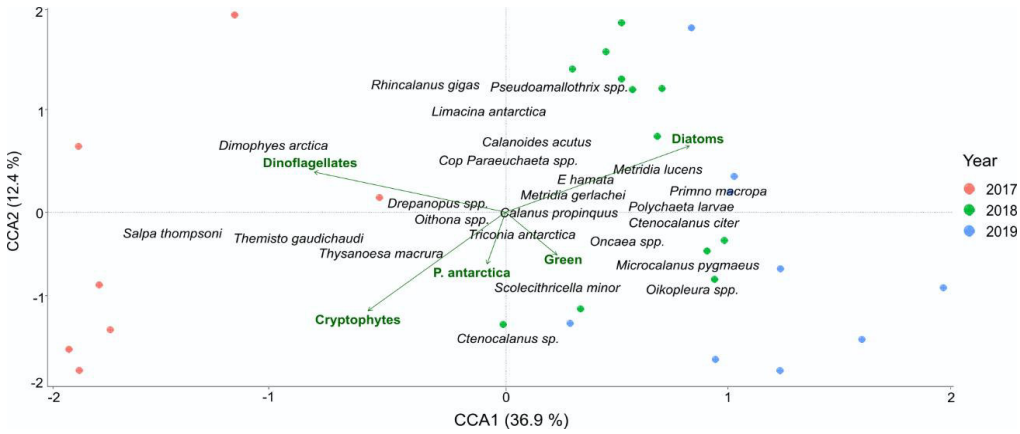


Figure 12: Canonical correspondence analysis (CCA) of surface meso- and macrozooplankton community relative to major phytoplankton groups within the upper 100 meters in the 3 years of sampling (2017, 2018, and 2019)

The analysis also reveals significant differences (p-value < 0.001) in the surface communities (first 100 m) in relation to the different phytoplankton groups, as observed through the PERMANOVA test, and highlights specific associations between phytoplankton and meso and macrozooplankton groups (Figure 12). Overall, diatoms were the group with the greatest significant impact on the structure of the meso and macrozooplankton community among the groups analyzed, and were strong associated to calanoid copepods, such as *C. propinquus*, *M. gerlachei*, *M. lucens* and *C. acutus*. On the other hand, cryptophytes were related to the salp *S. thompsoni*, the euphausiid *T. macrura*, the amphipod *T. gaudichaudii* and the cyclopoid copepod *Oithona* spp (Figure 12). Furthermore, despite being at the top of the plot, the calanoid copepods *Rhincalanus gigas*, *Pseudoamallothrix* spp., and the pteropod *Limacina antarctica* also showed associations with the diatom communities.

3.6. Influence of environmental variables on the meso – and macrozooplankton community

The canonical axes generated by Canonical Correspondence Analysis (CCA) explained 23% of the total variance in species abundance (Figure 13). Nevertheless, the CCA results allowed the identification of significant patterns in the spatial distribution of species and their associations with environmental variables, such as chlorophyll-*a* index, maximum temperature and salinity, stability, temperature variability (temperature index).

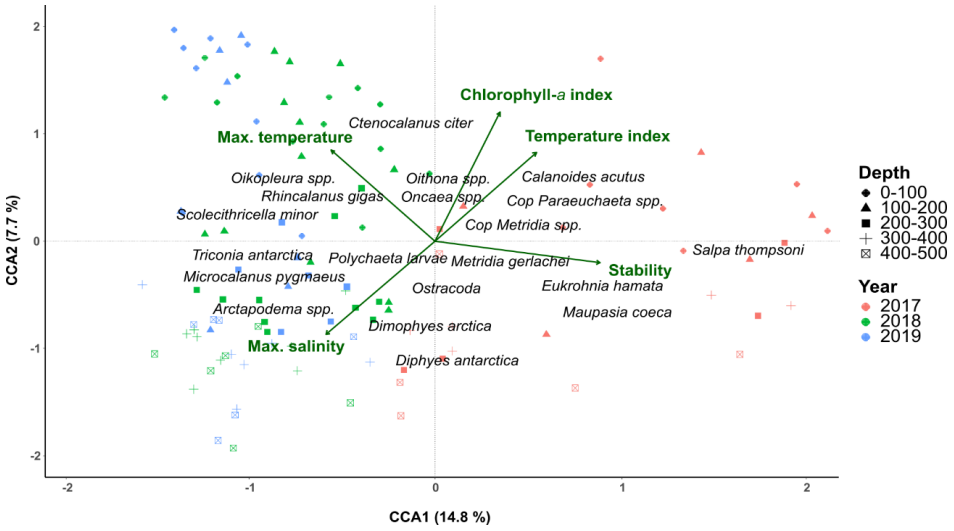


Figure 13: Canonical Correspondence Analysis (CCA) of the meso and macrozooplankton community in relation to the most significant environmental variables during the 3 years sampled.

The chlorophyll-*a*, temperature variation indices and stability correlated positively with the first axis (CCA1), mainly explaining the abundances observed in the 2017 samples. Furthermore, chlorophyll-*a* indices and temperature variation, together with the temperature maximum (representing the highest temperature recorded in each stratum, not necessarily at the surface), were responsible for much of the variation in the abundances of the samples from the first two strata, especially the latter being more important in 2018 and 2019. These variables also correlated positively with the second axis (CCA2).

The maximum salinity and stability were the variables that most explained the abundances of the intermediate and deep strata, over the three years, with stability being strongly associated with the variations in 2017 and the maximum salinity with the abundances of greater depths in 2018 and 2019.

Regarding the species displayed in the graph, stability was strongly associated with the abundance of Salps (*S. thompsoni*), copepods (*M. gerlachei*), chaetognats (*E. hamata*), polychaets (*Maupasia coeca*), as well as with copepodites of *Metridia* spp. Confirming the greater abundance of these taxa in places where the stability of the water column was greater. The chlorophyll-*a* and temperature variation indices explained the abundance of

the copepods *C. acutus*, *Oithona* spp. and copepodites of *Paraeuchaeta* spp. in the first two strata of the water column.

Triconia antarctica and *Microcalanus pygmaeus* showed negative correlations with CCA1 and CCA2, thus being associated with lower temperatures, confirming their predominant presence in colder and saline waters, associated with samples from the deepest or intermediate strata of 2018 and 2019. These species, together with Polychaeta larvae, the cnidarians *Arctapodema* spp., *Dimophyes arctica*, *Diphyes antarctica,* as well as ostracods, showed a positive association with maximum salinity values.

Ctenocalanus citer, *R. gigas,* and *Oikopleura* spp. were positively related to the CCA2 and, therefore, their abundances were explained by the maximum temperature found in the first two strata of the 2018 and 2019 samplings and by the chlorophyll-*a* variation index, indicating greater affinity for areas of greater productivity, such as in the first strata of the water column.

4. Discussion

4.2. Hydrographic conditions

The hydrographic variability across the NAP from 2017 to 2019 highlights distinct interannual differences in temperature and salinity patterns, particularly at the surface, as shown in the maps and T-S diagram (Figure 2 and 3). These variations reflected the influence of surrounding water masses, which shape the hydrography and stratification of the region [6,7,46]. The Bransfield Strait, in particular, is influenced by the intrusion of the Antarctic Circumpolar Current (ACC), which transports waters from the Bellingshausen Sea, including Antarctic Surface Water (AASW) and Circumpolar Deep Water (CDW) [47]. Additionally, dense water masses from the Weddell Sea, such as Dense Shelf Water (DSW), also contribute to the hydrographic complexity of the region [6,46,48].

The influence of waters from the Bellingshausen Sea was particularly evident in the surface warming, mainly in the Bransfield Strait over the three years, with a clear horizontal gradient at the surface and driving a greater stratification in the water column, increasing the stability, similar to observations from previous years [48–50]. In 2017, surface waters were warmer and less saline compared to the other years sampled, with a

shallower thermocline and MLD, and a significant presence of mCDW (a variety of CDW; [47]), mainly detected below the Antarctic Surface Water (AASW) at station #06, as also reported by Leonor and Muxagata [28].

The higher surface temperatures observed in 2017 probably is associated with a negative phase of the Southern Annular Mode (SAM), reported in the previous year (2016), which anomalously modified the wind pattern, resulting in the advection of warmer waters in the region during 2017 [51]. The SAM and the El Niño-Southern Oscillation (ENSO) are climatic phenomena that profoundly influence the climate dynamics of the Southern Ocean, especially in the NAP region, where they significantly alter and intensify regional wind patterns, thus modulating ocean water masses [50,51].

These conditions contrasted with 2018, when surface waters were colder and more saline. Furthermore, mCDW was detected at greater depths than in 2017, in other stations (#01, #02 in GS, and #09 in BS, near Deception Island). These findings align with previous studies detecting mCDW entering the Bransfield Strait from the southwest at the subsurface, reaching mid-strait regions [47], while also highlighting the dynamic contribution of transitional and local water masses to the hydrographic characteristics of the NAP. At the same time, waters from the Weddell Sea contributed to cold and dense waters in deeper layers, homogenizing the water column at eastern stations (#13, #15, #16 in 2018; #14, #17 in 2019) and reinforcing stratification in the western Bransfield Strait, consistent with previous studies [46,47,50]. Additionally, in the GS, the less saline and colder waters at the surface observed here probably originated from the melting of ice, favoring the increase in chlorophyll-*a* concentrations, as already seen by other authors [4,12]. In 2019, we observed almost the same hydrography conditions, however, in the GS the surface waters had an even lower salinity and shallower MLD than in 2018, probably affecting the phytoplankton community [27].

4.3. Phytoplankton community distribution

The phytoplankton community composition exhibited marked interannual variability. In 2017, we observed a higher abundance and dominance of smaller phytoplankton cells, such as dinoflagellates and cryptophytes, at most stations, with the exception of station #03 in the Gerlache Strait (GS), where diatoms were predominant. During oceanographic data collection that year, warmer and less saline waters resulted in shallower mixed layers

(<40 m) and greater stability of the water column, conditions that likely favored these smaller phytoplankton groups. This is because high proportions of cryptophytes are typically found at shallow depths in mixed layers, associated with freshwaters from meltwater inputs [11,27]. Furthermore, Costa et al. [52] reported elevated dinoflagellate concentrations during February and March in previous years, aligning with the sampling period in 2017. Notably, both dinoflagellates and cryptophytes exhibited a significant increase in February.

On the other hand, diatoms were the dominant group in #03 of 2017 and in almost all stations in 2018. Although diatoms generally accumulate more biomass in deeper waters [53], suggesting a preference for these conditions in 2018. However, this does not prevent some species from reaching high abundances in shallow mixed layers, such as at #03 in 2017. Given the diversity of the group in the NAP [53], it is unlikely that all diatom species are negatively affected by growth in shallow mixed layers [27]. It has been reported that pennate forms demonstrate great flexibility and ability to adapt to intense light conditions, which may favor their growth in waters with shallow mixed layer depths [54].

Samples from 2019 revealed distinct patterns across sites, with cryptophytes dominating the phytoplankton community at the Gerlache Strait (GS) stations and diatoms prevailing at the Bransfield Strait (BS) stations (Figure 4). This pattern was likely influenced by the less saline waters observed at the surface of GS during the year, which created stratification in the water column. Salinity was the main factor driving this stratification, likely due to the influence of glaciers dominating the region [7], creating an environment favorable for the development of cryptophytes [27]. In contrast, the dominance of diatoms in the Bransfield Strait in 2019 may be linked to the slight deepening of the mixed layer, as identified in this study and observed by other authors [53]. These differences between the two straits may be attributed to niche competition or segregation between diatoms and cryptophytes, a phenomenon reported by other studies but still not fully understood [3,4,11,12].

Elevated chlorophyll-*a* concentrations in the NAP are typically found in the western BS basin, in GS, and near the South Shetland Islands, decreasing toward the eastern BS [28,55,56]. This pattern was evident here over three years, where the highest chlorophyll-

a levels occurred in surface layers at GS stations and near Deception Island (#03, #05, #09; Figure 4). On contrary, the lowest (0.19 $mg.m^{-3}$) was eastern BS during 2017 at station #12, with a majority presence of smaller phytoplankton cells, and probably top-down control, which is an important driver to regulate phytoplankton biomass [57]. Diatoms were the primary contributors to the highest chlorophyll-*a* concentration, mainly in 2018, probably due to the lack of top-down control, since at these stations the zooplankton community was mostly at greater depths (Figure 8 and 9). Furthermore, according to superficial CCA analysis, diatoms emerged as the group with the most significant impact on the structure of the planktonic community of the surface (Figure 13), suggesting their crucial role in driving the variations in zooplankton composition observed here [58,59].

4.4. Meso and macrozooplankton and their relationship with phytoplankton community and oceanographic conditions

The zooplankton community observed during this study was similar in species composition to those previously reported for the region [24,28,49,60–62] and in the Southern Ocean [14,16,20,63]. However, for the first time, we recorded the presence of the genus *Dolioletta* spp. in two different stations (#10 and #15) of BS in 2018, not previously reported in the region, according to the Register Of Antarctic Marine Species (RAMS) [64]. Copepods were the most frequent, abundant, and diverse taxa in NAP over the three years, commonly reported as one of the major significant groups in the region [49,60,61].

In 2017, as already reported by Leonor and Muxagata [28], there was a predominance of larger copepods, such as *Metridia gerlachei*. This species was the most abundant and frequent, found in other studies as being a dominant omnivorous species in biomass in Antarctic waters [16,23,61,65]. The copepodites of *Metridia* spp. were also highly abundant, displaying a distribution pattern similar to that of the adults of *M. gerlachei*. This observation, as noted by King and LaCasella [65] during this time of year (March), is likely linked to their reproductive period.

Although the abundance of these calanoid copepods was still high in the other two years (2018 and 2019), the abundance of smaller copepods such as *C. citer*, *M. pygmaeus*, *Oithona* spp., and *T. antarctica* increased in 2018 and 2019. Previous studies suggest that

the copepod community undergoes size-related changes throughout the austral summer, transitioning from smaller to larger species [66,67]. This variation may be influenced by factors such as temperature and food availability [68]. In addition, it has been reported that the increase in cryptophytes favors smaller species such as *Oithona similis*, while larger copepods tend to migrate to deeper layers and consume larger particles [67–69]. In fact, in 2019, sampling occurred earlier (January/February) than in previous years, and higher abundances of smaller copepods, such as *C. citer* and *Oithona* spp., were observed in the first strata in stations dominated by cryptophytes, mainly in GS. Furthermore, we observed through the superficial CCA, a strong relationship of *Oithona* spp. with cryptophytes and *M. gerlachei* and *C. propinquos* with diatoms, which is supported by Atkinson [69], who observed that *Oithona similis* ingests small cells, whereas *C. propinquus* and *M. gerlachei* feed on larger cells. These patterns reinforce the influence of phytoplankton composition on the seasonal dynamics of copepods [67].

Additionally to the copepods, *S. thompsoni* was a major contributor to the observed differences between years, being present only in 2017 and absent in subsequent years. The responses of salps to environmental variations, such as temperature, food composition and concentration, are still not fully understood [70,71]. However, previous studies have identified that strong correlations between temperature and the influx of warmer waters have driven the population dynamics of *S. thompsoni*, increasing their abundance [24,49,70,72,73]. Conversely, lower temperatures can reduce their reproductive capacity [74], resulting in lower abundances or absence of this species. Furthermore, salps demonstrate sensitivity and limitations to food concentrations, with a preference for smaller phytoplankton cells [70,75,76]. In our study, CCA analyses indicated that salp abundances were associated with increased cryptophyte concentrations (Figure 12), higher surface temperatures—reflected by high temperature variation indices (indicating warmer surface conditions)—and increased water column stability (Figure 13), corroborating previous studies [49,60,77–79].

Plum et al. [60] reported that the presence of salps in the NAP favored larger mesozooplankton organisms, while negatively affecting smaller copepods. Thus, we assumed that in our study, the absence of salps in the 2018 and 2019 samples, in addition to being related to the lower temperatures observed in those years, may have contributed to the increase in the abundance of smaller copepods. These results reinforce the

significant impact of salps on structuring meso- and macrozooplankton communities in the NAP, as also observed by Plum et al. [60] and Kasyan et al. [73] and Criáles-Hernandez et al. [49].

Studies carried out in the last two decades have reported a considerable increase in the abundance of salps around the SO [13,60,79], especially in the NAP [49,73], where the ACC flow can advect these organisms to the region [80]. Meanwhile, krill abundance has been declining over the years having a major impact on the Antarctic marine food web, as it supports key predators such as whales and penguins [13,81–83]. The alternation between krill and salps in Antarctica is widely reported to be strongly influenced by environmental conditions and food availability [84,85]. Although salps were observed in our study only in 2017, and despite we noticing a slight increase in krill abundance in 2018 and 2019 samples, krill values were relatively low compared to other studies in the Antarctic Peninsula region [21,49,60]. Additionally, the majority of the euphausiid community observed consisted of juveniles.

This is likely due to the use of MultiNet in vertical trawls, as euphausiids are known to to escape from this type of trawl with this equipment [8,63]. Adult krill, in particular, may be very agile and could have escaped the slow vertical tows from the nets used in our study, further contributing to the low abundances observed. These findings also highlight the importance of considering methodological differences when interpreting krill and salp distribution patterns.

Although in lower abundances than copepods and salps, other groups also contributed significantly to the meso and macrozooplankton community in NAP. Chaetognaths were frequent in this study across all three years, with their distribution closely following that of copepods, their main prey [86,87]. *E. hamata* is one of the most abundant chaetognath species in the Southern Ocean [14,26,87], and widely distributed throughout the region [28]. However, their highest abundances were observed in the Gerlache Strait, where copepods, their main food source [87], were also most abundant.

Polychaete larvae also had significant abundances in this study, with the highest abundances occurring in 2018, in GS. High abundances of these larvae were reported in Marguerite Bay, the western Antarctic Peninsula [88], and in Prydz Bay [14]. The distribution in NAP of polychaete larvae abundance is still poorly known, but it is

believed that it occurs near shallow regions that will supply the larvae and distribute them according to the water circulation, which plays a fundamental role in benthic recruitment in polar areas [14].

The meso- and macrozooplankton community exhibited substantial interannual and vertical variations, reflecting the influence of hydrographic conditions and phytoplankton availability, as reported in previous studies in NAP [24,28,49,61,62].

4.5. Vertical distribution of meso-and macrozooplankton

Several authors have already observed DVM, with a nocturnal increase in zooplankton biomass at the surface of Antarctic waters, when there is increased feeding [16,23,89]. In fact, despite being marginally significant (p-value=0.041), the PERMANOVA test indicated significant differences in the abundances of samples collected during twilight and the day as also reported by Leonor & Muxagata [24] on surface samples collected with a CPR in this region. Previous studies suggest that DVM may depend on a species-by-species basis [16,90,91]. Here we only observed a considerable increase in community abundances in the first stratum in the nocturnal samples of stations #12 of 2017, dominated by salps, and #11 and #12 of 2018, dominated by copepods. However, contrary to what we expected, diversity did not increase at the surface during this period, being higher in the deeper strata. This is in agreement with Park and Wormuth [90], implying that not all species perform this vertical migration.

We believe that intrusive waters in BS and GS created niches favorable to diversity at certain depths [80], as observed in the mid-layers (200 - 400 m). Higher indices of diversity and abundance were reported in mid-layers than at the surface. This indicated that the intermediate and deep layers offer more diverse and stable habitats, such as predator refuge zones, while the surface layer presents greater predation pressure, greater environmental variability, and even limitations and competition for food resources [16,79,92]. However, we have to consider that almost all stations were sampled during the day period when most organisms are usually at greater depths [93]. Twilight sampling from stations #12 in 2017 and #11 and #12 in 2018 revealed a different pattern, with higher abundances observed in the first stratum. This highlights the importance of including sampling from both periods to capture the full scope of vertical migration and avoid underestimating surface layer diversity and abundance (Conroy et al. 2020).

Despite vertical differences, the dominance of copepods across all depths and years reinforces their central role in Antarctic zooplankton communities [21]. Normally in summer, high abundances of copepods such as *C. acutus, C. propinquus*, *M. gerlachei*, are seen in the first layers of the water column (0-200 m) [22]. However, since most of ours samplings occurred during daytime, most of the copepods abundances and diversity observed here were concentrated between 200–400 m in the three years, corroborating with other studies in the Antarctic Peninsula [16,21,28,61]. *Metridia gerlachei* has one of the highest vertical distributions, and emerged as a key species contributing to differences between strata, reinforcing its ecological significance [94]. However, their concentration on mid-layers, was consistent with previous studies, confirming them as a mid-water species [14,19,23,60,61,94]. The copepodites of *Metridia* spp. seems to follow the adult vertical distribution. These distributions may be related to the life cycle strategies of this species and to avoid predators, as suggested by Atkinson et al. [89] and King and LaCasella [65].

Smaller copepods, such as *Oithona* spp., *T. antarctica*, and *C. citer*, have been commonly reported in the upper layers of Antarctic waters [20,30,60,63]. In our study, indicator species analysis revealed that *Oithona* spp. was strongly associated with the first stratum, while *C. citer* showed a significant association with both the first and second strata. In contrast, *T. antarctica* was reported only in the deeper layers (200-500 m).

In addition to copepods and unlike other studies in NAP [60], Appendicularia showed low abundances, mainly concentrated in the upper layers (0 – 100 and 100 – 200 m). Studies in Prydz Bay suggested that *Oikopleura* spp., could be influenced by AASW at the surface [14], which is corroborated by our CCA results, which indicated higher abundances of this taxon related to higher temperatures in the first two strata, a typical characteristic of AASW (T° > 0) [47]. Furthermore, our study confirms the records of Leonor and Muxagata [24], who observed the presence of this taxon in surface samples carried out with the CPR in the NAP, with similar abundances in diurnal and twilight samples, associated with chlorophyll-*a*. These results reinforce the preference of *Oikopleura* spp. by superficial strata, regardless of the photoperiod, probably due to their feeding habits, since they are filter-feeding organisms, they have previously been related to chlorophyll-*a* in other studies [24,95].

Despite being found widely distributed throughout the water column, *S. thompsoni* were recorded in greater abundance on the upper layers (0 – 100 and 100 – 200 m). In regions of high productivity, such as areas with high concentrations of chlorophyll-*a*, salps tend to concentrate in the surface layers [16,20,79]. However, in our study, high surface abundances coincided with very low concentrations of chlorophyll-*a*, perhaps due to their feeding capacity, which ended up consuming the productivity in top-down control. Although less frequent, salps can also be found at greater depths [16,72,79,96], as observed here. This depends on local conditions, such as water column stability (higher in 2017) and food availability [16,79]. The vertical presence of salps at different depths greatly enhances the transport of carbon to deeper layers, especially due to their dense and rapidly sinking fecal pellets, playing a crucial role in the biogeochemical cycle [79]. In addition, their migration contributes to the active transport of carbon and nutrients between layers of the water column [72,79,96]. Here, we observe a migration pattern during the twilight period in station #12 of 2017, in BS, where their abundances increase in the first stratum.

Despite their low abundance, euphausiids (primarily juveniles) were more frequently observed in intermediate layers, particularly at stations sampled in 2018 with higher chlorophyll-*a* concentrations. Previous studies indicate that vertical distribution within the water column can vary with season and environmental conditions., and the occurrence of euphausiids in intermediate layers, especially in areas with elevated chlorophyll-*a* levels, reflects an adaptive strategy to enhance feeding efficiency while minimizing predation risk, particularly for juveniles [21,23,73]. However, surface abundances reported here may be underestimated due to the sampling method employed, as organisms could evade the net, particularly during daylight hours (when most sampling occurred), because of the increased visibility of the sampling gear [8].

On the other hand, ostracods emerged as a significant group in deeper layers across all locations and years, particularly at stations sampled during the day. Studies in the NAP have similarly recorded higher ostracod abundances below 200 meters, which can be attributed to their detritivorous feeding habits and the greater availability of organic particles at these depths [21,97,98]. Interestingly, in 2018, at stations #11 and #12 sampled during twilight, ostracods were also found in the upper strata, suggesting diel

vertical migration. This behavior has been documented around the Antarctic Peninsula [16], indicating a dynamic response to changing light conditions and prey availability.

Among the lower abundance groups, chaetognaths, polychaetes, and cnidarians showed higher densities in deeper layers, following the pattern widely documented in Antarctica, where carnivores tend to be more prevalent at greater depths [14,20,21]. This distribution is possibly related to the benefits of greater particle sedimentation and the availability of a more diverse food base in these regions [8,87]. For example, the chaetognath *Eukrohnia hamata*, one of the most abundant species of this phylum in the SO, is a predator whose distribution follows that of its prey, such as copepods, and is frequently found in deeper layers [28,87,99], a pattern also observed in this study. Cnidarians followed a similar trend, as previously reported by Panasiuk-Chodnicka et al. [100]. However, in nocturnal samples, we observed a vertical migration of hydromedusae to more superficial layers, which seemed to mirror the migration pattern of copepods observed here, which are their main prey in the Antarctic region [97].

Similarly, polychaetes and amphipods demonstrated vertical distribution patterns that seemed to be strongly associated with feeding and the specific environmental conditions of each depth layer. In the case of polychaetes, most of the abundances were represented by larvae at greater depths. Previous studies indicated that polychaete larvae are generally scarce in the epipelagic zone and that, although carnivorous in some cases, they can also feed on organic detritus, taking advantage of the greater availability of sedimented particles in deeper layers [14]. On the other hand, the absence of significant differences in larval distributions between diurnal and crepuscular samples suggests that additional factors, such as predator avoidance strategies, play a key role in shaping their vertical migration patterns in the region [8,101]. Furthermore, some larvae may exhibit weak or no diurnal vertical migration during the early stages of development, leading to a more homogeneous distribution throughout the water column [8,102].

Amphipods have been reported as significant components of temperate and cold-water pelagic ecosystems, reaching high biomass levels and serving as crucial prey for commercially important fish and squid stocks. In the northern regions of the Southern Ocean, they can be so abundant that they assume an ecological role similar to that of Antarctic krill [103]. This prominence in the food web may explain their vertical

distribution patterns, as observed in 2017, when amphipods were most abundant in the surface layers, resembling the distribution of *Salpa thompsoni* [104]. Their positioning in the water column may be influenced by feeding interactions, including the consumption of particulate matter filtered by salps or even direct predation on salp tissue [105]. These patterns suggest that environmental variations and trophic interactions play a critical role in shaping their vertical distribution.

Regarding the new report of the doliolid genus (*Dolioletta* spp.) in the region, doliolids generally occur abundantly in neritic areas of subtropical regions [106]. In addition, species of this genus have been observed in the upper mixed layer in shelf break regions [107]. However, in this study, the two specimens of *Dolioletta* spp. were recorded at greater depths (200 - 400 m), in colder and more saline waters. In this context, the presence of this genus may indicate that these organisms also take advantage of environmental fluctuations, potentially expanding their distribution to polar waters.

The observed vertical gradients in zooplankton abundance and diversity highlight the profound influence of depth on community structure. The variation in the vertical distribution of zooplankton over the years reflects, in part, the predominantly diurnal sampling times. In addition, this variation is closely linked to changes in water column stratification and stability, as already seen by Kasyan [61]. In 2017, greater stability was driven by higher surface temperatures in Bransfield Strait (BS) and lower salinities in Gerlache Strait (GS). In 2018 and 2019, BS showed lower stability with a slight deepening of the mixed layer, while GS, in 2019, exhibited lower surface salinity, contributing to the observed dynamics.

This water column stability directly influenced the composition of phytoplankton and, consequently, zooplankton. In 2017, in BS, greater stability due to temperature favored high abundances of salps, especially at the surface. In GS, in 2018 and 2019, lower salinity and greater stability benefited initially the presence of small copepods. The stratification of the water column, associated with shallower mixed layers, was strongly related to the increase in the concentration of cryptophytes. CCA analyses highlighted that cryptophytes were the phytoplankton group most correlated with these meso- and macrozooplankton groups, evidencing a crucial interaction between physical variables, phytoplankton composition, and zooplankton structure.

On the other hand, a homogeneous water column seems to favor the increase in the abundance of communities. The highest abundance of the meso- and macrozooplankton community was recorded at station #15, between 200-300 m, in 2018, where the water column was nearly homogeneous up to 500 m. This station is located in an area influenced by the waters of the Weddell Sea and the Scotia Sea, characterized by a unique mixing regime, which significantly contributes to the increase in zooplankton biomass, as previously documented by other researchers [60,90].

These detailed patterns emphasize the vertical complexity of the zooplankton community and the ecological roles of different taxa. However, further studies are needed, especially focusing on daytime and nighttime sampling at the same stations. Furthermore, it is important to consider that the stratification of the surface could be better detailed, since migration may be occurring at shallower depths, as already seen by some authors [8,24], and not being adequately captured in a 100 m interval. This factor may explain the absence of clear DVM patterns at some stations sampled at night.

5. Conclusion

The observed spatial differences in the distribution of the mesozooplankton community are closely linked to the heterogeneity of the water masses that enter the region and alter the properties of the surface and bottom. The oscillation of the stability of the water column observed here had a significant influence on the phytoplankton and zooplankton communities, with implications for Antarctic and global ecosystems. In sites of strong stability, the presence of opportunistic organisms, such as cryptophytes, supported salps in areas with warmer surface waters, as in 2017, and favored small copepods in surface conditions of lower salinity, as in 2019. In contrast, sites with weaker stability, together with a sinking of the mixed layer, as in 2018, favored the development of diatoms and the abundance of copepods, especially small calanoids (e.g., copepodites of *Metridia* spp. and *C. citer*). The stability of the water column proved to be a crucial parameter, directly influencing the composition and abundance of phytoplankton and zooplankton communities, between the surface and deep strata, standing out as a valuable proxy for predicting changes in community structure.

In addition, the differences in vertical distribution between surface and bottom were also influenced by the migration of some organisms, where particularly during periods of

reduced light, greater abundances were found at the surface, probably due to feeding habits, while during the day, greater abundances were found at greater depths, where more stable conditions and fewer variations in the water column seemed to be more favorable, especially for the early stages of *Metridia* spp..

Furthermore, this study expands the known distribution of the genus *Dolioletta* spp. to polar waters, highlighting its ability to persist in colder waters. The report reinforces the need for continued monitoring of meso- and macrozooplankton biodiversity in this region, which has been increasingly affected by rising temperatures in recent years.

These findings highlight the importance of considering horizontal and vertical variations, as well as temporal changes, to fully understand the ecological dynamics of these Antarctic marine ecosystems. These fluctuations in the patterns and composition found in the meso- and macrozooplankton community between locations and years have impacts on the efficiency of carbon and energy transfer to higher trophic levels, such as fish, birds, and marine mammals, which depend on these organisms. Therefore, monitoring and understanding these changes is crucial to predict and mitigate the impacts of climate change, ensuring the sustainability of these ecosystems and their role in the global climate balance.

Acknowledgements

This study is part of the Brazilian High Latitude Oceanography Group (GOAL) activities within the Brazilian Antarctic Program (PROANTAR). We sincerely thank the coordinators of the INTERBIOTA and NAUTILUS projects, E. R. Secchi and M. M. Mata, for their support. Our gratitude extends to the crew of the Brazilian Navy aboard the RV Almirante Maximiano, as well as the scientists and technicians from GOAL who contributed to the cruise and sampling efforts. We are also grateful to Simon Wright from the Australian Antarctic Division for providing the CHEMTAX v.1.95 software, and to C. R. B. Mendes and R. R. Costa for supplying the phytoplankton data. Additionally, we appreciate the contributions of R. Kerr and R. Torquato for providing physical data. We acknowledge the Zooplankton Laboratory (at FURG) team for their continuous support and collaboration throughout this study.

Author contributions: L.C.B. developed the main idea, led the writing and revisions, and created the figures for the manuscript. V.O.A. conducted the sampling, contributed to the conception of the work, co-supervised the project, and revised the manuscript. E.M. responsible for sample and data curation, funding acquisition and resources, contributed to the conception of the work, supervised the project, and revised the manuscript. Both V.O.A. and E.M. participated in the organization and writing of the final version of the manuscript. All authors contributed to the revision of the manuscript, read it, and approved the submitted version.

Funding: This work was supported by the projects INTERBIOTA, NAUTILUS, PROVOCCAR, ECOPELAGOS (Conselho Nacional de Desenvolvimento Científico e Tecnológico (CNPq) grant numbers 407889/2013-2, 405869/2013-4, 442628/2018-8, 442637/2018-7, respectively); L. C. Baldoni were supported by Ph.D. fellowship from CAPES (n° 88887.374525/2019-00) at the Programa de Pós-Graduação em Oceanografia Biológica, Universidade Federal do Rio Grande (FURG). E. Muxagata received CNPq researcher productivity grant no. 307633/2023-3.

References

[1] M.P. Meredith, J.C. King, Rapid climate change in the ocean west of the Antarctic Peninsula during the second half of the 20th century, Geophys. Res. Lett. 32 (2005) 2005GL024042. https://doi.org/10.1029/2005GL024042.

[2] M.P. Meredith, O. Schofield, L. Newman, E. Urban, M. Sparrow, The vision for a Southern Ocean Observing System, Curr. Opin. Environ. Sustain. 5 (2013) 306–313. https://doi.org/10.1016/j.cosust.2013.03.002.

[3] C.R.B. Mendes, V.M. Tavano, M.C. Leal, M.S. De Souza, V. Brotas, C.A.E. Garcia, Shifts in the dominance between diatoms and cryptophytes during three late summers in the Bransfield Strait (Antarctic Peninsula), Polar Biol 36 (2013) 537–547. https://doi.org/10.1007/s00300-012-1282-4.

[4] C.R.B. Mendes, V.M. Tavano, R. Kerr, T.S. Dotto, T. Maximiano, E.R. Secchi, Impact of sea ice on the structure of phytoplankton communities in the northern Antarctic Peninsula, Deep-Sea Res. Part II 149 (2018) 111–123. https://doi.org/10.1016/j.dsr2.2017.12.003.

[5] I.B.M. Orselli, A.C.O. Carvalho, T. Monteiro, B.Y. Damini, M.D. Carvalho-Borges, C. Albuquerque, R. Kerr, The marine carbonate system along the northern Antarctic Peninsula: current knowledge and future perspectives, An. Acad. Bras. Ciênc. 94 (2022) e20210825. https://doi.org/10.1590/0001-3765202220210825.

[6] T.S. Dotto, R. Kerr, M.M. Mata, C.A.E. Garcia, Multidecadal freshening and lightening in the deep waters of the Bransfield Strait, Antarctica, JGR Oceans 121 (2016) 3741–3756. https://doi.org/10.1002/2015JC011228.

[7] R. Kerr, M.M. Mata, C.R.B. Mendes, E.R. Secchi, Northern Antarctic Peninsula: a marine climate hotspot of rapid changes on ecosystems and ocean dynamics, Deep-Sea Res. Part II 149 (2018) 4–9. https://doi.org/10.1016/j.dsr2.2018.05.006.

[8] H. Flores, B.P.V. Hunt, S. Kruse, E.A. Pakhomov, V. Siegel, J.A. Van Franeker, V. Strass, A.P. Van De Putte, E.H.W.G. Meesters, U. Bathmann, Seasonal changes in the vertical distribution and community structure of Antarctic macrozooplankton and micronekton, Deep Sea Research Part I: Oceanographic Research Papers 84 (2014) 127–141. https://doi.org/10.1016/j.dsr.2013.11.001.

[9] M.R. Gleiber, D.K. Steinberg, O.M.E. Schofield, Copepod summer grazing and fecal pellet production along the Western Antarctic Peninsula, J. Plankton Res. 38 (2016) 732–750. https://doi.org/10.1093/plankt/fbv070.

[10] O. Schofield, M. Cimino, S. Doney, A. Friedlaender, M. Meredith, C. Moffat, S. Stammerjohn, B. Van Mooy, D. Steinberg, Antarctic pelagic ecosystems on a warming planet, Trends Ecol. Evol. (2024) S0169534724002003. https://doi.org/10.1016/j.tree.2024.08.007.

[11] C.R.B. Mendes, V.M. Tavano, T.S. Dotto, R. Kerr, M.S. De Souza, C.A.E. Garcia, E.R. Secchi, New insights on the dominance of cryptophytes in Antarctic coastal waters: A case study in Gerlache Strait, Deep-Sea Res. Part II 149 (2018) 161–170. https://doi.org/10.1016/j.dsr2.2017.02.010.

[12] M.A. Moline, H. Claustre, T.K. Frazer, O. Schofield, M. Vernet, Alteration of the food web along the Antarctic Peninsula in response to a regional warming trend, Glob. Change Biol. 10 (2004) 1973–1980. https://doi.org/10.1111/j.1365-2486.2004.00825.x.

[13] A. Atkinson, V. Siegel, E. Pakhomov, P. Rothery, Long-term decline in krill stock and increase in salps within the Southern Ocean, Nature 432 (2004) 100–103. https://doi.org/10.1038/nature02996.

[14] V. Venkataramana, A.U. Kerkar, R.K. Mishra, P. Sabu, N. Anilkumar, Hydrodynamics and zooplankton assemblages in Prydz Bay, East Antarctica, during the austral summer of 2017, Reg. Stud. Mar. Sci. 52 (2022) 102341. https://doi.org/10.1016/j.rsma.2022.102341.

[15] J. Berge, F. Cottier, Ø. Varpe, P.E. Renaud, S. Falk-Petersen, S. Kwasniewski, C. Griffiths, J.E. Søreide, G. Johnsen, A. Aubert, O. Bjærke, J. Hovinen, S. Jung-Madsen, M. Tveit, S. Majaneva, Arctic complexity: a case study on diel vertical migration of zooplankton, J. Plankton Res. 36 (2014) 1279–1297. https://doi.org/10.1093/plankt/fbu059.

[16] J.A. Conroy, D.K. Steinberg, P.S. Thibodeau, O. Schofield, Zooplankton diel vertical migration during Antarctic summer, Deep-Sea Res. Part I 162 (2020) 103324. https://doi.org/10.1016/j.dsr.2020.103324.

[17] A.J. Constable, J. Melbourne-Thomas, S.P. Corney, K.R. Arrigo, C. Barbraud, D.K.A. Barnes, N.L. Bindoff, P.W. Boyd, A. Brandt, D.P. Costa, A.T. Davidson, H.W. Ducklow, L. Emmerson, M. Fukuchi, J. Gutt, M.A. Hindell, E.E. Hofmann, G.W. Hosie, T. Iida, S. Jacob, N.M. Johnston, S. Kawaguchi, N. Kokubun, P. Koubbi, M. Lea, A. Makhado, R.A. Massom, K. Meiners, M.P. Meredith, E.J. Murphy, S. Nicol, K. Reid, K. Richerson, M.J. Riddle, S.R. Rintoul, W.O. Smith, C. Southwell, J.S. Stark, M. Sumner, K.M. Swadling, K.T. Takahashi, P.N. Trathan, D.C. Welsford, H. Weimerskirch, K.J. Westwood, B.C. Wienecke, D. Wolf-Gladrow, S.W. Wright, J.C. Xavier, P. Ziegler, Climate change and Southern Ocean ecosystems I: how changes in physical habitats directly affect marine biota, Glob. Change Biol. 20 (2014) 3004–3025. https://doi.org/10.1111/gcb.12623.

[18] D.L. Mackas, H. Sefton, C.B. Miller, A. Raich, Vertical habitat partitioning by large calanoid copepods in the oceanic subarctic Pacific during Spring, Prog. Oceanogr. 32 (1993) 259–294. https://doi.org/10.1016/0079-6611(93)90017-8.

[19] T.L. Hopkins, J.J. Torres, Midwater food web in the vicinity of a marginal ice zone in the western Weddell Sea, Deep-Sea Res. Part I 36 (1989) 543–560. https://doi.org/10.1016/0198-0149(89)90005-8.

[20] Y. Liu, Y. Wang, Y. Sun, G. Yang, K.M. Swadling, Zooplankton vertical stratification in the East-pacific and Indian sectors of the Southern Ocean, Front. Mar. Sci. 11 (2024) 1274582. https://doi.org/10.3389/fmars.2024.1274582.

[21] M. Marrari, K.L. Daly, A. Timonin, T. Semenova, The zooplankton of Marguerite Bay, western Antarctic Peninsula—Part II: Vertical distributions and habitat partitioning, Deep-Sea Res. Part II 58 (2011) 1614–1629. https://doi.org/10.1016/j.dsr2.2010.12.006.

[22] W. Lee, S. Kim, S.-H. Kang, H.-U. Bang, K.-H. Lee, I.-S. Kwak, Distribution and Abundance of Zooplankton in the Bransfield Strait and the Western Weddell Sea during Austral Summer, Ocean and Polar Res 26 (2004) 607–618. https://doi.org/10.4217/OPR.2004.26.4.607.

[23] L. Yebra, S. Hernández-León, C. Almeida, P. Bécognée, Metabolism and biomass vertical distribution of zooplankton in the Bransfield Strait during the austral summer of 2000, Polar Res 28 (2009) 415–425. https://doi.org/10.1111/j.1751-8369.2009.00116.x.

[24] C.M. Leonor, E. Muxagata, Interannual variability in surface mesozooplankton in the Western Antarctic Peninsula during two anomalous years, Deep-Sea Res. Part I 217 (2025) 104444. https://doi.org/10.1016/j.dsr.2025.104444.

[25] F.R. Cottier, G.A. Tarling, A. Wold, S. Falk-Petersen, Unsynchronised and synchronised vertical migration of zooplankton in a high Arctic fjord, Limnol. Oceanogr. 51 (2006) 2586–2599. https://doi.org/10.4319/lo.2006.51.6.2586.

[26] D.L. Mackas, W. Greve, M. Edwards, S. Chiba, K. Tadokoro, D. Eloire, M.G. Mazzocchi, S. Batten, A.J. Richardson, C. Johnson, E. Head, A. Conversi, T. Peluso, Changing zooplankton seasonality in a changing ocean: Comparing time series of zooplankton phenology, Prog. Oceanogr. 97–100 (2012) 31–62. https://doi.org/10.1016/j.pocean.2011.11.005.

[27] C.R.B. Mendes, R.R. Costa, A. Ferreira, B. Jesus, V.M. Tavano, T.S. Dotto, M.C. Leal, R. Kerr, C.A. Islabão, A.D.O.D.R. Franco, M.M. Mata, C.A.E. Garcia, E.R. Secchi, Cryptophytes: An emerging algal group in the rapidly changing Antarctic Peninsula marine environments, Glob. Change Biol. 29 (2023) 1791–1808. https://doi.org/10.1111/gcb.16602.

[28] C.M. Leonor, E. Muxagata, Vertical distribution of the zooplankton in the Antarctic Peninsula during the austral summer of 2017, An. Acad. Bras. Ciênc. 96 (2024) e20240144. https://doi.org/10.1590/0001-3765202420240144.

[29] A. Calbet, M. Alcaraz, D. Atienza, E. Broglio, D. Vaqué, Zooplankton biomass distribution patterns along the western Antarctic Peninsula (December 2002), J. Plankton Res. 27 (2005) 1195–1203. https://doi.org/10.1093/plankt/fbi081.

[30] A. Giraldo, M.I. Criales Hernández, M. Jerez Guerrero, D.F. Mojica Moncada, Epipelagic copepod assemblage in the Gerlache Strait (Antarctica) during the 2015 austral summer, BIM 48 (2019). https://doi.org/10.25268/bimc.invemar.2019.48.1.754.

[31] R. Avelina, L.C.D. Cunha, R. Kerr, C.O. Farias, C. Hamacher, M.M. Mata, Drivers and fluxes of dissolved organic carbon along the northern Antarctic Peninsula during late summer, An. Acad. Bras. Ciênc. 96 (2024) e20240573. https://doi.org/10.1590/0001-3765202420240573.

[32] M. Mackey, D. Mackey, H. Higgins, S. Wright, CHEMTAX - a program for estimating class abundances from chemical markers:application to HPLC measurements of phytoplankton, Mar. Ecol. Prog. Ser. 144 (1996) 265–283. https://doi.org/10.3354/meps144265.

[33] H.F. Steedman, Zooplankton Fixation and Preservation, Bernan Associates, 1976. https://books.google.com.br/books?id=3DwUAQAAIAAJ.

[34] R.R. Costa, C.R.B. Mendes, V.M. Tavano, T.S. Dotto, R. Kerr, T. Monteiro, C. Odebrecht, E.R. Secchi, Dynamics of an intense diatom bloom in the Northern Antarctic Peninsula, February 2016, Limnol. Oceanogr. 65 (2020) 2056–2075. https://doi.org/10.1002/lno.11437.

[35] R.R. Costa, C.R.B. Mendes, M.S.D. Souza, V.M. Tavano, E.R. Secchi, Chemotaxonomic characterization of the key genera of diatoms in the Northern Antarctic Peninsula, An. Acad. Bras. Ciênc. 94 (2022) e20210584. https://doi.org/10.1590/0001-3765202220210584.

[36] S.W. Wright, A. Ishikawa, H.J. Marchant, A.T. Davidson, R.L. Van Den Enden, G.V. Nash, Composition and significance of picophytoplankton in Antarctic waters, Polar Biol 32 (2009) 797–808. https://doi.org/10.1007/s00300-009-0582-9.

[37] P. Legendre, L. Legendre, Ecological resemblance, in: Developments in Environmental Modelling, Elsevier, 2012: pp. 265–335. https://doi.org/10.1016/B978-0-444-53868-0.50007-1.

[38] C. Cornwall, A. Horiuchi, C. Lehman, Sunrise/Sunset Calculator - NOAA, (n.d.). https://gml.noaa.gov/grad/solcalc/sunrise.html (accessed February 20, 2024).

[39] J. Oksanen, vegan: Community Ecology Package, (2022). https://github.com/vegandevs/vegan.

[40] H. Wickham, ggplot2: Elegant Graphics for Data Analysis, (2016). https://ggplot2.tidyverse.org.

[41] K. Clarke, R. Warwick, A further biodiversity index applicable to species lists: variation in taxonomic distinctness, Mar. Ecol. Prog. Ser. 216 (2001) 265–278. https://doi.org/10.3354/meps216265.

[42] M. De Cáceres, P. Legendre, M. Moretti, Improving indicator species analysis by combining groups of sites, Oikos 119 (2010) 1674–1684. https://doi.org/10.1111/j.1600-0706.2010.18334.x.

[43] M. Dufrene, P. Legendre, Species Assemblages and Indicator Species: The Need for a Flexible Asymmetrical Approach, Ecol. Monogr. 67 (1997) 345. https://doi.org/10.2307/2963459.

[44] M.O. Hill, Diversity and Evenness: A Unifying Notation and Its Consequences, Ecology 54 (1973) 427–432. https://doi.org/10.2307/1934352.

[45] C.J.F. Ter Braak, I.C. Prentice, A Theory of Gradient Analysis, in: Advances in Ecological Research, Elsevier, 1988: pp. 271–317. https://doi.org/10.1016/S0065-2504(08)60183-X.

[46] B.Y. Damini, R. Kerr, T.S. Dotto, M.M. Mata, Long-term changes on the Bransfield Strait deep water masses: Variability, drivers and connections with the northwestern Weddell Sea, Deep-Sea Res. Part I (2022) 103667. https://doi.org/10.1016/j.dsr.2021.103667.

[47] W.G.C. Huneke, O. Huhn, M. Schröeder, Water masses in the Bransfield Strait and adjacent seas, austral summer 2013, Polar Biol 39 (2016) 789–798. https://doi.org/10.1007/s00300-016-1936-8.

[48] A.L. Gordon, M. Mensch, D. Zhaoqian, W.M. Smethie, J. De Bettencourt, Deep and bottom water of the Bransfield Strait eastern and central basins, J. Geophys. Res. 105 (2000) 11337–11346. https://doi.org/10.1029/2000JC900030.

[49] M.I. Criales-Hernández, M. Jerez-Guerrero, S.A. Latandret-Solana, M.D. Gómez-Sánchez, Spatial distribution of meso- and macro-zooplankton in the Bransfield Strait and

around Elephant Island, Antarctic Peninsula, during the 2019–2020 austral summer, Polar Sci 32 (2022) 100821. https://doi.org/10.1016/j.polar.2022.100821.

[50] E.M. Ruiz Barlett, G.V. Tosonotto, A.R. Piola, M.E. Sierra, M.M. Mata, On the temporal variability of intermediate and deep waters in the Western Basin of the Bransfield Strait, Deep-Sea Res. Part II 149 (2018) 31–46. https://doi.org/10.1016/j.dsr2.2017.12.010.

[51] R.R. Torres Parra, A.L. Caicedo Laurido, J.D. Iriarte Sánchez, Hydrographic conditions during two austral summer situations (2015 and 2017) in the Gerlache and Bismarck straits, northern Antarctic Peninsula, Deep-Sea Res. Part II 161 (2020) 103278. https://doi.org/10.1016/j.dsr.2020.103278.

[52] R.R. Costa, A. Ferreira, M.S. De Souza, V.M. Tavano, R. Kerr, E.R. Secchi, V. Brotas, T.S. Dotto, A.C. Brito, C.R.B. Mendes, Physical-biological drivers modulating phytoplankton seasonal succession along the Northern Antarctic Peninsula, Environ. Res. 231 (2023) 116273. https://doi.org/10.1016/j.envres.2023.116273.

[53] R.R. Costa, C.R.B. Mendes, A. Ferreira, V.M. Tavano, T.S. Dotto, E.R. Secchi, Large diatom bloom off the Antarctic Peninsula during cool conditions associated with the 2015/2016 El Niño, Commun Earth Environ 2 (2021) 252. https://doi.org/10.1038/s43247-021-00322-4.

[54] K. Petrou, S.A. Kranz, S. Trimborn, C.S. Hassler, S.B. Ameijeiras, O. Sackett, P.J. Ralph, A.T. Davidson, Southern Ocean phytoplankton physiology in a changing climate, J. Plant Physiol. 203 (2016) 135–150. https://doi.org/10.1016/j.jplph.2016.05.004.

[55] M. Zhou, P.P. Niiler, J.-H. Hu, Surface currents in the Bransfield and Gerlache Straits, Antarctica, Deep-Sea Res. Part I 49 (2002) 267–280. https://doi.org/10.1016/S0967-0637(01)00062-0.

[56] C. Aracena, H.E. González, J. Garcés-Vargas, C.B. Lange, S. Pantoja, F. Muñoz, E. Teca, E. Tejos, Influence of summer conditions on surface water properties and phytoplankton productivity in embayments of the South Shetland Islands, Polar Biol 41 (2018) 2135–2155. https://doi.org/10.1007/s00300-018-2338-x.

[57] C.R.B. Mendes, M.S. De Souza, V.M.T. Garcia, M.C. Leal, V. Brotas, C.A.E. Garcia, Dynamics of phytoplankton communities during late summer around the tip of the Antarctic Peninsula, Deep-Sea Res. Part I 65 (2012) 1–14. https://doi.org/10.1016/j.dsr.2012.03.002.

[58] A. Hayward, S.W. Wright, D. Carroll, C. Law, P. Wongpan, A. Gutiérrez-Rodriguez, M.H. Pinkerton, Climate driven shifts in Antarctic phytoplankton groups: Implications of widespread diatom decline, (2024). https://doi.org/10.21203/rs.3.rs-5188031/v1.

[59] M.M. Deschamps, M. Boersma, L. Giménez, Responses of the mesozooplankton community to marine heatwaves: Challenges and solutions based on a long-term time series, J. Anim. Ecol. 93 (2024) 1524–1540. https://doi.org/10.1111/1365-2656.14165.

[60] C. Plum, A. Cornils, R. Driscoll, P. Wenta, T.H. Badewien, J. Niggemann, S. Moorthi, Mesozooplankton trait distribution in relation to environmental conditions and the presence of krill and salps along the northern Antarctic Peninsula, J. Plankton Res. 43 (2021) 927–944. https://doi.org/10.1093/plankt/fbab068.

[61] V.V. Kasyan, Structure and Spatial Distribution of Mesozooplankton Communities in the Atlantic Sector of the Southern Ocean, Oceanology 63 (2023) 550–558. https://doi.org/10.1134/S0001437023040057.

[62] O. Esquivel-Garrote, E. Muxagata, Composition patterns of surface mesozooplankton in the zonal fronts of Drake Passage, J. Plankton Res. 45 (2023) 853–869. https://doi.org/10.1093/plankt/fbad040.

[63] G. Yang, C. Li, Y. Wang, Y. Zhang, Vertical profiles of zooplankton community structure in Prydz Bay, Antarctica, during the austral summer of 2012/2013, Polar Biol 40 (2017) 1101–1114. https://doi.org/10.1007/s00300-016-2037-4.

[64] C. De Broyer, A. Clarke, P. Koubbi, E. Pakhomov, F. Scott, Register of Antarctic Marine Species – Doliolidae Bronn, 1862, (2023). https://www.marinespecies.org/rams./aphia.php?p=taxdetails&id=137215 (accessed October 20, 2023).

[65] A. King, E.L. LaCasella, Seasonal variations in abundance, diel vertical migration, and population structure of Metridia gerlachei at Port Foster, Deception Island, Antarctica, Deep-Sea Res. Part II 50 (2003) 1753–1763. https://doi.org/10.1016/S0967-0645(03)00091-2.

[66] M.D. Garcia, M.S. Hoffmeyer, M.C.L. Abbate, M.S. Barría De Cao, R.E. Pettigrosso, G.O. Almandoz, M.P. Hernando, I.R. Schloss, Micro- and mesozooplankton responses during two contrasting summers in a coastal Antarctic environment, Polar Biol 39 (2016) 123–137. https://doi.org/10.1007/s00300-015-1678-z.

[67] M.D. Garcia, M.S. Dutto, C.J. Chazarreta, A.A. Berasategui, I.R. Schloss, M.S. Hoffmeyer, Micro- and mesozooplankton successions in an Antarctic coastal environment during a warm year, PLoS ONE 15 (2020) e0232614. https://doi.org/10.1371/journal.pone.0232614.

[68] S. Hernández-León, P. Sangrà, P. Lehette, L. Lubián, C. Almeida, S. Putzeys, P. Bécognée, M.P. Andrade, Zooplankton biomass and metabolism in the frontal zones of the Bransfield Strait, Antarctica, J. Mar. Syst. 111–112 (2013) 196–207. https://doi.org/10.1016/j.jmarsys.2012.11.001.

[69] A. Atkinson, R.S. Shreeve, Response of the copepod community to a spring bloom in the Bellingshausen Sea, Deep-Sea Res. Part II 42 (1995) 1291–1311. https://doi.org/10.1016/0967-0645(95)00057-W.

[70] E.A. Pakhomov, P.W. Froneman, R. Perissinotto, Salp/krill interactions in the Southern Ocean: spatial segregation and implications for the carbon flux, Deep-Sea Res. Part II 49 (2002) 1881–1907. https://doi.org/10.1016/S0967-0645(02)00017-6.

[71] E.A. Pakhomov, B.P.V. Hunt, Trans-Atlantic variability in ecology of the pelagic tunicate Salpa thompsoni near the Antarctic Polar Front, Deep-Sea Res. Part II 138 (2017) 126–140. https://doi.org/10.1016/j.dsr2.2017.03.001.

[72] E.A. Pakhomov, J. Hall, M.J.M. Williams, B.P.V. Hunt, C.J. Stevens, Biology of Salpa thompsoni in waters adjacent to the Ross Sea, Southern Ocean, during austral summer 2008, Polar Biol 34 (2011) 257–271. https://doi.org/10.1007/s00300-010-0878-9.

[73] V.V. Kasyan, D.G. Bitiutskii, A.V. Mishin, O.A. Zuev, S.A. Murzina, P.V. Sapozhnikov, O.Yu. Kalinina, V.L. Syomin, G.D. Kolbasova, V.P. Voronin, E.S. Chudinovskikh, A.M. Orlov, Composition and Distribution of Plankton Communities in the Atlantic Sector of the Southern Ocean, Diversity 14 (2022) 923. https://doi.org/10.3390/d14110923.

[74] N. Henschke, E.A. Pakhomov, Latitudinal variations in Salpa thompsoni reproductive fitness, Limnol. Oceanogr. 64 (2019) 575–584. https://doi.org/10.1002/lno.11061.

[75] K.R. Sutherland, L.P. Madin, R. Stocker, Filtration of submicrometer particles by pelagic tunicates, Proc. Natl. Acad. Sci. U.S.A. 107 (2010) 15129–15134. https://doi.org/10.1073/pnas.1003599107.

[76] N. Henschke, E.A. Pakhomov, J. Groeneveld, B. Meyer, Modelling the life cycle of *Salpa thompsoni*, Ecol. Model. 387 (2018) 17–26. https://doi.org/10.1016/j.ecolmodel.2018.08.017.

[77] V.J. Loeb, J.A. Santora, Population dynamics of *Salpa thompsoni* near the Antarctic Peninsula: Growth rates and interannual variations in reproductive activity (1993–2009), Prog. Oceanogr. 96 (2012) 93–107. https://doi.org/10.1016/j.pocean.2011.11.001.

[78] B.P.V. Hunt, G.W. Hosie, The seasonal succession of zooplankton in the Southern Ocean south of Australia, part I: The seasonal ice zone, Deep-Sea Res. Part I 53 (2006) 1182–1202. https://doi.org/10.1016/j.dsr.2006.05.001.

[79] N. Henschke, S. Blain, Y. Cherel, C. Cotte, B. Espinasse, B.P.V. Hunt, E.A. Pakhomov, Population demographics and growth rate of Salpa thompsoni on the Kerguelen Plateau, J. Mar. Syst. 214 (2021) 103489. https://doi.org/10.1016/j.jmarsys.2020.103489.

[80] V. Loeb, E.E. Hofmann, J.M. Klinck, O. Holm-Hansen, Hydrographic control of the marine ecosystem in the South Shetland-Elephant Island and Bransfield Strait region, Deep-Sea Res. Part II 57 (2010) 519–542. https://doi.org/10.1016/j.dsr2.2009.10.004.

[81] N.S. Steiner, J. Bowman, K. Campbell, M. Chierici, E. Eronen-Rasimus, M. Falardeau, H. Flores, A. Fransson, H. Herr, S.J. Insley, H.M. Kauko, D. Lannuzel, L. Loseto, A. Lynnes, A. Majewski, K.M. Meiners, L.A. Miller, L.N. Michel, S. Moreau, M. Nacke, D. Nomura, L. Tedesco, J.A. Van Franeker, M.A. Van Leeuwe, P. Wongpan, Climate change impacts on sea-ice ecosystems and associated ecosystem services, Elementa Sci. Anthropocene 9 (2021) 00007. https://doi.org/10.1525/elementa.2021.00007.

[82] M. Czapanskiy, J. Santora, K. Dietrich, M. Cimino, E. Hazen, C. Reiss, R. Veit, Sea-ice and macrozooplankton distribution as determinants of top predator community structure in Antarctic winter, Mar. Ecol. Prog. Ser. 738 (2024) 57–73. https://doi.org/10.3354/meps14609.

[83] E. Seyboth, S. Botta, C.R.B. Mendes, J. Negrete, L. Dalla Rosa, E.R. Secchi, Isotopic evidence of the effect of warming on the northern Antarctic Peninsula ecosystem, Deep-Sea Res. Part II 149 (2018) 218–228. https://doi.org/10.1016/j.dsr2.2017.12.020.

[84] D.G. Bitiutskii, E.Z. Samyshev, N.I. Minkina, V.V. Melnikov, E.S. Chudinovskih, S.I. Usachev, P.A. Salyuk, A.N. Serebrennikov, O.A. Zuev, A.M. Orlov, Distribution and Demography of Antarctic Krill and Salps in the Atlantic Sector of the Southern Ocean during Austral Summer 2021–2022, Water 14 (2022) 3812. https://doi.org/10.3390/w14233812.

[85] B.W. Pietzsch, A. Schmidt, J. Groeneveld, D. Bahlburg, B. Meyer, U. Berger, The impact of salps (*Salpa thompsoni*) on the Antarctic krill population (*Euphausia superba*): an individual-based modelling study, Ecol Process 12 (2023) 50. https://doi.org/10.1186/s13717-023-00462-9.

[86] R. Giesecke, H.E. González, Distribution and feeding of chaetognaths in the epipelagic zone of the Lazarev Sea (Antarctica) during austral summer, Polar Biol 35 (2012) 689–703. https://doi.org/10.1007/s00300-011-1114-y.

[87] V. Øresland, Feeding and predation impact of the chaetognath Eukrohnia hamata in Gerlache Strait, Antarctic Peninsula, Mar. Ecol. Prog. Ser. 63 (1990) 201–209. https://doi.org/10.3354/meps063201.

[88] J. Ameneiro, B. Mouriño-Carballido, J. Parapar, E. Vázquez, Abundance and distribution of invertebrate larvae in the Bellingshausen Sea (West Antarctica), Polar Biol 35 (2012) 1359–1373. https://doi.org/10.1007/s00300-012-1177-4.

[89] A. Atkinson, P. Ward, R. Williams, S.A. Poulet, Diel vertical migration and feeding of copepods at an oceanic site near South Georgia, Mar. Biol. 113 (1992) 583–593. https://doi.org/10.1007/BF00349702.

[90] C. Park, J.H. Wormuth, Distribution of antarctic zooplankton around Elephant Island during the austral summers of 1988, 1989, and 1990, Polar Biol 13 (1993). https://doi.org/10.1007/BF00238756.

[91] K.N. Kosobokova, R.R. Hopcroft, Diversity and vertical distribution of mesozooplankton in the Arctic's Canada Basin, Deep-Sea Res. Part II 57 (2010) 96–110. https://doi.org/10.1016/j.dsr2.2009.08.009.

[92] P. Ward, G.A. Tarling, S.E. Thorpe, Mesozooplankton in the Southern Ocean: Spatial and temporal patterns from Discovery Investigations, Prog. Oceanogr. 120 (2014) 305–319. https://doi.org/10.1016/j.pocean.2013.10.011.

[93] G.C. Hays, H. Kennedy, B.W. Frost, Individual variability in diel vertical migration of a marine copepod: Why some individuals remain at depth when others migrate, Limnol. Oceanogr. 46 (2001) 2050–2054. https://doi.org/10.4319/lo.2001.46.8.2050.

[94] M.D.G. Lopez, M.E. Huntley, Feeding and diel vertical migration cycles of Metridia gerlachei (Giesbrecht) in coastal waters of the Antarctic Peninsula, Polar Biol 15 (1995). https://doi.org/10.1007/BF00236120.

[95] E.M. Giménez, A.C. Nocera, B. Temperoni, G. Winkler, Appendicularians and marine snow in situ vertical distribution in Argentinean Patagonia, J. Plankton Res. 45 (2023) 239–254. https://doi.org/10.1093/plankt/fbac072.

[96] J. Nishikawa, A. Tsuda, Diel vertical migration of the tunicate Salpa thompsoni in the Southern Ocean during summer, Polar Biol 24 (2001) 299–302. https://doi.org/10.1007/s003000100227.

[97] T.L. Hopkins, Food web of an Antarctic midwater ecosystem, Mar. Biol. 89 (1985) 197–212. https://doi.org/10.1007/BF00392890.

[98] V.G. Chavtur, N.V. Kruk, Vertical Distribution of Pelagic Ostracods (Ostracoda, Halocyprinidae) in the Australian–New Zealand Sector of the Southern Ocean, Russ. J. Mar. Biol. 29 (2003) 90–99. https://doi.org/10.1023/A:1023996306419.

[99] A.P. Mackey, A. Atkinson, S.L. Hill, P. Ward, N.J. Cunningham, N.M. Johnston, E.J. Murphy, Antarctic macrozooplankton of the southwest Atlantic sector and Bellingshausen Sea: Baseline historical distributions (Discovery Investigations, 1928–1935) related to temperature and food, with projections for subsequent ocean warming, Deep-Sea Res. Part II 59–60 (2012) 130–146. https://doi.org/10.1016/j.dsr2.2011.08.011.

[100] A.A. Panasiuk-Chodnicka, M.I. Żmijewska, M. Mańko, Vertical migration of Siphonophora (Cnidaria) and their productivity in the Croker Passage, the Antarctic, Pol. Polar Res. 35 (2014) 115–131. https://doi.org/10.2478/popore-2014-0007.

[101] W. Nordhausen, Distribution and diel vertical migration of the euphausiid *Thysanoessa macrura* in Gerlache Strait, Antarctica, Polar Biol 14 (1994). https://doi.org/10.1007/BF00239170.

[102] N. Garcia-Herrera, A. Cornils, J. Laudien, B. Niehoff, J. Höfer, G. Försterra, H.E. González, C. Richter, Seasonal and diel variations in the vertical distribution, composition, abundance and biomass of zooplankton in a deep Chilean Patagonian Fjord, PeerJ 10 (2022) e12823. https://doi.org/10.7717/peerj.12823.

[103] C. Havermans, H. Auel, W. Hagen, C. Held, N.S. Ensor, G. A. Tarling, Predatory zooplankton on the move: Themisto amphipods in high-latitude marine pelagic food webs, in: Advances in Marine Biology, Elsevier, 2019: pp. 51–92. https://doi.org/10.1016/bs.amb.2019.02.002.

[104] J. Donnelly, T.T. Sutton, J.J. Torres, Distribution and abundance of micronekton and macrozooplankton in the NW Weddell Sea: relation to a spring ice-edge bloom, Polar Biol 29 (2006) 280–293. https://doi.org/10.1007/s00300-005-0051-z.

[105] L.P. Madin, G.R. Harbison, The associations of Amphipoda Hyperiidea with gelatinous zooplankton—I. Associations with Salpidae, Deep-Sea Res. I 24 (1977) 449–463. https://doi.org/10.1016/0146-6291(77)90483-0.

[106] G.-A. Paffenhöfer, D.M. Gibson, Determination of generation time and asexual fecundity of doliolids (Tunicata, Thaliacea), J. Plankton Res. 21 (1999) 1193–1189.

[107] A.I. Pinchuk, S.D. Batten, W.W. Strasburger, Doliolid (Tunicata, Thaliacea) Blooms in the Southeastern Gulf of Alaska as a Result of the Recent Marine Heat Wave of 2014–2016, Front. Mar. Sci. 8 (2021) 625486. https://doi.org/10.3389/fmars.2021.625486.

APÊNDICE 2

Artigo submetido ao periódico *Polar Biology*, o qual encontra-se em revisão.

Meso and macrozooplankton distribution across water column during a 20-hours experiment in the Bransfield Strait, Northern Antarctic Peninsula

Meso and macrozooplankton distribution across water column during a 20-hours experiment in the Bransfield Stêndicerait, northern Antarctic Peninsula

Letícia Cazarin Baldoni*[1,4], Raul Rodrigo Costa[2,4], Vanessa Ochi Agostini[3], Carlos Rafael Borges Mendes[2,4], Erik Muxagata[1,4]

[1]Laboratório de Zooplâncton, Universidade Federal do Rio Grande, Instituto de Oceanografia, Av. Itália, km 8, 96203-900 Rio Grande, RS, Brazil

[2]Laboratório de Fitoplâncton e Microorganismos Marinhos, Universidade Federal do Rio Grande, Instituto de Oceanografia, Av. Itália, km 8, 96203-900 Rio Grande, RS, Brazil

[3]Regenera Moléculas do Mar, Prédio 43421, Av. Bento Gonçalves, 9500 - 117 - Agronomia, 91501-970 Porto Alegre, RS, Brazil

[4]Programa de Pós-Graduação em Oceanografia Biológica, Universidade Federal do Rio Grande, Instituto de Oceanografia, Av. Itália, km 8, 96203-900 Rio Grande, RS, Brazil

Abstract

Phytoplankton and zooplankton organisms are important constituents of the Antarctic marine food-web and play important roles in carbon export. This study analysed the composition and vertical distribution of meso- and macrozooplankton along with the phytoplankton community composition during 20 hours in February 2017 at a fixed station in the central basin of the Bransfield Strait. The water column was stratified, resulting in the dominance of cryptophytes in phytoplankton community. The meso- and macrozooplankton community showed a vertical distribution patterns linked to water column dynamics and food availability across layers, which led an accumulation of salps at the surface during all sampling periods. Calanoid copepods were the main taxa in deeper layers. These results suggest that variations in salps dominance at surface change the vertical migration dynamics through the water column. These findings provide substantial insights into how salp and copepod distributions shape meso- and macrozooplankton community structure, with potential implications for food web interactions and carbon flux in the Bransfield Strait.

Key words: Community structure, macrozooplankton, vertical migration, Southern Ocean

1. Introduction

The Southern Ocean (SO) is crucial for Earth's climate due to the thermohaline circulation, climate regulation, and biological carbon sequestration, particularly during the productive seasons in spring and summer (Meredith et al. 2013; Constable et al. 2014; Landschützer et al. 2015; Henley et al. 2019; Orselli et al. 2022). However, significant warming of the upper layer that has been occurring in recent decades is altering hydro physical conditions, and transforming the structure and distribution of plankton communities, leading to notable changes in the Antarctic pelagic ecosystem (Turner et al. 2014; Meredith and King 2005; Convey et al. 2009).

This warming has contributed to a shift in phytoplankton composition, with cryptophytes becoming dominant over diatoms, particularly in the Northern Antarctic Peninsula (NAP), associated with low salinity and warm stratified waters (Moline et al. 2004; Mendes et al. 2018a). This process directly affects the zooplankton community, altering its composition, distribution, and abundance (Atkinson et al. 2004, Atkinson et al. 2019; Moline et al. 2004; Montes-Hugo et al. 2009). As zooplankton link primary production to higher trophic levels, these changes have cascading effects on the entire pelagic ecosystem (Schofield et al. 2024).

The structure of zooplankton communities varies with environmental factors like temperature, chlorophyll-*a*, sea-ice and salinity (Atkinson et al. 2004; Henley et al. 2019). Locally, life cycles, trophic interactions, and primary production cycles shape the distribution of meso- and macrozooplankton (Swadling et al. 2010). In addition to changes in horizontal distribution, vertical shifts take place depending on factors such as region or season of the year (Hosie et al. 2000).

In dynamic regions such as the Bransfield Strait, located in the NAP, the complex hydrography and seasonal shifts in sea-ice actively shape both phytoplankton and zooplankton communities (Mendes et al. 2012; Criales-Hernández et al. 2022). Mesozooplankton generally peak in upper layers under favorable conditions, while deeper waters host different species, some entering periods of inactivity, while others remain active, impacting mesozooplankton populations through predation (Calbet et al. 2005). Changes in water column stratification further drive these vertical shifts,

particularly during the austral summer, complexing zooplankton migration patterns and community composition (Calbet et al. 2005; Liu et al. 2024).

The zooplankton community adjust their depth throughout the day to balance food availability, light irradiance and predation risk, typically ascending to the surface to feed at night and descending to greater depths during the day (Lampert 1989). Body size and grazing interactions also contribute to shaping their distribution (Cisewski and Strass 2016). This vertical movement, driven by diel, seasonal, and ontogenetic migrations, plays a key role in carbon transport to the deep ocean, affecting carbon flux (Turner 2014).

Integrated assessments and syntheses across trophic levels are crucial for improving our understanding of ecosystem variability and the potential impacts of climate change. In order to fully grasp, the role of meso- and macrozooplankton in Antarctic carbon export, particularly in dynamic regions like the Bransfield Strait, comprehensive studies of their vertical distribution and composition are needed (Conroy et al. 2020). Despite existing research focusing mainly on specific taxa and shelf waters, there remain significant gaps in our knowledge of communities throughout water column (Calbet et al. 2005; Garcia et al. 2020). This study addresses these gaps by investigating the composition and vertical distribution of meso- and macrozooplankton over a 500-meter depth range during a 20-hour period in the Bransfield Strait, aiming to shed light on their role in carbon sequestration and their response to environmental changes.

2. Material and Methods

2.1 Field sampling

This study was conducted on board the RV Almirante Maximiano of the Brazilian Navy, as part of the INTERBIOTA project ("Biological Interactions in marine ecosystems around the Antarctic Peninsula under different impacts of climate change") during the Austral summer of 2017. Sampling was carried out between March 3rd and 4th at station B42 (62°17'09''S; 57°02'53''W) located in the Bransfield Strait. This station was chosen since it is located above the Peninsula Front (Fig. 1; Ferreira et al. 2020). The Peninsula Front is a surface front that separates Transitional Zonal Water with Bellingshausen influence (TBW) from Transitional Zonal Water with Weddell Sea (TWW) (Sangrà et al. 2011).

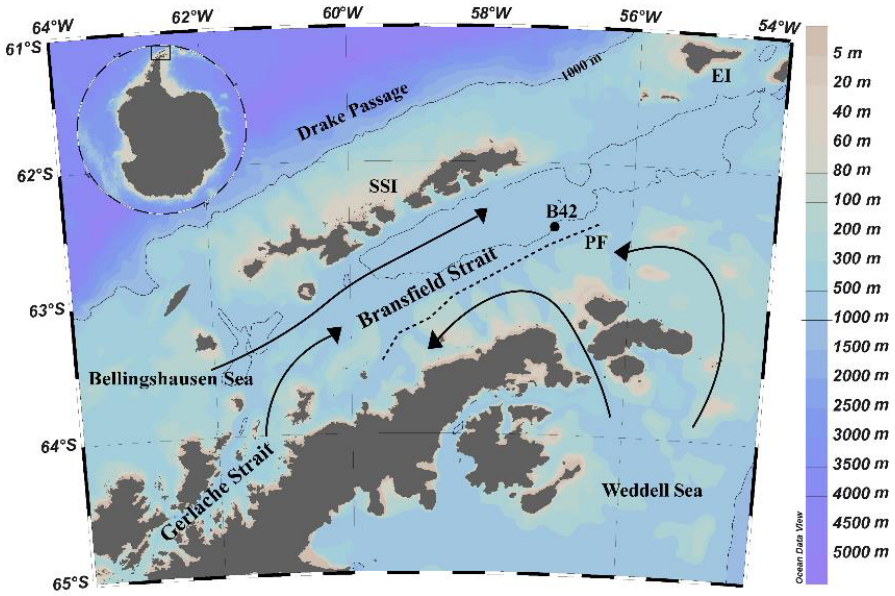


Fig. 1 Map of the Northern Antarctic Peninsula showing the location of the B42 oceanographic station in the Bransfield Strait (B42), with a schematic representation of the influence of adjacent waters, following Zhou et al. (2002), Huneke et al. 2016 and Sangrà et al. (2017). Arrows represent the inflow of Bellingshausen Sea, Gerlache Strait and Weddell Sea waters in Bransfield Strait. SSI = South Shetland Islands, EI = Elephant Island. Dashed line show the surface Peninsula Front (PF)

2.1.1 Physical data

We collected hydrographic data to assess water column dynamics using a Sea-Bird CTD/Carousel (SBE 911+) system equipped with 24 Niskin bottles, profiling down to 500 m. During a 20-hour period, we collected seawater samples (0.5 – 2.5 L) at depths of 5, 25, 50, 75, 100, and 150 m at 4-hour intervals (T1 – 5:07 pm; T2 – 10:28 pm; T3 – 1:08 am; T4 – 5:49 am; T5 – 9:05 am GMT) to assess hydrographic data and phytoplankton groups. We establish the sampling times based on daytime, night-time, information from the NOAA website: https://gml.noaa.gov/grad/solcalc/sunrise.html. Specifically, T1, T2, and T5 correspond to daytime samples, while T3 and T4 represent night-time samples.

2.1.2 Phytoplankton

To evaluate phytoplankton biomass and composition variability, we filtered the water samples collected with the CTD through Whatman® GF/F glass fiber filters under

low vacuum. We then froze the filters in liquid nitrogen for later High-Performance Liquid Chromatography (HPLC) and Chemical Taxonomy (CHEMTAX) analysis (Mackey et al. 1996).

2.1.3 Meso and Macrozooplankton

A MultiNet® (Type Midi - Hydrobios) equipped with 300 μm nets was vertically trawled at station B42 across five strata (500–400 m, 400–300 m, 300–200 m, 200–100 m, and 100–0 m). The trawls occurred at 4-hour intervals (T1 – 5:07 pm; T2 – 10:28 pm; T3 – 1:08 am; T4 – 5:49 am; T5 – 9:05 am GMT) over a 20-hour period on 3 March 2017 to measure meso-macrozooplankton variability. The filtered volume was derived trough the flowmeter coupled to the Multinet. After collection, zooplankton samples were fixed with a 4% formalin solution neutralized with borax (Steedman 1976).

2.2 Physical measurements

Seawater thermodynamic calculations were performed with the Thermodynamic Equation of Seawater - 2010 (TEOS-10). The seawater potential density (kg m^{-3}) referenced to 0 dbar was determined for each CTD cast based on seawater conservative temperature, absolute salinity, and pressure data. To examine the water column physical structure, the mixed layer depth (MLD; m) was calculated as the depth at which seawater potential density deviates from its 10 m depth value by a threshold of 0.03 kg m^{-3} (de Boyer Montégut et al. 2004). In addition, we also used the seawater potential density to calculate water column stability (x10^{-6} m^{-1}) as a function of buoyancy frequency by the local gravity, as described by Costa et al. (2020).

2.3. Laboratory analysis

The concentration of Chl-*a* and class-specific accessory pigments were measured by HPLC as described in Costa et al. (2020). The absolute (mg m^{-3} Chl-*a*) and relative (%) contribution of phytoplankton chemotaxonomic groups were estimated via CHEMTAX software v1.95 (Mackey et al. 1996). Seven algal groups were chosen for CHEMTAX analysis based on initial pigment ratios derived for the NAP (Mendes et al. 2018, Costa et al. 2022). The groups resolved include diatoms Type-A, diatoms Type-B, dinoflagellates Type-A, dinoflagellates Type-B, cryptophytes, haptophytes Type 8

(*Phaeocystis antarctica* Karsten, 1905), and green flagellates. The diatoms (sum of diatoms Type-A and diatoms Type-B) and the dinoflagellates (sum of dinoflagellates Type-A and dinoflagellates Type-B), were grouped as the same chemotaxonomic group. CHEMTAX results were optimized following Wright et al. (2009). The procedure of quality control was performed by microscopic analysis.

Three types of Chl-*a* degradation products: chlorophyllide-*a* (Chlide-*a*), pheophytin-*a* (Phytin-*a*), and pheophorbide-*a* (Phide-*a*) were identified and quantified by HPLC analysis. Phaeopigments have long been observed in the fecal pellets of zooplankton organisms (Coelho et al. 2011). Therefore, we used the sum of the Phytin-*a* and Phide-*a* as a proxy of grazing pressure, and Chlide-*a* as the senescence of phytoplankton cells. These two indices were divided by the total of degradation products plus Chl-*a* (sum of Chl-*a*, Phytin-*a*, Phide-*a*, and Chlide-*a*), and represented as a percentage (Costa et al. 2021).

All zooplankton samples were examined under a stereo microscope, where all organisms present were quantified and identified. Larval stages and immature forms (e.g copepodites) were identified to a higher taxonomic level due to difficulties in identification, while adult forms were identified to the lowest possible taxonomic level. The identification was conducted based on the descriptions from Bouillon (1999), Bradford-Grieve et al. (1999), Pugh (1999), Gibbons et al. (1999), Thuesen and Álamo (1999), Vinogradov (1999), Esnal and Daponte (1999), Casanova (1999), van der Spoel and Dadon (1999) and Razouls et al. (2023) (Biodiversity of Marine Planktonic Copepods resource - available at http://copepodes.obs-banyuls.fr/en). We expressed abundances as org.1000 m^{-3}.

2.4. Statistical analysis

The environmental parameters were treated and the average temperature, salinity, turbidity, and density for each sampled depth stratum were obtained. To summarize the patterns in the meso- and macrozooplankton community structure, we performed a Non-Metric Multidimensional Scaling (nMDS) using the Bray-Curtis similarity index on the Hellinger transformed abundance of zooplankton species (org.1000m^{-3}) that occurred in more than 10% of the samples. This transformation reduced the influence of numerically

dominant species on the analysis (Legendre and Legendre 2012). The "Envifit" function was applied to explore the relationship between the zooplankton community and environmental variables in the nMDS ordination, testing for significance using a permutation test (999 interactions). This allowed us to obtain p-values for the influence of each environmental variable on species distribution, and the vectors were overlaid on the nMDS plots.

A PERMANOVA test based on 999 permutations were conducted to determine significant differences in community composition between different sample times and layers, using the R "vegan" package (Oksanen et al. 2019). Indicator Species Analysis (ISA) with the "indicspecies" package (De Caceres and Legendre 2010) were also conducted to identify species strongly associated with particular strata. 95% confidence level (p-value ≤ 0.05) were used to identify indicator species (Dufrêne and Legendre 1997).

Diversity indices for different strata and sampling times were obtained using Hill numbers, including the exponential of the Shannon-Weaver index (Exp H′) and the inverse of the Simpson index (1/D) (Hill 1973). Pielou's evenness index (H'/ln(S)) represented species evenness, where S indicates total species richness at the site. All diversity indices and statistical analyses were calculated using R v.4.2.0 (R Core R Development Core Team 2022).

3. Results

3.1. Oceanographic conditions

The water temperature in the upper 100 meters ranged from -0.30°C to 1.48°C, with the lowest temperature (-1.17°C) recorded at 400-500 meters during T1 at 17:07 (GMT), and the highest (1.48°C) observed at the surface during T5 at 09:05. Salinity varied from 34.03 to 34.53, with the minimum at the T1 surface and the maximum in the deeper layers during T2 (Fig. 2). Mixed layer depth (MLD) was relatively deep (> 60 m) during all sampling times (from T1 to T5) with values around 80 m (Fig 2).

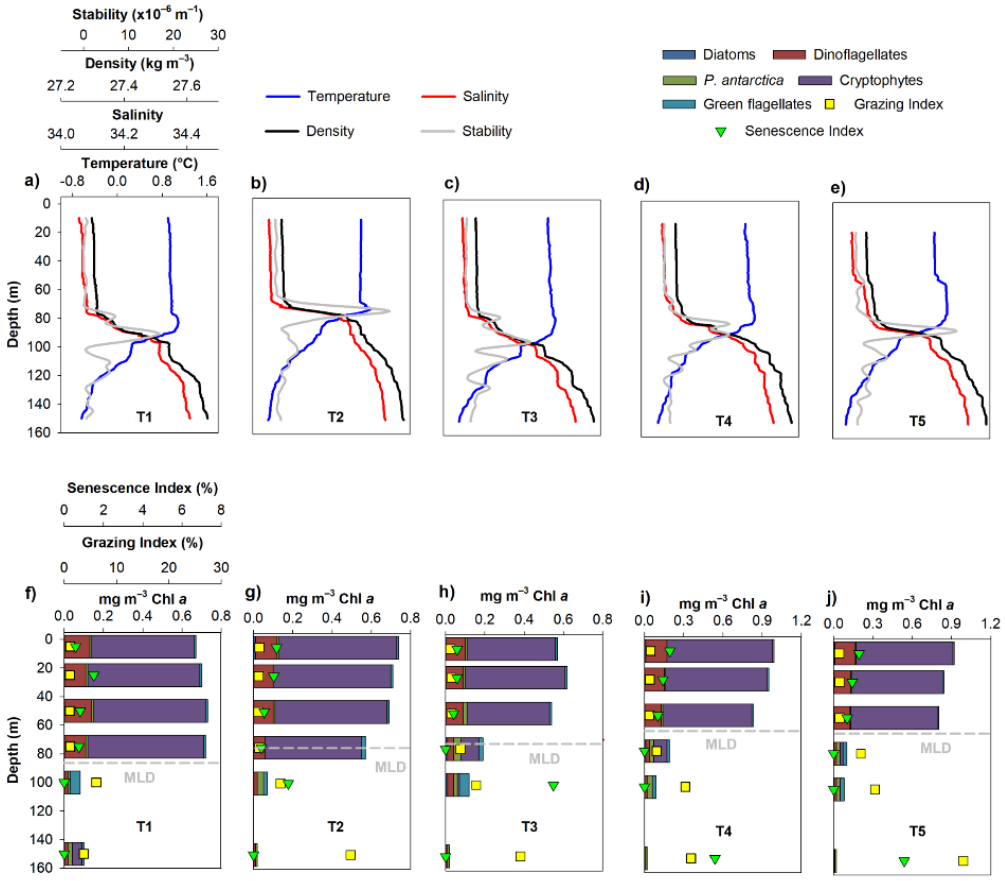


Fig. 2 (a – e) Vertical profiles of water column temperature (°C), salinity, density (kg m^{-3}) and stability (x10^{-6} m^{-1}) in the top panel. (f - j) Depth distribution of phytoplankton groups' biomass (mg m^{-3} Chl-*a*), grazing index (%) and senescence index (%) in the lower panel. Diatoms (blue), dinoflagellates (dark red), *P. antarctica* (green), cryptophytes (purple) and green flagellates (light blue) are shown. Dashed gray line represents mixed layer depth (MLD; m)

The TS-diagram showed a stratified water column at the B42 station, with TBW occupying the upper layers down to 120 m, characterized by warmer and less saline water, and TWW influencing the deeper, colder, and saltier layers (Fig. 3).

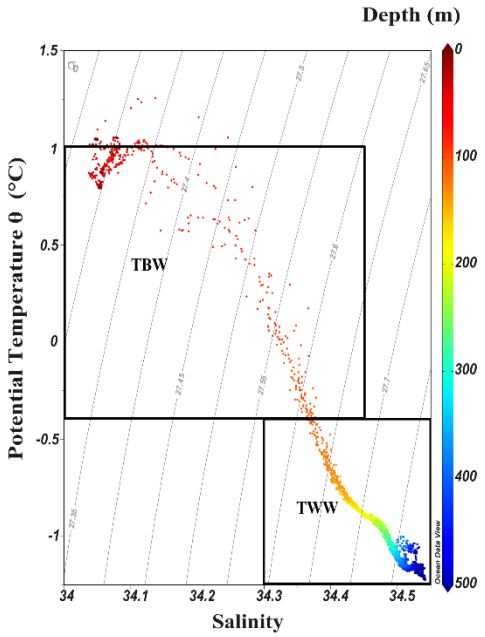


Fig. 3 T–S diagram for B42 oceanographic station from the Bransfield Strait with the waters masses observed: Transitional Zonal Water with Bellingshausen Sea influence (TBW), Transitional Zonal Water with Weddell Sea influence (TWW)

3.2 Phytoplankton community

The phytoplankton biomass accumulation was relatively low ranging from 0.57–0.98 mg m^{-3} Chl-*a*. There was an increase from T1-T3 to T4-T5 (Fig. 2). Cryptophytes dominated the composition of the phytoplankton community, while diatoms were almost absent (Fig. 2). The macronutrient concentrations were not limiting to phytoplankton biomass accumulation, with dissolved inorganic nitrogen, phosphate, and silicic acid exceeding 21 µM, 1.5 µM, and 80 µM, respectively (Supplementary Table S1). The grazing index remained stable within the MLD at low levels (0.9–1.15%) but increased significantly below the MLD (2.32–26.28%) (Fig. 2). The senescence index increased from T1 to T5 (0.41–2.59%) (Fig. 2), indicating phytoplankton community deterioration over the study period.

3.3 Meso- and macro-zooplankton community composition

A total of 4039 organisms from 65 taxa were identified across 25 zooplankton samples (Online Resource 2). Of these, 23 taxa were either in early developmental stages or too damaged to be identified at the species level. Copepoda dominated the samples

with 92% of frequency of occurrence and a relative abundance (R.A.) of 59.45%, followed by Thaliacea at 21.61% R.A. (Online Resource 2). In total, we identified 42 zooplankton species, including 26 copepod species, 2 Euphausiacea, 4 Amphipoda, 3 Thaliacea, 2 Chaetognatha, 2 Siphonophora, 2 Polychaeta, and 1 Pteropoda. The most abundant species were *Salpa thompsoni* (5698 org.1000 m^{-3}), followed by *Metridia gerlachei* (3500 org. 1000 m^{-3}), and *Oithona similis* (1313 org.1000 m^{-3}). All the taxa identified in the samples are shown in Online Resource 2.

3.4 Diel vertical distribution

Vertical profiles of abundance of the dominant zooplanktonic groups are given in Fig. 4. Higher abundances were concentrated in the deeper layers, except for salps that clearly dominated the surface layer (80% R.A., Fig. 4). The highest zooplankton abundance (13265 org.1000m^{-3}) was recorded during daylight at T1 (05:07 pm) between 400-500 m. The lowest zooplankton abundance (341 org.1000m^{-3}) occurred at T5 (09:05 am) between 100-200 m.

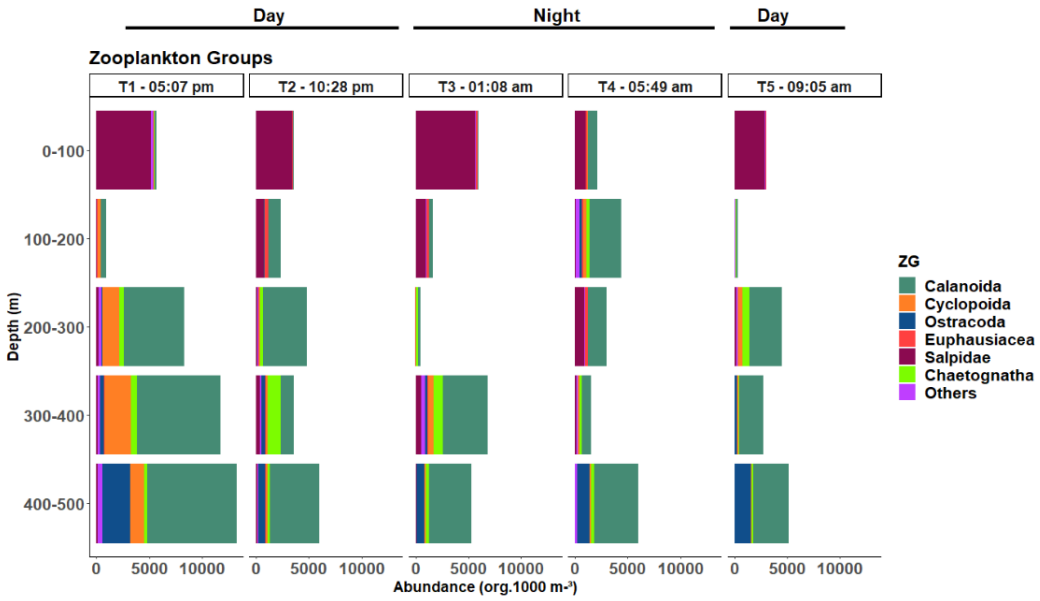


Fig. 4 Vertical distribution of the main zooplanktonic groups in each sampling time of B42 station in 2017 where: T1 -5:07 pm; T2 -10:28 pm; T3 - 1:08 am; T4 -5:49 am and T5 - 9:05 am. Day and night period is also indicated

In the surface layer (0-100 m), the highest zooplankton abundance occurred at T3 (01:08 am, 5953 org.1000m-3). Between depths of 100 and 200 m, zooplankton abundance was higher at T4 (05:49 am, 4345 org.1000m-3). Maximum zooplankton abundances of the strata below 200 m (200-300, 300-400, 400-500 m) occurred during T1 (05:07 pm).

In general, species richness increased with the depth, with lowest values in the surface layer (0–100 m) and highest values in the deeper layers (from 300 to 500 m), during the day and night (Table 1). Despite that, zooplankton diversity indexes, Shannon-Weaver index (Exp H') and the inverse of Simpson index (1/D) were higher in intermediate layers than in deeper layer, mainly between 100 and 200 m at night (T4 05:49 am). The lowest diversity index was in the surface, early in the morning, during T5 (09:05 am) (Table 1). However, the highest number of species (21) was found at 400-500 m in the afternoon during T1 (05:07 pm) (Table 1). Species showed a more even distribution in intermediate depths compared to the surface and deep layers, regardless of the sampling time (Table 1).

Table 1 Diversity indexes calculated for each strata and each sampling time. Species richness (S), Exponential of Shannon-Waver index (Exp H'), the inverse of Simpson index (1/D) and Pielou's evenness index (J)

Diversity indexes	Strata	T1	T2	T3	T4	T5
S	0-100	10	4	4	6	4
	100-200	3	7	6	12	5
	200-300	7	8	3	4	11
	300-400	15	9	11	6	3
	400-500	**21**	9	11	9	9
Exp H'	0-100	1.49	1.23	1.24	3.25	1.19
	100-200	2.82	3.51	2.89	**10.32**	4.37
	200-300	4.95	3.76	2.46	2.85	7.14
	300-400	6.13	5.18	6.29	5.36	2.36
	400-500	4.59	3.89	2.37	2.99	3
1/D	0-100	1.15	1.08	1.09	2.52	1.06
	100-200	2.66	2.97	2.19	**9.13**	3.76
	200-300	4.23	2.51	2.13	2.58	5.42
	300-400	4.36	4.03	5.02	5	2.05
	400-500	2.27	2.56	1.48	1.84	2.02
J	0-100	0.17	0.15	0.15	0.65	0.12
	100-200	**0.94**	0.64	0.59	0.93	0.91
	200-300	0.82	0.63	0.81	0.75	0.81
	300-400	0.66	0.74	0.76	0.93	0.78
	400-500	0.5	0.61	0.36	0.49	0.49

Aggregate forms of *S. thompsoni* (sexual generation, blastozooids) dominated the observed salp population at surface layers during all sampling times, especially during the night at 01:08 am (Fig. 5). Salps were relatively scarce below 300 m and at T4-T5, the abundance of salps decreased in the surface (0-100 m; Fig. 4).

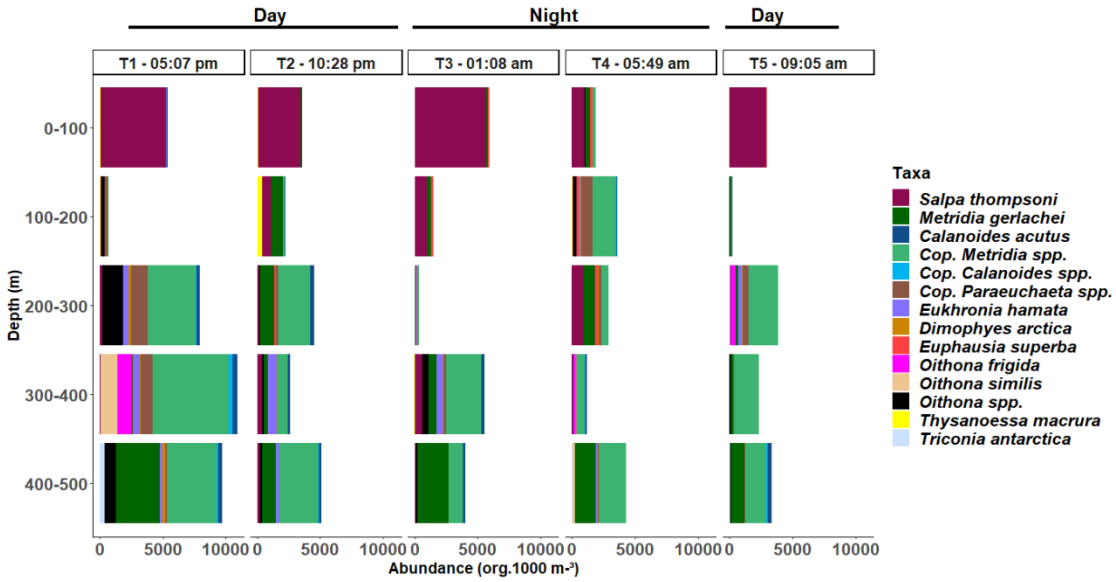


Fig. 5 Vertical distribution of the main meso- and macrozooplanktonic taxa in each sampling time of B42 station in 2017 where: T1 -5:07 pm; T2 -10:28 pm; T3 - 1:08 am; T4 -5:49 am and T5 - 9:05 am. Day and night period is also indicated

In contrast with the surface layer, copepods dominated (74%) the community of the deeper layers (from 300 to 500 m). *M. gerlachei* and *Calanoides acutus* were the most abundant species of Calanoida (Table 1). Most adults of *M. gerlachei* were restricted to the deeper layer (400-500 m, Fig. 5) during the day and the copepodites between the 200 to 400 m (Fig. 5). There was an increase in the abundance of adults at night, which were observed in the surface layer, following by copepodites just below (100 – 200 m). At T5, early morning, adult abundance decreased at the surface and increased at 400-500 m, while copepodites increased between 200-400 m. *C. acutus*, the second most abundant copepod, concentrated between 200-400 m and was restricted to 100-200 m at night (Fig. 5). Other adults calanoid species were restricted to depths greater than 200 m. However, we observed an increase in copepodites abundances of *Calanoides* spp., and *Paraeuchaeta* spp. during the night period (T4) in upper layers (100-200 m, Fig. 5).

Species of *Oithona* also strongly represented the copepod community. Small copepods remained fairly constant throughout the water column at all sampling time but were more concentrated below 200 m (Fig. 5). Overall, copepod abundances increased with depth while the proportion of *S. thompsoni* decreased (Fig. 5). Ostracods and chaetognaths made up a large portion of the deep zooplankton community (Fig. 4), where *Eukrohnia hamata* was the most abundant species (676 org.1000m^{-3}) at 300-400 m, and ostracods (2647 org.1000 m^{-3}) dominated at 400-500 m, especially during the day (T1 and T5, Fig. 5).

Cnidarian taxa appeared at different depths, mostly in the deepest layers, with a slight increase near the surface during the night (T3 01:08 am and T4 05:49 am). Only four cnidarian taxa were identified (Online Resource 2), with *Dimophyes arctica* being the most abundant species among them (265 org.1000m^{-3}) at 400-500 m (Fig. 5).

Euphausiids were sparse, with only two species identified: *Euphausia superba* and *Thysanoessa macrura*. Almost all specimens of *E. superba* were juveniles and found in deeper layers during the day and in shallower depths during the night. Only one adult was found at surface during the night (T3 at 01:08 am). In contrast, abundances of *T. macrura* were higher at surface layer during the day, while during the night they were found in deep layers (Fig. 5). The highest abundance of *E. superba* (259 org.1000m^{-3}) occurred during the night at T4 (05:49 am) between 200-300 m, while *T. macrura* peaked (372 org. 1000m^{-3}) at T2 (10:28 pm) between 100-200 m (Fig. 5).

The nMDS analysis revealed distinct groups of samples across different depth layers (Fig. 6). The abundance and composition of the 17 main species (present in over 10% of the samples) showed little variation over the different sampling times (T1–T5) (PERMANOVA $p > 0.05$) but differed significantly between depth strata (PERMANOVA $p < 0.001$).

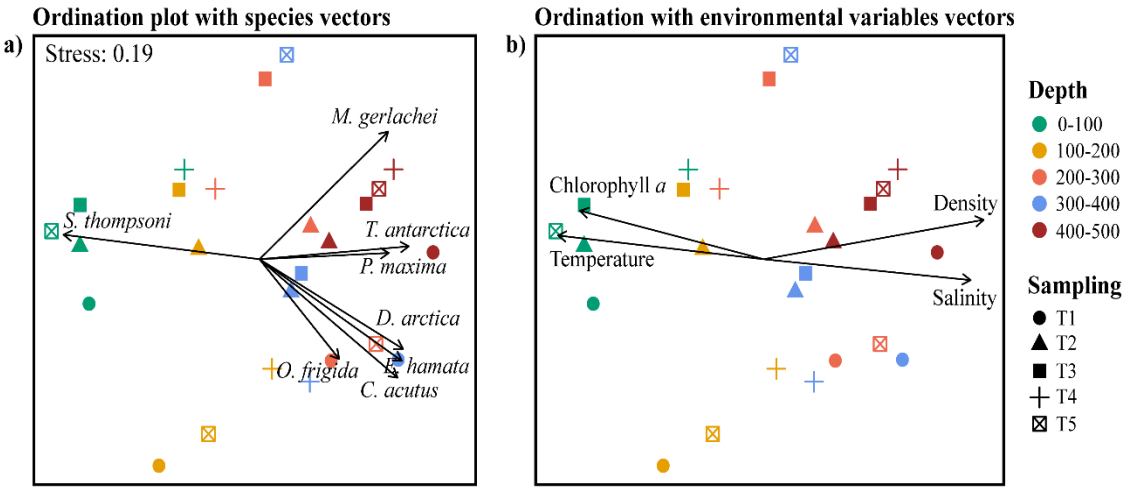


Fig. 6 Non-metric multidimensional scaling (nMDS) of the main zooplanktonic species collected in B42 station in 2017. Vectors show the significant species (a) and environmental variables (b) with nMDS ordination of samples

Environmental variables on the nMDS plot (Fig. 6) showed an interaction between the surface community (0-100 m) and factors such as temperature and chlorophyll-a. Indicator species analysis confirmed that *S. thompsoni* was strongly associated with the surface layer ($p < 0.001$), where higher temperatures and chlorophyll-a concentrations were recorded (Fig. 6). In contrast, the abundant copepod, *M. gerlachei*, was linked to the deepest stratum (400-500 m) ($p < 0.001$). Additionally, *E. hamata* was associated with intermediate depths (200-400 m) ($p < 0.05$).

4. Discussion

4.1. Influence of oceanographic properties of the water column on the interactions of phytoplankton and zooplankton

The T-S diagram shows the expected stratification in the water column, with warmer, less saline waters from the Bellingshausen Sea influence surface layers, while colder, saltier waters from the Weddell Sea affect deeper layers (>120 m) (Sangrà et al. 2011; Huneke et al. 2016; Criales-Hernández et al. 2022; Frey et al. 2022). The distribution of plankton community, both vertically and horizontally, is shaped by these water masses, which play a key role across different ocean layers and regions of NAP (Mendes et al. 2018; Costa et al. 2020; Criales-Hernández et al. 2022). The advection of

warmer waters from the Bellingshausen Sea contributes to nutrient-rich waters in the surface layers (Online Resource 1), coming from productive coastal areas, particularly the Gerlache Strait (Zhou et al. 2002; Ferreira et al. 2020; Costa et al. 2021).

The dominance of cryptophytes in the surface layers is linked to a stratified shallow mixing layer (~20 m) influenced by localized glacier meltwater and potential light stress (Mendes et al. 2018a, b, 2023). However, station B42, located far from coastal areas, is unlikely to experience significant glacier meltwater input. Cryptophytes are known for thriving in environments with limited competition, especially under adverse conditions (Henley et al. 2019; Costa et al. 2023; Mendes et al. 2023). The lack of large diatoms, the dominant phytoplankton group in the NAP (Costa et al. 2021, 2023), suggests that cryptophytes dominance could be due to the absence of competition. The lack of diatoms in our analysis (Fig. 2) could be attributed to deep mixed layer depths (>60 m) during our 20-hour sampling, preventing their development. Large diatom blooms, such as those observed in the Gerlache Strait during an El Niño event in 2016, occur in more stable waters (Costa et al. 2020, 2021). Despite abundant macronutrients and no micronutrient limitations for phytoplankton growth (Annett et al. 2017; Sherrell et al. 2018), the role of water column appears to have shaped the phytoplankton community observed in this study.

Over the study period, grazing index values rapidly increased below MLD, indicating a sinking process of the fecal pellets, and we also observed a deterioration process of phytoplankton community composition with increasing values of senescence index (Fig. 2), which is also correlated with grazing pressure (Costa et al. 2023). Therefore, these results further support the grazing activity of local meso- and macrozooplankton assemblages on phytoplankton community during the different sampling times.

The top-down control may drive phytoplankton biomass accumulation. However, the cryptophytes kept a relatively high standard stock during the 20h experiment (Fig. 2). This result raises a question, how could cryptophytes thrive under grazing? Unfortunately, our results and approaches cannot answer this question. Future studies should focus on cryptophytes' to understand better the coupling between phytoplankton and zooplankton species along the NAP.

4.2 Meso- and macrozooplankton community composition and vertical distribution

In this study, all the taxa identified are commonly recorded in the SO (Ward et al. 2014; Razouls et al. 2023; Schaafsma et al. 2024). Copepods and *S. thompsoni* were the most abundant meso- and macrozooplankton forms in terms of abundance, converging with previous studies in the region (Cabal et al. 2002; Ward et al. 2005; Marrari et al. 2011; Ochoa et al. 2016; Giraldo et al. 2019; Garcia et al. 2020; Criales-Hernández et al. 2022). Less abundant groups, including Amphipoda, Chaetognatha, Cnidaria, Pteropoda, Polychaeta and Appendicularia, generally exhibit varying abundances distributions in different regions of the Southern Ocean (Ward et al. 2005; Swadling et al. 2010; Conroy et al. 2020).

Although studies in the Antarctic Peninsula often report high euphausiid abundance (Ashjian et al. 2004; Calbet et al. 2005; Marrari et al. 2011; Siegel et al. 2013; Tarling et al. 2018; Criales-Hernández et al. 2022), our study found unexpectedly low values. This likely stems from the employment of the MultiNet in vertical hauls (Wiebe and Benfield 2003) and the ability of euphausiids to evade capture by nets (Atkinson et al., 2012). Our findings indicated approximately a tenfold decrease in adult krill abundance compared to observations with oblique tows using other equipment like the IKMT-500, in Bransfield Strait (Criales-Hernández et al. 2022). Furthermore, oblique trawls with the bongo net in the same region also generally capture more euphausiids (Plum et al. 2021; Kasyan 2023).

We observed significant variations in the vertical distribution of specific mesozooplankton groups throughout different periods of the day. This behaviour aligns with the common vertical migration reported for several species in the Antarctic Ocean (Atkinson et al. 1992; Lopez and Huntley 1995; Hays et al. 2001; Hernandez-Leon et al. 2001; Hunt et al. 2003; Hunt and Hosie 2005, 2006). This daily movement probably explains the observed variations in abundance along the vertical profiles. However, the PERMANOVA analysis revealed no significant differences in species abundance across sampling times, suggesting minimal influence of vertical migrations. A notable exception occurred at night, when a decrease in surface salps abundance coincided with an increase in copepods and krill. This was further supported by an increase in diversity and equitability indexes values (Table 1). These results align with other studies around the

NAP (Hopkins 1985; Lopez and Huntley 1995; King and LaCasella 2003; Ward et al. 2007; Siegel et al. 2013; Conroy et al. 2020; Ichii et al. 2020), likely indicating a competition between these species due to the feeding behaviour.

Our results revealed two distinct meso- and macrozooplankton communities: one in the surface layer dominated by *S. thompsoni* and another in the deeper layers dominated by calanoid copepods. These communities may be partially driven by water column dynamics and the availability of food throughout it (Conroy et al. 2020; Liu et al. 2024). Consistent with our sampling period, previous research has demonstrated that the abundance of dominant salps increase in late summer due to the persistence of relatively warm surface waters in March and the presence of high cryptophytes biomass creating favourable conditions (Moline et al. 2004; Hunt and Hosie 2006)

In the deeper layers, the abundance of copepods was highest than surface layers. *M. gerlachei* was the most abundant copepod, which is a common calanoid in the Antarctic Peninsula and plays a key role in the Southern Ocean's carbon cycle and trophic structure as both grazer and prey (Calbet and Irigoien 1997; King and LaCasella, 2003; Conroy et al. 2020). Considered as a mid-water species (Hopkings and Torres 1988) and consistent with previous studies (Lopez and Huntley 1995; Yebra et al. 2009; Venkataramana et al. 2022), *M. gerlachei* was predominantly found in the 300-500 m depth layers. It has already been reported that *M. gerlachei* begins its migration to shallower depths, for feeding mainly during the night (Lopez and Huntley 1994), despite its omnivorous nature (Hopkins 1985), consuming phytoplankton, especially during the summer and spring months (Hopkins and Torres 1989). Despite differences in sampling times, vertical migrations did not significantly alter the community's vertical distribution, except at T4 when a decrease in salps abundance at the surface allowed *M. gerlachei* and krill to increase, indicating potential competition for space and food. Furthermore, *M. gerlachei* adapts its feeding strategies based on food availability at different depths, allowing it to exploit multiple ecological niches and minimize competition (Yang et al. 2018). Its distribution appears unrelated to water column properties, likely influenced more by food resources.

Several calanoid copepodites were present during the study period. We observed a possible ontogenetic migration of *Calanoides* spp., *Metridia* spp., and *Paraeuchaeta*

spp. during the nocturnal period (T3 and T4). This was indicated by increased abundances of adults (531 org. 1000 m^{-3}) and copepodites (2759 org. 1000 m^{-3}) in the surface (0–100 m) and subsurface layers (100–200 m) compared to daytime (T1), when their numbers were much lower (32 and 276 org. 1000 m^{-3}, respectively). During T5, these calanoids were scarce at the surface but increased significantly (6756 org. 1000 m^{-3}) in deeper strata (200–500 m). Similar ontogenetic migrations have been noted off the Antarctic Peninsula (Michels et al. 2012; Yang et al. 2017; Conroy et al. 2020; Liu et al. 2024).

Small copepods, such as *T. antarctica* and adults of *Oithona* spp., concentrated at deeper layers (200–500 m) during the study, with abundances of 353 and 4105 org.1000 m^{-3}, respectively. In deeper layers, the decrease in phytoplankton biomass combined with the increase in sinking particles could be advantageous for omnivores, scavengers, or predators (Nishikawa & Tsuda, 2001; Conroy et al. 2020). Other authors have observed these copepods feeding below 100 m on fecal pellets from surface organisms, including salps (González and Smetacek 1994; Svensen and Nejstgaard 2003; Dagg et al. 2014). These larger pellets, which may contain undigested phytoplankton (Gilli et al. 2006), enable other zooplankton at greater depths to ingest these particulate organic materials during the sinking process (González and Smetacek 1994; Cavan et al. 2015). Therefore, the high salp abundances in the surface layers (Fig. 4) suggests that *T. antarctica* and *Oithona spp.* could be feeding on their sinking fecal pellets, which likely explains these copepods taxa accumulations at deeper layers throughout the study period.

In addition to copepods, deeper layers also showed increased abundances of Chaetognata, Polychaeta, Cnidaria and Ostracada. Chaetognats, polychaets and cnidarians are all carnivorous predators that typically follow copepods distributions such as *Oncaea* spp., *M. gerlachei*, and *Paraeuchaeta* spp. (Hopkins 1985), which were the most abundant copepods taxa in our study (Online Resource 2). During the summer, off the Antarctic Peninsula, they remain in deeper layers to feed on abundant copepods (Conroy et al. 2020), supporting a clear predator-prey in these groups.

Meanwhile, Ostracoda, primarily detritivores, are more abundant at greater depths due to the higher availability of organic particles sinking from the surface (Conroy et al. 2020). Although ostracods maintained their distributions at deeper layers, during the nocturnal period they were found in lower abundance (172 org.1000 m^{-3}) in the 100-200

m layer. Similarly, studies in the NAP reported ostracods more abundant below 200 m (Hopkins 1985, Marrari et al. 2011) and generally, on the contrary, scarce in the lower epipelagic waters (0-200 m; Blachowiak-Samolyk & Angel 2007), consistent with our observations.

Our findings suggest that local water masses and the feeding behavior of macrozooplankton, particularly salps, driven vertical distribution patterns. Increasing salp abundance in Northern Antarctic Peninsula waters poses potential implications for regional food webs and biodiversity (Henley et al. 2019). Future research on the role of salps as both grazers and prey will be vital for understanding changes in carbon export to the deep ocean.

5. Conclusion

The vertical distribution of meso- and macrozooplankton in this study aligns with oceanographic conditions and food availability across the sampled water layers. Higher temperatures, lower salinity, and increased phytoplankton biomass in the upper layers likely influenced the abundance and diversity of key zooplankton groups. The stabilized shallow mixing layer, with the dominance of cryptophytes, may serve as a primary food source for salps at the surface. In periods of high phytoplankton biomass, some zooplankton may remain at the surface to feed, pausing their vertical migration (Cisewski and Strass 2016). However, the observed dominance of *S. thompsoni* in surface waters may have formed a barrier, hindering other species from completing their migrations and reaching the upper layers in significant numbers. The increasing frequency of salp blooms could have major ecological impacts on the regional food web and carbon cycling, affecting both surface and deep-water communities. This underscores the need for further research to understand the expanding role of salps and their complex interactions in Antarctic ecosystems.

Authors' Contributions: L.C.B. elaborated the principal idea, lead the writing and revisions and drawing the figures of the manuscript. R.R.C. and C.R.B.M. carried out the HPLC/CHEMTAX analysis. R.R.C. contributed to the elaboration of figures and texts referring phytoplankton. V.O.A. carried out the sampling. E.M. contributed to the conception of this work, supervised and reviewed the manuscript. R.R.C., C.R.B.M.,

V.O.A. and E.M. contributed to the organization and writing of the final version of the manuscript. All authors contributed to manuscript revision, read, and approved the submitted version.

Acknowledgements

This study is part of the Brazilian High Latitude Oceanography Group (GOAL) activities in the Brazilian Antarctic Program (PROANTAR). This study was conducted within the projects INTERBIOTA, NAUTILUS, PROVOCCAR, ECOPELAGOS (Conselho Nacional de Desenvolvimento Científico e Tecnológico (CNPq) grant numbers 407889/2013-2, 405869/2013-4, 442628/2018-8, 442637/2018-7, respectively). We thank the coordinators of the mentioned projects, E. R. Secchi and M. M. Mata. We thank the crew of the Brazilian Navy on board of the RV Almirante Maximiano as well as several scientists and technicians from GOAL participating in the cruise for their valuable help during sampling. We are grateful to Simon Wright, from the Australian Antarctic Division, for providing the CHEMTAX v.1.95 software. L. C. Baldoni and R. R. Costa were granted with Ph.D. and M.Sc. fellowships, respectively, from Coordenação de Aperfeiçoamento de Pessoal de Nível Superior (CAPES) at the Programa de Pós-graduação em Oceanografia Biológica (Universidade Federal do Rio Grande - FURG). Carlos R.B. Mendes received CNPq researcher productivity grant no. 312569/2021-1. E. Muxagata received CNPq researcher productivity grant no. 307633/2023-3.

Compliance with Ethical Standards

There is no conflict of interest.

References

Annett AL, Fitzsimmons JN, Séguret MJ, Lagerström M, Meredith MP, Schofield O, Sherrell RM (2017) Controls on dissolved and particulate iron distributions in surface waters of the Western Antarctic Peninsula shelf. Mar. Chem. 196: 81–97.

Ashjian CJ, Rosenwaks GA, Wiebe PH, et al (2004) Distribution of zooplankton on the continental shelf off Marguerite Bay, Antarctic Peninsula, during Austral Fall and Winter, 2001. Deep-Sea Res II 51:2073–2098. https://doi.org/10.1016/j.dsr2.2004.07.025

Atkinson A, Hill SL, Pakhomov EA, et al (2019) Krill (Euphausia superba) distribution contracts southward during rapid regional warming. Nature Clim Change 9:142–147. https://doi.org/10.1038/s41558-018-0370-z

Atkinson A, Schmidt K, Fielding S, et al (2012) Variable food absorption by Antarctic krill: Relationships between diet, egestion rate and the composition and sinking rates of their fecal pellets. Deep-Sea Res II 59–60:147–158. https://doi.org/10.1016/j.dsr2.2011.06.008

Atkinson A, Siegel V, Pakhomov E, Rothery P (2004) Long-term decline in krill stock and increase in salps within the Southern Ocean. Nature 432:100–103. https://doi.org/10.1038/nature02996

Atkinson A, Ward P, Williams R, Poulet SA (1992) Diel vertical migration and feeding of copepods at an oceanic site near South Georgia. Mar Biol 113:583–593. https://doi.org/10.1007/BF00349702

Blachowiak-Samolyk K, Angel MV (2007) A year round comparative study on the population structures of pelagic Ostracoda in Admiralty Bay (Southern Ocean). Hydrobiologia 585:67–77. https://doi.org/10.1007/s10750-007-0629-2

Bouillon J (1999) Hydromedusae. In: Boltovskoy D (ed) South Atlantic Zooplankton. Bachyuys, Netherlands, pp 385-466

Bradford-Grieve JM, Markhasev EL, Rocha CEF, Abiahy B (1999) Copepoda. In: Boltovskoy D (ed) South Atlantic Zooplankton. Bachyuys, Netherlands, pp 869-1098

Cabal A, Alvarez-Marqués F, Acuña L, Quevedo M, Gonzalez-Quirós R, Huskin I, Fernández D, Rodriguez VC & Anadón R (2002) Mesozooplankton distribution and grazing during the productive season in the Northwest Antarctic Peninsula (FRUELA cruises). Deep-Sea Res II 49. https://doi.org/10.1016/S0967-0645(01)00128-X

Calbet A, Alcaraz M, Atienza D, et al (2005) Zooplankton biomass distribution patterns along the western Antarctic Peninsula (December 2002). J Plankton Res 27:1195–1203. https://doi.org/10.1093/plankt/fbi081

Calbet A, Irigoien X (1997) Egg and faecal pellet production rates of the marine copepod *Metridia gerlachei* northwest of the Antarctic Peninsula. Polar Biol 18:273–279. https://doi.org/10.1007/s003000050188

Casanova JP (1999) Chaetognatha. In: Boltovskoy D (ed) South Atlantic Zooplankton. Bachyuys, Netherlands, pp 1353-1374

Cavan EL, Le Moigne FAC, Poulton AJ, et al (2015) Attenuation of particulate organic carbon flux in the Scotia Sea, Southern Ocean, is controlled by zooplankton fecal pellets. Geophys Res Lett 42:821–830. https://doi.org/10.1002/2014GL062744

Cisewski B, Strass VH (2016) Acoustic insights into the zooplankton dynamics of the eastern Weddell Sea. Progr Oceanogr 144:62–92. https://doi.org/10.1016/j.pocean.2016.03.005

Coelho H, Cartaxana P, Brotas V, et al (2011) Pheophorbide a in Hydrobia ulvae faecal pellets as a measure of microphytobenthos ingestion: variation over season and period of day. Aquat Biol 13:119–126. https://doi.org/10.3354/ab00356

Conroy JA, Steinberg DK, Thibodeau PS, Schofield O (2020) Zooplankton diel vertical migration during Antarctic summer. Deep-Sea Res I 162:103324. https://doi.org/10.1016/j.dsr.2020.103324

Constable AJ, Melbourne-Thomas J, Corney SP, et al (2014) Climate change and Southern Ocean ecosystems I: how changes in physical habitats directly affect marine biota. Glob Change Biol 20:3004–3025. https://doi.org/10.1111/gcb.12623

Convey P, Bindschadler R, Di Prisco G, et al (2009) Antarctic climate change and the environment. Antarct Sci 21:541–563. https://doi.org/10.1017/S0954102009990642

Costa RR, Ferreira A, de Souza MS, et al (2023) Physical-biological drivers modulating phytoplankton seasonal succession along the Northern Antarctic Peninsula. Environ Res 231:116273. https://doi.org/10.1016/j.envres.2023.116273

Costa RR, Mendes CRB, Ferreira A, et al (2021) Large diatom bloom off the Antarctic Peninsula during cool conditions associated with the 2015/2016 El Niño. Commun Earth Environ 2:252. https://doi.org/10.1038/s43247-021-00322-4

Costa RR, Mendes CRB, de Souza MS, et al (2022) Chemotaxonomic characterization of the key genera of diatoms in the Northern Antarctic Peninsula. An Acad Bras Ciênc 94:e20210584. https://doi.org/10.1590/0001-3765202220210584

Costa RR, Mendes CRB, Tavano VM, et al (2020) Dynamics of an intense diatom bloom in the Northern Antarctic Peninsula, February 2016. Limnol Oceanogr 65:2056–2075. https://doi.org/10.1002/lno.11437

Criales-Hernández MI, Jerez-Guerrero M, Latandret-Solana SA, Gómez-Sánchez MD (2022) Spatial distribution of meso- and macro-zooplankton in the Bransfield Strait and around Elephant Island, Antarctic Peninsula, during the 2019–2020 austral summer. Polar Sci 32:100821. https://doi.org/10.1016/j.polar.2022.100821

Dagg MJ, Jackson GA, Checkley DM (2014) The distribution and vertical flux of fecal pellets from large zooplankton in Monterey bay and coastal California. Deep-Sea Res I 94:72–86. https://doi.org/10.1016/j.dsr.2014.09.001

De Boyer Montégut C, Madec G, Fischer AS, et al (2004) Mixed layer depth over the global ocean: An examination of profile data and a profile-based climatology. J Geophys Res 109:2004JC002378. https://doi.org/10.1029/2004JC002378

De Cáceres M, Legendre P, Moretti M (2010) Improving indicator species analysis by combining groups of sites. Oikos 119:1674–1684. https://doi.org/10.1111/j.1600-0706.2010.18334.x

Dufrene M, Legendre P (1997) Species Assemblages and Indicator Species: The Need for a Flexible Asymmetrical Approach. Ecol Monogr 67:345. https://doi.org/10.2307/2963459

Esnal GB, Daponte MC (1999) Doliolida. In: Boltovskoy D (ed) South Atlantic Zooplankton. Bachyuys, Netherlands, 1409-1422

Esnal GB, Daponte MC (1999) Salpida. In: Boltovskoy D (ed) South Atlantic Zooplankton. Bachyuys, Netherlands, pp 1423-1444

Ferreira A, Costa RR, Dotto TS, et al (2020) Changes in Phytoplankton Communities Along the Northern Antarctic Peninsula: Causes, Impacts and Research Priorities. Front Mar Sci 7:576254. https://doi.org/10.3389/fmars.2020.576254

Frey DI, Krechik VA, Morozov EG, et al (2022) Water Exchange between Deep Basins of the Bransfield Strait. Water 14:3193. https://doi.org/10.3390/w14203193

Garcia MD, Dutto MS, Chazarreta CJ, et al (2020) Micro- and mesozooplankton successions in an Antarctic coastal environment during a warm year. PLoS ONE 15:e0232614. https://doi.org/10.1371/journal.pone.0232614

Gibbons MJ, Spiridonov VA, Tarling GA (1999) Euphausiacea. In: Boltovskoy D (ed) South Atlantic Zooplankton. Bachyuys, Netherlands, pp 1241-1280

Gili J, Rossi S, Pagès F, et al (2006) A new trophic link between the pelagic and benthic systems on the Antarctic shelf. Mar Ecol Prog Ser 322:43–49. https://doi.org/10.3354/meps322043

Giraldo A, Criales Hernández MI, Jerez Guerrero M, Mojica Moncada DF (2019) Epipelagic copepod assemblage in the Gerlache Strait (Antarctica) during the 2015 austral summer. BIM 48:. https://doi.org/10.25268/bimc.invemar.2019.48.1.754

González H, Smetacek V (1994) The possible role of the cyclopoid copepod Oithona in retarding vertical flux of zooplankton faecal material. Mar Ecol Prog Ser 113:233–246. https://doi.org/10.3354/meps113233

Hays GC, Kennedy H, Frost BW (2001) Individual variability in diel vertical migration of a marine copepod: Why some individuals remain at depth when others migrate. Limnol Oceanogr 46:2050–2054. https://doi.org/10.4319/lo.2001.46.8.2050

Henley SF, Schofield OM, Hendry KR, et al (2019) Variability and change in the west Antarctic Peninsula marine system: Research priorities and opportunities. Progr Oceanogr 173:208–237. https://doi.org/10.1016/j.pocean.2019.03.003

Hernández-León S, Portillo-Hahnefeld A, Almeida C, et al (2001) Diel feeding behaviour of krill in the Gerlache Strait, Antarctica. Mar Ecol Prog Ser 223:235–242. https://doi.org/10.3354/meps223235

Hopkins TL (1985) Food web of an Antarctic midwater ecosystem. Mar Biol 89:197–212. https://doi.org/10.1007/BF00392890

Hopkins TL, Torres JJ (1989) Midwater food web in the vicinity of a marginal ice zone in the western Weddell Sea. Deep-Sea Res Part I 36:543–560. https://doi.org/10.1016/0198-0149(89)90005-8

Hosie GW, Schultz MB, Kitchener JA, et al (2000) Macrozooplankton community structure off East Antarctica (80-150°E) during the Austral summer of 1995/1996

Huneke WGC, Huhn O, Schröeder M (2016) Water masses in the Bransfield Strait and adjacent seas, austral summer 2013. Polar Biol 39:789–798. https://doi.org/10.1007/s00300-016-1936-8

Hunt BPV (2003) The Continuous Plankton Recorder in the Southern Ocean: a comparative analysis of zooplankton communities sampled by the CPR and vertical net hauls along 140 E. J Plankton Res 25:1561–1579. https://doi.org/10.1093/plankt/fbg108

Hunt BPV, Hosie GW (2005) Zonal structure of zooplankton communities in the Southern Ocean South of Australia: results from a 2150km continuous plankton recorder transect. Deep-Sea Res I 52:1241–1271. https://doi.org/10.1016/j.dsr.2004.11.019

Hunt BPV, Hosie GW (2006) The seasonal succession of zooplankton in the Southern Ocean south of Australia, part I: The seasonal ice zone. Deep-Sea Res I 53:1182–1202. https://doi.org/10.1016/j.dsr.2006.05.001

Ichii T, Mori Y, Mahapatra K, et al (2020) Body length-dependent diel vertical migration of Antarctic krill in relation to food availability and predator avoidance in winter at South Georgia. Mar Ecol Prog Ser 654:53–66. https://doi.org/10.3354/meps13508

Kasyan VV (2023) Structure and Spatial Distribution of Mesozooplankton Communities in the Atlantic Sector of the Southern Ocean. Oceanology 63:550–558. https://doi.org/10.1134/S0001437023040057

King A, LaCasella EL (2003) Seasonal variations in abundance, diel vertical migration, and population structure of Metridia gerlachei at Port Foster, Deception Island, Antarctica. Deep-Sea Res II 50:1753–1763. https://doi.org/10.1016/S0967-0645(03)00091-2

Lampert W (1989) The Adaptive Significance of Diel Vertical Migration of Zooplankton. Funct Ecol 3:21. https://doi.org/10.2307/2389671

Landschützer P, Gruber N, Haumann FA, et al (2015) The reinvigoration of the Southern Ocean carbon sink. Science 349:1221–1224. https://doi.org/10.1126/science.aab2620

Liu Y, Wang Y, Sun Y, et al (2024) Zooplankton vertical stratification in the East-pacific and Indian sectors of the Southern Ocean. Front Mar Sci 11:1274582. https://doi.org/10.3389/fmars.2024.1274582

Lopez MDG, Huntley ME (1995) Feeding and diel vertical migration cycles of Metridia gerlachei (Giesbrecht) in coastal waters of the Antarctic Peninsula. Polar Biol 15:. https://doi.org/10.1007/BF00236120

Mackey M, Mackey D, Higgins H, Wright S (1996) CHEMTAX - a program for estimating class abundances from chemical markers:application to HPLC measurements of phytoplankton. Mar Ecol Prog Ser 144:265–283. https://doi.org/10.3354/meps144265

Marrari M, Daly KL, Timonin A, Semenova T (2011) The zooplankton of Marguerite Bay, western Antarctic Peninsula—Part II: Vertical distributions and habitat partitioning. Deep-Sea Res II 58:1614–1629. https://doi.org/10.1016/j.dsr2.2010.12.006

Mendes CRB, Costa RR, Ferreira A, et al (2023) Cryptophytes: An emerging algal group in the rapidly changing Antarctic Peninsula marine environments. Glob Change Biol 29:1791–1808. https://doi.org/10.1111/gcb.16602

Mendes CRB, De Souza MS, Garcia VMT, et al (2012) Dynamics of phytoplankton communities during late summer around the tip of the Antarctic Peninsula. Deep-Sea Res I 65:1–14. https://doi.org/10.1016/j.dsr.2012.03.002

Mendes CRB, Tavano VM, Dotto TS, et al (2018a) New insights on the dominance of cryptophytes in Antarctic coastal waters: A case study in Gerlache Strait. Deep-Sea Res II 149:161–170. https://doi.org/10.1016/j.dsr2.2017.02.010

Mendes CRB, Tavano VM, Kerr R, et al (2018b) Impact of sea ice on the structure of phytoplankton communities in the northern Antarctic Peninsula. Deep-Sea Res II 149:111–123. https://doi.org/10.1016/j.dsr2.2017.12.003

Meredith MP, King JC (2005) Rapid climate change in the ocean west of the Antarctic Peninsula during the second half of the 20th century. Geophys Res Lett 32:2005GL024042. https://doi.org/10.1029/2005GL024042

Meredith MP, Schofield O, Newman L, et al (2013) The vision for a Southern Ocean Observing System. Curr Opin Environ Sustain 5:306–313. https://doi.org/10.1016/j.cosust.2013.03.002

Michels J, Schnack-Schiel SB, Pasternak A, et al (2012) Abundance, population structure and vertical distribution of dominant calanoid copepods on the eastern Weddell Sea shelf during a spring phytoplankton bloom. Polar Biol 35:369–386. https://doi.org/10.1007/s00300-011-1083-1

Moline MA, Claustre H, Frazer TK, et al (2004) Alteration of the food web along the Antarctic Peninsula in response to a regional warming trend. Global Change Biology 10:1973–1980. https://doi.org/10.1111/j.1365-2486.2004.00825.x

Montes-Hugo M, Doney SC, Ducklow HW, et al (2009) Recent Changes in Phytoplankton Communities Associated with Rapid Regional Climate Change Along the Western Antarctic Peninsula. Science 323:1470–1473. https://doi.org/10.1126/science.1164533

Nishikawa J, Tsuda A (2001) Diel vertical migration of the tunicate Salpa thompsoni in the Southern Ocean during summer. Polar Biol 24:299–302. https://doi.org/10.1007/s003000100227

Ochoa N, Bonicelli J, López D (2016) Comunidad del zooplancton antártico en el Estrecho de Bransfield y alrededores de la Isla Elefante: Enero 2006. PERÚ ANTAR XVI. Bol Inst Mar Perú 31: 64–70

Oksanen J, et al (2012) Vegan: Community Ecology Package. R package Version 2.0-4. http://CRAN.Rproject.org/package=vegan.

Orselli IBM, Carvalho ACO, Monteiro T, et al (2022) The marine carbonate system along the northern Antarctic Peninsula: current knowledge and future perspectives. An Acad Bras Ciênc 94:e20210825. https://doi.org/10.1590/0001-3765202220210825

Plum C, Cornils A, Driscoll R, et al (2021) Mesozooplankton trait distribution in relation to environmental conditions and the presence of krill and salps along the northern Antarctic Peninsula. J Plankton Res 43:927–944. https://doi.org/10.1093/plankt/fbab068

Pugh P (1999) Siphonophorae. In: Boltovskoy D (ed) South Atlantic Zooplankton. Bachyuys, Netherlands, pp 467-512

Razouls C, Desreumaux N, Kouwenberg J, de Bovée F (2023). Biodiversity of Marine Planktonic Copepods (morphology, geographical distribution and biological data) (Sorbonne University, CNRS). Available online at: http://copepodes.obs-banyuls.fr/en (Accessed May 10, 2023).

Sangrà P, Gordo C, Hernández-Arencibia M, et al (2011) The Bransfield current system. Deep-Sea Res I 58:390–402. https://doi.org/10.1016/j.dsr.2011.01.011

Schaafsma FL, Matsuno K, Driscoll R, et al (2024) Zooplankton communities at the sea surface of the eastern Indian sector of the Southern Ocean during the austral summer of 2018/2019. Prog Oceanogr 226:103303. https://doi.org/10.1016/j.pocean.2024.103303

Schofield O, Cimino M, Doney S, et al (2024) Antarctic pelagic ecosystems on a warming planet. Trends in Ecology & Evolution S0169534724002003. https://doi.org/10.1016/j.tree.2024.08.007

Sherrell RM, Annett AL, Fitzsimmons JN, Roccanova VJ, Meredith MP (2018) A “shallow bathtub ring” of local sedimentary iron input maintains the Palmer Deep biological hotspot on the West Antarctic Peninsula shelf. Philos. Trans. Roy. Soc. A Math. Phys. Eng. Sci. 376: 2122. https://doi.org/10.1098/rsta.2017.0171

Siegel V, Reiss CS, Dietrich KS, Haraldsson M, Rohardt G (2013) Distribution and abundance of Antarctic krill (*Euphausia superba*) along the Antarctic Peninsula. Deep-Sea Res I 77: 63–74. https://doi.org/10.1016/j.dsr.2013.02.005

Steedman HF (1976) Monographs on oceanographic methodology No 4 - Zooplankton fixation and preservation. The UNESCO Press, Paris

Svensen C, Nejstgaard JC (2003) Is sedimentation of copepod faecal pellets determined by cyclopoids? Evidence from enclosed ecosystems. J Plankton Res 25:917–926. https://doi.org/10.1093/plankt/25.8.917

Swadling KM, Kawaguchi S, Hosie GW (2010) Antarctic mesozooplankton community structure during BROKE-West (30°E–80°E), January–February 2006. Deep-Sea Res II 57:887–904. https://doi.org/10.1016/j.dsr2.2008.10.041

Tarling GA, Ward P, Thorpe SE (2018) Spatial distributions of Southern Ocean mesozooplankton communities have been resilient to long-term surface warming. Glob Change Biol 24:132–142. https://doi.org/10.1111/gcb.13834

Thuesen E, Álamo MAF (1999) Polychaeta. In: Boltovskoy D (ed) South Atlantic Zooplankton. Bachyuys, Netherlands, pp 595-620

Turner J, Barrand NE, Bracegirdle TJ, et al (2014) Antarctic climate change and the environment: an update. Polar Rec 50:237–259. https://doi.org/10.1017/S0032247413000296

Van der Spoel S, Dadon JR (1999) Pteropoda. In: Boltovskoy D (ed) South Atlantic Zooplankton. Bachyuys, Netherlands, pp 649-706

Venkataramana V, Kerkar AU, Mishra RK, et al (2022) Hydrodynamics and zooplankton assemblages in Prydz Bay, East Antarctica, during the austral summer of 2017. Reg Stud Mar Sci 52:102341. https://doi.org/10.1016/j.rsma.2022.102341

Vinogradovi G (1999) Amphipoda. In: Boltovskoy D (ed) South Atlantic Zooplankton. Bachyuys, Netherlands, pp 1141-1240

Ward P, Shreeve R, Whitehouse M, et al (2005) Phyto- and zooplankton community structure and production around South Georgia (Southern Ocean) during Summer 2001/02. Deep-Sea Res I 52:421–441. https://doi.org/10.1016/j.dsr.2004.10.003

Ward P, Tarling GA, Thorpe SE (2014) Mesozooplankton in the Southern Ocean: Spatial and temporal patterns from Discovery Investigations. Prog Oceanogr 120:305–319. https://doi.org/10.1016/j.pocean.2013.10.011

Ward P, Whitehouse M, Shreeve R, et al (2007) Plankton community structure south and west of South Georgia (Southern Ocean): Links with production and physical forcing. Deep-Sea Res I 54:1871–1889. https://doi.org/10.1016/j.dsr.2007.08.008

Wiebe PH, Benfield MC (2003) From the Hensen net toward four-dimensional biological oceanography. Prog Oceanogr 56:7–136. https://doi.org/10.1016/S0079-6611(02)00140-4

Wright SW, Ishikawa A, Marchant HJ, et al (2009) Composition and significance of picophytoplankton in Antarctic waters. Polar Biol 32:797–808. https://doi.org/10.1007/s00300-009-0582-9

Yang G, Li C, Wang Y, Peng Q (2018) Copepod feeding strategies in the epipelagic to bathypelagic zone of Prydz Bay, Antarctica: an assessment through fatty acids and stable isotopes. Polar Biol 41:1307–1317. https://doi.org/10.1007/s00300-018-2286-5

Yang G, Li C, Wang Y, Zhang Y (2017) Vertical profiles of zooplankton community structure in Prydz Bay, Antarctica, during the austral summer of 2012/2013. Polar Biol 40:1101–1114. https://doi.org/10.1007/s00300-016-2037-4

Yebra L, Hernández-León S, Almeida C, Bécognée P (2009) Metabolism and biomass vertical distribution of zooplankton in the Bransfield Strait during the austral summer of 2000. Polar Res 28:415–425. https://doi.org/10.1111/j.1751-8369.2009.00116.x

Zhou M, Niiler PP, Hu J-H (2002) Surface currents in the Bransfield and Gerlache Straits, Antarctica. Deep-Sea Res I: Oceanographic Research Papers 49:267–280. https://doi.org/10.1016/S0967-0637(01)00062-0

Online Resources

Online Resource 1: Macronutrient concentrations during the sampling intervals from T1 to T5. DIN = Dissolved Inorganic Nitrogen

Sampling times	DIN (µM)	Phosphate (µM)	Silicate (µM)
T1	22.3	1.6	91.4
T2	22.1	1.6	89.8
T3	23.4	1.7	92.5
T4	22.1	1.6	82.2
T5	21.4	1.6	94.6

Online Resource 2: Taxonomic groups found in the 25 zooplankton samples collected at station B42. FO = Frequency of occurrence, RA = Relative Abundance, Max. Ab. = Maximum Abundance and N = Number of specimens found, N.I. = Not identified

Taxa	F. O. (%)	R. A. (%)	Max Ab. (org. 1000 m^{-3})	N
Hidrozoa				
N. I.	4	0.05	53	2
Rhopalonematidae	4	0.05	59	2
Siphonophora				
N. I.	4	0.02	36	32
Diphyes antarctica Moser, 1925	16	0.17	103	7
Dimophyes arctica (Chun, 1897)	52	0.89	265	36
Polychaeta				
Vanadis antarctica (McIntosh, 1885)	28	0.20	69	8
Vanadis longissima (Levinsen, 1885)	4	0.02	24	1
Larvae	24	0.45	156	18
Pteropoda				
Spongiobranchaea australis d'Orbigny, 1836	4	0.02	34	1
Ostracoda N.I.	60	7.08	2647	286
Copepoda				
Calanoides acutus (Giesbrecht, 1902)	60	2.43	375	98
Calanus propinquus Brady, 1883	8	0.05	31	2
Copepodite Calanidae	8	0.07	63	3
Copepodite *Calanoides* spp.	32	0.67	313	27
Rhincalanus gigas Brady, 1883	8	0.05	29	2
Rhincalanus nasutus Giesbrecht, 1888	4	0.02	29	1
Ctenocalanus citer Heron & Bowman, 1971	4	0.02	25	1
Microcalanus pygmaeus (Sars G.O., 1900)	8	0.10	103	4
Copepodite *Clausocalanus* sp.	4	0.07	100	3
Aetideus arcuatus (Vervoort, 1949)	4	0.02	29	1
Aetideopsis antarctica (Wolfenden, 1908)	8	0.10	88	4
Chiridius gracilis Farran, 1908	8	0.10	83	4
Gaetanus tenuispinus (Sars G.O., 1900)	8	0.05	32	2
Paraeuchaeta biloba Farran, 1929	4	0.05	63	2
Paraeuchaeta exigua (Wolfenden, 1911)	24	0.17	53	7
Copepodite *Paraeuchaeta* spp.	52	3.61	1367	146
Scaphocalanus curtus (Farran, 1926)	4	0.02	29	1
Scaphocalanus elongatus Scott A., 1909	4	0.05	59	2
Scolecithricella minor minor (Brady, 1883)	20	0.15	54	6
Scolecithricella vittata (Giesbrecht, 1893)	4	0.07	86	3
Scottocalanus securifrons (Scott T., 1894)	4	0.02	34	1
Copepodite *Scaphocalanus* sp.	4	0.02	29	1
Copepodite Scolecithricidae	12	0.10	69	4
Haloptilus ocellatus Wolfenden, 1905	4	0.02	29	1
Haloptilus oxycephalus (Giesbrecht, 1889)	4	0.02	29	1
Heterorhabdus lobatus Bradford, 1971	4	0.02	28	1
Heterorhabdidae	4	0.02	29	1
Metridia gerlachei Giesbrecht, 1902	92	13.37	3500	540
Metridia longa (Lubbock, 1854)	28	0.25	63	10
Copepodite *Metridia* spp.	80	30.38	6063	1227

Copepodite *Centropages* sp.	4	0.02	26	1
Labidocera sp.	4	0.02	32	1
Copepodite N.I.	28	0.64	342	26
Oithona frigida Giesbrecht, 1902	12	1.31	1125	53
Oithona similis Claus, 1866	8	1.16	1313	47
Oithona spp.	56	3.61	1667	246
Triconia antarctica (Heron, 1977)	28	0.45	353	18
Agetus flaccus (Giesbrecht, 1891)	4	0.07	88	3
Amphipoda				
Eusirus microps Walker, 1906	4	0.02	26	1
Cyllopus lucasi Spence Bate, 1862	8	0.05	32	2
Vibilia antarctica Stebbing, 1888	16	0.12	65	5
Vibilia armata Bovallius, 1887	24	0.17	53	7
Manca Stage	8	0.05	32	2
Euphausiacea				
Thysanoessa macrura G.O. Sars, 1883	24	0.62	372	25
Euphausia superba Dana, 1850	4	0.02	23	1
Calyptopis	4	0.05	63	2
Furcilia	48	1.06	259	43
Chaetognata				
N. I.	52	2.01	541	81
Eukrohnia hamata (Möbius, 1875)	60	2.85	676	115
Pseudosagitta maxima (Conant, 1896)	32	0.40	88	16
Pseudosagitta spp.	4	0.15	158	6
Appendicularia				
Oikopleura sp.	8	0.07	59	3
Fritillaria sp.	4	0.05	69	2
Thaliacea				
Salpa maxima Forskål, 1775	8	0.05	31	2
Salpa thompsoni Foxton, 1961	84	21.49	5698	960
Ihlea racovitzai (Van Beneden & De Selys Longchamp, 1913)	8	0.07	54	3

APÊNDICE 3

Artigo a ser submetido na *Ocean and Coastal Research*, em processo de finalização.

First Record of *Desmonema glaciale* Larson, 1986 ephyrae in the Northern Antarctic Peninsula

First Record of *Desmonema glaciale* Larson, 1986 ephyrae in the Northern Antarctic Peninsula

Baldoni, Letícia Cazarin*[1,2], von Montfort, Guilherme [1,2], Jordano, Mayara Almeida[3], Nagata, Renato Mitsuo[1,2], Erik Muxagata[1,2]

[1]Laboratório de zooplâncton, Instituto de Oceanografia, Universidade Federal do Rio Grande, Av. Itália, km 8, 96203-000 Rio Grande, RS, Brazil

[2]Programa de Pós-Graduação em Oceanografia Biológica – PPGOB

[3]Departamento de Zoologia, Instituto de Biociências, Universidade de São Paulo

*Corresponding author: l.baldoni.lb@gmail.com

Abstract

The Northern Antarctic Peninsula (NAP) is a region experiencing rapid environmental changes, with significant impacts on marine ecosystems, making it a hotspot for studies on biodiversity. Here, we describe, for the first time, an early *Desmonema* ephyra in the central basin of the Bransfield Strait, collected during February 2018. The specimen, measuring 12.2 mm in diameter is characterized by four fully developed adradial tentacles and four tentacular buds, poorly developed oral arms, and smooth umbrellar lobes. Based on size, morphological comparisons and distribution of the other three known species in this genus we suggest that this individual belongs to *Desmonema glaciale.* Although adults of this large (<1.2 m bell diameter) scyphozoan medusa are often found in Antarctic waters, this record represents the youngest specimen ever described for the species. The presence of *D. glaciale* ephyra in this region highlights the ecological role of this ecosystem for the development of large gelatinous predators, in the context of rapid climate-driven changes. The detection of early life stages of large gelatinous predators provides valuable insights into reproductive success and population dynamics in changing environments, especially since jellyfish blooms have been increasingly recognized as indicators of ecosystem shifts. This record contributes to our understanding of cnidarians' life cycles and biodiversity in the Antarctic. It underscores the importance of monitoring early life stages to better predict ecological responses to climate change.

Keywords: Scyphozoa, Cyaneidae, Northern Antarctic Peninsula, Ephyra

Introduction

The Southern Ocean is renowned for its unique biodiversity and its key role in regulating the global climate and supporting unique marine ecosystems (Constable et al 2014). The Northern Antarctic Peninsula (NAP) is one of the regions experiencing the most rapid climate change, with profound effects on environmental patterns and local biological

communities (Mendes et al. 2013, Atkinson et al. 2019, Henley et al. 2020), including zooplankton, an essential component of marine food webs (Atkinson et al. 2004, Richardson 2008).

Among zooplanktonic organisms, cnidarians stand out as important predators due to their efficiency in capturing prey using specialized nematocysts. This group, which includes jellyfish, anemones, and hydroids, is widely distributed across marine environments, ranging from shallow tropical waters to polar regions (Mayer 1910, Kramp 1961, Mianzan & Cornelius 1999, Jarms et al. 2023). In the Southern Ocean, cnidarians play critical roles in energy transfer and carbon flux, influencing ecological dynamics and biogeochemical cycles (Ekau et al. 2018). Jellyfish, in particular, act as both predators and prey, competing with other zooplankton for resources while also serving as a food source for larger predators such as seabirds and fish (Lucas et al. 2014, Hays et al. 2018). Despite their ecological significance, the biodiversity and distribution of cnidarians in Antarctic waters remain underexplored. This knowledge gap is particularly pronounced for early pelagic life stages, such as ephyrae, the juveniles of scyphozoan jellyfish.

Ephyrae, released from benthic polyps, are characterized by their distinct morphology relative to the adult counterparts, their short duration and represent a critical transition stage before the adult (Schiariti et al. 2008, Jordano et al. 2022). However, identifying this stage in nature is challenging due to morphological similarities between species, and because its occurrence in the wild is often underestimated due to sampling constraints (Holst 2012, Jordano et al. 2022). Their small size, fragility, and rapid developmental changes further complicate field sampling and laboratory studies (Straehler-Pohl & Jarms, 2010). Detecting ephyrae in the natural environment can provide valuable insights into the environmental factors regulating jellyfish production and help identify early patterns of mass jellyfish occurrence (Nagata et al. 2021). Previous studies have primarily focused on species known from laboratory cultures (Pitt 2000), while natural records remain scarce. One of the few documented records of young specimens of *Desmonema* L. Agassiz, 1862 is that of Browne (1909), who described some individuals of *Desmonema gaudichaudi* (Lesson, 1830) (as *Desmonema chierchiana* Vanhöffen, 1888) near the Falkland Islands (51° 42' 0" S), measuring between 14 mm and 25 mm. In Antarctic Waters, large medusae of *Desmonema glaciale* Larson, 1986 up to 1.2 m in bell diameter have been recorded during samplings carried out with nets (Ward 1989, Larson & Harbison 1990, Lindsay et al. 2023) and divings (Brueggeman 2023, Jarms et al. 2023). The species is found around the continent and it is endemic to Antarctic waters (Larson 1986, Jarms et al. 2023). Younger specimens, however, have never been morphologically described. In this context, the present study reports, for the first time, the occurrence of an ephyra of the genus *Desmonema* in the Northern Antarctic Peninsula.

Sampling was conducted on board the RV Almirante Maximiano of the Brazilian Navy. The specimen was collected in a vertical trawl (100-0 m) with a Multinet (equipped with 300 μm nets) at station #10 (63° 16' 40.8" S, 59° 16' 33.6" O), localized in the central

basin of the Bransfield Strait (NAP), in February of 2018. Samples were immediately preserved in 4% formalin buffered with borax.

Hydrographic data (temperature and salinity) were collected to evaluate the dynamics of the water column using a Sea-Bird CTD (conductivity–temperature–depth instrument)/Carrousel 911+system® equipped with 24 five-liter Niskin bottles in all stations.

Samples were analyzed under a stereomicroscope, and the organisms present in the zooplankton samples were quantified and identified following descriptions by Browne (1908), Larson (1986), and Mianzan and Cornelius (1999). The specimen found was deposited in the collection of marine zooplankton and ichthyoplankton of the Centro de Biodiversidade Subtropical (CBS-ZPKT 0201).

Results

At station #10, we identified low surface temperatures, ranging from -0.63 to 0.79 °C (0-100 m), and surface salinities ranging from 34.3 to 34.4. In addition, low stability of the water column ($1.21x10^{-6}m^{-1}$) with a deeper mixed layer (34 m) was found when compared with other stations sampled in 2018, indicating a homogeneous water column.

From 49 samples collected in 2018, more than 413 individuals of planktonic cnidarians were identified. Only one ephyra of *Desmonema* spp. was found in the surface layer of station #30, in the central basin of Bransfield Strait.

Diagnosis

One ephyra transparent with a whitish hue, measuring 12.2 mm in diameter (Fig. 1). Umbrella is thin and flat, with a circular stomach of about 4.3 mm of maximum width, featuring radiating pouches separated by radial septa. Eight adradial groups of tentacles, four consisting of longer and thicker tentacles, interspersed with four tentacular buds (white arrow in Fig. 1 - A). The tentacles located within the bell margin, adjacent to the distal edge of the gastric pouches (Fig. 1 - C). Circular musculature is present and radial musculature absent. Eight rhopalia, four perradial, and four interradial (Fig. 1 - A and B). The stomach contained four interradial bundles of gastric filaments, and four oral arms hung from the mouth, slightly longer than the bell radius (white arrow in Fig. 1 - D). Marginal lobes less pronounced, with the cleft structure indicating ongoing development. The marginal canal system, which connects the stomach pouches to the marginal lobes, not fully developed and the series of bifurcations observed in older specimens not present.

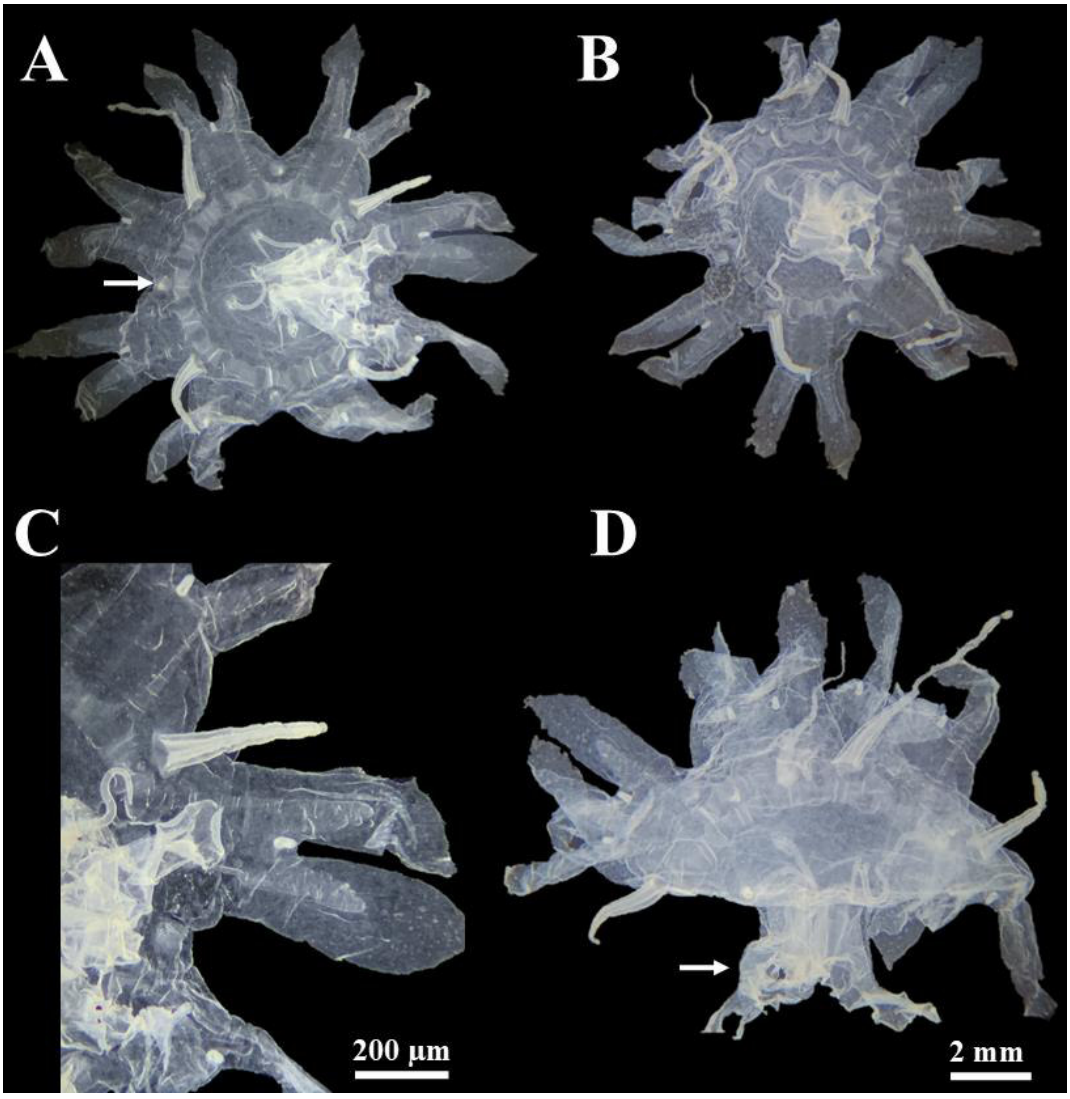


Figure 1 - Specimen of *Desmonema glaciale* sampled at Bransfield Strait. A) oral view, the white arrow indicates tentacle bud. B) Aboral view. C) Lappet detail. D) Lateral view, white arrow indicates oral arms. Scale: 2mm for figures A, B and D; 200µm figure C.

Discussion

Despite being an individual at an early stage of development, characterized by the absence of velar lobes, poorly developed oral arms, and only four tentacles and four tentacular buds (instead of the eight tentacles, or group of tentacles, that appear in more advanced stages), our specimen shows morphological characteristics that classify it as an ephyra of Semaeostomeae. The smooth lobes of the umbrella reinforce this identification (Jordano et al. 2022). Within this group, we ruled out its inclusion in Ulmaridae, as no digitiform structures were observed on the oral arms (i.e. digitata), which are typical of this group, but also shared with Rhizostomeae. The pattern of tentacle development and insertion, the shape of marginal lobes, and the presence of circular musculature only, reinforce that this specimen belongs to the genus *Desmonema.* There are four known species in

Desmonema (Worms 2025), which can be determined by counting the number of tentacles per adradial grouping and by the arrangement of canals in the marginal lappets (Larson 1986). Young individuals of these species can not be distinguished morphologically (Larson 1986). *D. glaciale* holds the lowest number of tentacles (<10) per grouping, which are also thicker when considering individuals larger than 20 cm in diameter (Larson 1986). *Desmonema comatum* Larson 1986 holds more than 100 tentacles, while *D. gaudichaudi* has between 10 to 60 per group (Larson 1986). Distribution is important as well as *D. comatum* occurs in temperate and subantartic waters of Argentina (35o-55oS), whereas *D. gaudichaudi* is circum-subantartic (35o-55oS) (Larson 1986, Schiariti et al. 2018, Jarms & Morandini 2019). *Desmonema scoresbyanna* Gershwin & Zeidler 2008 was described in southern Australian coastal waters. Therefore, *D. glaciale* stands out as the only species found in Antarctic waters (Larson 1986, Jarms et al. 2023), which therefore ultimately defined the determination of the species.

Browne (1909) described *D. gaudichaudi* (as *D. chierchiana*) ephyrae in a juvenile stage, with eight adradial groups of tentacles, each group containing one long and four to six-minute tentacles or tentacle buds. Our specimen, however, shows only four fully developed adradial tentacles (one per umbrella quadrant), while the other adradial clefts exhibit tentacular buds. This confirms that the specimen here described is at an earlier stage of development, than those documented by Browne (1909), and possibly the youngest ever reported for the species. This is corroborated by the size of the specimen (Fig. 1). Browne (1909) reported an ephyra with a diameter of 14 mm, while our individual is only 12.2 mm. As bell diameter is a determining factor for the emergence of new structures in jellyfish (Jordano et al. 2022) described. Furthermore, if we consider that both individuals were similar in size, while ours still had only one thick tentacle or one rudiment per adradial group, while those described by Browne (1909) already had more than four tentacles, this comparison further reinforces the identification of the present individual as *D. glaciale*.

The NAP is a hydrological region that encompasses the Bransfield Strait (Kerr et al. 2018a). This strait has a dynamic circulation, which varies seasonally and is influenced by warmer and lower saline waters from the Bellingshausen Sea, and colder and more saline waters from the Weddell Sea (Sangrà et al. 2011). The ephyra was found in the central basin of the Bransfield Strait, in an area under the influence of colder and relatively saline waters, resulting from the mixing of local water masses with waters from the Weddell Sea (Huneke et al. 2016). The occurrence of this specimen in colder waters of Antarctica also makes it unlikely that this specimen belongs to other subantarctic species of the genus. The presence of *Desmonema* ephyra in the NAP adds to the morphological description of the development of this species, contributing valuable insights into its life cycle and early stages. However, there are few records on its biology. Diving observations of *Desmonema* at Signy Island, South Orkney Islands, indicate that

this jellyfish is common in neritic waters and functions as a benthopelagic predator (White & Bone, 1972). In South Georgia, gelatinous organisms appear to be common prey for seabirds and fish, particularly when krill populations are depleted (Brierley & Watkins, 1995). Furthermore, a previous study reported that the radial canals of *Desmonema* specimens were infested with hyperiid amphipods (White and Bone 1972), demonstrating the further ecological importance of these organisms. While the identification of this specimen as *Desmonema glaciale* is supported by its geographical location, environmental conditions, and morphological similarities to described specimens (Browne, 1908; Larson, 1986), definitive species-level confirmation would require molecular analysis. The early life stages of jellyfish, such as ephyrae, are susceptible to environmental variability, and their presence may provide insights into the reproductive success and population dynamics of jellyfish in polar regions (Lucas et al. 2012). Furthermore, the predator-prey ecological role of jellyfish in marine ecosystems highlights the importance of understanding their life history and distribution (Ekau et al. 2018). As such, this record contributes to our knowledge of cnidarian biodiversity in Antarctica and raises important questions about the ecological implications of the proliferation of these jellyfish.

Conclusion

Based on morphological comparisons and the geographical distribution, we describe, for the first time, an ephyra of *Desmonema glaciale*, representing the youngest stage ever described of this species. However, due to the limitations of analysis based exclusively on morphology, we recommend the application of molecular techniques for definitive confirmation. Such an approach is essential, especially at early stages of development, when diagnostic characteristics may be incomplete. This study broadens our understanding of the biodiversity and life cycle of Antarctic jellyfish, reinforcing the presence of *D. glaciale* in the region and contributing to the documentation of its early stages of development.

References

Atkinson A, Hill SL, Pakhomov EA, Siegel V, Reiss CS, Loeb VJ, Steinberg DK, Schmidt K, Tarling GA, Gerrish L, Sailley SF (2019) Krill (Euphausia superba) distribution contracts southward during rapid regional warming. Nature Clim Change 9:142–147.

Atkinson A, Siegel V, Pakhomov E, Rothery P (2004) Long-term decline in krill stock and increase in salps within the Southern Ocean. Nature 432:100–103.

Brierley A, Watkins J (1996) Acoustic targets at South Georgia and the South Orkney Islands during a season of krill scarcity. Mar Ecol Prog Ser 138:51–61.

Browne ET (1909) X.—The Medusæ of the Scottish National Antarctic Expedition. Trans R Soc Edinb 46:233–251.

Brueggeman P (2023) Underwater Field Guide to Ross Island & McMurdo Sound, Antarctica, Volume 2: Cnidaria.

Constable AJ, Melbourne-Thomas J, Corney SP, Arrigo KR, Barbraud C, Barnes DKA, Bindoff NL, Boyd PW, Brandt A, Costa DP, Davidson AT, Ducklow HW, Emmerson L, Fukuchi M, Gutt J, Hindell MA, Hofmann EE, Hosie GW, Iida T, Jacob S, Johnston NM, Kawaguchi S, Kokubun N, Koubbi P, Lea M, Makhado A, Massom RA, Meiners K, Meredith MP, Murphy EJ, Nicol S, Reid K, Richerson K, Riddle MJ, Rintoul SR, Smith WO, Southwell C, Stark JS, Sumner M, Swadling KM, Takahashi KT, Trathan PN, Welsford DC, Weimerskirch H, Westwood KJ, Wienecke BC, Wolf-Gladrow D, Wright SW, Xavier JC, Ziegler P (2014) Climate change and Southern Ocean ecosystems I: how changes in physical habitats directly affect marine biota. Global Change Biology 20:3004–3025.

Ekau W, Auel H, Hagen W, Koppelmann R, Wasmund N, Bohata K, Buchholz F, Geist S, Martin B, Schukat A, Verheye HM, Werner T (2018) Pelagic key species and mechanisms driving energy flows in the northern Benguela upwelling ecosystem and their feedback into biogeochemical cycles. Journal of Marine Systems 188:49–62.

Hays GC, Doyle TK, Houghton JDR (2018) A Paradigm Shift in the Trophic Importance of Jellyfish? Trends in Ecology & Evolution 33:874–884.

Henley SF, Schofield OM, Hendry KR, Schloss IR, Steinberg DK, Moffat C, Peck LS, Costa DP, Bakker DCE, Hughes C, Rozema PD, Ducklow HW, Abele D, Stefels J, Van Leeuwe MA, Brussaard CPD, Buma AGJ, Kohut J, Sahade R, Friedlaender AS, Stammerjohn SE, Venables HJ, Meredith MP (2019) Variability and change in the west Antarctic Peninsula marine system: Research priorities and opportunities. Progress in Oceanography 173:208–237.

Holst S (2012) Morphology and development of benthic and pelagic life stages of North Sea jellyfish (Scyphozoa, Cnidaria) with special emphasis on the identification of ephyra stages. Mar Biol 159:2707–2722.

Huneke WGC, Huhn O, Schröeder M (2016) Water masses in the Bransfield Strait and adjacent seas, austral summer 2013. Polar Biol 39:789–798.

Jarms G, Morandini AC, Schmidt-Rhaesa A, Giere O, Straehler-Pohl I (eds) (2023) World atlas of jellyfish: Scyphozoa except Stauromedusae, 1st digital edition. Dölling und Galitz Verlag, München Hamburg.

Jordano MDA, Miyake H, Nagata RM, Morandini AC (2022) Patterns of morphological development in Scyphozoa ephyrae (Cnidaria, Medusozoa). Mar Biodivers 52:31.

Kerr R, Mata MM, Mendes CRB, Secchi ER (2018) Northern Antarctic Peninsula: a marine climate hotspot of rapid changes on ecosystems and ocean dynamics. Deep Sea Research Part II: Topical Studies in Oceanography 149:4–9.

Larson RJ (1986) Pelagic Scyphomedusae (Scyphozoa: Coronate and Semaeostomeae of the Southern Ocean. Antarctic Research Series 41:59–165.

Larson RJ, Harbison GR (1990) Medusae from Mcmurdo Sound, Ross Sea including the descriptions of two new species, Leuckartiara brownei and Benthocodon hyalinus. Polar Biol 11.

Lindsay DJ, Grossmann MM, Montenegro J, Morandini AC (2023) A new subfamily of ulmarid scyphomedusae, the Santjordiinae, with a description of Santjordia pagesi gen. et sp. nov. (Cnidaria: Scyphozoa: Discomedusae: Semaeostomeae: Ulmaridae) from the Sumisu Caldera, Ogasawara Islands, Japan. Zootaxa 5374:533–551.

Lucas CH, Jones DOB, Hollyhead CJ, Condon RH, Duarte CM, Graham WM, Robinson KL, Pitt KA, Schildhauer M, Regetz J (2014) Gelatinous zooplankton biomass in the global oceans: geographic variation and environmental drivers. Global Ecology and Biogeography 23:701–714.

Mendes CRB, Tavano VM, Leal MC, De Souza MS, Brotas V, Garcia CAE (2013) Shifts in the dominance between diatoms and cryptophytes during three late summers in the Bransfield Strait (Antarctic Peninsula). Polar Biol 36:537–547.

Mianzan H, Cornelius P (1999) Cubomedusae and Scyphomedusae. In: *South Atlantic Zooplankton*. Demetrio Boltovskoy, Leiden, The Netherlands, p 513–560

Nagata RM, Teixeira-Amaral P, Lemos VR, Jordano MA, Muxagata E, Morandini AC (2021) First description of wild-collected ephyrae of Lychnorhiza lucerna (Cnidaria, Scyphozoa). An Acad Bras Ciênc 93:e20190574.

Pitt KA (2000) Life history and settlement preferences of the edible jellyfish Catostylus mosaicus (Scyphozoa: Rhizostomeae). Marine Biology 136:269–279.

Richardson AJ (2008) In hot water: zooplankton and climate change. ICES Journal of Marine Science 65:279–295.

Sangrà P, Gordo C, Hernández-Arencibia M, Marrero-Díaz A, Rodríguez-Santana A, Stegner A, Martínez-Marrero A, Pelegrí JL, Pichon T (2011) The Bransfield current system. Deep Sea Research Part I: Oceanographic Research Papers 58:390–402.

Schiariti A, Kawahara M, Uye S, Mianzan HW (2008) Life cycle of the jellyfish Lychnorhiza lucerna (Scyphozoa: Rhizostomeae). Mar Biol 156:1–12.

Straehler-Pohl I, Jarms G (2010) Identification key for young ephyrae: a first step for early detection of jellyfish blooms. Hydrobiologia 645:3–21.

Ward P (1989) The distribution of zooplankton in an Antarctic fjord at South Georgia during summer and winter. Antartic science 1:141–150.

Anexo - © Copyright Statement - GOAL / LEOC 2022

Banco de Dados Oceanográficos do GRUPO DE OCEANOGRAFIA DE ALTAS LATITUDES (GOAL) e do LABORATÓRIO DE ESTUDOS DOS OCEANOS E CLIMA (LEOC).

**Todos os dados físicos, químicos e biológicos gerados pelo GOAL e/ou LEOC estão disponíveis nas coleções ODV para serem utilizados por pesquisadores e alunos participantes dos grupos de pesquisa parceiros/colaboradores.

**É proibido o envio das coleções para terceiros, sem a prévia autorização do Coordenador do GOAL ou do LEOC.

****

Coleções Disponíveis com dados processados:

DATABASE_GOAL_2003_2019_v01 : Coleção com dados físicos e químicos dos cruzeiros dos projetos GOAL (2003, 2004, 2005), SOS-CLIMATE (2008, 2009, 2010),

POLARCANION/PROOASIS (2011, 2013, 2014), NAUTILUS/INTERBIOTA (2015, 2016, 2017, 2018, 2019).

NAUTILUS_v03a : Coleção com inserção de dados AT e CT corrigidos dos cruzeiros

NAUTILUS/INTERBIOTA (2015, 2016, 2017, 2018, 2019).

Caso pretenda utilizar os dados para publicação, por favor informar e solicitar a anuência/autorização dos coordenadores abaixo:

Dr. Mauricio M. Mata - mauricio.mata@furg.br (Coordenador PROVOCCAR)

Dr. Rodrigo Kerr - rodrigokerr@furg.br (Coordenador GOAL e LEOC, e Coordenador Adjunto PROVOCCAR, Responsável dados físicos e químicos)

Dr. Eduardo R. Secchi - edu.secchi@furg.br (Coordenador ECOPELAGOS e ECOMEGA, Responsável dados biológicos Cetáceos)

Dr. Carlos Rafael B. Mendes - crbmendes@furg.br (Coordenador GOAL e LABFITO, Coordenador Adjunto ECOPELAGOS, Responsável dados biológicos Plâncton)

© Grupo de Oceanografia de Altas Latitudes / Laboratório de Estudos dos Oceanos e Clima – 2022

Anexo: Dados ambientais de 2017 utilizados nas análises.

Ano	Estação	Local	Profundidade	Méd. Temp	Média Sal.	Média Chl-*a*	Min. Temp	Min. Sal	Min. Chl-*a*	Max. Temp	Max. Sal	Max Chl-*a*	Ind. Temp	Ind. Sal.	Ind. Chl-*a*	PCM	Estabilidade
2017	#03 - D	Gerlache	0-100	0.822	33.993	0.583	0.051	33.466	0.106	1.621	34.334	3.208	1.511	0.716	3.102	13	5.48
2017	#03 - D	Gerlache	100-200	-0.241	34.376	0.101	-0.412	34.327	0.084	0.035	34.429	0.172	0.533	0.109	0.088	13	5.48
2017	#03 - D	Gerlache	200-300	-0.486	34.447	0.077	-0.574	34.432	0.068	-0.425	34.463	0.107	0.117	0.049	0.039	13	5.48
2017	#03 - D	Gerlache	300-400	-0.577	34.482	0.070	-0.628	34.463	0.063	-0.484	34.497	0.143	0.135	0.032	0.079	13	5.48
2017	#03 - D	Gerlache	400-500	-0.693	34.503	0.067	-0.759	34.497	0.061	-0.628	34.508	0.126	0.163	0.017	0.065	13	5.48
2017	#04 - D	Gerlache	0-100	1.091	34.005	1.738	0.124	33.313	0.175	2.459	34.356	5.553	2.374	1.060	5.378	16	7.17
2017	#04 - D	Gerlache	100-200	-0.058	34.424	0.096	-0.213	34.356	0.070	0.120	34.476	0.205	0.327	0.124	0.135	16	7.17
2017	#04 - D	Gerlache	200-300	-0.290	34.490	0.070	-0.401	34.473	0.063	-0.194	34.500	0.102	0.230	0.047	0.039	16	7.17
2017	#08 - D	Bransfield	0-100	0.659	34.260	0.734	0.659	34.155	0.293	1.615	34.354	1.892	1.851	0.237	1.600	22	2.27
2017	#08 - D	Bransfield	100-200	-0.482	34.405	0.168	-0.482	34.361	0.098	-0.175	34.432	0.395	0.462	0.077	0.298	22	2.27
2017	#08 - D	Bransfield	200-300	-0.785	34.448	0.107	-0.785	34.431	0.082	-0.675	34.463	0.181	0.281	0.041	0.100	22	2.27
2017	#08 - D	Bransfield	300-400	-0.890	34.470	0.081	-0.890	34.462	0.064	-0.867	34.484	0.128	0.083	0.034	0.063	22	2.27
2017	#08 - D	Bransfield	400-500	-0.977	34.503	0.064	-0.977	34.484	0.057	-0.929	34.519	0.086	0.084	0.028	0.028	22	2.27
2017	#06 - D	Bellingshausen	0-100	1.404	34.033	0.623	1.404	33.798	0.077	3.234	34.405	1.122	3.461	0.692	1.045	30	5.41
2017	#06 - D	Bellingshausen	100-200	1.159	34.572	0.063	1.159	34.413	0.056	1.507	34.648	0.105	1.033	0.259	0.049	30	5.41
2017	#06 - D	Bellingshausen	200-300	1.495	34.668	0.058	1.495	34.634	0.055	1.670	34.694	0.073	0.370	0.211	0.019	30	5.41
2017	#10 - D	Bransfield	0-100	0.099	34.190	0.587	0.099	34.048	0.159	1.045	34.336	1.082	1.932	0.343	0.923	17	2.41
2017	#10 - D	Bransfield	100-200	-0.950	34.358	0.161	-0.950	34.336	0.109	-0.683	34.376	0.697	0.367	0.056	0.588	17	2.41
2017	#10 - D	Bransfield	200-300	-1.109	34.397	0.124	-1.109	34.376	0.085	-1.064	34.426	0.310	0.108	0.052	0.226	17	2.41
2017	#10 - D	Bransfield	300-400	-1.132	34.462	0.090	-1.133	34.426	0.068	-1.114	34.484	0.381	0.045	0.055	0.313	17	2.41
2017	#10 - D	Bransfield	400-500	-1.102	34.500	0.068	-1.102	34.486	0.060	-1.087	34.511	0.112	0.022	0.028	0.052	17	2.41
2017	#11 - D	Bransfield	0-100	0.978	34.137	1.035	0.978	33.970	0.432	2.138	34.375	1.540	0.556	0.078	1.108	33	3.46
2017	#11 - D	Bransfield	100-200	-0.766	34.421	0.253	-0.766	34.377	0.128	-0.350	34.460	0.466	0.546	0.082	0.339	33	3.46
2017	#11 - D	Bransfield	200-300	-1.021	34.494	0.103	-1.021	34.460	0.080	-0.904	34.520	0.141	0.214	0.039	0.061	33	3.46
2017	#11 - D	Bransfield	300-400	-0.935	34.529	0.073	-0.935	34.520	0.062	-0.850	34.535	0.132	0.032	0.034	0.070	33	3.46
2017	#11 - D	Bransfield	400-500	-1.061	34.537	0.063	-1.061	34.534	0.055	-0.987	34.540	0.080	0.169	0.036	0.025	33	3.46
2017	#12 - T	Bransfield	0-100	0.839	34.228	0.284	0.839	34.069	0.082	2.268	34.395	0.501	2.945	0.431	0.419	36	3.41
2017	#12 - T	Bransfield	100-200	-0.752	34.440	0.069	-0.752	34.392	0.057	-0.513	34.469	0.101	0.129	0.042	0.044	36	3.41
2017	#12 - T	Bransfield	200-300	-0.976	34.490	0.056	-0.976	34.469	0.053	-0.872	34.509	0.067	0.127	0.026	0.015	36	3.41
2017	#12 - T	Bransfield	300-400	-1.091	34.520	0.054	-1.091	34.510	0.051	-1.062	34.528	0.079	0.132	0.035	0.028	36	3.41
2017	#12 - T	Bransfield	400-500	-1.094	34.535	0.054	-1.094	34.529	0.051	-1.088	34.541	0.059	0.026	0.023	0.008	36	3.41

Anexo: Dados ambientais de 2018 (1 de 2) utilizados nas análises.

Ano	Estação	Local	Profundidade	Méd. Temp	Média Sal.	Média Chl-*a*	Min. Temp	Min. Sal	Min. Chl-*a*	Max. Temp	Max. Sal	Max Chl-*a*	Ind. Temp	Ind. Sal.	Ind. Chl-*a*	PCM	Estabilidade
2018	#12 - T	Bransfield	0-100	0.666	34.290	1.470	-0.545	34.171	0.077	1.954	34.414	5.595	2.496	0.287	5.518	34	2.66
2018	#12 - T	Bransfield	100-200	-0.665	34.455	0.076	-0.781	34.414	0.061	-0.532	34.492	0.096	0.258	0.084	0.035	34	2.66
2018	#12 - T	Bransfield	200-300	-0.815	34.503	0.067	-0.847	34.492	0.061	-0.782	34.507	0.104	0.052	0.018	0.043	34	2.66
2018	#12 - T	Bransfield	300-400	-0.879	34.513	0.064	-0.926	34.507	0.058	-0.845	34.521	0.098	0.098	0.017	0.040	34	2.66
2018	#12 - T	Bransfield	400-500	-0.969	34.526	0.058	-1.017	34.521	0.054	-0.926	34.530	0.068	0.079	0.012	0.014	34	2.66
2018	#13 -D	Bransfield	0-100	1.114	34.251	2.191	0.878	34.236	1.740	1.271	34.279	2.733	0.068	0.010	0.993	76	0.65
2018	#13 -D	Bransfield	100-200	0.587	34.324	1.131	0.278	34.280	0.289	0.872	34.400	2.406	0.731	0.115	2.117	76	0.65
2018	#15 - D	Bransfield	0-100	1.138	34.229	1.863	0.723	34.197	0.306	1.451	34.276	3.554	1.183	0.161	3.212	54	1.58
2018	#15 - D	Bransfield	100-200	0.219	34.362	0.233	0.059	34.277	0.118	0.718	34.401	0.394	0.273	0.094	0.276	54	1.58
2018	#15 - D	Bransfield	200-300	0.046	34.428	0.116	-0.008	34.400	0.087	0.097	34.448	0.145	0.154	0.040	0.059	54	1.58
2018	#15 - D	Bransfield	300-400	-0.283	34.484	0.068	-0.586	34.449	0.053	-0.009	34.506	0.105	0.590	0.058	0.053	54	1.58
2018	#15 - D	Bransfield	400-500	-0.736	34.516	0.055	-0.818	34.506	0.051	-0.587	34.519	0.059	0.144	0.019	0.008	54	1.58
2018	#16 - D	Bransfield	0-100	-1.015	34.217	0.290	-1.196	34.042	0.117	-0.632	34.310	0.455	0.605	0.291	0.338	16	2.11
2018	#16 - D	Bransfield	100-200	-1.248	34.399	0.139	-1.323	34.310	0.094	-1.196	34.475	0.248	0.112	0.133	0.154	16	2.11
2018	#11 - T	Bransfield	0-100	1.060	34.250	2.483	-0.486	34.162	0.079	2.505	34.375	6.654	2.814	0.253	6.575	19	2.96
2018	#11 - T	Bransfield	100-200	-0.565	34.447	0.063	-0.613	34.376	0.056	-0.488	34.485	0.102	0.140	0.117	0.047	19	2.96
2018	#11 - T	Bransfield	200-300	-0.640	34.509	0.056	-0.706	34.485	0.053	-0.564	34.524	0.063	0.155	0.049	0.010	19	2.96
2018	#11 - T	Bransfield	300-400	-0.881	34.523	0.054	-0.981	34.522	0.052	-0.706	34.528	0.059	0.267	0.015	0.007	19	2.96
2018	#11 - T	Bransfield	400-500	-1.015	34.532	0.053	-1.047	34.527	0.051	-0.966	34.535	0.060	0.043	0.010	0.009	19	2.96
2018	#09 - D	Bransfield	0-100	0.863	34.220	6.073	0.198	34.024	1.593	1.553	34.351	10.178	0.902	0.306	8.585	15	2.91
2018	#09 - D	Bransfield	100-200	0.481	34.463	0.412	0.147	34.352	0.074	0.705	34.518	1.838	0.281	0.193	1.763	15	2.91
2018	#09 - D	Bransfield	200-300	0.872	34.556	0.072	0.704	34.518	0.061	1.000	34.597	0.175	0.319	0.084	0.114	15	2.91
2018	#10 - D	Bransfield	0-100	0.058	34.352	1.024	-0.620	34.318	0.269	0.787	34.388	1.890	1.547	0.125	1.621	34	1.21
2018	#10 - D	Bransfield	100-200	-0.887	34.423	0.175	-0.967	34.389	0.094	-0.627	34.444	0.353	0.214	0.062	0.259	34	1.21
2018	#10 - D	Bransfield	200-300	-0.974	34.462	0.093	-1.037	34.446	0.080	-0.931	34.476	0.147	0.136	0.028	0.067	34	1.21
2018	#10 - D	Bransfield	300-400	-1.057	34.483	0.081	-1.076	34.475	0.068	-1.035	34.490	0.157	0.028	0.020	0.089	34	1.21
2018	#10 - D	Bransfield	400-500	-1.081	34.501	0.067	-1.098	34.489	0.060	-1.068	34.512	0.093	0.010	0.018	0.033	34	1.21
2018	#08 - D	Bransfield	0-100	0.225	34.324	1.035	-0.330	34.285	0.432	0.590	34.390	1.540	0.556	0.078	1.108	49	1.15
2018	#08 - D	Bransfield	100-200	-0.519	34.415	0.253	-0.704	34.387	0.128	-0.322	34.443	0.466	0.546	0.082	0.339	49	1.15
2018	#08 - D	Bransfield	200-300	-0.809	34.460	0.103	-0.871	34.442	0.080	-0.702	34.473	0.141	0.214	0.039	0.061	49	1.15
2018	#08 - D	Bransfield	300-400	-0.882	34.484	0.073	-0.889	34.473	0.062	-0.870	34.495	0.132	0.032	0.034	0.070	49	1.15
2018	#08 - D	Bransfield	400-500	-0.826	34.507	0.063	-0.877	34.495	0.055	-0.743	34.526	0.080	0.169	0.036	0.025	49	1.15

Anexo: Dados ambientais de 2018 (2 de 2) utilizados nas análises.

Ano	Estação	Local	Profundidade	Méd. Temp	Média Sal.	Média Chl-*a*	Min. Temp	Min. Sal	Min. Chl-*a*	Max. Temp	Max. Sal	Max Chl-*a*	Ind. Temp	Ind. Sal.	Ind. Chl-*a*	PCM	Estabilidade
2018	#05 - D	Gerlache	0-100	0.615	34.102	1.885	-0.116	33.576	0.136	1.846	34.355	8.643	1.811	0.751	8.508	15	5.44
2018	#05 - D	Gerlache	100-200	-0.031	34.420	0.105	-0.180	34.356	0.062	0.083	34.474	0.230	0.237	0.142	0.168	15	5.44
2018	#05 - D	Gerlache	200-300	-0.264	34.487	0.064	-0.327	34.476	0.058	-0.122	34.501	0.080	0.228	0.033	0.022	15	5.44
2018	#05 - D	Gerlache	300-400	-0.368	34.509	0.060	-0.410	34.501	0.054	-0.327	34.514	0.067	0.078	0.015	0.013	15	5.44
2018	#03 - D	Gerlache	0-100	0.516	34.068	0.864	0.055	33.803	0.142	1.079	34.362	2.178	1.065	0.555	2.036	40	3.99
2018	#03 - D	Gerlache	100-200	-0.111	34.420	0.097	-0.244	34.362	0.070	0.053	34.450	0.161	0.274	0.094	0.092	40	3.99
2018	#03 - D	Gerlache	200-300	-0.306	34.475	0.066	-0.348	34.450	0.058	-0.245	34.490	0.102	0.102	0.039	0.044	40	3.99
2018	#03 - D	Gerlache	300-400	-0.390	34.503	0.060	-0.423	34.490	0.055	-0.348	34.512	0.103	0.090	0.026	0.048	40	3.99
2018	#03 - D	Gerlache	400-500	-0.428	34.522	0.057	-0.498	34.512	0.054	-0.366	34.526	0.069	0.096	0.015	0.016	40	3.99
2018	#02 - D	Gerlache	0-100	0.910	34.043	0.825	0.390	33.616	0.110	1.781	34.272	2.083	1.381	0.702	1.972	16	4.77
2018	#02 - D	Gerlache	100-200	0.522	34.425	0.094	0.361	34.276	0.074	0.839	34.560	0.136	0.390	0.213	0.061	16	4.77
2018	#02 - D	Gerlache	200-300	0.962	34.598	0.068	0.849	34.563	0.058	1.079	34.627	0.115	0.324	0.101	0.058	16	4.77
2018	#02 - D	Gerlache	300-400	1.237	34.660	0.058	1.079	34.627	0.054	1.357	34.685	0.071	0.262	0.057	0.017	16	4.77
2018	#01 - D	Gerlache	0-100	1.028	33.987	2.058	0.763	33.811	0.495	1.241	34.195	4.492	0.474	0.394	3.996	20	3.62
2018	#01 - D	Gerlache	100-200	0.737	34.391	0.187	0.623	34.197	0.068	0.888	34.524	1.397	0.252	0.341	1.329	20	3.62
2018	#01 - D	Gerlache	200-300	0.938	34.542	0.069	0.888	34.524	0.063	0.961	34.551	0.091	0.071	0.031	0.028	20	3.62
2018	#01 - D	Gerlache	300-400	0.974	34.556	0.066	0.959	34.550	0.062	0.986	34.562	0.093	0.026	0.012	0.031	20	3.62

Anexo: Dados ambientais de 2019 utilizados nas análises.

Ano	Estação	Local	Profundidade	Méd. Temp	Média Sal.	Média Chl-*a*	Min. Temp	Min. Sal	Min. Chl-*a*	Max. Temp	Max. Sal	Max Chl-*a*	Ind. Temp	Ind. Sal.	Ind. Chl-*a*	PCM	Estabilidade
2019	#14 - D	Bransfield	0-100	0.959	34.339	2.730	0.684	34.303	0.767	1.267	34.403	4.619	0.689	0.112	3.852	36	0.26
2019	#14 - D	Bransfield	100-200	0.375	34.437	0.349	0.055	34.403	0.094	0.682	34.483	0.779	0.748	0.092	0.685	36	0.26
2019	#14 - D	Bransfield	200-300	-0.148	34.510	0.078	-0.491	34.485	0.065	0.079	34.533	0.118	0.327	0.033	0.054	36	0.26
2019	#14 - D	Bransfield	300-400	-0.454	34.546	0.065	-0.679	34.532	0.057	-0.307	34.553	0.080	0.544	0.057	0.024	36	0.26
2019	#14 - D	Bransfield	400-500	-0.784	34.537	0.061	-0.856	34.535	0.058	-0.677	34.541	0.088	0.162	0.019	0.030	36	0.26
2019	#17 - D	Bransfield	0-100	-0.599	34.497	0.415	-0.829	34.493	0.292	-0.451	34.507	1.892	0.332	0.110	1.594	70	0.01
2019	#12 - D	Bransfield	0-100	0.186	34.329	1.392	-0.287	34.107	0.118	0.964	34.454	3.850	1.991	0.430	3.732	60	0
2019	#12 - D	Bransfield	100-200	-0.394	34.499	0.092	-0.487	34.454	0.070	-0.287	34.531	0.144	0.133	0.078	0.074	60	0
2019	#12 - D	Bransfield	200-300	-0.421	34.545	0.068	-0.512	34.531	0.064	-0.376	34.553	0.074	0.185	0.026	0.010	60	0
2019	#12 - D	Bransfield	300-400	-0.808	34.538	0.065	-0.901	34.536	0.061	-0.534	34.546	0.080	0.445	0.075	0.019	60	0
2019	#12 - D	Bransfield	400-500	-0.969	34.540	0.063	-1.095	34.540	0.059	-0.902	34.543	0.074	0.063	0.008	0.015	60	0
2019	#11 - T	Bransfield	0-100	0.634	34.291	1.797	-0.155	34.109	0.272	1.193	34.420	3.082	1.402	0.329	2.810	21	0.02
2019	#11 - T	Bransfield	100-200	-0.254	34.471	0.219	-0.391	34.420	0.177	-0.151	34.503	0.367	0.076	0.031	0.106	21	0.02
2019	#11 - T	Bransfield	200-300	-0.451	34.516	0.060	-0.621	34.501	0.056	-0.325	34.524	0.063	0.137	0.015	0.006	21	0.02
2019	#11 - T	Bransfield	300-400	-0.659	34.533	0.059	-0.737	34.524	0.055	-0.566	34.541	0.072	0.152	0.018	0.062	21	0.02
2019	#11 - T	Bransfield	400-500	-0.848	34.540	0.056	-0.978	34.540	0.053	-0.714	34.541	0.092	0.187	0.009	0.039	21	0.02
2019	#03 - D	Gerlache	0-100	0.552	34.218	1.110	0.099	34.053	0.232	1.253	34.386	1.989	1.066	0.358	1.757	23	0.25
2019	#03 - D	Gerlache	100-200	-0.080	34.458	0.158	-0.231	34.386	0.110	0.107	34.494	0.389	0.357	0.090	0.279	23	0.25
2019	#03 - D	Gerlache	200-300	-0.230	34.519	0.077	-0.308	34.497	0.064	-0.077	34.529	0.106	0.102	0.036	0.042	23	0.25
2019	#03 - D	Gerlache	300-400	-0.353	34.534	0.061	-0.398	34.522	0.056	-0.291	34.537	0.075	0.110	0.016	0.019	23	0.25
2019	#03 - D	Gerlache	400-500	-0.480	34.540	0.057	-0.521	34.537	0.053	-0.399	34.541	0.065	0.154	0.016	0.012	23	0.25
2019	#05 - D	Gerlache	0-100	0.869	34.129	1.671	0.005	33.783	0.345	1.827	34.381	3.567	1.871	0.562	3.223	20	-0.06
2019	#05 - D	Gerlache	100-200	-0.203	34.450	0.176	-0.289	34.384	0.078	-0.003	34.497	0.371	0.219	0.121	0.294	20	-0.06
2019	#05 - D	Gerlache	200-300	-0.162	34.530	0.066	-0.255	34.498	0.056	-0.069	34.538	0.087	0.321	0.034	0.030	20	-0.06
2019	#05 - D	Gerlache	300-400	-0.470	34.534	0.056	-0.553	34.532	0.053	-0.259	34.539	0.070	0.190	0.012	0.017	20	-0.06
2019	#05 - D	Gerlache	400-500	-0.571	34.538	0.055	-0.578	34.536	0.052	-0.555	34.540	0.060	0.012	0.007	0.008	20	-0.06
2019	#08 - D	Bransfield	0-100	0.536	34.252	0.837	-0.192	34.001	0.277	1.423	34.405	2.197	2.135	0.505	1.921	33	0.12
2019	#08 - D	Bransfield	100-200	-0.457	34.441	0.246	-0.607	34.404	0.119	-0.192	34.469	0.445	0.386	0.078	0.326	33	0.12
2019	#08 - D	Bransfield	200-300	-0.697	34.492	0.099	-0.794	34.470	0.076	-0.615	34.515	0.136	0.164	0.041	0.060	33	0.12
2019	#08 - D	Bransfield	300-400	-0.663	34.522	0.076	-0.724	34.513	0.064	-0.616	34.537	0.117	0.154	0.037	0.054	33	0.12
2019	#08 - D	Bransfield	400-500	-0.468	34.557	0.064	-0.623	34.537	0.059	-0.351	34.568	0.087	0.334	0.038	0.028	33	0.12
2019	#07 - D	Bellingshausen	0-100	0.994	34.142	0.647	0.344	33.973	0.167	1.773	34.322	2.340	1.727	0.447	2.173	21	0.05
2019	#07 - D	Bellingshausen	100-200	-0.060	34.452	0.105	-0.270	34.325	0.066	0.333	34.519	0.299	0.409	0.130	0.233	21	0.05
2019	#06 - T	Bellingshausen	0-100	0.506	34.072	1.292	-0.648	33.851	0.130	1.568	34.413	2.698	2.044	0.545	2.569	37	0.4
2019	#06 - T	Bellingshausen	100-200	0.989	34.541	0.075	0.406	34.416	0.057	1.265	34.625	0.129	0.856	0.222	0.073	37	0.4
2019	#06 - T	Bellingshausen	200-300	1.396	34.665	0.057	1.266	34.626	0.054	1.513	34.700	0.064	0.204	0.067	0.010	37	0.4